

Aus der Medizinischen Klinik mit Schwerpunkt Nephrologie
und Internistische Intensivmedizin
der Medizinischen Fakultät Charité – Universitätsmedizin Berlin

DISSERTATION

**Molecular profiling of sex-specific podocyte stress response in response to
mTOR inhibition**

zur Erlangung des akademischen Grades

Doctor of Philosophy (PhD)

vorgelegt der Medizinischen Fakultät

Charité – Universitätsmedizin Berlin

von

Ola Al Diab

aus Jordanien

Datum der Promotion: 25.06.2023

Table of contents

Abbreviations	v
Table of figures	vii
Abstract	ix
Abstrakt	xi
1. INTRODUCTION	
1.1 Sex-specific differences in kidney diseases	1
1.2 Glomerular filtration barrier, podocytes and proteinuria	2
1.3 Podocyte homeostasis and injury	5
1.4 Podocyte stress responses	6
1.5 mTOR and its role in podocytes and the kidney	7
1.6 Rapamycin - mechanism of action, clinical use and adverse effects	10
1.7 Scope of the thesis, hypothesis and objectives	12
2. MATERIALS AND METHODS	
2.1 Materials	14
2.1.1 Chemical substances, buffer and gel recipes and kits.....	14
2.1.2 Primers	18
2.1.3 Antibodies.....	18
2.1.4 Equipment	20
2.2 Methods	21
2.2.1 Animal model and genotyping.....	21
2.2.2 Experimental design.....	22
2.2.3 Glomeruli and podocyte isolation	24
2.2.4 Assessment of renal function.....	25
2.2.5 Histology.....	26
2.2.5.1 Embedding and sectioning.....	26
2.2.5.2 Stainings using paraffin-embedded renal tissue sections.....	26
2.2.5.3 Immunofluorescent actin staining, microscopic analysis and quantification.....	26
2.2.6 Gene expression analysis.....	28
2.2.6.1 Total RNA extraction, measurement and RNA sequencing	28
2.2.6.2 Quantitative real time PCR (qRT-PCR).....	30

2.2.7 Protein isolation and western blot analysis	30
2.2.8 Proteomics	31
2.2.9 Metabolomics	31
2.2.10 Statistical Analysis.....	32

3. RESULTS

3.1 Functional effects of mTOR inhibition in male and female mice.....	33
3.2 Effect of mTOR inhibition on renal morphology.....	36
3.3 Effect of mTOR inhibition on mTOR protein expressions and signalling.....	38
3.3.1 Sexual dimorphism of mTOR complex protein expressions in vehicle and rapamycin treated mice.....	38
3.3.2 Effect of rapamycin on mTORC1 signaling in male and female mice	39
3.3.3. Effect of rapamycin on mTORC2 regulation in male and female mice.....	40
3.3.4 Effect of rapamycin on energy sensor AMPK and stress kinase activation ERK1/2 in male and female mice.....	42
3.4 Sexual dimorphism of podocyte transcriptome and transcriptional stress responses to mTOR inhibition with rapamycin	44
3.4.1 Overview of RNA sequencing dataset.....	44
3.4.2 Gene set enrichment analyses of significant sexually dimorphic and treatment-related differentially expressed genes.....	50
3.4.2.1 Gene set enrichment analyses of significant sexually dimorphic genes	50
3.4.2.2 Gene set enrichment analyses of treatment-related differentially expressed genes.....	53
3.4.2.3 Sexually dimorphic responses to rapamycin in functionally relevant gene subgroups.....	55
3.4.3 Gene set enrichment analysis (GSEA) of whole transcriptome	56
3.4.4 Transcriptional differences in selected GO terms which appeared significantly enriched in GSEA of the whole transcriptome	58
3.4.4.1 GOs including genes relevant for podocyte proteostasis.....	58
3.4.4.2. GO's including genes relevant for podocyte energy homeostasis and metabolism.....	62
3.4.4.3 GO's including genes relevant for adaptation processes in response to stress..	66
3.4.4.4 GO's including genes relevant for podocyte structure and cell-cell interactions..	73

3.4.4.5 Sex- and treatment-specific transcriptional differences in genes coding for mTOR-signaling related proteins.....	80
3.4.5 Validation of gene expression levels for selected genes.....	82
3.5 Podocyte-specific proteomics and effect of mTOR inhibition on protein levels of selected podocyte relevant structural and functional protein groups	84
3.5.1 Podocyte-specific proteomics revealed sexual dimorphism in vehicle control mice .	84
3.5.2 GO enrichment analysis of proteomics of vehicle control podocytes revealed that females have an increased abundance of mitochondrial oxidative phosphorylation proteins and basal cell proteins	86
3.5.3 Focus on sexual dimorphism in mitochondrial respiratory chain proteins and metabolic proteins related to glycolysis, TCA cycle and pentose phosphate pathway.....	88
3.5.4 Focus on sexual dimorphism in oxidative stress response proteins in podocytes..	90
3.5.5 Focus on sexual dimorphism in proteins related to the post-translational modification in podocytes..	91
3.5.6 Focus on sexual dimorphism in podocyte-specific structural proteins and proteins related to podocyte homeostasis and function	92
3.5.7 Sexual dimorphism in proteins involved in major cellular response and cell fate Pathways.....	93
3.6 Integration of transcriptomics and proteomics data.....	94
3.7 Analyses of selected protein expression levels in renal cortex tissues of all experimental groups to investigate sexually dimorphic responses to rapamycin treatment on protein level.....	95
3.7.1 Sexual dimorphic responses to mTOR inhibition on expression of mitochondrial oxidative proteins.....	95
3.7.2 Sexual dimorphic responses to mTOR inhibition on podocyte-specific proteins.....	97
3.7.3 Effect of rapamycin on cytoskeletal and focal adhesion proteins.....	99
3.7.4 Sexual dimorphism in autophagy and apoptosis marker protein expressions.....	104
3.8 Effect of mTOR inhibition on renal cortex metabolism.....	106
4. DISCUSSION.....	111
4.1 Mouse model and experimental design.....	112
4.1.1 Mouse model.....	112

4.1.2 Choice for the use of mTOR inhibition to investigate sexual dimorphic stress responses in podocytes	113
4.1.3 Sample size.....	113
4.1.4 Validation of RNA-seq and proteomics data.....	114
4.2 Lack of physiological and morphological alterations in response to mTOR inhibition with rapamycin in both sexes	115
4.3 Sexual dimorphic expressions of mTOR complex components, related signaling molecules and responses to rapamycin treatment	116
4.4 Intrinsic and treatment-related sexual dimorphism of podocyte genes and proteins.	117
4.4.1 Sexual dimorphic GO enrichments in podocyte genes and proteins.....	117
4.4.2 Sexual dimorphism in major podocyte-specific genes and proteins relevant for podocyte structure.....	120
4.4.3 Intrinsic and treatment-related sexual dimorphism in podocyte cellular energy homeostasis.....	123
4.4.4 Sexual dimorphism in redox proteins.....	124
4.4.5 Sexual dimorphism in proteostasis-regulating genes and proteins	125
4.4.6 Sexual dimorphism in kinases relevant for podocyte homeostasis	126
4.4.7 Sexual dimorphism in transcription factors.....	127
4.5 Sexual dimorphic metabolic responses to rapamycin	128
4.6 Study limitations.....	132
4.7 Outlook and Conclusions.....	133
5. REFERENCES.....	134
6. APPENDIX.....	145
7. STATUARY DECLARATION.....	155
8. CURRICULUM VITAE.....	156
9. ACKNOWLEDGEMENT.....	159

Abbreviations

AA	Amino acid
ACTN4	α -actinin-4
AKI	Acute kidney injury
AKT	Protein kinase B
AMPK	MP-activated protein kinase
ARHGAP32	Rho GTPase activating protein 32
ATF6	activating transcription factor 6
BHLHE40	basic helix-loop-helix family member e40
CD151	Cluster of Differentiation 151
CD2AP	CD2-associated protein
CKD	chronic renal disease
CME	clathrin-dependent
COX7a2	cytochrome c oxidase subunit 7A2
CTSL	cathepsin L
DAG	dystroglycan
DAAM2	dishevelled associated activator of morphogenesis 2
DE	Differential expressed
DMSO	Dimethyl sulfoxide
DN	diabetic nephropathy
ECM	Extracellular matrix
EMT	epithelial-to-mesenchymal transition
ESRD	End stage renal disease
FA	Focal adhesion
FACS	fluorescence-activated cell sorting
FC	Fold change
FDR	False discover rate
FKBP12	FK506-binding protein (FKBP) 12
FP	foot processes
FSGS	focal segmental glomerulosclerosis
GBM	glomerular basement membrane
GFB	glomerular filtration barrier
GFP	green fluorescent protein
GO	Gene ontology
GSEA	Gene set enrichment analysis
GUT	glucose transporters
ILK	Integrin-linked kinase
IRE1 α	inositol-requiring enzyme 1 α
KEGG	Kyoto Encyclopedia of Genes and Genomes
LC3	Microtubule-associated proteins
LFQ	label-free quantification
Log2FC	log ₂ -fold change
MSig	molecular signature

mSIN	mammalian stress-activated protein kinase interaction protein 1
μg	microgram
μL	microliter
MUP	major urinary proteins (s)
NPHS1	nephrin
NPHS2	podocin
OXPPOS	Oxidative phosphorylation
PAS	Periodic acid-Schiff
PCA	principal component analysis
PFA	Paraformaldehyde
PGC-1α	Peroxisome proliferator-activated receptor-gamma coactivator
PI3K	phosphatidylinositol 3-kinase-related kinase
PKD	polycystic kidney disease
Podxl	podocalyxin
PPP	pentose phosphate pathway
Prdx	peroxiredoxin
PTMs	Post-translational modifications PTMs
qPCR	Quantitative real time PCR
RNA-seq	RNA sequencing
RPKB	Read per kilo base
Rpl13a	Ribosomal protein L13a
SD	slit diaphragm
SDE	significantly differentially expressed
SGK1	glucocorticoid-induced protein kinase 1
SLC6a6	Solute carrier family 6 member 6
SRL	sirolimus
TCA	tricarboxylic acid
TF	transcription factors
TJP1 / ZO1	Tight junction protein 1/ Zonula occludens-1
UPR	unfolded protein response
UPS	ubiquitin-proteasome system
VEGF	Vascular endothelial growth factor
WT1	Wilms tumor-1
WB	western blot
YWHAZ	Tyrosine 3-Monooxygenase/Tryptophan 5-Monooxygenase Activation Protein Zeta
4EBP1	eukaryotic translation initiation factor 4E-binding protein 1

Table of figures

Figure 1	Gender differences in the incidence of ESRD
Figure 2	Glomerular filtration barrier
Figure 3	Structure and molecular components of podocytes
Figure 4	mTOR signaling pathway
Figure 5	Representative agarose gel for the genotyping for Tomato and Cre recombinase PCR
Figure 6	Schematic presentation of the experimental design
Figure 7	Scheme for podocyte cell isolation technique
Figure 8	Representative results from FACS cell sorting
Figure 9	RNA quality control
Figure 10	Urinary parameters, glucose, albumin and total protein excretion
Figure 11	Histological morphology of glomeruli from vehicle and rapamycin-treated male and female mice
Figure 12	Assessment of renal fibrosis levels by Sirius red staining and collagen immunohistochemistry
Figure 13	Expression of mTOR complex proteins
Figure 14	mTORC1 signaling pathway activation
Figure 15	mTORC2 signaling pathway activation
Figure 16	Expression and activation of AMPK and ERK1/2 in renal cortex tissue in all experimental groups.
Figure 17	Podocyte-specific genes detected in the current and previously reported transcriptomic studies
Figure 18	Principal component analysis
Figure 19	Sex- and treatment-specific transcriptional differences
Figure 20	Venn diagram demonstrating overlap of intrinsic sexually dimorphic genes and DE genes in response to rapamycin treatment in each sex
Figure 21	Sexual dimorphism does not relate to sex chromosomes
Figure 22	Panther Protein Class categorization of the intrinsically significant sexually dimorphic podocyte genes
Figure 23	Gene ontology enrichment analyses of sexually dimorphic genes which were intrinsically overexpressed either in males or in females
Figure 24	Functional annotation graphs for the significantly differentially regulated genes by treatment in male podocytes
Figure 25	Sexual dimorphism in responses to rapamycin in functionally relevant subgroups of sexually dimorphic genes
Figure 26	Heatmap of significant sexually dimorphic ribosomal genes, translational factors and genes involved in ribosome biogenesis of podocytes from all experimental groups
Figure 27	Sexual dimorphism of PTM-related genes
Figure 28	Sexually dimorphic response of mitochondrial genes coding for proteins of the oxidative phosphorylation system
Figure 29	Gene expression changes of glycolysis and TCA cycle genes in male and female podocytes in response to rapamycin
Figure 30	Redox genes show sexual dimorphic expression levels at baseline and with rapamycin.
Figure 31	Apoptotic genes respond differently to rapamycin in male and female podocytes
Figure 32	Gene expression changes of signaling pathway in male and female podocytes in response to rapamycin

Figure 33	Sexual dimorphism in TFs genes
Figure 34	GSEA analysis of GOs related to focal adhesion, regulation of cytoskeleton different expression at baseline and after rapamycin
Figure 35	heatmap of the log ₂ FC expression for highly expressed SD, ECM and focal adhesion molecules. between all experimental groups
Figure 36	GSEA analysis of GOs related to podocyte-cytoskeleton specific genes
Figure 37	KEGG graph for endocytosis
Figure 38	Sexual dimorphism in podocyte endocytic genes
Figure 39	Effect of rapamycin on mTOR pathway
Figure 40	Validation of differentially expressed genes (DEGs) between male and female podocytes.
Figure 41	Validation of differentially regulated genes in response to rapamycin in male podocytes
Figure 42	Volcano plot of significantly sex-DE expressed proteins
Figure 43	GO enrichment analysis revealed enrichment of cell part and mitochondrial proteins in female podocytes
Figure 44	GO-term overexpressed in male and female podocyte protein vehicle groups with FC>2
Figure 45	Log ₂ FC of LFQ values of male versus female podocyte proteins of the oxidative chain
Figure 46	Log ₂ FC of LFQ values of male versus female podocyte proteins of the glycolysis pathway
Figure 47	Log ₂ FC of LFQ values of male versus female podocyte proteins for podocyte-specific and structural proteins.
Figure 48	Integration of transcriptomics and proteomics data
Figure 49	Sexual dimorphic expression of mitochondrial proteins
Figure 50	Sexual dimorphism in selected podocyte-specific proteins
Figure 51	Sexual dimorphism in cytoskeletal filament proteins
Figure 52	Cytoskeletal staining of renal cortex tissue sections from vehicle and rapamycin treated male and female mice and quantification
Figure 53	Expression of Rho-GTPases and sexual dimorphic responses to rapamycin treatment in renal cortex tissue
Figure 54	Expression and regulation of selected ECM and focal adhesion proteins in renal cortex tissue of male and female vehicle and rapamycin treated mice
Figure 55	Marker protein expressions for autophagy and apoptosis in renal cortex tissue of male and female vehicle and rapamycin treated mice
Figure 56	Accumulation of amino acids after rapamycin treatment
Figure 57	Rapamycin effect on main metabolites of the central carbon metabolism
Figure 58	Rapamycin effect on nucleobases metabolites

Abstract

Strong sexual dimorphism exists in many kidney diseases, progression to End-Stage Kidney Disease and renal graft functions. However, molecular mechanisms remain poorly understood. Podocytes are the most important cell-type of the glomerulus regulating integrity and function of the glomerular filtration barrier. Sex differences in their molecular components and functional stress responses might be crucial for these clinically relevant sex differences. Therefore, these cells were chosen as targets for the following study investigating intrinsic sexual dimorphism on genomic and proteomic levels and sex-specific differences in response to mTOR inhibition by rapamycin in an *in vivo* stress model in mice. Metabolomic studies of renal cortex tissues from the same experimental groups were included to investigate the functional consequences of sexual dimorphic molecular signatures.

Male and female ROSAmT/mG-NHPS2(podocin)Cre mice with GFP-expression restricted to podocytes were treated with rapamycin or vehicle for three weeks. Renal functional parameters were monitored using metabolic cages prior to sacrifice. The genetic mouse model allowed isolation of highly pure podocytes by sequential perfusion of kidneys and fluorescence activated cell sorting after tissue digestion. Kidneys were perfused for subsequent podocyte isolations for sequencing and proteomics or directly snap frozen for histology and metabolomics. qRT-PCR, western blots and immunohistological stainings were performed for validation of omics studies and further molecular characterizations.

Although kidney function and morphology remained normal in all experimental groups, RNA sequencing revealed strong intrinsic sex-differences with more than 1700 mRNA transcripts significantly sex-differently expressed. Furthermore, stress responses due to mTOR inhibition displayed sexual dimorphism in transcriptomes and metabolomes and signaling differences as assessed by western blots. Gene set enrichment analyses of sequencing data pointed to sex-differences in enriched GOs related to transcription, cytoskeleton and focal adhesion in male and mitochondria and translation in female podocytes. Proteomics displayed in addition to significant enrichment in mitochondrial proteins increased abundance of basal cell proteins in females. Rapamycin treatment abolished significant sex differences, yet rather due to increased changes in male podocytes whereas the female transcriptome remained more stable towards treatment-induced changes. Metabolomics further supported this finding that females appeared to be less sensitive towards mTOR inhibition by showing less accumulation of amino acid pool and glycolysis metabolites after rapamycin.

In conclusion, for the first-time podocyte-specific sexual dimorphism in gene regulation and protein expression patterns were identified together with sex-different metabolic changes in stress responses, which might contribute significantly to sex differences in renal disease susceptibilities and progression.

Abstrakt

Viele Nierenerkrankungen, die zeitliche Entwicklung hin zum terminalen Nierenversagen, sowie die Funktion von Nierentransplantaten weisen einen starken sexuellen Dimorphismus auf. Die zugrundeliegenden molekularen Mechanismen sind jedoch weiterhin nur unzureichend erforscht. Podozyten sind die wichtigsten glomerulären Zellen, die die Integrität und Funktion des glomerulären Filters regulieren. Geschlechterunterschiede in ihren molekularen Komponenten und funktionellen Stressantworten könnten dafür eine entscheidende Rolle spielen. Daher wurden diese Zellen in der folgenden Arbeit ausgewählt, um intrinsische Geschlechterunterschiede auf Genom- und Proteomebene, sowie sex-spezifische Unterschiede in der Stressantwort durch mTOR-Signalweghemmung mittels Rapamyzin in einem *in vivo* Mausmodell zu untersuchen. Um Auswirkungen auf den Metabolismus zu adressieren, wurden die Studien durch Metabolomics von Nierenkortexgewebe der gleichen experimentellen Gruppen ergänzt.

Männliche und weibliche ROSAmT/mG-NHPS2(podocin)Cre-Mäuse mit spezifischer GFP-Expression auf Podozyten wurden 3 Wochen mit Rapamyzin oder Vehikel behandelt. Metabolische Käfige ermöglichten eine genaue Bestimmung der Nierenfunktionsparameter. Aufgrund des genetischen Mausmodells konnten spezifisch reine Podozytenfraktionen nach Nierenperfusion, Verdauungsschritten und fluoreszenzaktiviertem Zellsortieren isoliert werden. Diese wurden für Sequenzierungen und Proteomics verwendet. Weitere Nieren wurden für histologische Analysen und Metabolomics direkt schockgefroren. qRT-PCR, Westernblots and immunohistologische Färbungen wurden zur Validierung der Omicsstudien und für weitere molekulare Charakterisierungen eingesetzt.

Trotz normaler Nierenfunktion und Nierenmorphologie bei allen experimentellen Gruppen fanden sich bei der RNA-Sequenzierung hochsignifikante Geschlechterunterschiede bei mehr als 1700 mRNA-Transkripten. Veränderungen induziert durch die Stressantwort auf mTOR-Hemmung wiesen ebenso sexuellen Dimorphismus im Transkriptom und Metabolom auf, sowie Signalwegsunterschiede, wie mithilfe von Westernblots gezeigt werden konnte. Gengruppen-Enrichment Analysen deuteten auf Geschlechterunterschiede in angereicherten Genontologien für Transkription, Zytoskelett und Fokale Adhäsionen in männlichen und mitochondrialer Proteine und Translation in weiblichen Podozyten hin. Proteomics wies zusätzlich zu mitochondrialen Proteinen eine Anreicherung von basalen Zellproteinen bei weiblichen Podozyten auf. Rapamyzin beseitigte die signifikanten Geschlechterunterschiede, allerdings eher aufgrund erhöhter Veränderungen bei männlichen Podozyten bei insgesamt stabilerem weiblichen Transkriptom.

Metabolomics bestätigte dieses sex-differente Verhalten in Bezug auf Rapamycinbehandlung. Weibliche Podozyten erschienen stressresistenter und zeigten eine geringere Akkumulation im Aminosäurenpool und von Metaboliten der Glykolyse als männliche Podozyten.

Zusammenfassend konnte in dieser Arbeit erstmals gezeigt werden, dass Podozyten signifikante Unterschiede in der Genregulation und Proteinexpression aufweisen zusammen mit geschlechtsspezifischen metabolischen Stressanpassungen, was entscheidend zu den Geschlechterunterschieden der Entwicklung von Nierenerkrankungen und deren Progress beitragen könnte.

1. Introduction

There is increasing evidence that „cell sex matters“ (1). This has been documented in numerous physiological processes and specific immune responses, disease prevalence, treatments and clinical outcomes in renal neurodegenerative, cardiovascular diseases, cancers, responses to immunotherapeutic agents and transplantation (2-7) . Further research on sex-specific cellular responses has the great potential to design better prevention or treatment strategies in a wide variety of diseases in today`s era of personalized medicine.

1.1 Sex-specific differences in kidney diseases

Beside the brain and the liver, the kidneys display a high degree of sexual dimorphism concerning disease incidence, prevalence and clinical progression. In general, more pre-dialytic men progress faster to end stage renal disease (ESRD) compared to women (Figure 1) and have a higher mortality (8) with polycystic kidney disease (PKD), membranous nephropathy, immunoglobulin A nephropathy, focal segmental glomerulosclerosis (FSGS) and chronic renal disease (CKD) of unknown etiology (2, 9). In addition, male sex is associated with increased ischemia-reperfusion injury and delayed recovery as well as higher susceptibility for nephrotoxin–induced renal injury (10, 11). In contrast, females have a higher prevalence for systemic lupus erythematosus and allograft failure compared to men (7) The sex of the donor organ can lower the risk of allograft failure in women, with female kidneys being more favorable (8). Conflicting data exist regarding diabetic nephropathy (DN) (2, 9, 12).

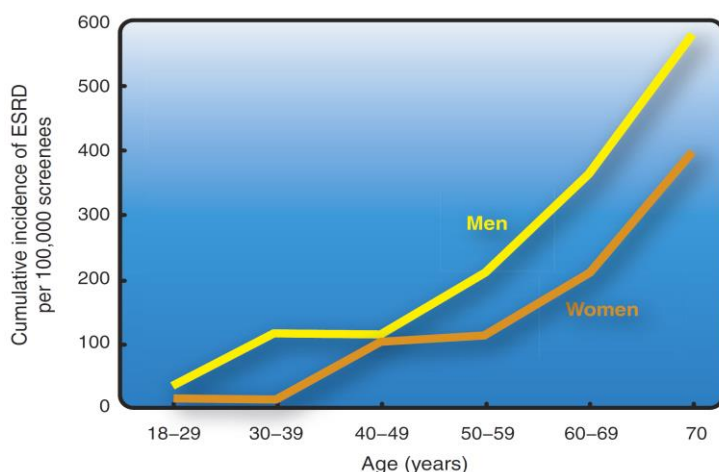


Figure 1. Gender differences in the incidence of ESRD. Reproduced with permission, Copyright Elsevier (13).

The exact mechanisms underlying these differences are still unclear, yet, many factors have been suggested such as sex hormones with protective effects of estrogen and its influences on cellular metabolism as nitric oxygen metabolism and oxidative stress the impact of comorbidities and life style, renal mass or nephron number, systemic or glomerular hemodynamics, cardiovascular diseases and hypertension as a leading cause of CKD (2, 8, 9, 12).

One of the first studies on cellular and molecular sex differences in the kidney has been reported by Yabuki et al. in 1999, demonstrating that proximal tubular epithelium exhibited sexual dimorphism in the structure of the brush border in mouse kidneys (14). Recently, sex differences have been described in renal proximal tubular cell transporters and electrolyte homeostasis (15-17). Still, only few studies have been published investigating the underlying molecular differences between both sexes in the whole kidney and not in isolated cells (18-20).

1.2 Glomerular filtration barrier, podocytes and proteinuria

One major function of the kidneys is the filtration of blood, removal of waste and maintenance of water and electrolyte homeostasis. The ultrafiltration of plasma in the kidney occurs through the capillary wall of the glomerulus which enables the flux of water, cationic molecules, electrolytes and small solutes while retaining plasma proteins and macromolecules based on size and charge selectivity. The filtration barrier in the glomerulus (GFB) is composed of three layers: (i) the fenestrated endothelial cells (ii) glomerular basement membrane (GBM) and (iii) the podocytes (21, 22). Figure 2 illustrates the components of the filtration barrier.

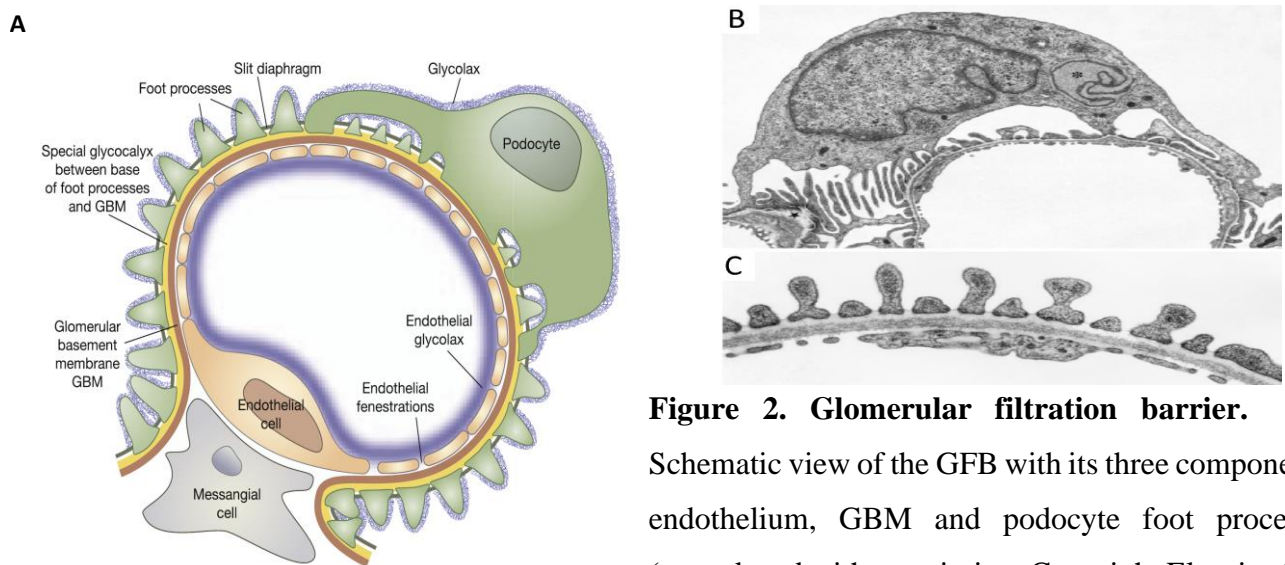


Figure 2. Glomerular filtration barrier. (A) Schematic view of the GFB with its three components: endothelium, GBM and podocyte foot processes (reproduced with permission, Copyright Elsevier (23). (B,C) electron microscope images showing a podocyte cell body which is connected to the capillary wall by its foot processes and the three layers of the GBM (24).

The fenestrated endothelial cells are mainly composed of glycocalyx (proteoglycans and sialoproteins) which impede the leakage of free albumin and other proteins. Any change in the amount or composition would affect their function. Vascular endothelial growth factor (VEGF) is

considered as a major molecule in the cross-talk between endothelial cells and podocytes, and has been linked to proteinuria in many glomerular diseases (22, 25).

Podocytes are attached to the outer membrane of the GBM, which components are synthesized by the glomerular endothelial cells and the podocytes. The essential components are type IV collagen, laminin, proteoglycan-agrin and nidogens (22, 26). The net negative charge of the GBM is a crucial component of the glomerular capillary wall filtration barrier to plasma albumin which is also negatively charged and repelled by the GBM (26). The podocytes are terminally differentiated epithelial cells. They consist of three morphologically and functionally different segments: cell body, major processes and foot processes (FP). Interdigitating slit diaphragm (SD) proteins connect podocytes to each other and constitute a critical layer of the GFB (27). The FP are in contact with three different membranes, the glomerular basal membrane, SD proteins and the apical membrane through different proteins, linkers and by microtubules and microfilaments with actin filaments (22, 26, 28). (Figure 3)

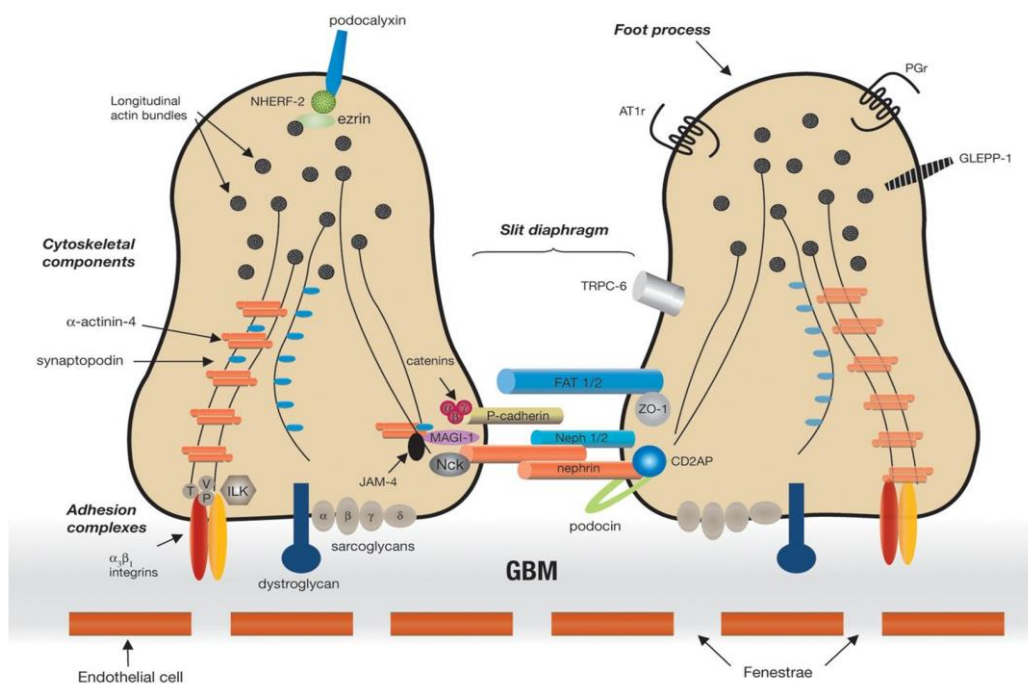


Figure 3. Structure and molecular components of podocytes. (adapted from Michaud J.L and C.R Kenndy, Clin Sci (Lond), reproduced with permission, Copyright Portland Press (29).

Podocytes are anchored to the outer membrane of the GBM via multiple receptors and transmembrane proteins, including Syndecan1/4 (30), $\alpha\beta$ dystroglycan (encoded by *DAG1*), $\alpha\beta$ 1

integrin and tetraspanin CD151. Paxillin, vinculin and talin also connect FBs to the GBM through $\alpha 3\beta 1$ integrin complex at the focal adhesion (22, 30). Integrin-linked kinase (ILK) acts as anchoring protein with integrins at the focal adhesion binding to α -actinin-4 (ACTN4) (30) (Figure 3).

Many proteins are well-known podocyte markers and play a critical role in podocyte function, such as transmembrane proteins nephrin (NPHS1), Neph1, fat-1, P-cadherins and catenins. The intracellular domain of nephrin has been shown to associate with the actin cytoskeleton and to link with adapter proteins such as CD2-associated protein (CD2AP), Nck proteins (22, 26, 30) and ZO-1 (24). In addition to the regulation of the actin cytoskeleton nephrin can induce antiapoptotic signaling (31).

Another SD-associated protein is podocin (NPHS2) which is exclusively expressed in podocytes, localizes at the insertion site of the SD and plays a major role as mechano-sensor, maintenance of the actin cytoskeleton, nephrin-anchor and nephrin-NEH1 induced signaling (22, 27, 30). Podocin expression is regulated by the transcription factor LMX1B (30).

Podocytes' proper function, morphology and structural integrity are highly dependent on the cytoskeletal architecture. Podocytes contain (i) longitudinal actin microfilaments and the meshwork of actin filaments as actin, α -actinin-4 and myosin (ii) Vimentin-rich intermediate filaments and (iii) microtubules as α -tubulin and β -tubulin. The function of the cytoskeleton is regulated through the small GTPases mainly RhoA, Rac1 and Cdc42 (30, 32) and Rhoophilin-1(33).

α -actinin-4 is enriched in FP, crosslinks actin filaments and acts as scaffold of protein complexes. α -actinin-4 is regulated by synaptopodin, a proline-rich-actin associated proteins, a key organizer for the actin cytoskeleton (30) and an upstream regulator of RhoA (32).

Other actin-associated proteins involve TRPC6, cortactin, cofilin (32) myosin (myosin II and 1E, Hsp27, palladin, ZO-1, podocalyxin (an anionic glycoalyx transmembrane protein covering the podocyte surface, and linking to the actin cytoskeleton through ezrin and inverted formin 2 (IFN2) (34) and the podocyte foot processes proteins Schip1 and Pdlim2 (35, 36). Recently, SRGAP2a which colocalizes with synaptopodin, has been attributed an important role in podocyte structure and motility. Knockdown causes suppressed podocyte motility through inactivation of RhoA and Cdc42 but not Rac1 (37).

The importance of the podocyte in the development of proteinuria has been emerged from the discoveries of many mutations in genes encoding podocyte proteins or GBM such as podocin, nephrin, collagen, ACTN4 and others (21, 22, 25, 27, 30).

1.3 Podocyte homeostasis and injury

Whereas genetic studies have contributed essentially to the understanding of podocyte biology and function, genetic defects account for only a minority of glomerular diseases. Podocyte structure and function are determined and maintained through a complex interaction between different proteins, organization of the actin and microtubule cytoskeleton, and factors and signaling pathways between the GBM, FP and SD.

Due to their unique structure, components and interaction with other glomerulus cells, podocytes are sensitive to toxins, antibodies, mechanical and oxidative stress, immune-complexes, cytokines and complement activation which occurs in many glomerular diseases, (24, 38), high levels of TGF- β (24), hyperglycemia, dyslipidemia (39) and many other factors. Any physiological or pathological interference or changes in podocytes intracellular junctions, SD structure and complexes, GBM structure and the podocyte–GBM interaction, dysfunction of the actin cytoskeleton, apical membrane domain or associated proteins, disturbances in the transcriptional regulation, pathways and factors regulating podocyte function, can contribute to the pathogenesis of podocytes, podocytopenia and proteinuria (40, 41).

Mitochondrial dysfunction or genetic mutation also has been associated with podocyopathies, examples are; Mpv17, GRP78, PGC-1 α genes (42-46). Other intracellular events which are involved in the progression of podocyte injury and glomerular diseases include endoplasmic reticulum (ER) stress, production of ROS and proteases, all influencing homeostasis and causing podocyte injury,

Heat shock proteins (HSPs) mediate a diverse range of cellular functions, prominently including folding and regulatory processes of cellular repair and are also regulated by ROS. Hsp90, Hsp25/27, Hsp70 are one of the main regulated chaperone-like proteins in podocytes injury, as well as Hsp27 which is involved in actin cytoskeletal regulation (47). Moreover, HSPB1 has been found to be expressed in podocytes and controls a wide range of biological activities, including actin stabilization and protection from stress and apoptosis. It is upregulated in ER stress as a protective mechanism (48).

Additionally, the unfolded protein response (UPR) is part of the proteostasis and has been reported to affect pathogenesis in CKD and podocytes (42). In the ER the pathway is activated to restore ER homeostasis (till certain limit) through the action of inositol-requiring protein 1 (IRE1), activating transcription factor 6 (ATF6) and PKR-like ER kinase (PERK), transmembrane sensors, which are usually bound to the ER chaperon GRP78. During stress GRP78 dissociates,

binds to the unfolded proteins, releases the transducers and causes a sequence of transcriptional factor changes and upregulation of XBP1, ATF4, REA1 and CHOP. However, excessive activation induces apoptosis of the cells.

The majority of intracellular proteins are degraded by the ubiquitin-proteasome system (UPS) which consists of enzymes, which ubiquitinate or deubiquitinate target proteins, and the 26S proteasome system. It has been recently shown that the UPS system is upregulated by persistent glomerular injury in such as minimal change disease, FSGS, and DN(49).

Finally, miRNA play a role in podocyte homeostasis and podocytopathies. Dicer is the enzyme responsible for miRNA generation. In dicer-mutation specific to podocyte mouse model mice developed proteinuria 4 to 5 weeks after birth and died several weeks later showing structural glomerular defects (50).

1.4 Podocyte stress responses

Podocytes are able to adapt to stressful conditions in order to maintain their function upon encountering different stimuli. As part of their adaptation response, they hypertrophy and alter their molecular composition by up-regulation of many proteins such as metallothionein, intermediate filaments and by reorganization of FP structures. These early events occur without visible changes in morphology or function. However, when podocytes exceed their intrinsic capacity to encounter prolonged and/or severe injury foot process effacement, detachment, and cell death (through apoptosis or necrosis) occur finally leading to podocyte loss. In addition, cytoskeleton disorganization and endothelial cell responses with activation of the coagulation cascade, chemokine receptor expression, adhesion molecule abnormalities and lipid peroxidation occur (38), the GBM is no longer intact and proteinuria occurs (21, 25).

Subsequent anatomic events resulting from podocyte injury include mesangial expansion, the appearance of denuded areas of the GBM, synechia formation (adhesion to Bowman's capsule), focal and global glomerulosclerosis further contributing to interstitial injury and fibrosis. It has been postulated that these changes start with more than 20 % of podocyte loss (28) and ultimately lead to glomerulosclerosis and end-stage renal failure (40).

1.5 mTOR and its role in podocytes and the kidney

According to current knowledge, the mechanistic target of rapamycin (mTOR) signaling network emerges as a key pathway controlling renal epithelial cells and regulating a variety of renal epithelial processes ranging from podocyte size control, regenerative capacity of proximal tubular cells in acute kidney injury, water and salt transport balance in the collecting ducts , as well as regulating endocytosis and nutrient transport in proximal tubular cells and renal immune cells and vascular endothelial cell homeostasis (51-54).

mTOR is a 289-kDa serine/threonine kinase, a member of the phosphatidylinositol 3-kinase-related kinase (PIKK) family of protein kinases (PI3K-related kinase) that forms the catalytic subunit of two structurally and functionally distinct complexes, mTOR complex 1 (mTORC1) and 2 (mTORC2) (55-59). In mTORC1, mTOR is associated with regulatory-associated protein of mTOR (raptor) - which is fundamental for the assembly and stability and acts as a scaffold and recruitment for specific mTORC1 substrates such as S6K1 and 4EBP1. mTORC2 is defined by the rapamycin insensitive component rictor, mSIN (mammalian stress-activated protein kinase interaction protein 1) and Protor-1/2. Like raptor within mTORC1, rictor acts as a scaffold protein and facilitates both, the assembly of mTORC2 and the interaction of mTORC2 with its substrates AKT, PKC, SGK1 and regulators. mTORC1 and mTORC2 have different sensitivities to rapamycin and are implicated in divergent physiological functions such as glucose homeostasis, immune responses, cardiac homeostasis, aging and health span, muscle mass and function, immune function, adipocyte function and lipid metabolism, and pathological conditions such as cancer, cardiac and kidney diseases, obesity, type 2 diabetes, epilepsy, chronic neurodegenerative disorders (56, 57, 59-64) . Figure 4 gives an overview of the signaling of the two mTOR complexes and the various cellular functions.

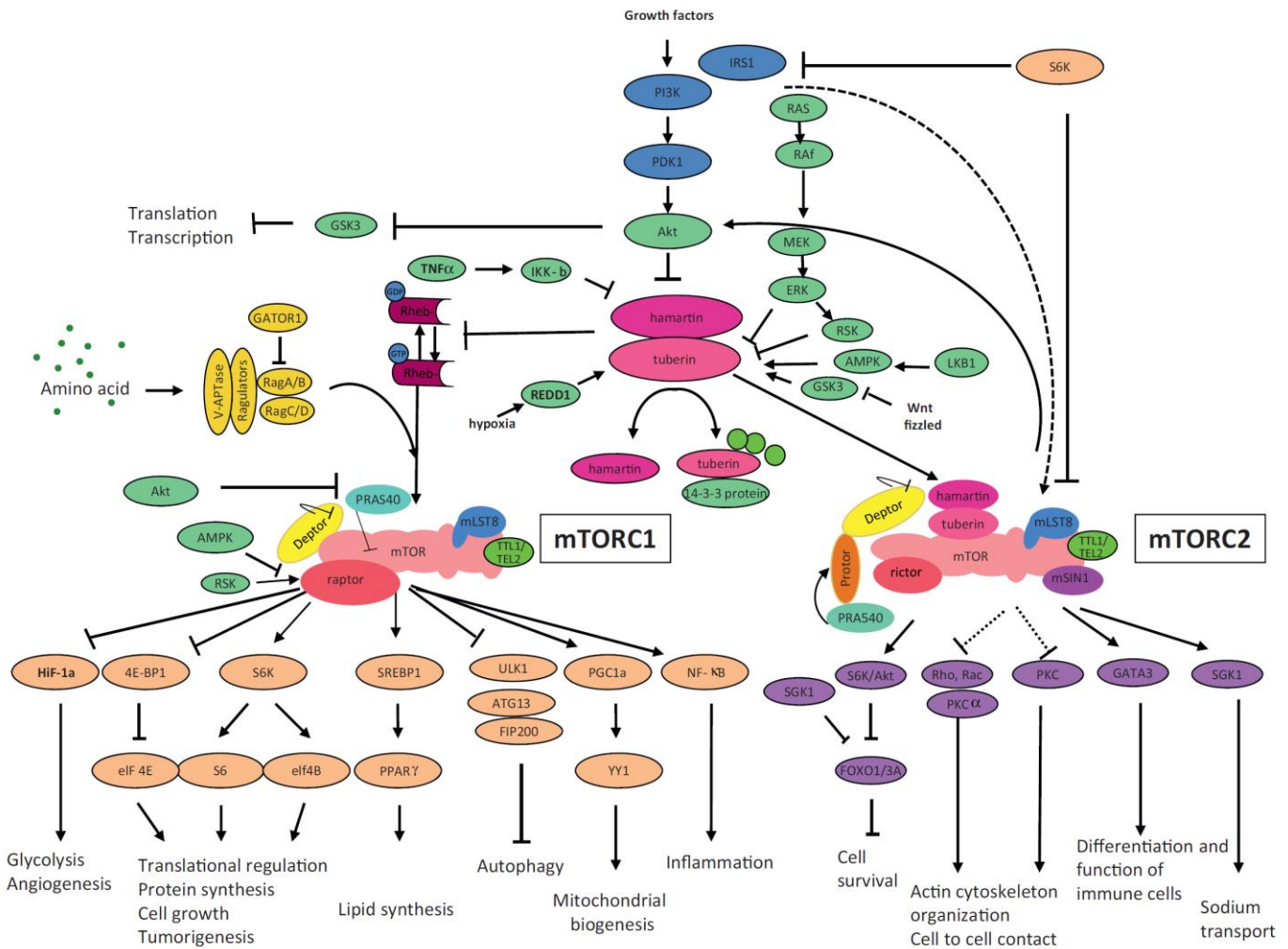


Figure 4. mTOR signaling pathway. mTORC1 controls protein synthesis mainly via S6K, mitochondrial biogenesis via PGC1 α and autophagy, while mTORC2 regulates cell survival and actin cytoskeleton. Reproduced with permission, Copyright Elsevier (59).

The development of different transgenic mouse models gave insight into the importance of the mTOR pathway in the podocyte and kidney physiology and pathology, either by the activation or inhibition of mTORC1 and mTORC2 activity (65, 66) and has proven the necessity of balanced mTORC activities to maintain podocyte homeostasis (65, 67, 68).

Extensive evidence has indicated the importance of mTOR signaling pathway in both control of podocyte function and in podocyte injury (69) and any alteration in mTOR activity can lead to different changes including glomerular basement membrane thickness, podocyte loss, mesangial expansion, glomerular hypertrophy, cyst formation and albuminuria, as resulted in many kidney disease such as DN, PKD, inherited hamartoma syndromes (55) and such changes could be

delayed and/or reversed by mTORC1 inhibition with rapamycin or everolimus as in FSGS and membranous nephropathy, minimal change and other glomerular diseases (67, 68).

The fundamental impact of mTORCs in the kidney has been further underlined by the study of Gödel et al., in which a double knockout of raptor and rictor resulted in dramatic renal failure and rapid death. Raptor knockout at early stage caused more podocyte injury and progressive glomerulosclerosis and foot process broadening and effacement compared to mTORC2 ablation (65). Yet not only loss of mTOR signaling is detrimental for the kidney, but also increased activation of the mTORCs. High mTORC1 activity has been shown to cause a mis-localization of nephrin (66), suppress autophagy and induce endoplasmic reticulum ER stress (55, 67). Furthermore, increased mTORC1 activity caused irreversible structural changes and podocyte hypertrophy in early stages of DN (70). In such contexts of experimental DN (66) and nutritional overload (71), mTOR inhibition has been found to protect against podocyte damage.

mTOR is also involved in epithelial-to-mesenchymal transition (EMT). Several studies have shown that rapamycin inhibits EMT in animal models with different forms of CKD (72) by inhibition of Rheb/mTORC1 signaling that has been found to be activated in myofibroblasts, activated kidney fibroblasts and interstitial fibrosis (73). Inhibition of mTOR by rapamycin in CKD has furthermore been shown to ameliorate the glomerular changes, the interstitial inflammation, fibrosis, and loss of renal function associated with CKD and moreover, a reduction in glomerular hypertrophy, decreased expression of proinflammatory and profibrotic cytokines, less infiltration of the interstitium by inflammatory cells, and renal fibrosis (72).

Additional in vitro data have shown the involvement of mTORC2 in renal tubular Na⁺ balance regulation (74). Numerous studies point towards an essential role for mTORC2-AKT signalling for podocyte function, organization and maintenance (75-77). Canaud et al. showed that AKT2 - an isoform expressed mainly in podocytes - is essential for podocyte protection and survival and the reduction of AKT2 levels caused foot process effacement in the mouse model. mTOR inhibition by rapamycin decreased AKT2 phosphorylation leading to albuminuria in kidney transplant patients which was accompanied with increased glomerular apoptosis (75), reviewed in (70). In another study, AKT2 was found to control dephosphorylation of p130Cas by TGFβ1 leading to podocyte hypertrophy and matrix protein accumulation (76).

mTORC2 controls proliferation and survival primarily by activation of several members of the AGC subfamily of kinases including protein kinase C (PKC) α , PKC δ , PKC γ , PKC ϵ which regulate various aspects of cytoskeletal remodeling, cell migration (57, 58, 78) and cell polarity (79) by the activation of Rho and Rac1, two G proteins and major regulators of the cytoskeleton. PKC α also phosphorylates paxillin and induces its localization to focal adhesions (78, 79). mTORC2 is responsible for the activation of serum and glucocorticoid-induced protein kinase 1 (SGK1), a kinase which controls ion transport and stimulates sodium reabsorption in the distal nephron by increasing the activity of the aldosterone- regulated epithelial sodium channel (ENaC) (58, 78, 79).

1.6 Rapamycin - mechanism of action, clinical use and adverse effects

In 1999, rapamycin was the first pharmacological agent of mTORC1 inhibitors to be approved by the FDA to prevent graft rejection in kidney transplant patients. Since then, it has been widely used as immunosuppressant after transplantation. Other rapamycin analogs have been approved later, including temsirolimus for advanced renal cell carcinoma, everolimus for the prevention of solid organ transplant rejection and treatment of breast, renal and neuroendocrine tumors. (80) zotarolimus and ridaforolimus (57). In addition to its use as an immunosuppressant, rapamycin is employed in drug eluting stents in coronary artery diseases, graft versus host disease, rheumatoid arthritis, and several neurological disorders (57).

Upon entering the cell, rapamycin interacts with a 12 kDa protein named FK506-binding protein (FKBP) 12. The resulting FKBP12-rapamycin (FRB) complex inhibits mTORC1 signaling by interfering with the association of mTOR and Raptor and subsequently down-regulates mTORC1 activity (57, 80). However, not all downstream targets are inhibited, such as 4E-BP1 and ULK1, which are involved in protein translation and autophagy (57).

Free rapamycin is capable of binding to and inhibiting mTORC1, but the affinity of this interaction is increased by approximately three orders of magnitude in the presence of FKBP12. Hence, the FKBP12-rapalog complex functions as an allosteric inhibitor of the mTOR catalytic domain, which may explain observations that this complex is a potent but partial antagonist of mTORC1-dependent responses in mammalian cells (81).

In contrast, the FRB domain of mTOR within mTORC2 is not exposed, so that mTORC2 cannot be inhibited by rapamycin binding comparably to mTORC1. Yet, prolonged rapamycin exposure

can lead to decreased mTOR expression, thereby reducing the formation of mTORC2 with decreased activation of AKT (57, 79, 82).

In 2003, rapamycin was reported for the first time to cause proteinuria in renal transplant recipients after conversion from calcineurin inhibitors to rapamycin (83). Since then, multiple studies have documented proteinuria after liver, kidney, pancreatic and heart transplantation (84-87). In addition to low molecular weight proteinuria, it has been reported that patients may develop phosphaturia, hypokalemia and reduced megalin expression under sirolimus (SRL) therapy. Yet, there is evidence that not all transplanted patients who converted to an SRL-based regimen experienced worsening of kidney function, some reported no change or even improved function.

The role of rapamycin in podocyte integrity and function has been further investigated in both animal models and human podocyte cells. In human podocytes, prolonged rapamycin treatment (120 hours) caused a reduction of several mTOR signaling pathway components and decreased expression of slit diaphragm proteins including nephrin, TRPC6 and Nck. Functionally, rapamycin impaired the migration and adhesion of podocytes with a slight increase in apoptosis (88). However, shorter rapamycin treatment for 48 hours, led to only reduced WT1, phosphorylated AKT and VEGF (which control podocin/CD2AP interaction) levels (89). High doses of SRL induced a permanent alteration of the SD and the cytoskeleton with a reduction in nephrin, podocin, CD2ap, and derangement of stress fibers (90). The reduction in podocyte nephrin expression was not related to the extent of proteinuria in transplanted patients (91). In addition, a study in C57Bl/6 mice showed that the reduction in podocyte-related proteins (WT1, synaptopodin, nephrin, Cd2AP and podocin) and fibrosis-related TGF beta was not enough to induce proteinuria after rapamycin treatment for 24 days with 3 different doses (92).

So far, the impact of sex on the highly variable levels of proteinuria development in transplant patients has not been investigated yet.

1.7 Scope of the thesis, hypothesis and objectives

Despite recent advances in our understanding of podocyte biology, sexual dimorphism of podocytes has never been investigated in physiological or disease models and the progression to CKD, as well as responses to treatments and adverse effects remain elusive. Several groups worldwide have been focusing on the mechanism by which mTOR influence podocyte homeostasis and pathological response resulting in podocyte FP effacement and proteinuria, still there is lack of research including sex as a variable and the examination of underlying cause in research designs and reporting. In addition, many studies are conducted on males or mixed sexes without always indicating the sex or the failure to include adequate numbers of males and females to allow for sex- and gender-based analyses.

A large body of evidence demonstrates sex differences in protein filtration in a large variety of kidney diseases and ischemic injury (20, 93, 94). However why some kidney transplant patients treated with mTOR inhibitors develop proteinuria and the majority of recipients of other solid organs improve their kidney function remains a conundrum. Sexual dimorphism of podocyte genes and protein expressions might contribute to understand these differences in addition to sex-specific glomerular disease susceptibilities and clinical courses.

Aim of this thesis was therefore to test the hypothesis that podocytes have sexual dimorphic gene expression which further leads to different stress responses towards mTOR inhibition, thereby influencing transcriptional regulation and cellular homeostasis of podocytes in a sex-specific manner.

To address this question, a genetic mouse model, ROSAmT/mG-NHPS2(podocin) Cre mice with membrane targeted GFP restricted to podocytes, was used which allowed specific isolation and molecular analyses of podocytes by FACS sorting from male and female mice. As a stress model, mTOR inhibition with rapamycin was induced *in vivo* for three weeks prior to analyses.

The study had the following objectives:

1. to investigate intrinsic sexual dimorphism on genomic and protein levels of podocytes from vehicle treated male and female mice by RNA sequencing (RNA-seq) and proteomics

2. to study sexual dimorphic responses to mTOR inhibition on transcriptional regulation and podocyte homeostasis in podocytes from male and female mice after 3 weeks of rapamycin treatment
3. to study mTOR-related signaling pathway activations and functional consequences of the stress response induced by mTOR inhibition in renal cortex tissue from male and female mice by western blots and immunohistochemistry
4. to identify sex-specific responses to stress in energy-providing metabolic pathways from renal cortex tissue from male and female vehicle and rapamycin-treated mice by metabolomics.

Understanding the sex-specific transcriptional, translational and metabolic regulation of decisive key factors for podocyte homeostasis and stress responses could provide a deeper knowledge for tailoring targeted-individualized mTOR inhibitor therapies and glomerular diseases at the podocyte molecular level.

2. MATERIAL AND METHODS

2.1 Materials

2.1.1 Chemical substances, buffer and gel recipes and kits

Table 1. Chemicals and Solutions	Manufacturer
Acrylamide (37.5:1) Rotiphorese® Gel 30	Carl Roth
Agarose	Serva
Albumin Fraction V, BSA	Carl Roth
Ammonium persulfate (APS)	Sigma-Aldrich
BICIN	Carl Roth
Bis-Tris	AppliChem
Diethylpyro-carbonate (DEPC)	Sigma-Aldrich
Dimethyl sulphoxide (DMSO)	Sigma-Aldrich
dNTPs	Promega
dNTP Mix	Applied Biosystems
Dithiothreitol (DTT)	Sigma-Aldrich
Dulbecco's Phosphate Buffered Saline (PBS)	Biochrom
Ethylenediaminetetra-acetic acid (EDTA)	Carl Roth
Ethanol 99.8%	Carl Roth
Glycerin	Carl Roth
β-Glycerophosphate disodium salt hydrate	AppliChem
Hydrochloric acid (37%)	Carl Roth
Isol-RNA Lysis Reagent	5Prime
Methanol	Carl Roth
MOPS	AppliChem
M-MuLV Reverse Transcriptase	BioLabs
Nonfat dried milk powder	AppliChem
NaF (Sodium Fluoride)	AppliChem
N-lauroyl-Sarkosine	Sigma-Aldrich
3-(N-morpholino)-propanesulfonic acid (MOPS)	AppliChem
2-Propanol	Carl Roth
Protease Inhibitor Tablets, Complete Mini	Roche Applied Science

Ponceau S	Carl Roth
RNase Inhibitor	Applied Biosystems
Sodium azide	Sigma-Aldrich
Sodium chloride	Carl Roth
Sodium hydroxide	Sigma-Aldrich
Sodium pyrophosphate	AppliChem
Sodium dodecyl sulfate (SDS) Pellets	Carl Roth
SuperSignal West Pico	Thermo Scientific
SuperSignal West Dura	Thermo Scientific
WesternBright Sirius	Advansta
Tetramethylethyldiamin (TEMED)	Sigma-Aldrich
Tris	Carl Roth
Tween®20	Carl Roth
Tris-HCl	Sigma-Aldrich
Triton X-100	Sigma
Trizol	Invitrogen
Xylol	Sigma-Aldrich
Paraformaldehyde	Bio-rad
Coomassie stain	Bio-rad
3-Amino-9-Ethylcarbazole AEC chromogen	Agilent
O.C.T compound	Tissue-Tek
SYBER green	Sigma-Aldrich

Table 2. Buffer recipes

Buffer	Reagent	Final Conc.
Blocking buffer	Nonfat dried milk powder	5% m/v
	ad 1x TBS-T	
BICIN transfer buffer 1x	BICIN	25 mM
	Bis-Tris	25 mM
	EDTA, pH 8.0	1 mM
	Ethanol	10-15% v/v
Gel buffer 3.5x, pH 6.5-6.8	Bis-Tris	1.25 M

Glycin stripping buffer, pH 2.0	Glycin	25 mM
	SDS	1% m/v
Laemmli buffer 5x	Tris-HCl, pH 7.5	250 mM
	DTT	500 mM
	Glycerol	30% v/v
	SDS	5% m/v
	Bromphenol blue	0.25% m/v
MOPS running buffer 1x, pH 7.7	MOPS	50 mM
	Tris	50 mM
	EDTA, pH 8.0	1 mM
	SDS	0.1% m/v
PBS (Ca²⁺ - /Mg²⁺ -free), pH 7.3	NaCl	137 mM
	KCl	2.7 mM
	Na ₂ HPO ₄	9 mM
	KH ₂ PO ₄	2.3 mM
TBE buffer 1x, pH 8.0	Tris	89 mM
	Boric acid	89 mM
	EDTA	2 mM
TBS-T buffer 1x, pH 7.6-8.0	Tris	50 mM
	NaCl	150 mM
	Tween 20	0.1% v/v
TE buffer 1x pH.9	Tris-base	10 mM
	EDTA	1mM
	Tween 20	0.05% v/v
RIPA lysis buffer	Tris-HCl, pH 8.0	
	SDS	10% v/v
	β-Glycerolphosphat	10% v/v
	NaF	10% v/v
	Na ₃ VO ₄	5% v/v
	Sodium pyrophosphate	40% v/v
Citrate buffer pH 6	Citric acid (anhydrous)	10mM
	Tween 20	0.05% v/v

HBSS 10X pH 7.4	KCl	5.4mM
	Na ₂ HPO ₄ x 7H ₂ O	0.3mM
	KH ₂ PO ₄	0.4mM
	NaHCO ₃	4.2mM
	NaCl	137mM
	D-Glucose	5.6mM
	CaCl ₂ x 2H ₂ O	1.3mM
	MgCl ₂ x 6H ₂ O	0.5mM
	MgSO ₄ x 7H ₂ O	0.6mM
PFA 4%	HCl (1M)	0.1mM
	NaOH (1 M)	0.1mM
	Paraformaldehyde powder	4% v/v
	PBS pH.7.4	

Table 3. MOPS-BICIN gel formulation

Running gel	8.5%	10%	12.5%	15%	Stacking gel 6%
H2O	3.63	3.19	2.53	1.76	1.25
30% AA mix	2.53	2.97	3.63	4.4	500
3.5X gel buffer	2.53	2.53	2.53	2.53	750
10% APS	110	110	110	110	37.5
TEMED	11	11	11	11	6.25

30% AA mix: De-gased 30-acrylamid-stock-solution with 0.8% Bis-acrylamid (37.5:1)

Table 4. Kits

	Manufacturer
DC™ Protein Assay	Bio-Rad
FastStart Universal SYBR Green Master (Rox)	Roche
TaKaRa kit	Takara bio

2.1.2 Primers

Table 5 . Primers used for qPCR

Sequences Gene	Forward primer (5' 3')	Reverse primer (5' 3')
Arhgap32	TCCGACCTAGAAGACCCAGA	AGTCAACATCCTCAGCCGAA
Bhlhe40	TATCTCATCCCACCATCGGC	GCCAAAGGAGAAGGGAGTCT
Cd151	TACCTAGCCACGGCCTACAT	GCAATGATCTCCAGGAGGAA
Cox7a2	GACCATCAGCACCACCTCAC	CTTCTTGGGAAATGCAGCCA
Ctstl	TGTAGCAGCAAGAACCTCGA	TGTCCCGGTCTTTGGCTATT
Daam2	AAGCTGCCAAAGTCAACCTG	TCCTGCTCTCCGAAATGTGT
Hdgf	ACTCCCCTAAACGTCCCAAG	TCTCATGATCTCTGACGCC
Podocin (Nphs2)	GTGTCCAAAGCCATCCAGTT	GGAAGCTGAGGCACAAAGAC
RP113	CCCTCCACCCTATGACAAG	TTCTCCTCCAGAGTGGCTGT
Slc6a6	AAAATGGTGGAGGTGCGTTC	ACACAATGACGATGGATGCG
Tjp1	CAACAGGTACAGGCCAGAGG	CAGAGGAGGGACAACACTGCAG
Ywhaz	TCTGGCCCTCAACTTCTCTG	CCTGCTTCTGCTTCATCTCC

2.1.3 Antibodies

Table 6. Antibodies used for immunohistochemistry

Antibodies	origin	Dilution	Manufacturer
Collagen type 1	Rabbit	1:200	Abcam 34710
WT1	Rabbit	1:100	Abcam 89901
Phalloidin-iFluor 647		1:100	Abcam176759

Antibodies	origin	Dilution	Manufacturer
Phospho-P70 Thr389	Rabbit	1:1000	RD AF8963
P70	Rabbit	1:3000	RD AF8962
Phospho-mTOR Ser2448	Rabbit	1:1000	Cell signaling 5536
mTOR	Rabbit	1:1000	Cell signaling 2972
P62 (SQSTM1)	Rabbit	1:1000	Cell signaling
Phospho-4EBP1 Ser65	Rabbit	1:1000	Cell signaling 9451
4EBP1	Rabbit	1:1000	Cell signaling 9452S
Rictor	Rabbit	1:1000	Cell signaling 9476
Raptor	Rabbit	1:600	Cell signaling 2280
Phospho-AKT Ser473	Rabbit	1:1000	Cell signaling 4060S
Phospho-AKT Thr308	Rabbit	1:1000	Cell signaling 2965S
AKT	Rabbit	1:1000	Cell signaling 9272
LC3B	Rabbit	1:1000	Novus NB100-2220
Phospho-ERK1/2(pp42/44)	Rabbit	1:1000	Cell signaling 9106
ERK(p42/44 MAPK)	Rabbit	1:1000	Cell signaling 9102
Phospho-AMPK α 1/2 (Thr 172)	Rabbit	1:500	Santa cruz 33524
AMPK	Rabbit	1:1000	Santa cruz 2532
Anti-GAPDH, monoclonal	Mouse	1:5000	Hytest 5G4
Wilms Tumor -1 (WT1)	Rabbit	1:750	Abcam 89901
Integrin β 1	mouse	1:1000	BD bioscience 610467
Phospho-paxillin Tyr118	rabbit	1:1000	Cell signaling 2541
Phospho -myocin light chain-2 Ser19	mouse	1:1000	Cell signaling 3675
Talin-1	rabbit	1:1000	Abcam 71333
Vimentin	mouse	1:1000	Santa cruz (E-5) 373717
Collagen IV	rabbit	1:1000	Abcam 6586
Podocin	rabbit	1:750	Abcam50339
Claudin-1	mouse	1:1000	Santa cruz (A-9)166338
β -actin	mouse	1:5000	Sigma A5441
α -tubulin	mouse	1:6000	SigmaT9026
Laminin β 2	mouse	1:1000	Santa cruz (C4) 59980

α -Actinin 4 (ACTN4)	Rabbit	1:1000	Abcam 59468
Nephrin	Rabbit	1:1000	Abcam 58968
COQ2	Rabbit	1:1000	Abcam 89706
OXPPOS	Rabbit	-	Abcam 110413
Synaptopodin	mouse	1:1000	Santa cruz (D-9) 515842
ATP5b	mouse	1:1000	Santa cruz (E-1)- 55597
ZO-1	Rabbit	1:1000	Invitrogen 61-7300
SDHB	mouse	1:1000	Santa cruz (G-10) 271548
UQCRC2	mouse	1:1000	Santa cruz 390378
Rho-GTPases kit	Rabbit	1:1000	Cell signaling kit 9968
Caspase3	Rabbit	1:1000	Cell Signaling 9665
Bcl2	mouse	1:1000	Santa cruz (C-2) 7387
Collagen IV	rabbit	1:1000	Abcam6586
PRAS40	Rabbit	1:1000	Cell signaling 2691
Secondary antibodies			
Peroxidase-conjugated AffiniPure Donkey Anti-Mouse IgG		1:20000	Dianova
Peroxidase-conjugated AffiniPure Donkey Anti-Rabbit IgG		1:15000	Dianova

2.1.4 Equipment

Equipment	Manufacturer
Applied Biosystems® StepOnePlus Real-Time PCR System	Thermo Fisher Scientific
Shandon Excelsior ES® A78410120 issue 3	Thermo Fisher Scientific
Microtome HM 355 S	Microm- Thermo Fisher Scientific
Cryostar NX70 387928 issue7	Thermo Fisher Scientific
Gel documentation system, Syngene G:BOX Chemi XRQ	VWR
UV-transilluminator Gene Flash	SYNGENE
HistoStar™ A810101000	Thermo Fisher Scientific
fluorescence microscope	Zeiss

2.2 Methods

2.2.1 Animal model and genotyping

12-18 weeks old male and female homozygous ROSAmT/mG-NHPS2 (podocin) Cre mice - a cell membrane-targeted carrying double fluorescent and expressing Cre recombinase under the NHPS2 (podocin) promoter - were a generous gift of T.B. Huber (University of Freiburg, Germany) and were used in this project. This genetic modification allows specific separation of green fluorescent protein (GFP)-positive podocytes from the GFP-negative non-podocyte glomerular fraction by fluorescence-activated cell sorting (FACS) (95). Breeding was performed according to standard procedures. All animals were kept under specific pathogen free (SPF) environment with a standard 12:12 h light-dark cycle and had ad libitum access to water and standard chow throughout the entire experiments. All animal experiments were conducted in accordance to the animal welfare guidelines of the Charité Universitätsmedizin Berlin and were approved by the local authorities (LaGeSo, G0241/15 Berlin, Germany).

For genotyping, genomic DNA was extracted from tail biopsies (≤ 3 millimeter (mm)) for Cre-genotypic confirmation. Biopsies were boiled at 95 °C for 8 minutes in a 20 μ L mixture volume of 20 μ l F-132 extraction buffer and 0,25 μ l DNA release additive (1X). Samples were cooled down and centrifuged for few seconds before storage at 4⁰ C for genotyping.

DNA was amplified with Cre-specific primers (Forward primer: CGTACTGACGGTGGGAGAA, Reverse primer: CCCGGCAAACAGGTAGTT) for polymerase chain reactions (PCR)-based genotyping using TaKaRa kit according to manufacturer protocol, with annealing at 57° C for 1.20 minutes. Additionally, mice were tested for mT/mG, DNA was amplified with Tomato specific primers (Forward primer: CTCTGCTGCCTCCTGGCTTCT), (reverse -wild type CGAGGCGGATCACAAGCAATA , reverse -mutant type TCAATGGGCGGGGTCGTT). The PCR products were separated in 1% agarose gel in TBE buffer at 85 voltage (V) for 45 min and visualized under UV light after staining with GelRed™ (Biotium). (Figure 5)

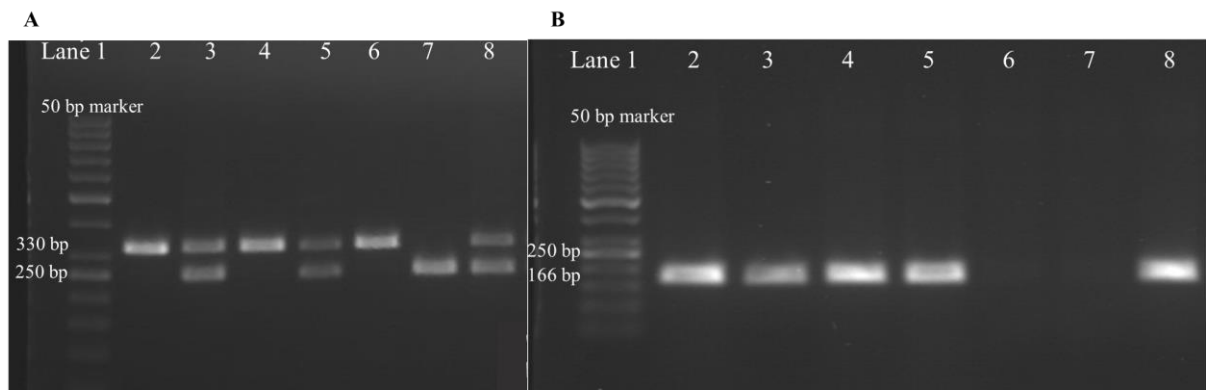


Figure 5. Representative agarose gel for the genotyping for Tomato and Cre recombinase PCR. (A) a DNA size marker was applied to the first lane, PCR product of 330 bp long fragment (2,4) indicates Tomato wild type and product of 250bp (lane 7) indicate mutant for Tomato, only mutant mice were used for further breeding. (B) presence of the PCR product of 166 bp long fragment (lane 2-5,8) indicate Cre positive ROSAmT/mG-NHPS2 and were used for further podocyte isolation. Mice tested negative for Cre recombinase were used for staining, protein analysis and metabolomics.

2.2.2 Experimental design

Mice were divided into four experimental groups:

1. Male ROSAmT/mG-NHPS2 Cre mice with vehicle treatment
2. Male ROSAmT/mG-NHPS2 Cre mice with rapamycin treatment
3. Female ROSAmT/mG-NHPS2 Cre mice with vehicle treatment
4. Female ROSAmT/mG-NHPS2 Cre mice with rapamycin treatment

Rapamycin was injected into the peritoneal cavity at a concentration of 1.5 mg/kg body weight or vehicle (DMSO) every third day during the experimental period of 3 weeks. Effective drug delivery was confirmed by measuring trough level from EDTA blood samples 24h after the last injection (trough concentration 19 -25 ng/ml). One day before the end of the 3 weeks of treatment, all mice were transferred into metabolic cages for urine collection for 24 h. Then, mice were either perfused and treated as described below for podocyte isolation or directly sacrificed by exsanguination after sedation by intra-peritoneal ketamine injection (10mg/kg). Blood, urine, and kidney tissue samples were collected. (Figure 6)

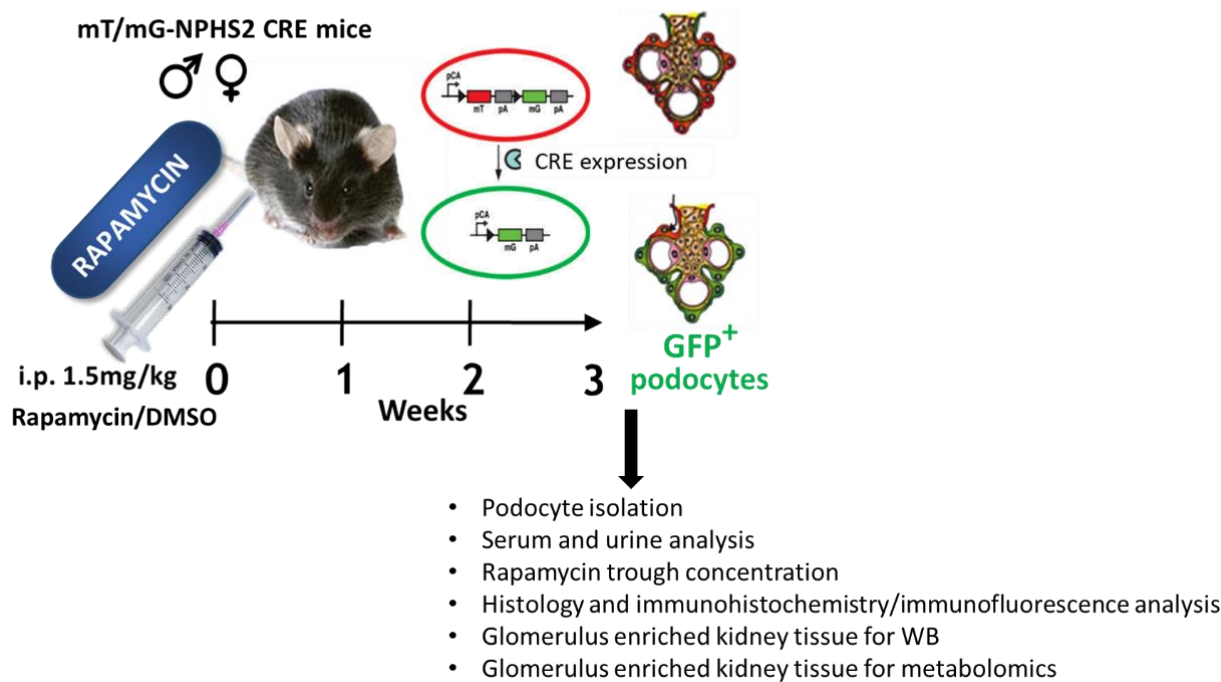


Figure 6. Schematic presentation of the experimental design.

Renal tissues designated for histology or western blot were washed with normal saline (0.9% NaCl), cut into four pieces, and then were either immediately (i) fixed in 4% paraformaldehyde for paraffin embedding (ii) embedded in O.C.T for cyro-sectioning or (iii) snap frozen in liquid nitrogen and stored at -80°C for subsequent mRNA or protein extraction. Table 8 indicates the number of mice used per experimental group to allow the use of diverse analytical methods.

Table 8. Number of mice from different experimental groups analyzed by indicated methods

Experiment	male vehicle	male rapamycin	female vehicle	female rapamycin
RNA-seq	5-10	5-10	4-10	5-10
Proteomics	6	6	6	6
Histology	6-8	6-8	6-8	6-8
IHC, IF	6	6	6	6
qPCR, Western blot	10	10	10	10
Metabolomics	6-10	6-10	6-10	6-10

2.2.3 Glomeruli and podocyte isolation

To obtain pure podocyte fractions for later molecular analyses, a specific method had been recently established in the lab. Renal perfusion and digestion steps were performed by two postdocs of Dragun's lab. FACS sorting and analyses were part of this thesis work.

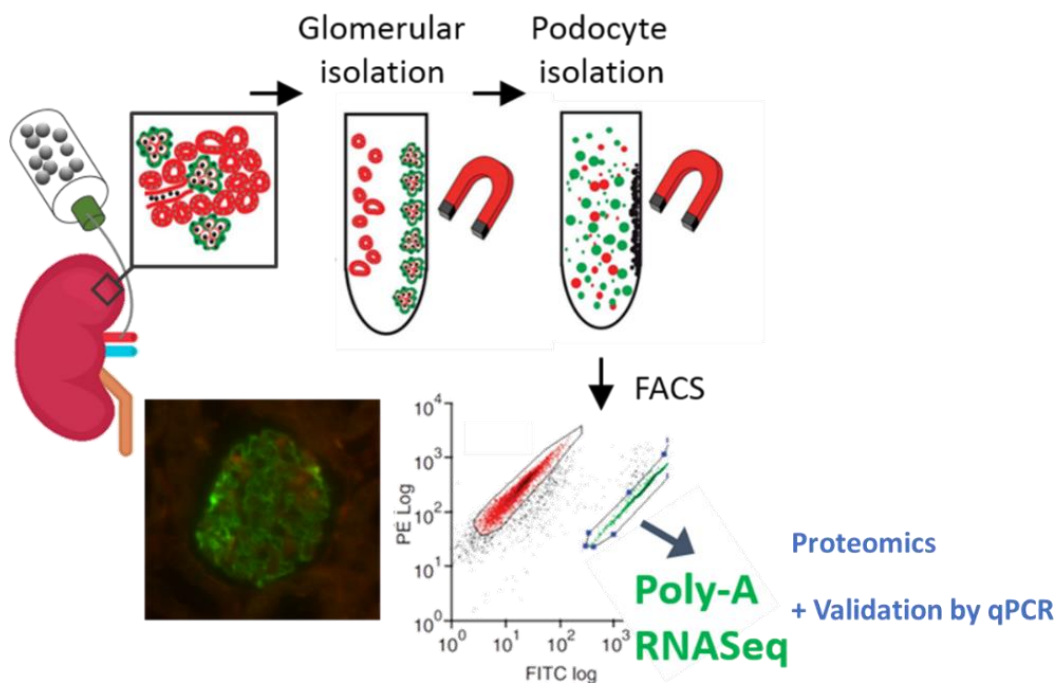


Figure 7. Scheme for podocyte cell isolation technique. Podocyte isolation was performed according to Boerries et al., reproduced with permission, Copyright Elsevier (95).

To separate GFP-expressing (GFP+) podocytes from GFP-negative (GFP-) glomerular cells, a BioRad S3 cell sorter (Biorad) with a Laser excitation at 488nm was used. Only viable cells were sorted (laser excitation 380 nm) and green GFP+ podocyte fractions were directly frozen on dry ice and stored at -80°C for further RNA sequencing and proteomics. Continuous methodological optimization allowed for 92-98% purity and a yield of approximately 117.000 - 450.000 podocytes per mouse. Table 9 summarizes average number of podocytes isolated used for RNA-seq and proteomics.

Table 9. Number of podocyte cells sorted per experimental group used for RNA/ proteomics

Sex (n)	Treatment	Average number of podocyte cells isolated
Male (6)	rapamycin	371,153.8
Male (8)	vehicle	339,805.3
Female (6)	rapamycin	250,310.5
Female (8)	vehicle	224,958

Flow cytometric analysis and FACS sorting from glomerular single cell suspension were performed using BioRad S3 Cell Sorter. Cell size and granularity was measured in forward (FSC) and side-scatter (SSC) [left] with subsequent analysis of Tomato (R2) [middle] and GFP (R1) positive cells [right] (Figure 8).

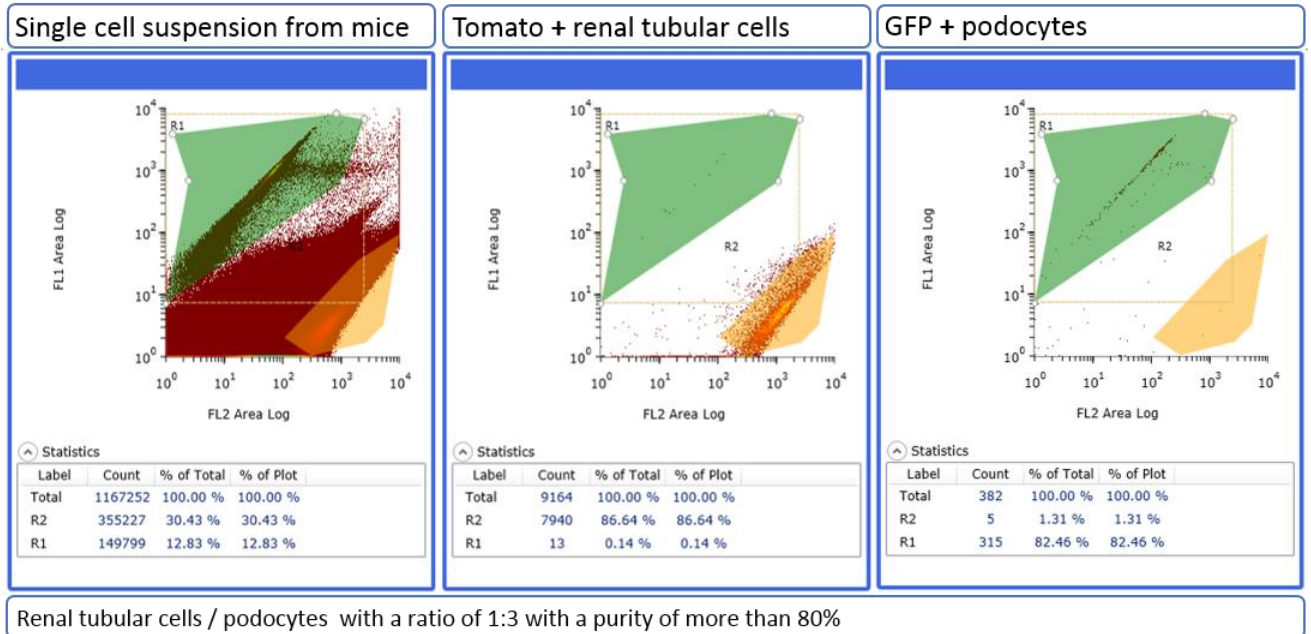


Figure 8: Representative results from FACS cell sorting. podocyte cell sorting showed a good separation on FL1 with separation ratio of 1:3 from other glomerular cells.

2.2.4 Assessment of renal function

Prior to animal sacrifice, blood was drawn, coagulated and centrifuged at $5,000 \times g$ for 10 min to collect serum. 24 h urine samples from the metabolic cages were centrifuged at $5,000 \times g$ for 10 min, supernatant was collected and stored at $-80C^0$ for further analysis.

Serum creatinine, urea, sodium, glucose, osmolality, albumin and total protein in serum and urine were determined at Labor Berlin (Charité Campus Virchow-Klinikum, Berlin, Germany).

To determine albuminuria, urinary protein samples were separated by BICIN-MOPS electrophoresis together with BSA standards ranking from 0.25 - 1 μ g. Protein detection was performed using coomassie blue staining according to manufacturer protocol (Bio-Rad).

2.2.5 Histology

2.2.5.1 Embedding and sectioning

Paraformaldehyde-fixed kidney specimen were immersed in paraffin using a standard protocol for tissue embedding. Kidney tissues were fixed overnight with 4% PFA and stored in 70% ethanol for further preparative steps. Tissues were dehydrated through an ascending series of graded alcohol concentrations (50,70, 80, 96 and 100 %) to displace the water, placed in xylol using Shandon Excelsior ES® A78410120 issue 3 (Thermo scientific, Germany). The next day, the samples were heated and infiltrated with liquid paraffin 62 °C using Thermo scientific HistoStar™ A810101000 issue 2 (Thermo scientific), and stored at 4C⁰. Paraffin-blocks were cut into 4 µm-thick sections with a microtome (Thermo Fisher), transferred to microscope slides and dried over night at room temperature. For cryo-sections, kidneys were directly embedded in Tissue-Tek O.C.T. (Sakura, Japan) after harvesting and cut into 4-6 µm sections using Thermo scientific Cryostar NX70 387928 issue7 (Thermo scientific), slides were dried and stored at - 80 °C for further staining.

2.2.5.2 Staining using paraffin-embedded renal tissue sections

Paraffin-embedded renal tissue sections were deparaffinized and rehydrated through Roti-clear (3×10 min), 100% ethanol, 96%, 80%, 70%, and 50% ethanol and distilled water (each 1×5 min). Then, specific stainings were performed as summarized in table 10.

2.2.5.3 Immunofluorescent actin staining, microscopic analysis and quantification

4 µm thick renal sections were defrosted and pre-washed with PBS-Triton 0.3% for 15 min at RT. To block endogenous peroxidases, sections were immersed in 0.3% H₂O₂ for 10 min, washed three times, then incubated with Phalloidin 647 (1:100, Abcam176759) for two hours at RT prepared in BPS as manufacturer protocol. After washing three times with PBS for 5 min, nuclear counterstaining was performed with DAPI for 15min and then slides were mounted with Aqua polymount mounting medium. Images of actin filaments were evaluated in at least 20 glomeruli each mouse FoV at 200× magnification under a fluorescence microscope at Ex/Em = 650/665 nm (Zeiss, Jena, Germany). The quantification of positive signals was evaluated as intensity of positive area per glomerulus.

Table 10. Summary of staining performed using paraffin-embedded staining

Staining	Summarized method after deparaffination
Periodic acid–Schiff (PAS) staining Demonstrate the thickness of glomerular basement membrane	<ol style="list-style-type: none">1- Immersion in 0.5% periodic acid solution for 5 min,2- Schiff's reagent for 30 min at room temperature3- Mayer's hematoxylin for 1min and rinsing with tap water for few minutes,4- Dehydration in an ascending ethanol series and 15 minutes in Roti-Clear,5- Mounting with Entellan® a xylene-based mounting medium.
Picro-Sirius Red staining visualization of collagen I and III fibers (fibrosis)	<ol style="list-style-type: none">1- Immersion in 0.5% Picro-Sirius Red Solution for 60 min at room temperature2- Rinsing quickly in two changes of 0.005% Acetic acid solution3- Rinsing and dehydrate in absolute alcohol and for 15 minutes in xylene4- Mounting with Entellan®.
Immunohistochemistry staining	
WT1 staining	<ol style="list-style-type: none">1- Antigen Retrieval using Tris-EDTA buffer pH.9 (TE) for 40 min at 95⁰C using water bath2- Blocking of endogenous peroxidase by 0.3 % H₂O₂ for 20 min,3- Blocking with 5% goat serum solution in TBS-T buffer for 30 min at room temperature4- Incubation with WT1 antibody (1:300) at 4⁰C overnight.5- Incubation with the anti-Rabbit 1:1000 secondary antibody for 60 min at room temperature.6- Visualization was performed using AEC (Agilant) for 30 minutes for WT17- Counterstained with Hematoxylin for 90 seconds8- Mounting with Aqua polymount aqueous mounting medium.

	<p>9- Control sections were subjected to secondary antibody only (blank).</p> <p>10- Images were evaluated in at least 50 Glomeruli each mouse FoV at 200× magnification under a fluorescence microscope (Zeiss, Jena, Germany).</p>
Collagen I staining	<ol style="list-style-type: none"> 1- Antigen retrieval with high-temperature Citrate buffer pH.6. 2- Incubated in 1% hydrogen peroxide 3- 5% goat serum blocking for 60 min; 4- Incubated with primary antibodies Collagen I 1:100 (abcam34710) overnight at 4⁰C overnight. 5- Incubation with the anti-Rabbit 1:1000 secondary antibody for 60 min at room temperature. 6- Visualization by incubation with the AEC chromogen for 10 minutes, 7- Counter stained with Hematoxylin and further mounted with Aqua polymount aqueous mounting medium. <p>Images of Collagen I were evaluated in at least 30 Glomeruli each mouse FoV at 200× magnification under a fluorescence microscope (Zeiss, Jena, Germany).</p>
All analysis for positive signal was done using image J software	

2.2.6 Gene expression analysis

2.2.6.1 Total RNA extraction, measurement and RNA-seq

Total podocyte specific RNA was purified from podocyte isolations of 5 female vehicle-treated, 6 rapamycin-treated animals and each 5-male vehicle/rapamycin-treated animals by transfer of Trizol-Ethanol lysed samples to Zymo-Spin IC Column, and used for RNA sequencing. RNA extraction yielded intact high-quality material with a mean RNA integrity number (RIN) of 9.2 ± 0.47 (Figure 9).

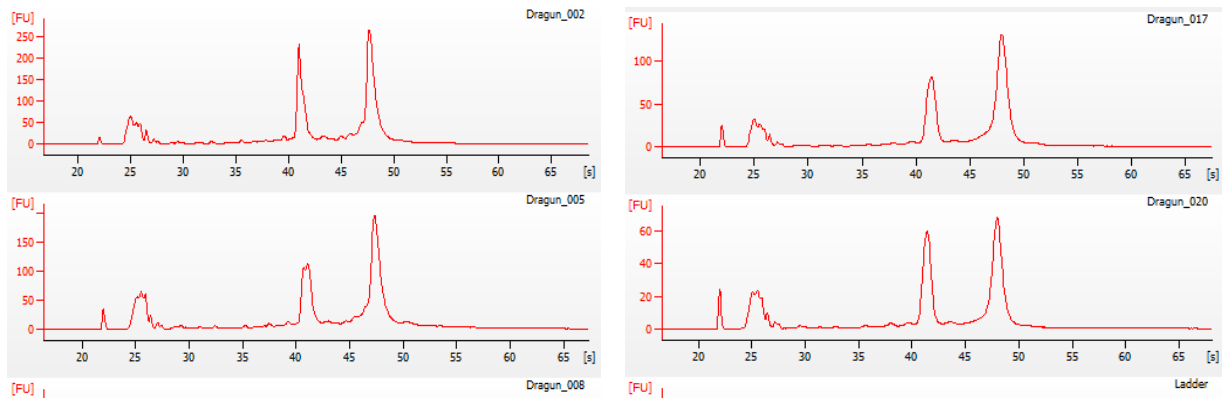


Figure 9: RNA quality control. Bioanalyzer run indicating valid 18S / 28S ratio and RNA Integrity Number (RIN) using Agilent 2100 bioanalyzer RNA testing.

Sequencing reads were mapped to mm10_GRCm38.p4 using STAR 2.5.0b, intersected with Ensembl GRCm38_mm10 gene models using GenomicRanges (96) and counted with the Bioconductor package Rsubread (97). Further analysis was done using DESeq2 (98). Expression changes of transcripts were called significant if the adjusted p-value was lower than 0.05. The principal component analysis (PCA) was done on regularized log transformed read counts.

Subsequent library preparation and RNA sequencing was performed in collaboration with Prof. Rajewsky, MDC Berlin and was performed by Dr.rer.nat Sünkel, Christin. Briefly, after generating cDNA libraries from Poly-A selected mRNA (NEB Next Ultra II Directional RNA Library Prep Kit) the obtained DNA was validated with the Agilent TapeStation platform (TapeStation D1000 HS – Kit) and deep RNA sequencing (2x75 per lane) was carried out on a Illumina Hiseq4000 system. Sequencing performance provided 36-46 million paired-end reads per sample detecting 84% of all transcripts uniquely mapping sequences aligned to only one single gene within the genome. Further statistical analyses and comparisons to other databases of DE genes were performed by Eric Blanc, BIH Bioinformatics Core Unit, Charité – Universitätsmedizin Berlin. Further detailed gene set enrichment analyses were subject of thesis work and performed by Ola Al Diab using PANTHER database (99, 100), GSEA software (45, 101) and Enrichr (102-104). Heatmaps were developed using Heatmapper (105).

2.2.6.2 Quantitative real time PCR (qRT-PCR)

For RNA-seq results validation, total RNA was extracted from isolated podocyte using Qiazol (Qiagen) according to the manufacturer's protocol. RNA pellets were dissolved in 0.1% DEPC water and the concentration was measured by NanoDrop® Spectrophotometer.

For cDNA generation, 1,000 ng of total RNA was reverse-transcribed to cDNA by M MuLV Reverse Transcriptase using Oligo dT primer, according to the manufacturer's recommendations. Specific oligonucleotide primers were designed using the database of the National Center for Biotechnology Information (NCBI). The generation of the primers was in advance using the Primer3 software (<http://primer3.sourceforge.net/releases.php>) and the quantitative real time PCR was conducted on a ABI® StepOnePlus Real Time PCR system (Applied Biosystems, Foster City, CA, USA) using SYBER GREEN. Each amplification reaction was performed in duplicate and Hdgf and Ywhaz was used for normalization. The primer sequences are listed in Table 5 and were synthesized by Bioglegio, Netherlands.

2.2.7 Protein isolation and western blot analysis

Stored cortex-renal tissues were snap-frozen in liquid nitrogen and immersed into ice-cold cryotubes containing grinding matrix (Lysing Matrix D Bulk, white beads) and gold ceramic sphere beads (gold bead, PEQLAB) containing RIPA lysis buffer containing protease and phosphatase inhibitors. The homogenization was carried out using mechanical tissue disruptor (MP Biomedical FastPrep 24 Tissue Homogenizer) twice for 20 sec. Samples were centrifuged for few seconds and incubated with the addition of 1:100 of 10% SDS solution on ice for 20 min, then vortexed and incubated on ice for more 10 minutes. Samples were centrifuged next at 14,000×g, 4 °C for 20 minutes. Protein concentrations were determined by using the BioRad DC™ (BioRad, Danmark) protein assay in triplicates.

Protein lysates (60 µg of protein per lane) were dissolved in Laemmli buffer, denatured at 95 °C for 5 min and stored in -20° C until use. Samples were applied on 8, 10, 12 and 15% BICIN gel (Table 2) with a protein marker (Protein Marker VI) as a ladder, and run with MOPS buffer at a start with a voltage of 80 V for 30 min and further separation was achieved at 130 V.

Proteins were transferred to ethanol-activated PVDF membranes (GE Healthcare, Amersham, UK) within BICIN buffer in a transfer chamber (biorad Germany) at 1 A for 2 h. Blocking was carried out using 5% non-fat milk in TBST for 1 h followed by incubating with primary antibodies of interest (Table 7) overnight at 4°C. Thereafter, the membranes were washed three times with TBST and then incubated with a secondary antibody for 1 h at RT. Bands were visualized with an

enhanced chemiluminescence system according to the manufacturer's instructions. The development procedure was supported with the digital image system of Syngene G:BOX Chemi XRQ, VWR machine. If further antigen detection was required, membranes were incubated in stripping buffer for 30 minutes at 52°C. After further washing cycles and a blocking step, the membranes were reused for subsequent antibody probes.

2.2.8 Proteomics

Proteomics was performed in collaboration with Dr. med. Markus Rinschen in NephroLab, Cologne. In brief, proteins were extracted from snap frozen podocytes, digested and analyzed on a QExactive Plus mass spectrometer coupled to a nanoLC proxeon device using a 1h gradient as described previously (106). Detailed gene set enrichment analyses were subject of thesis work and performed by Ola Al Diab using Enrichr.

2.2.9 Metabolomics

Metabolomics was performed in collaboration with Prof. Kirwan lab, MDC Berlin, tissue extraction and analysis was performed by Dr.rer.nat Raphaela Fritsche. In summary, for tissue extraction 50 mg of cortex-enriched renal tissue was used from 6 cortex-enriched kidney tissue for each experimental group. The tissue was lysed by addition of 1 mL/50 mg tissue MeOH:CHCl₃:Aqua (5:2:1, v/v/v) mixture. Polar samples were extracted using Precellys 24 Tissue Lyser (Peqlab) combined with an N₂ cooling unit (Cryolys). Part of samples were pooled after extraction and used as a quality control sample to test the technical variability of the instrument. They were prepared alongside the samples in the same way.

Metabolite analysis was performed on a Pegasus 4D GCxGC TOFMS-System (LECO Corporation, St. Joseph, MN, USA) complemented with an auto-sampler (Gerstel MPS DualHead with CAS4 injector, Mühlheim an der Ruhr, Germany). Gas chromatographic separation was performed on an Agilent 7890 (Agilent Technologies, Santa Clara, CA, USA), equipped with a VF-5 ms column (Agilent Technologies, Santa Clara, CA, USA) of 30 m length, 250 µm inner diameter, and 0.25 µm film thickness. Helium was used as the carrier gas with a flow rate of 1.2 mL/min. The spectra were recorded in a mass range of 60 to 600 m/z with 10 spectra/sec. The GC-MS chromatograms were processed with the ChromaTOF software (LECO Corporation, St. Joseph, MN, USA) including baseline assessment, peak picking and computation of the area and height of peaks without a calibration by using an in-house created reference and library containing the top 3 masses by intensity for 45 metabolites related to the central carbon metabolism. Data were exported to the software tool MetMax (<http://gmd.mpimp-golm.mpg.de/apps/metmax>) and

merged by an *in-house* written R script. The metabolites were considered valid when they appeared in minimum of n=3 biological replicates. Data were normalized to cinnamic acid (internal standard). Relative quantities were used. The quality control samples were analyzed separately. Glutamine and glutamic acid were removed for data analysis since there are known conversion problems. Data were analyzed to confirm correct metabolite annotation and for outliers (<https://www.graphpad.com/quickcalcs/Grubbs1.cfm>). Sixteen statistically significant (p<0.05) outliers were removed. Wilcoxon rank sum test (p < 0.05) was used for statistics between the different conditions. The ratios between females and males or rapamycin and control were calculated and for better visualization the log2 from the ratio was generated.

2.2.10 Statistics

Statistical analysis of quantifications of western blots and stainings, as well as for physiological data and qRT-PCR were performed by Ola Al Diab using Graphpad PrismTM software version 7.0 (USA). Data are represented as mean ± standard error (SE). n represents the number of biological replicates. All data were tested for significance using Kruskal Wallis and Mann-Whitney test, where applicable and unless otherwise specified, and only results with P<0.05 were considered statistically significant.

Bioinformatics analysis for RNA sequencing data was performed by Dr Eric Blanc from the Core Unit Bioinformatics CUBI in Berlin Institute of Health (BIH)/ Charité – Universitätsmedizin Berlin using Bioconductor package DESeq2. Bioinformatics analysis for proteomics was done by Dr. Markus Rinschen, Medizinische Klinik und Poliklinik, Universitätsklinikum Hamburg-Eppendorf.

Statistical analysis for comparison of metabolites between experimental groups was performed by Dr.rer.nat Raphaela Fritsche, BIH Metabolomics Core Unit, using Wilcoxon rank sum test.

Gene set enrichment analysis for RNA sequencing and proteomics was performed by Ola Al Diab using GSEA software, Enrichr and Panther database. Only results with P<0.05 were considered statistically significant.

3. Results

3.1 Functional effects of mTOR inhibition in male and female mice

mTOR is a master regulator of growth and metabolism and serves as an integrator for diverse cellular stresses (107). Clinically, mTOR inhibitors are frequently used as immunosuppressants and in oncology due to their antiproliferative effects. Yet, their use has been implicated in increased serum glucose levels, insulin resistance and variable deteriorations of kidney function in both, patients and animal models (55, 60).

It was therefore first of all important to thoroughly characterize metabolic parameters and renal function of all male and female mice after three weeks of rapamycin treatment which was administered in a dosage reaching comparable to clinically used serum trough levels of 19-25 ng/ml, vehicle (DMSO) treated mice served as controls.

Table 11 summarizes the physiological parameters measured including serum analyses and urine parameters obtained by metabolic cages at the end of the three-week treatment period. All physiological parameters including kidney function and urine analysis did not show any significant changes comparing sex and treatment by multi-group analyses with Kruskal-Wallis test except for body weight and urine creatinine (Table 11). Rapamycin treatment led to non-significant reduction in body weight of 1.5% in male mice with no change in females. Vice versa, male mice maintained their kidney weights whereas female rapamycin treated mice displayed significantly lighter right kidneys compared to vehicle treated female mice (110.75 ± 12.47 vs. 45.5 ± 14.9 , $p < 0.05$). Mice of all groups maintained normal activities without any signs of health problems.

Glucose, serum electrolytes and kidney functional parameters remained within normal range during the three weeks of rapamycin treatment in all experimental groups indicating no clinically relevant compromise of kidney function in response to rapamycin treatment in either sex during the experimental period. However, even if not reaching statistical significance in Kruskal-Wallis testing comparing all experimental groups, there were obvious intra-sexual changes in glucose excretion by rapamycin treatment suggesting sex-specific drug effects on glucose metabolism and/or renal tubular glucose reabsorption mechanisms. Though, it should be added, that only two male and two female mice in rapamycin treated groups showed a higher level of glucose in the urine (as an outliers, performed by ROUT test), and the remaining had comparable range to vehicle groups with an average level of 21.09 ± 6.07 and 31.0 ± 18.78 mg/dl in males and females, respectively (Figure 10A). In addition, serum glucose concentration increased by 15 % in females in response to rapamycin treatment whereas it remained constant in male mice. Despite of the fact

that other functional parameters of the mice which showed higher glucose levels in serum and urine were within normal ranges, they were not included in further RNA sequencing or proteomics.

Table 11: Clinical and physiological parameters of experimental study groups

Parameters	male vehicle (n=9)	male rapamycin (n=8)	female vehicle (n=8)	female rapamycin (n=8)	p value
Body weight (g) - day 1	28,15±3.8	28,27±2.98	24,69±3.61	23,21±3.47	0.027
Body weight (g) - day 21	27.7±3.68	27.3±3.23	23.92±2.28	22.6±2.55	0.008
Body weight loss (%)	1.5	3.2	2.15	2.11	
Right kidney weight (mg)	181,98±33.37	177,16±39.24	145,5±14.9	110,75±12.47	0.006
	male vehicle (n=6)	male rapamycin (n=11)	female vehicle (n=7)	female rapamycin (n=9)	
Serum parameters					
Creatinine (mg/dl)	0,23±0,05	0,22±0,04	0,22±0,04	0,21±0,03	0.902
Urea (mg/l)	74,67±20,62	74,27±21,64	58,43±13,6	67,22±12,79	0.335
Na ⁺ (mmol/l)	156,5±5,17	153,36±2,84	153,63±2,13	153,1±5,23	0.395
Glucose (mg/dl)	171±32,34	171,3±61,01	124,71±40,75	143,57±39,09	0.286
Osmolality (mosmol/kg)	346,17±11,97	343,45±9,64	330,5±5,19	345,11±9,75	0.086
Urine parameters					
24-hour urine volume (ml)	1,82±0.83	1,6±1.04	1,42±0.74	1,59±0.99	0.817
Creatinine (mg/dl)	17,07±7,21	19,86±3,16	17,07±7,21	14,35±2,65	0.021
Urea (g/l)	43,8±13,24	41,42±5,23	43,8±13,24	40,95±4,82	0.936
Na ⁺ (mmol/l)	85,11±17,81	81,09±13,96	85,11±17,81	77±15,95	0.153
Glucose (mg/dl)	19.3±5.5	38,95±42,02	23,87±14,91	70,38±88,55	0.434
Osmolality (mosmol/kg)	1218,22±364,12	1205,45±155,93	1218,22±364,12	1156,4±106,15	0.904
Total Protein (mg/l)	2934±290.5	2084,91±963	534±443,38	228,2±83,57	<0.0001
Albumin (mg/l)	5.33±21,21	4±1,15	22±21,21§	<3	0.534
Albumin/Crea ratio (mg/g)	21,5±7,42	18,71±4,45	22,5±7,42	21,2±5,17	0.714

§ one vehicle-treated female showed mild microalbuminuria, and when removed, Albumin measurement was 3.8±0.6 mg/l. Mice were weight every third day on the injection day. Calculation was based on day 1 and day 21 prior to sacrifice. The percentage of body weight (BW) loss was calculated by the ratio of BW on day 21 / BW on day 1 x100. Only right kidneys could be weighed as left kidneys were in situ perfused with HBSS and PFA for histology. Kruskal-Wallis test was used to compare the four experimental groups. Data is represented as mean ± standard deviation.

The urine specimens were obtained from spot urine samples and 24-hour urine collection to measure total protein excretion and to determine albumin to creatinine ratio to evaluate the kidney function. In addition to the urine analyses by the Charité and Vivantes laboratory Labor Berlin (Table 11, Figure 10C), SDS-PAGE and Coomassie stains of random urinary samples from 24-hour urine collections were performed. Bovine albumin standards ranking from 0.25 - 1µg were co-applied to allow quantification. The Coomassie stain revealed the absence of microalbuminuria except for one vehicle treated female mouse with an albumin concentration of 37 mg/L (as

determined by turbidimetry) which is just slightly above the lower limit for microalbuminuria of 30 mg/L and was excluded from further transcriptomic, proteomics and metabolomics analysis. Otherwise, almost no albumin (4-7mg/L) could be detected in the urine of all animals tested (n=5 per group). Total protein excretion was higher in male mice compared to females due to higher expression and excretion of major urinary proteins (MUPs) in male mice. There was no effect of rapamycin on total urine excretion as well as on albumin to creatinine ratio in both sexes in males, yet as determined by Mann-Whitney test, treatment effect in females showed significant decreased total protein excretion in females. (Figure 10 B, C, D).

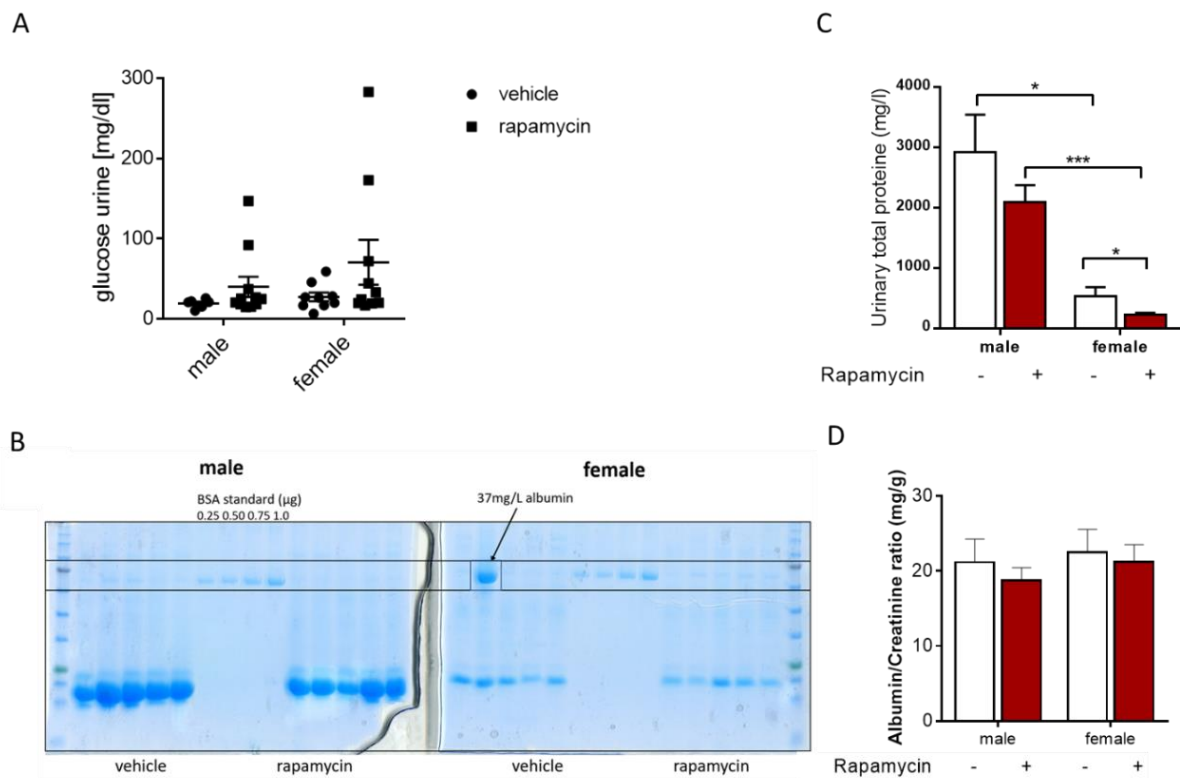


Figure 10. Urinary parameters, glucose, albumin and total protein excretion

(A) Urine glucose increased non-significantly in response to rapamycin in both sexes, yet to a higher level in females. (B) Urinary albumin was determined using SDS-PAGE gels. Except for one sample from a vehicle treated female mouse, no microalbuminuria could be observed in all groups (upper band). Lower bands correspond to the excretion of MUPs which was expectedly higher in male mice. (C) Total protein in the urine was significantly higher in male mice compared to females independently from treatment due to higher male expression and secretion of MUPs. Rapamycin did alter protein excretion only in female $P < 0.05$, tested by Mann-Whitney test. (D) Urinary albumin to creatinine ratio was comparable in male and female mice and was not affected by treatment.

3.2 Effect of mTOR inhibition on renal morphology

Paraffin embedded kidney sections were stained with PAS in order to investigate the effect of mTOR inhibition on renal vascular and glomerular morphology. We observed gross normal renal morphology in vehicle and rapamycin treated animals of both sexes. Focussing on the glomerular compartment and podocytes, 50 randomly selected glomeruli per mouse (n=5 per group) were evaluated. There were no arterial hyalinosis or fibrinoid necrosis. Furthermore, no obvious abnormalities of glomerular mesangium or extracellular matrix expansion within the bowman's capsule could be observed indicating absence of adverse remodelling at this time point (Figure 11).

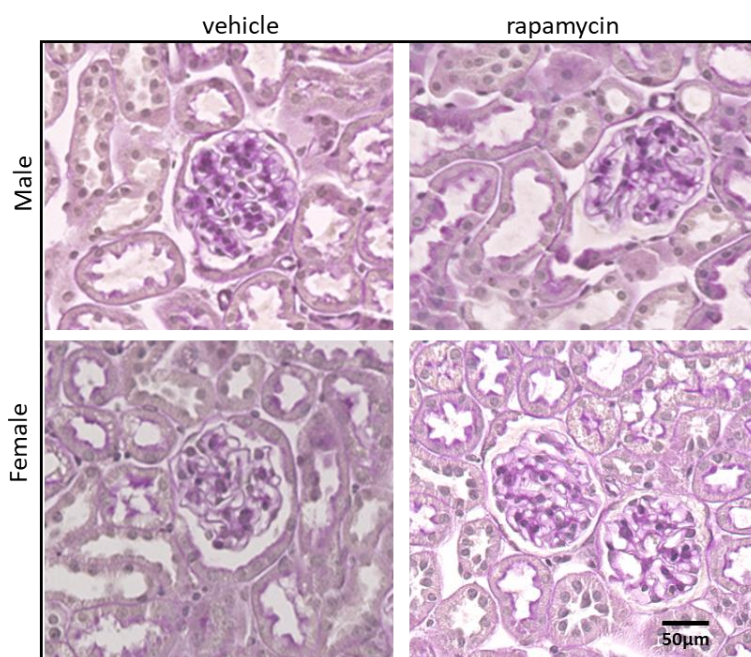


Figure 11. Histological morphology of glomeruli from vehicle and rapamycin-treated male and female mice. Shown are representative PAS staining, n=5 per group.

Tubulointerstitial fibrosis is a hallmark of progressive chronic kidney diseases. Treatment with rapamycin has been shown to ameliorate interstitial inflammation and fibrosis (108) Sirius red staining was performed to investigate the levels of fibrosis in both sexes and in response to rapamycin treatment. 50 randomly selected glomeruli per mouse (n=3-4 per group) were evaluated. Analysis revealed no significant fibrosis within both, the glomerular segment and in the remaining renal tissue of rapamycin and vehicle treated animals of both sexes (less than 4 % of glomerular area in all groups) (Figure 12). However, although not reaching significantly high levels to cause obvious, clinically relevant fibrosis, female mice showed stronger Sirius red staining when treated with rapamycin, whereas male mice showed decreased levels in response to rapamycin treatment. To investigate this issue further, collagen I immunohistochemistry was performed in paraffin embedded kidney sections. Collagen I deposition is a well-known marker

for fibrosis in the kidney. Increased levels of collagen I indicate the formation of fibrotic tissue and later scarring with disease progression. The analysis of 50 glomeruli per mouse (n=3 per group) yielded a comparable result as the Sirius red staining with female mice having increased collagen-I levels in the rapamycin treatment group and males showing reduced levels after rapamycin compared to vehicle treated male mice. In summary, results of staining indicate that three weeks of rapamycin treatment had no adverse effect on renal morphology or physiological kidney function.

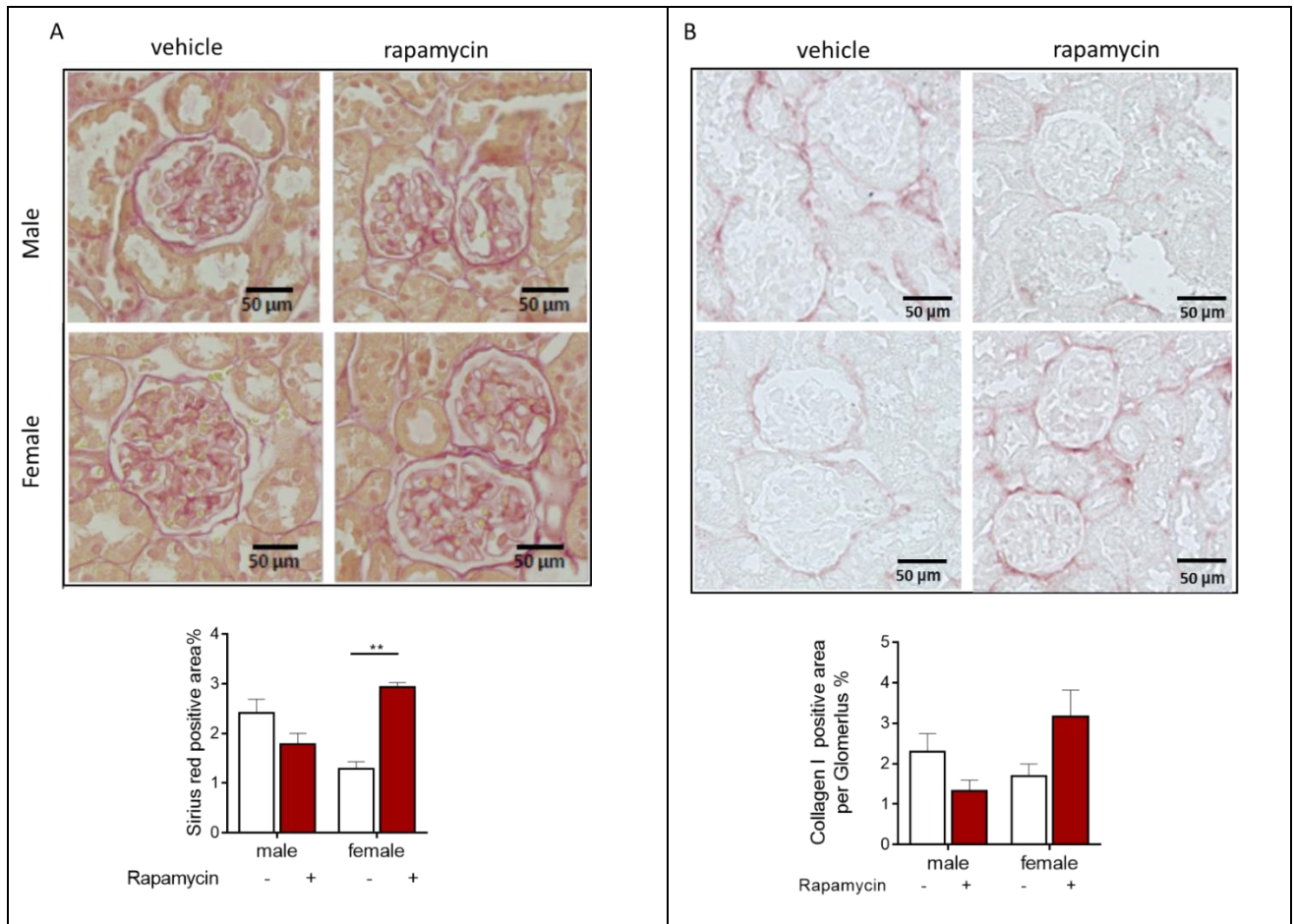


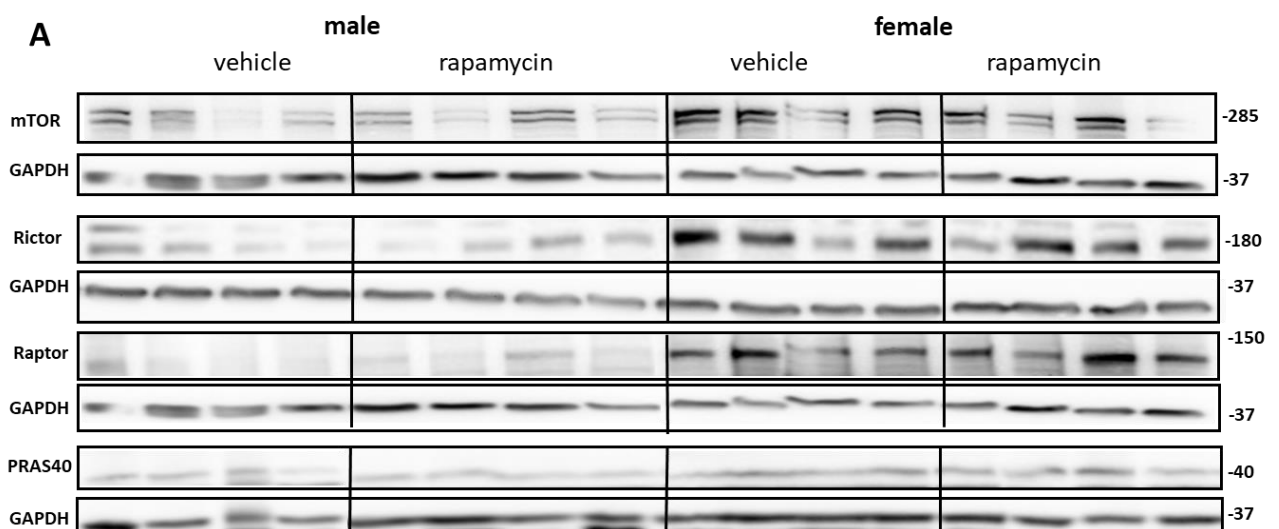
Figure 12: Assessment of renal fibrosis levels by Sirius red staining and collagen immunohistochemistry. (A) Representative staining with Picro Sirius red and quantification, n=4 mice per group except for female vehicle n=3 (B) and immunostainings for collagen I (n=3 per group). kidney sections of vehicle and rapamycin treated male and female mice are shown, image J showed increased Sirius positive signal after rapamycin treatment in females but not in males, Kruskal–Wallis test was used.

3.3 Effect of mTOR inhibition on mTOR protein expressions and signalling

Adequate rapamycin dosage to achieve trough levels comparable to clinically effective dosages had been confirmed by serum samples during the treatment in both male, and female mice (see 3.1). To further characterize pharmacological effective mTOR inhibition in renal tissue itself, especially in the absence of significant changes in kidney function and gross morphology, expression of mTOR complex proteins and activation levels were assessed in renal cortical tissues by western blots. Due to the limited biological material of isolated podocytes, which were used for deep RNA sequencing and qualitative proteomics, and to be able to assess signaling independently from confounders of the isolation procedure of the podocytes by different digestion steps and by FACS, protein lysates from snap frozen renal cortical tissues were taken for these analyses.

3.3.1 Sexual dimorphism of mTOR complex protein expressions in vehicle and rapamycin treated mice

Interestingly, the expression of mTOR, raptor and rictor showed high sexual dimorphism. These proteins were higher in female compared to male irrespective of treatment and reached highly significant differences for raptor and rictor ($0.01 > p\text{-value} < 0.05$ between vehicle groups). Treatment with rapamycin however did not change mTOR complex protein expressions in each sex. PRAS40 expression, an important component, substrate and regulator of mTORC1(109) did not show any sex or treatment differences. (Figure 13).



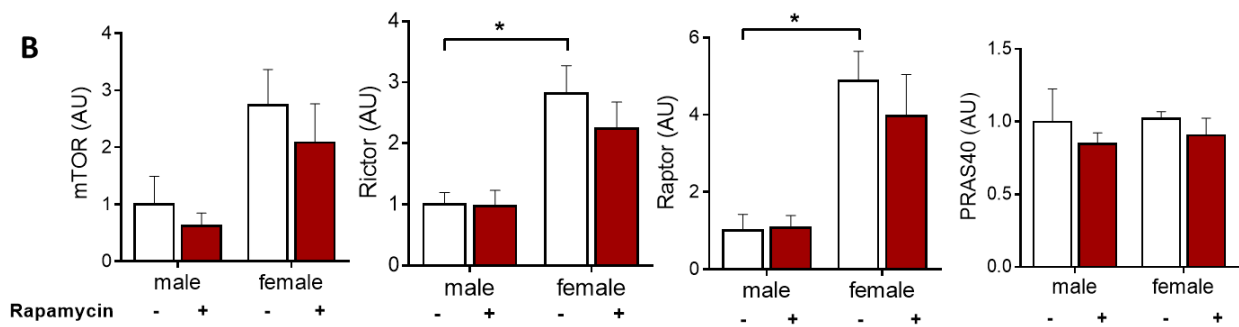


Figure 13. Expression of mTOR complex proteins. (A) Protein lysates of renal cortex tissues from 4 different mice per group were prepared and subjected to gel electrophoresis. Specific antibodies against mTOR, raptor, rictor and PRAS40 were used to detect their protein expressions in male and female vehicle and rapamycin treated groups. (B) Densitometric quantification showed a higher level of mTOR complex proteins in females compared to males. GAPDH was used as loading control. Kruskal–Wallis test was used and results are expressed as mean +/- SEM, * $p < 0.05$, ** $p < 0.01$.

3.3.2 Effect of rapamycin on mTORC1 signaling in male and female mice

It is well known that mTORC1 phosphorylates two well characterized downstream targets, S6K1 (p70S6k) and 4E-BP1 (eIF-4E binding protein) (110), whereas 4E-BP1 has been reported to be rapamycin insensitive (111). As p70SK phosphorylation at Thr389 indicates mTORC1 activation levels it was predominantly used to investigate the effect of rapamycin in male and female mice. In both sexes, mTORC1 activity decreased to less than half in response to rapamycin treatment compared to vehicle with highly significant reduction in females ($p < 0.05$). As expected, the other mTORC1 downstream kinase 4-EBP1 was not largely affected by treatment (Figure 14). Also, the level of p-p70S6K^{Thr389} and basal p70S6k showed sex differences at baseline (according to western blots from male and female samples run side by side on the same gel, data not shown).

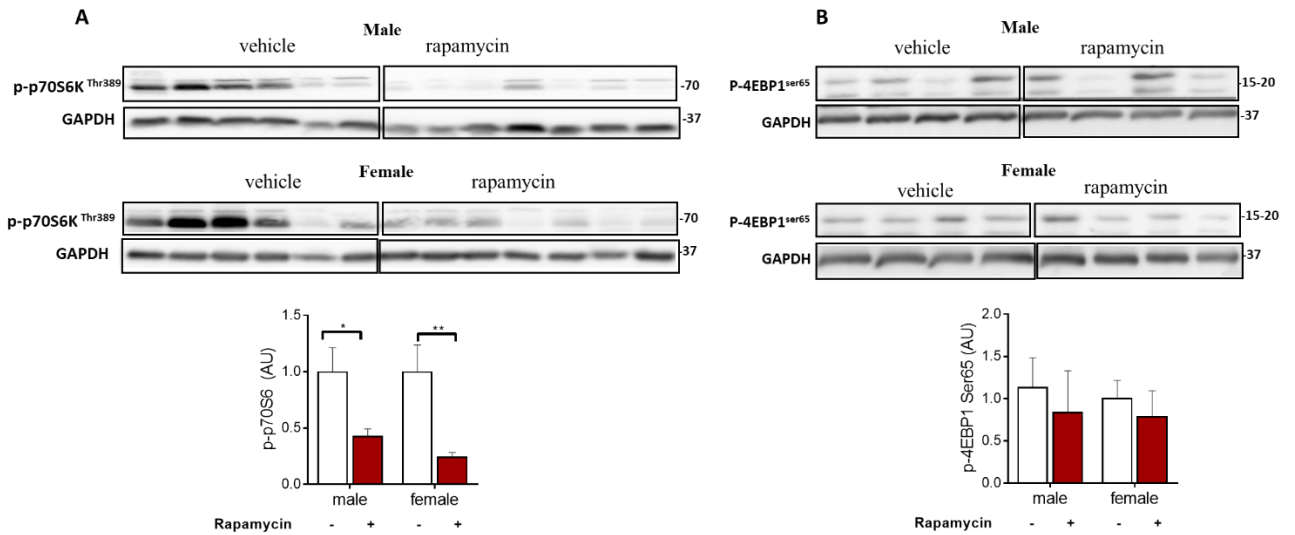


Figure 14. mTORC1 signaling pathway activation. (A) Representative western blots are shown for p-p70S6K^{Thr389} (left panels) and p-4EBP1^{Ser65} (right panels) downstream targets of mTORC1 from renal cortex tissue lysates of vehicle female and male mice (n=6 for each sex for p-p70S6K^{Thr389}, n=4 for p-4EBP1^{Ser65}) and rapamycin treated male and female mice (n=7 for each sex for p-p70S6K^{Thr389}, n=4 for p-4EBP1^{Ser65}). GAPDH was used as loading control. (B) Quantitative analyses were performed by Kruskal–Wallis test, normalized to GAPDH and are shown as mean +/- SEM, * 0.01 > p-value < 0.05.

3.3.3 Effect of rapamycin on mTORC2 regulation in male and female mice

mTOR phosphorylation at Ser2481 is commonly used as a marker of intact mTORC2 and its activity (112). Significantly increased phosphorylation of mTOR at Ser2481 was found in female vehicle and rapamycin treated mice compared to male mice. The increased mTORC2 activation in female mice was also confirmed by the assessment of mTORC2 effector protein kinase B (AKT) phosphorylation at Ser471 which showed higher levels in female mice compared to male mice already under baseline conditions with almost three times higher phosphorylation levels (p<0.05). Rapamycin treatment decreased AKT phosphorylation at Ser471, whereas it slightly increased in male. Furthermore, PDK-1 dependent and mTORC2 - independent AKT phosphorylation at Thr308, which contributes to full activation of AKT kinase, was also significantly higher in female vehicle compared to male vehicle mice and remained high in females in response to rapamycin treatment whereas it increased in males about three-fold with

rapamycin treatment. AKT protein itself was about equally expressed in male and female independent of treatment (Figure 15).

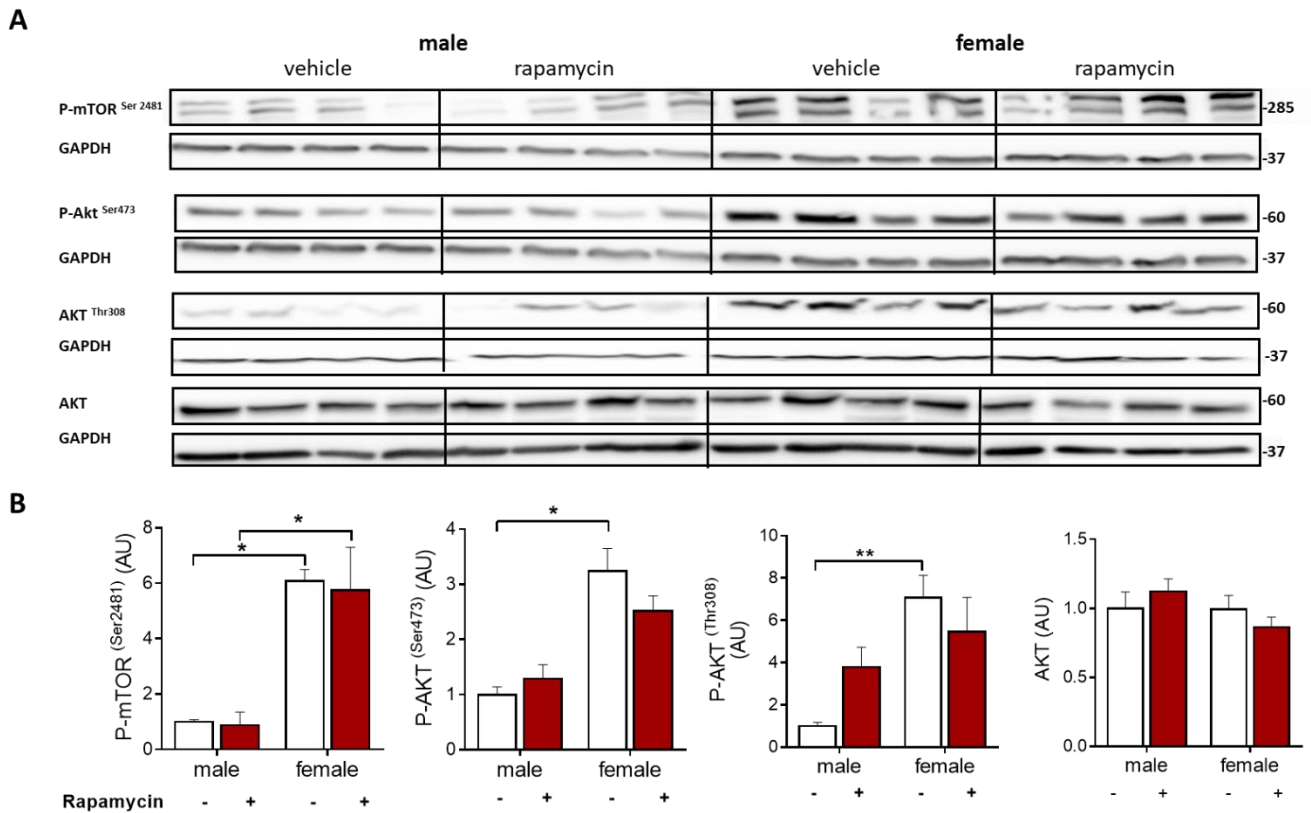


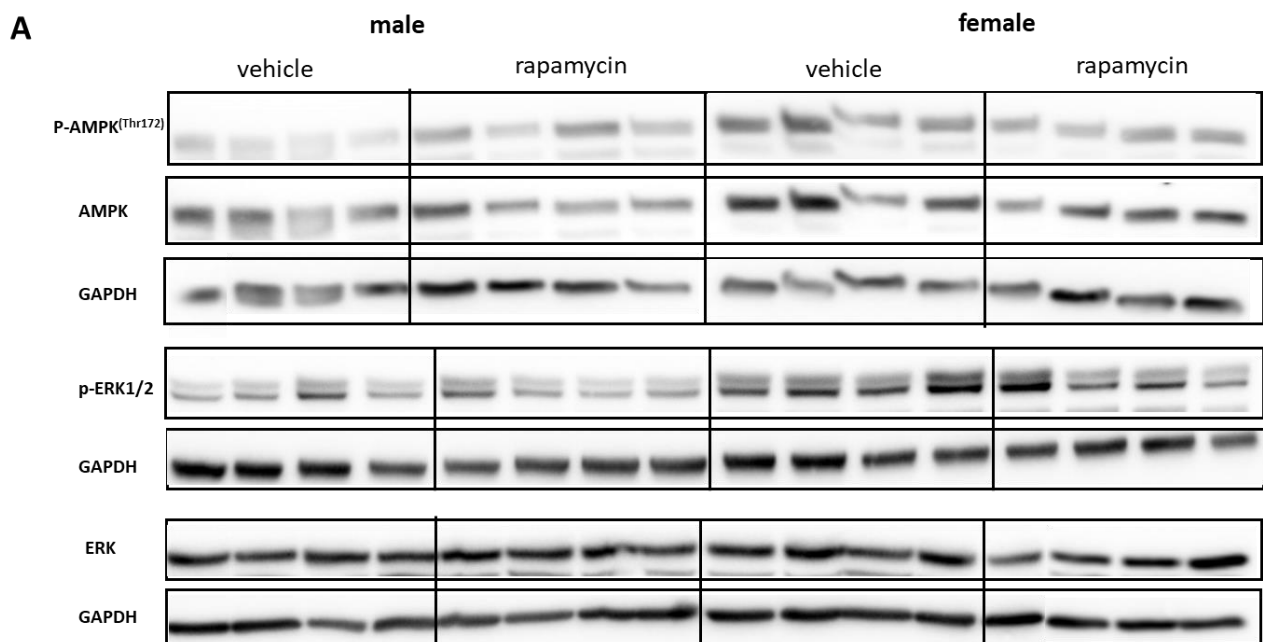
Figure 15. mTORC2 signaling pathway activation. (A) Representative western blots are shown for p-mTOR-^{S2481} and mTORC2 downstream target p-AKT^{Ser471} and p-AKT^{Thr308} (n=4 for each group). GAPDH was used as loading control. (B) Quantitative analyses were performed of phosphospecific bands normalized to GAPDH and Kruskal–Wallis test was applied. Results are expressed as mean +/- SEM, *p<0.05, **p<0.01.

To summarize, mTOR complex proteins mTOR, raptor and rictor show higher expression levels in female compared to male mice. Rapamycin caused a decrease of mTORC1 in both, male and female mice, whereas there was a tendency to increased mTORC2 in males compared to decreased mTORC2 activation in females in response to rapamycin.

3.3.4 Effect of rapamycin on energy sensor AMPK and stress kinase activation ERK1/2 in male and female mice

The serine/threonine protein kinase AMPK regulates energy metabolism and is considered as main sensor of cellular energy status. When AMP: ATP / ADP:ATP ratio increases under energy stress, AMPK is activated by phosphorylation at Thr172 and restores energy balance by promoting catabolic processes that generate ATP and by inhibiting protein synthesis. AMPK potently promotes autophagy through activation of ULK1 and inhibition of mTORC1 activity via phosphorylation of Tsc2 and phosphorylation and inhibition of raptor, thereby decreasing protein synthesis. Moreover, activation of AMPK promotes glucose uptake by phosphorylating TBC1D1 (TBC domain family, member 1) and TXNIP (thioredoxin-interacting protein), which control the translocation and cell-surface levels of glucose transporters GLUT4 and GLUT1 and improves glycolysis (113).

In this study, rapamycin treatment led to a significantly decreased p-AMPK at Thr172 only in female but not in male renal cortices, indicating an overall better balanced energy status in females in response to rapamycin compared to males (Figure 16). However, stress kinase ERK1/2, a multifunctional serine/threonine kinase that is able to phosphorylate numerous substrates, including protein kinases, signal effectors, receptors, cellular scaffold proteins and nuclear transcriptional regulators unexpectedly showed a reduction in response to rapamycin in both, male and females with higher baseline level in females compared to males.



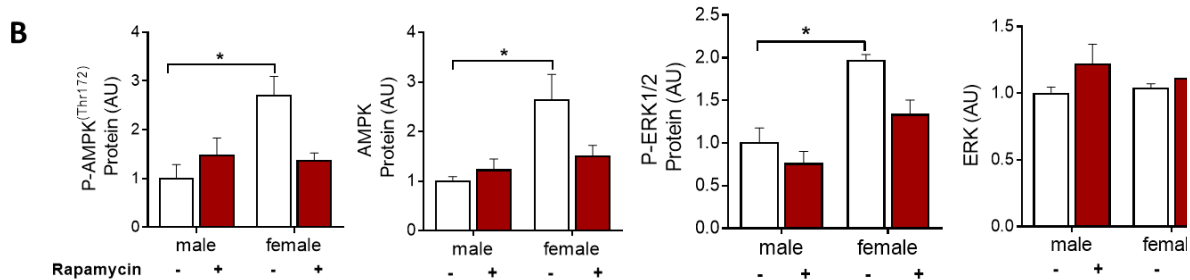


Figure 16. Expression and activation of AMPK and ERK1/2 in renal cortex tissue in all experimental groups. (A) p-AMPK and p-ERK1/2 showed significantly higher levels in female vehicle compared to male. Rapamycin treatment reduced p-AMPK only in females, p-ERK1/2 in both sexes (n=4 for each group). (B) Quantification of western blots using image J. Kruskal–Wallis test was used and results are expressed as mean +/- SEM, *p<0.05, **p<0.01.

3.4 Sexual dimorphism of podocyte transcriptome and transcriptional stress responses to mTOR inhibition with rapamycin

3.4.1 Overview of RNA sequencing dataset

After thorough phenotyping of male and female mice treated with vehicle or rapamycin for 3 weeks with regard to kidney morphological and functional sex differences, podocytes were isolated to investigate potential sexual dimorphic podocyte specific transcriptomes and transcriptional stress responses to mTOR inhibition. RNA was extracted from snap frozen specimen of freshly isolated podocytes and polyA-mRNA was prepared from five biological replicates of each group. One biological replicate of the male and female vehicle groups had to be excluded from further sequencing due to low RNA quality and abnormal kidney function test. Sequencing performance provided 36-46 million paired end reads per sample detecting 84% of all transcripts uniquely mapping sequences aligned to only one single gene within the genome.

There was high conformity between podocyte specific transcripts of own data with different podocyte specific RNA-seq datasets reported in the literature (95, 114-116) proving validity of the podocyte isolation method and subsequent preparative steps for sequencing (Figure 17).

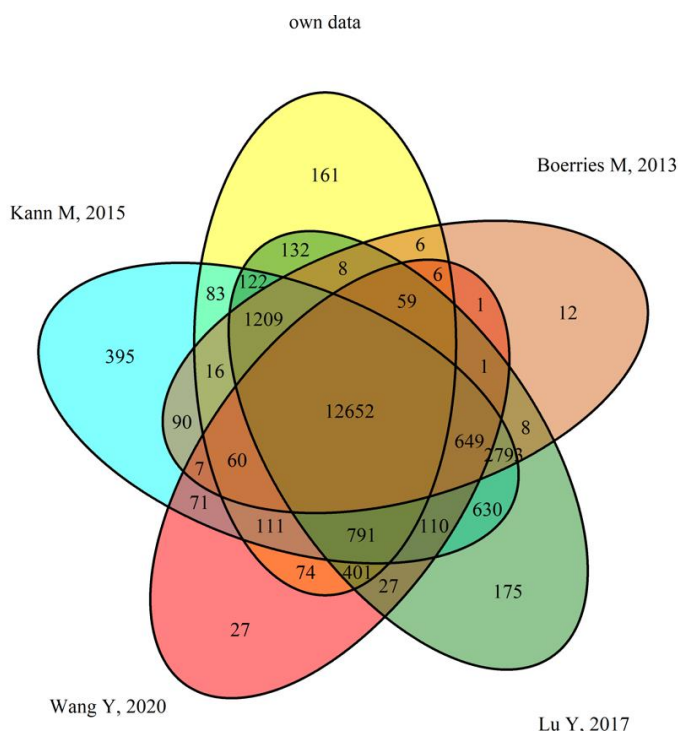


Figure 17. Podocyte-specific genes detected in the current and previously reported transcriptomic studies. Venn diagram showing the number of common or unique genes detected in reported podocyte datasets (95, 114-116).

The principal component analysis (PCA) of transformed sequencing data indicated a clear separation of male and female transcriptomes in the first principal component that explained 26%

of all variability and a second component with 12% variability. Furthermore, male and female transcriptomes showed separate clustering under baseline (vehicle treatment) indicating intrinsic sex-differences in the podocyte-specific transcriptome. Remarkably, these differences in podocyte gene expression decreased significantly between male and female mice by rapamycin treatment (Figure 18). The comparison between samples was based on expression levels using the variance-stabilization algorithm implemented in DESeq2.

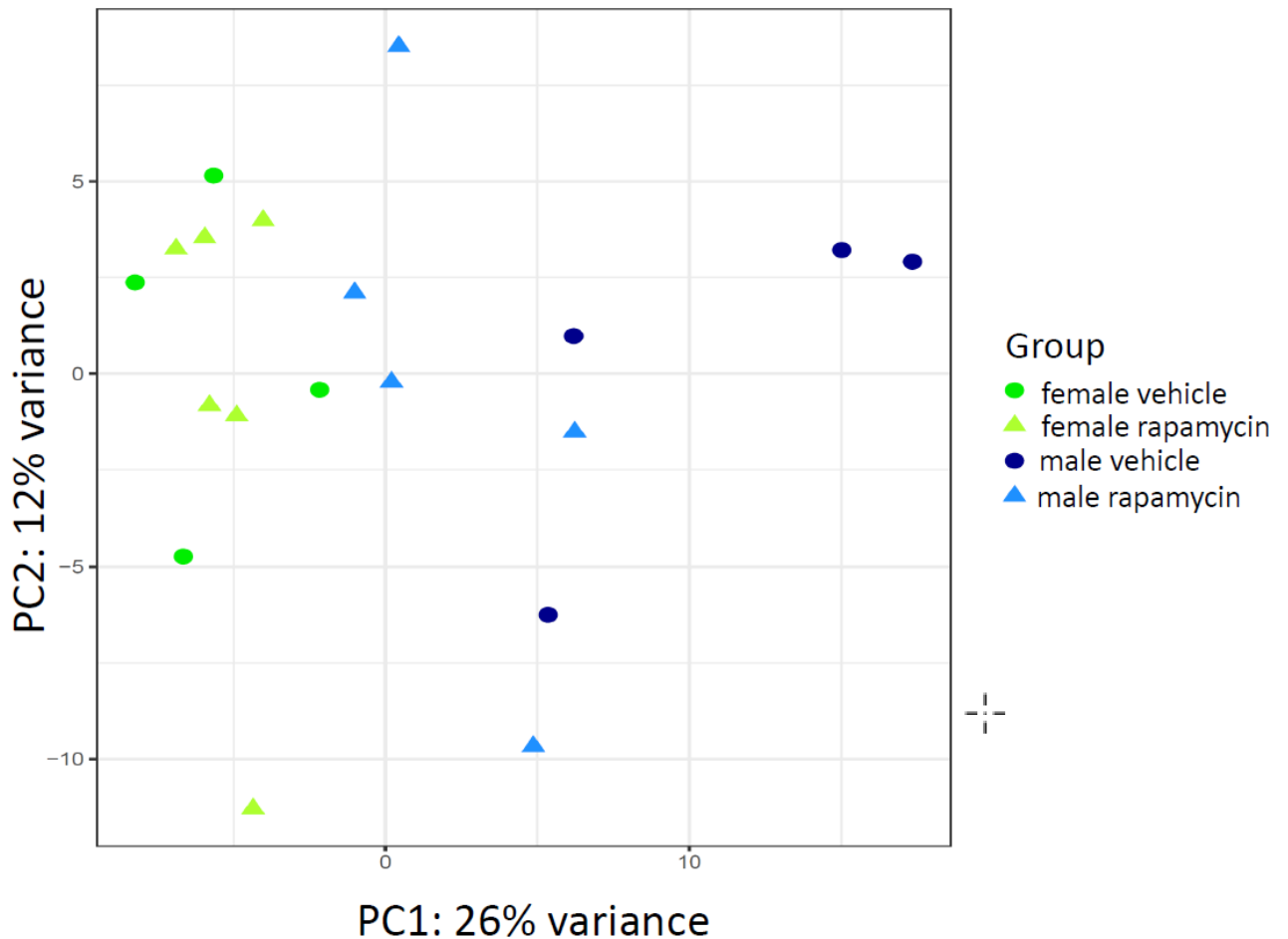


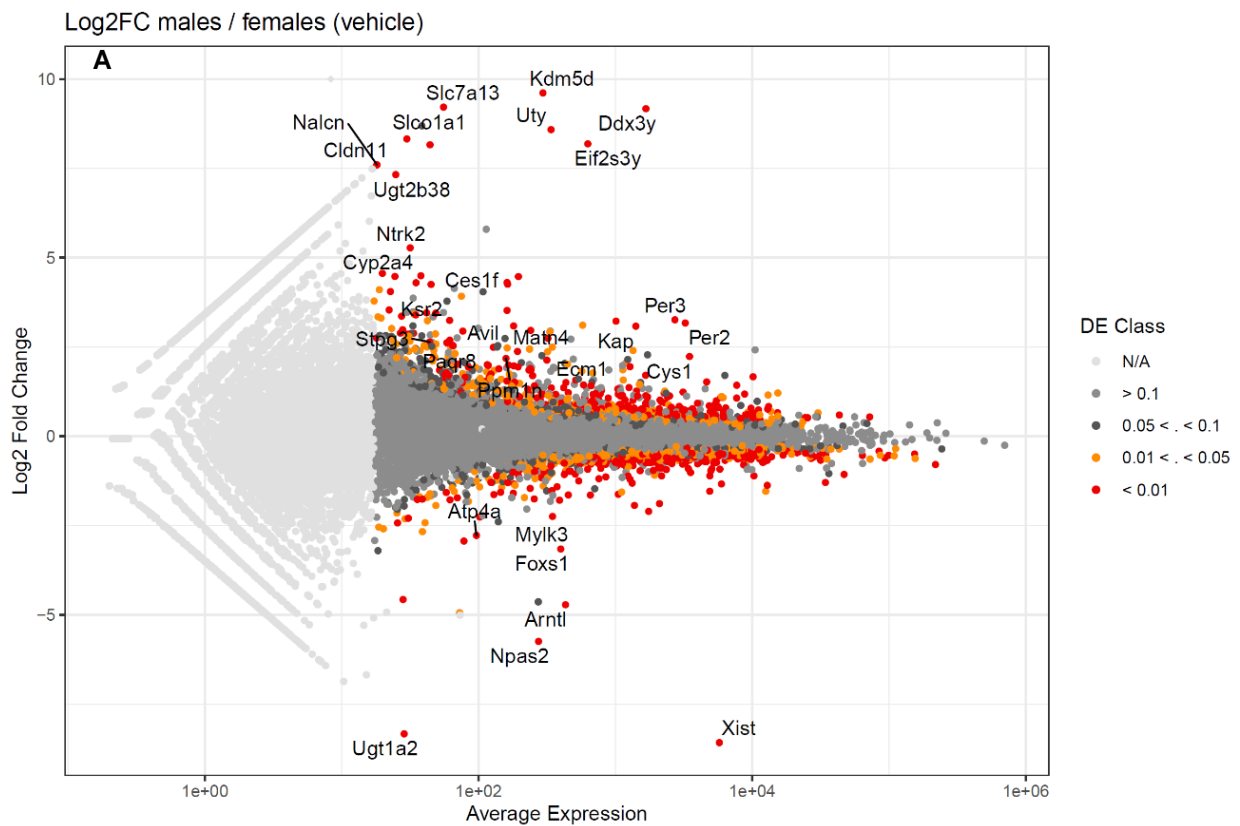
Figure 18. Principal component analysis

The top 500 most varying genes (variance-stabilized expression values, without taking experimental design into account) were used for the PCA. Results revealed sex-dependent separation of transcriptomes between male and female vehicle mice (blue / green dots) and sexually dimorphic changes in response to rapamycin treatment (blue / green triangles).

In order to compare the gene transcription of podocytes from different groups mean normalized expression was calculated using single sequencing read numbers for each gene. Differences

between gene transcript counts were calculated as log₂-fold change (Log₂FC) and adjusted p-values (adj. p-value) below $p < 0.05$ were considered statistically different. With these conditions, 1768 genes were detected to be significantly differentially expressed (DE) between male and female podocytes under baseline (vehicle treatment) (xlsx-gene lists in Appendix, Table 1). Of them, 942 genes (53.28%) were upregulated in female podocytes (437 genes with $p < 0.01$) and 826 genes (46.72%) were upregulated in male podocytes (353 genes $p < 0.01$) (Figure 19 A). Interestingly, only 53 genes were regulated between male and female podocytes after rapamycin with $p < 0.05$ (Figure 19 B, gene list in Appendix, Table 2). Moreover, a functional interaction analysis was done on the interaction of treatment effect between male and female mice, which revealed that only few genes were significantly differentially expressed between male and female podocytes (Figure 19 C).

The previously relatively high number of sexually dimorphic genes was dramatically reduced to only 32 DE genes in the functional interaction analysis. Yet, most of these genes were regulated in males and related to metabolic process, endocytosis and regulation of cytoskeletal function. Female podocytes only significantly regulated three genes: *Ptgds*, *Dip2b* and *Ankrd33b* with p adj. value < 0.05 (xlsx-gene lists in Appendix, Table 3).



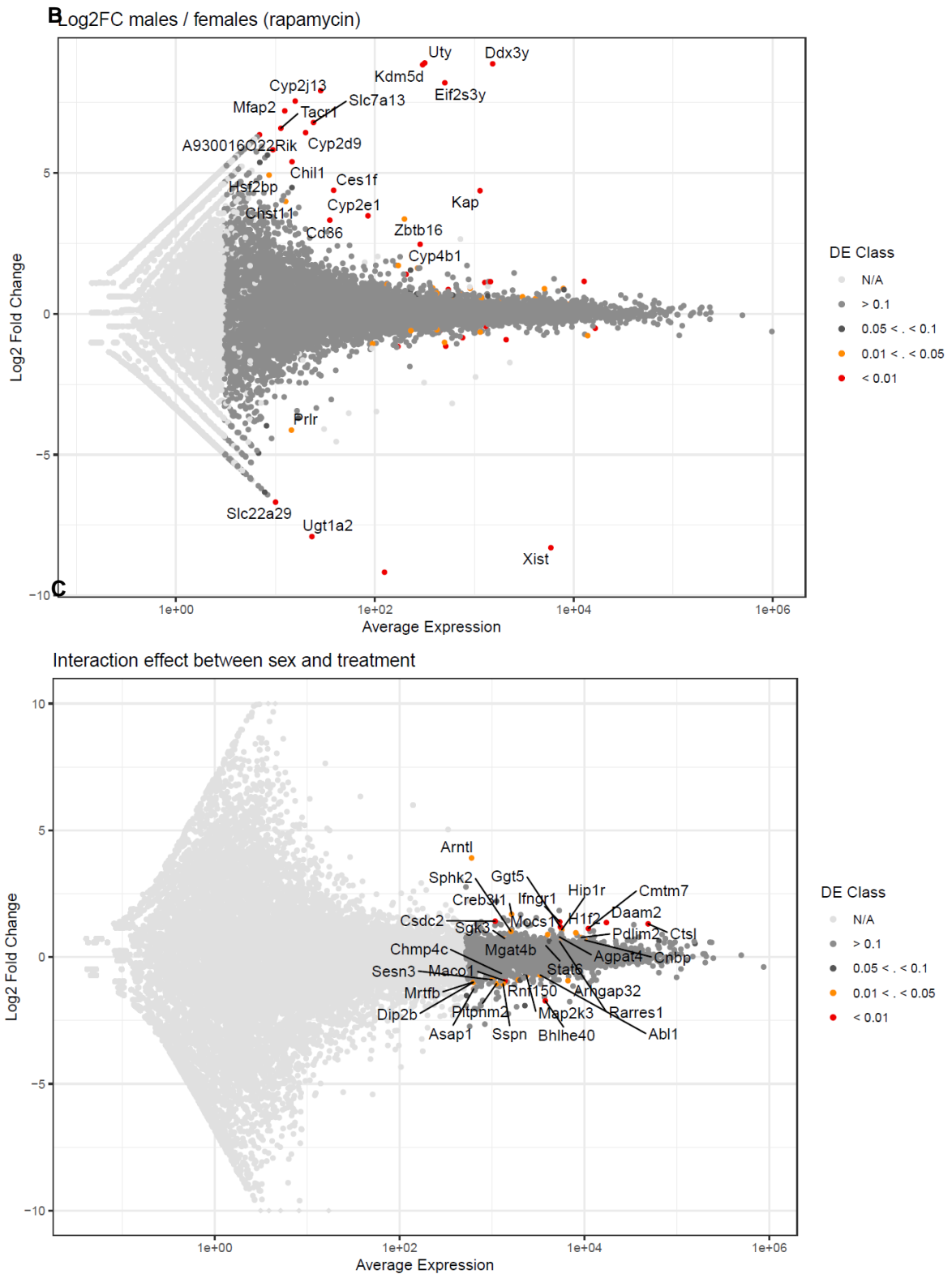


Figure 19: Sex- and treatment-specific transcriptional differences. Scatter blots showing distribution of gene copy numbers of podocytes as normalized counts per transcript versus Log2FC males/female of (A) vehicle and (B) rapamycin treated (C) Results of functional interaction analysis of treatment effect in each sex. Colours indicate significance levels (red: $p < 0.01$, orange: $0.01 < p < 0.05$, grey: non-significantly DE).

Whereas vehicle comparison revealed a high number of sexually dimorphic mitochondrial, ribosomal and others genes (further details see below), rapamycin treated male and female mice displayed no significantly differentially expressed mitochondrial genes or genes coding for ribosomal proteins. Most genes that were significantly different in rapamycin treated showed already sexually dimorphic expression under vehicle conditions (except for *Ggt5*, *Hlf2*, *Hip1r*, *Stat6*, *Sgk3*, *Sesn3* being only DE in podocytes of rapamycin treated male and female mice) (Figure 20, xlsx-gene list in Appendix, Table 2).

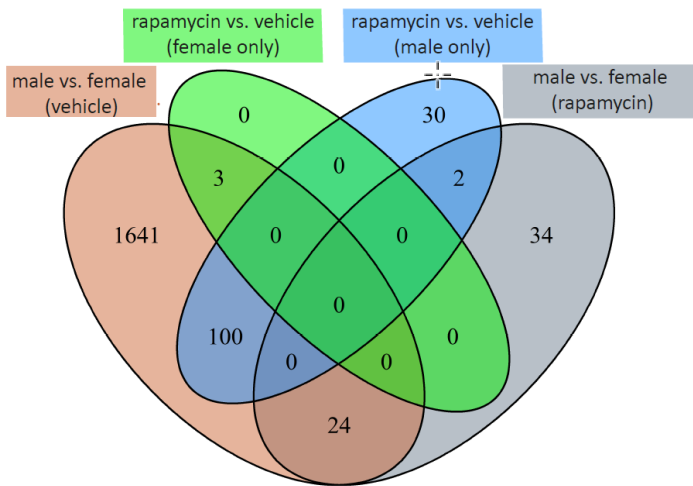


Figure 20. Venn diagram demonstrating overlap of sexually dimorphic genes and DE genes in response to rapamycin treatment in each sex.

To rule out any confounder that may have contributed to the number of sex-differentially expressed genes under baseline, the dataset was first compared to normalized expression for different glomerular cell type marker genes (16 cell types) (117). DE genes were not related/overexpressed in other cell types but only to podocytes, confirming the high purity of podocyte isolation and ruling out contamination by other cell types of the glomeruli as a reason for the high number of sexually dimorphic genes (data not shown). Next, the localization of the DE genes on specific chromosomes was investigated. As shown in Figure 21 genes on the X chromosome were not more differentially expressed than genes on autosomes for all experimental groups. Interestingly, mitochondrial genes clustered strongly for sex, but not for treatment (Figure 21 B).

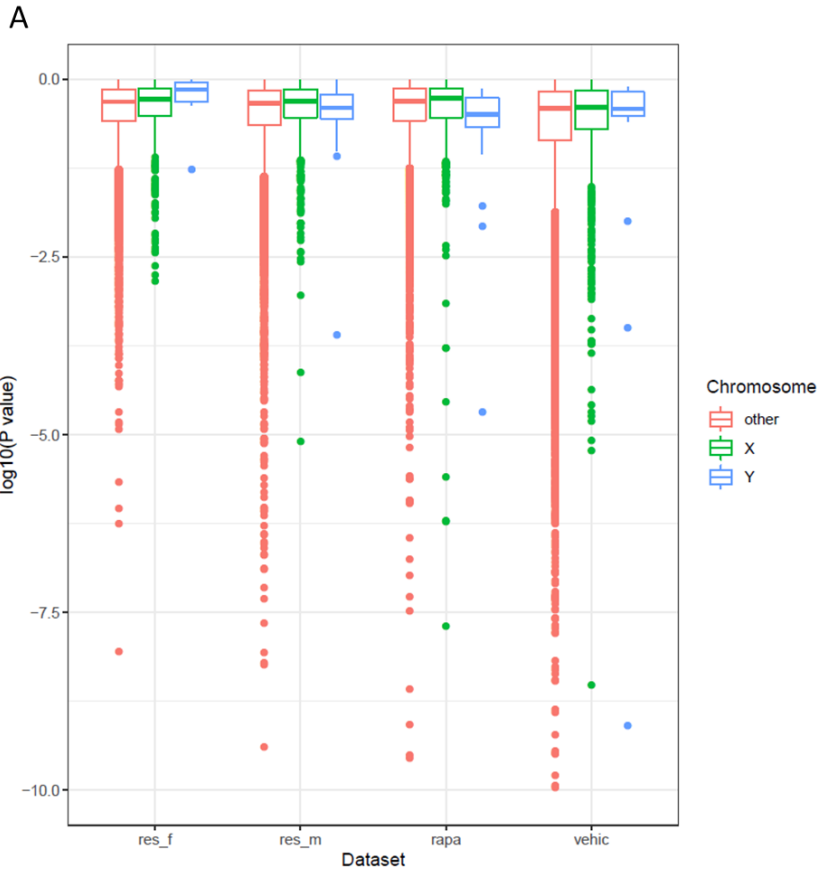
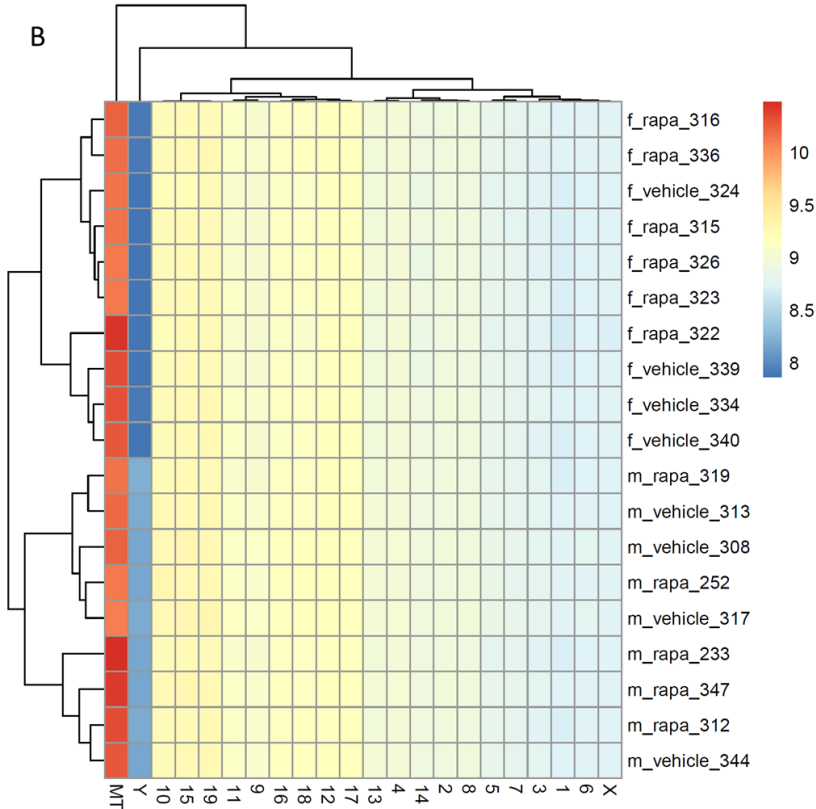


Figure 21. Sexual dimorphism does not relate to sex chromosomes. (A) Dot blot showing the significant differences of p-value for all podocyte genes. Blue and green dots visualize sex chromosomal genes, and red dots visualize autosomal genes, (B) heatmap of the average normalized expression by sample and by chromosome.



3.4.2 Gene set enrichment analyses of significant sexually dimorphic and treatment-related differentially expressed genes

3.4.2.1 Gene set enrichment analyses of significant sexually dimorphic genes

In 2004, Rinn et al. firstly described sex differences in gene expressions in the kidney (19). Several further studies followed, not only showing intrinsic sex differences, but also different responses to injury (18, 20, 115, 118-120). Overrepresented gene ontology (GO) terms in murine kidneys included e.g. major metabolic processes (20). Gene ontology analyses of the top 100 DE genes (p value<0.01 and RPKB>4Kb) of podocytes from vehicle mice of this thesis study showed enrichment in mitochondrial genes, translation/ribosomal, metabolic and cellular junction/focal adhesion related genes (heatmap for top 100 DE genes is in Appendix, Figure 1). To further investigate which GO terms were significantly enriched in sexually dimorphic genes in podocytes from vehicle and rapamycin-treated mice, GO term enrichment analyses were performed, mainly by Panther database version 16.0 for GO-slim (released 12.2020) and GO ontology (released 02.2021) and Enrichr enrichment analysis tool for Kyoto Encyclopedia of Genes and Genomes (KEGG), Wiki pathways and molecular signature (mSig)-Hallmark enrichment. Figure 22 summarizes categories of protein classes for all intrinsically sexually dimorphic genes.

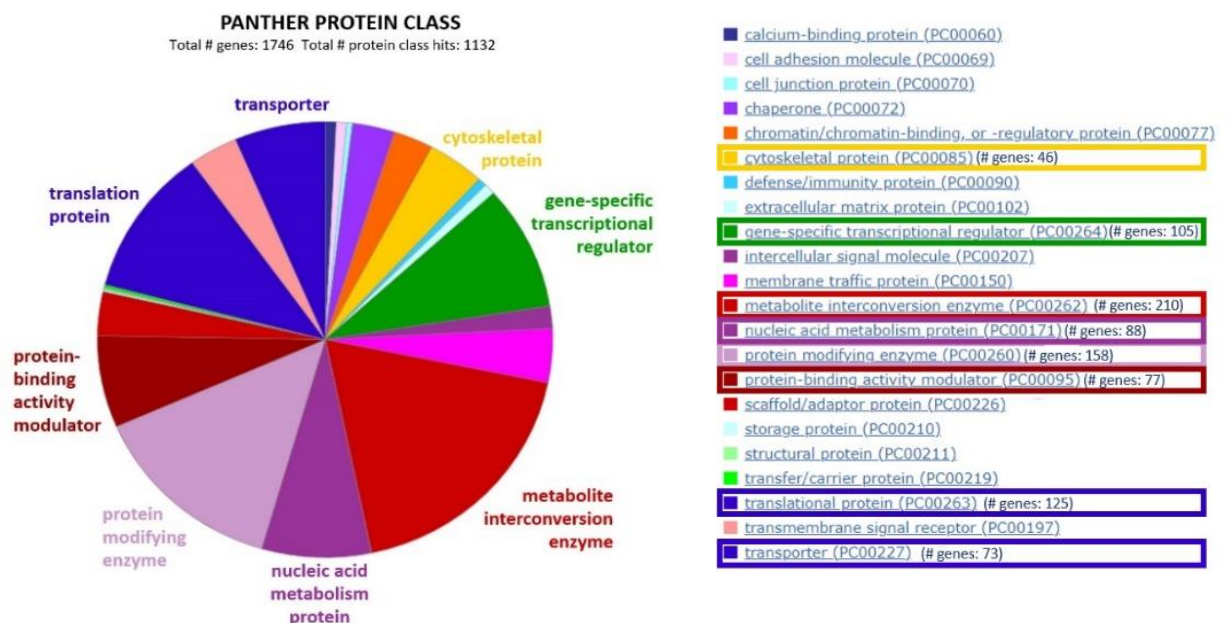
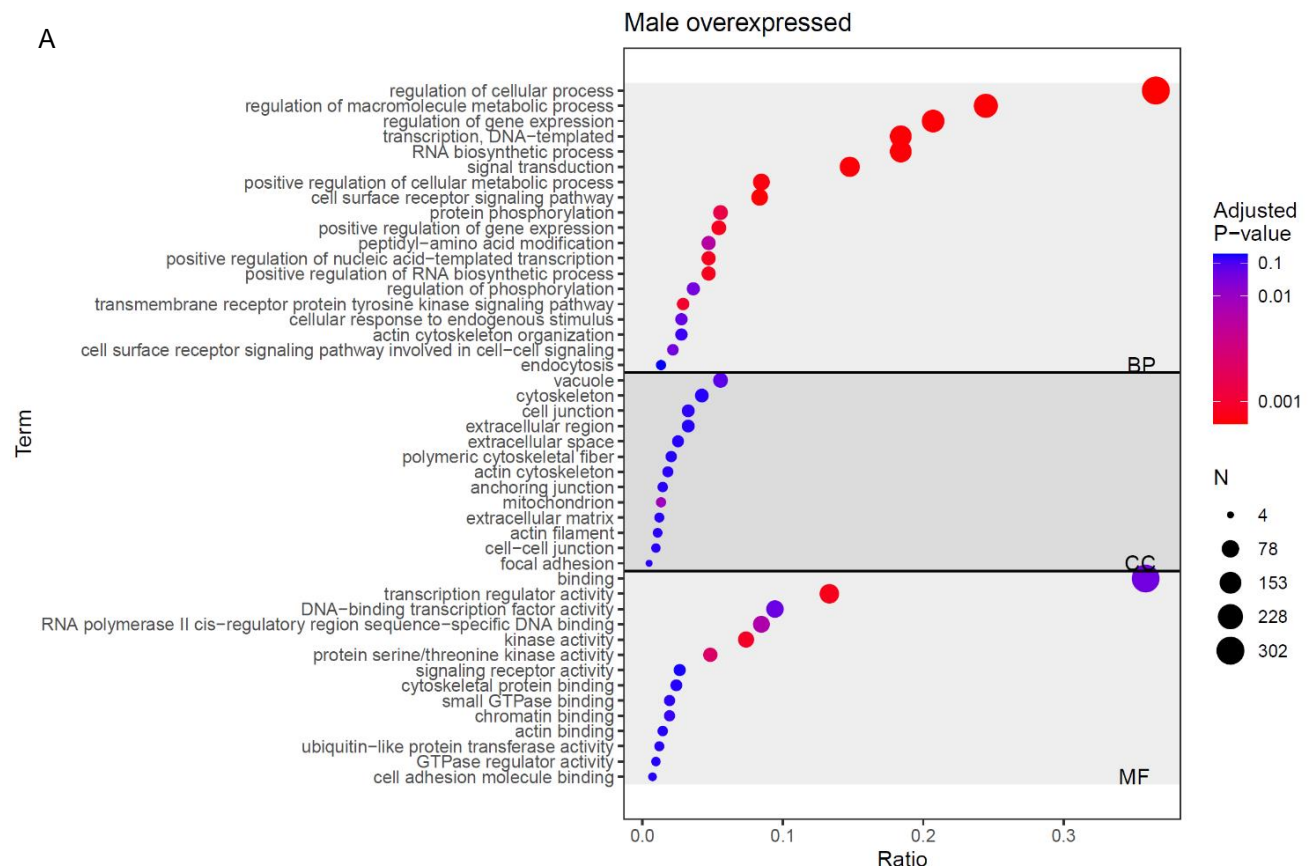


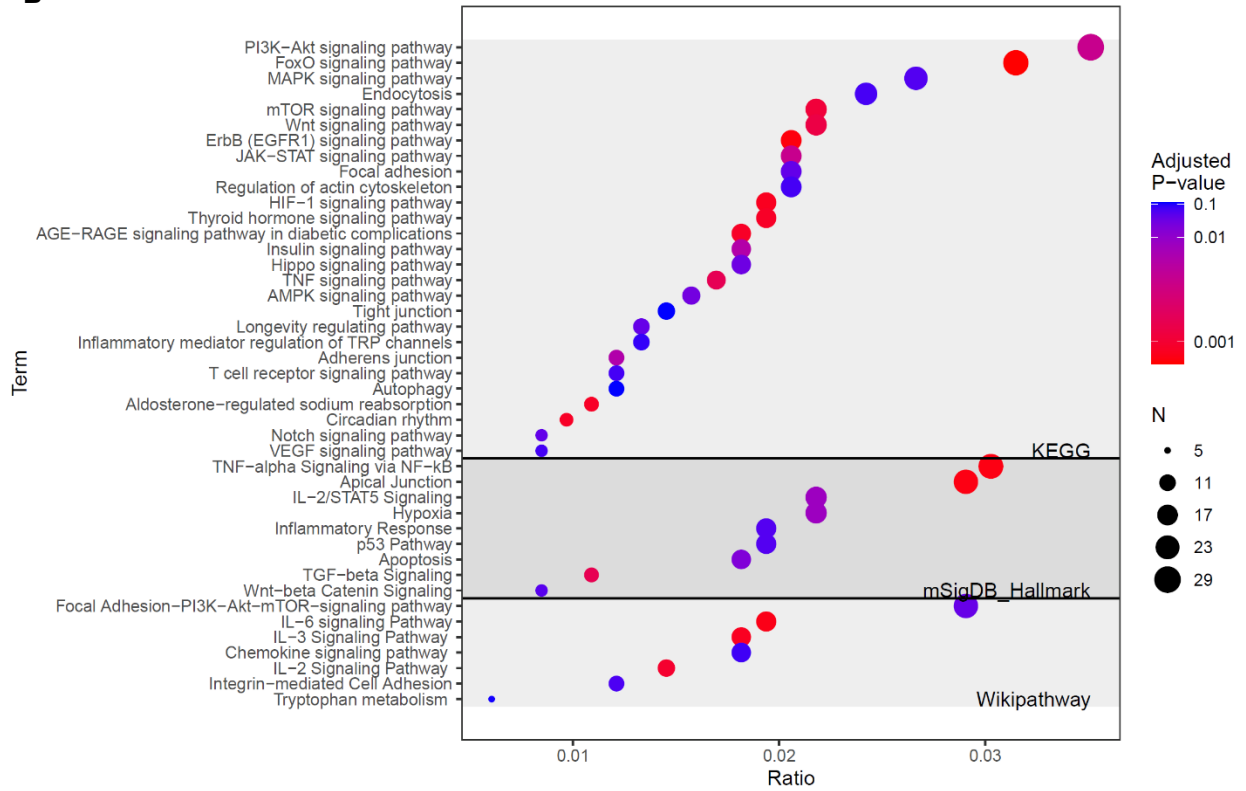
Figure 22. Panther Protein Class categorization of the intrinsically significant sexually dimorphic podocyte genes. 1768 podocyte genes significantly differentially expressed between male and female vehicle treated mice were analyzed using Panther database for GO term “protein class”. See colour legend beside for detailed specification of categories.

Next, GOs were extracted from Panther GO-Slim for sex-DE genes with $p\text{-value} < 0.05$ and $FDR < 0.1$ and gene number > 4 . Interestingly, functional annotation of these 1768 DE genes showed that male and female podocytes had sexually dimorphic genes that were enriched in distinct GOs and pathways. Males had higher expression of genes related to “transcription” and “gene expression”, “kinase activity and signal transduction”, “cytoskeleton and small GTPases regulating activity” (Figure 23A). Females had higher expression levels of genes related to “mitochondrial-oxidation phosphorylation”, “translational initiation factors” and “ribosome”, “protein metabolic process”, “protein modifying activity” including proteolysis, glycosylation and protein folding (Figure 23C). In addition, Enrichr was used to extract enriched KEGG, Wiki pathways and mSig-hallmark. In males, pathways involved in “regulating actin cytoskeleton”, “integrin-mediated cell adhesion”, “hypoxia”, “apoptosis”, “inflammation-related”, “PI3K-AKT, mTOR, MAPK, VEGF signaling pathways” were enriched (Figure 23B). In contrast, females showed pathways enrichment in “oxidation phosphorylation”, “ribosome”, “endocytosis”, “protein export”, “TCA cycle” and “peroxisome” (Figure 23D).



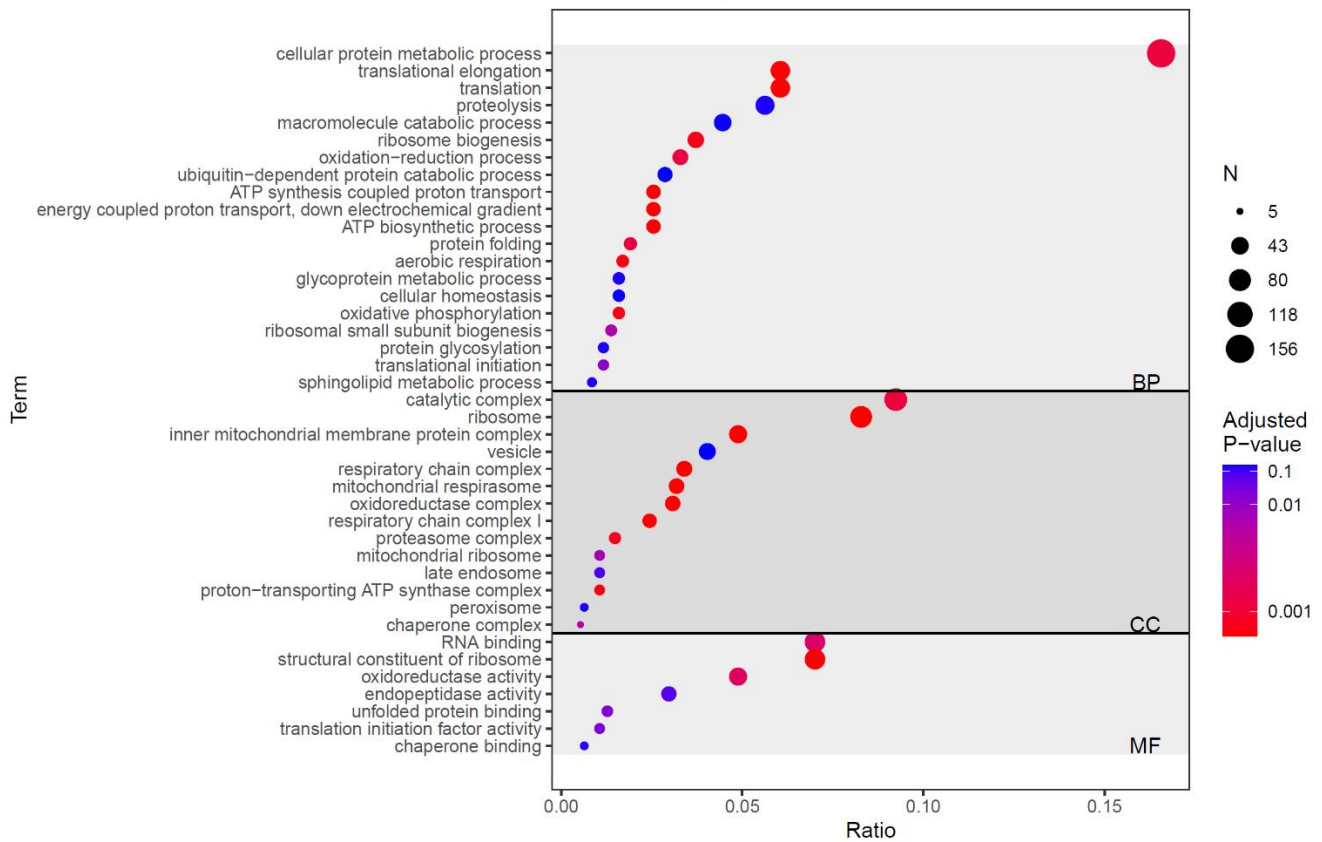
B

Male pathways



C

Female overexpressed



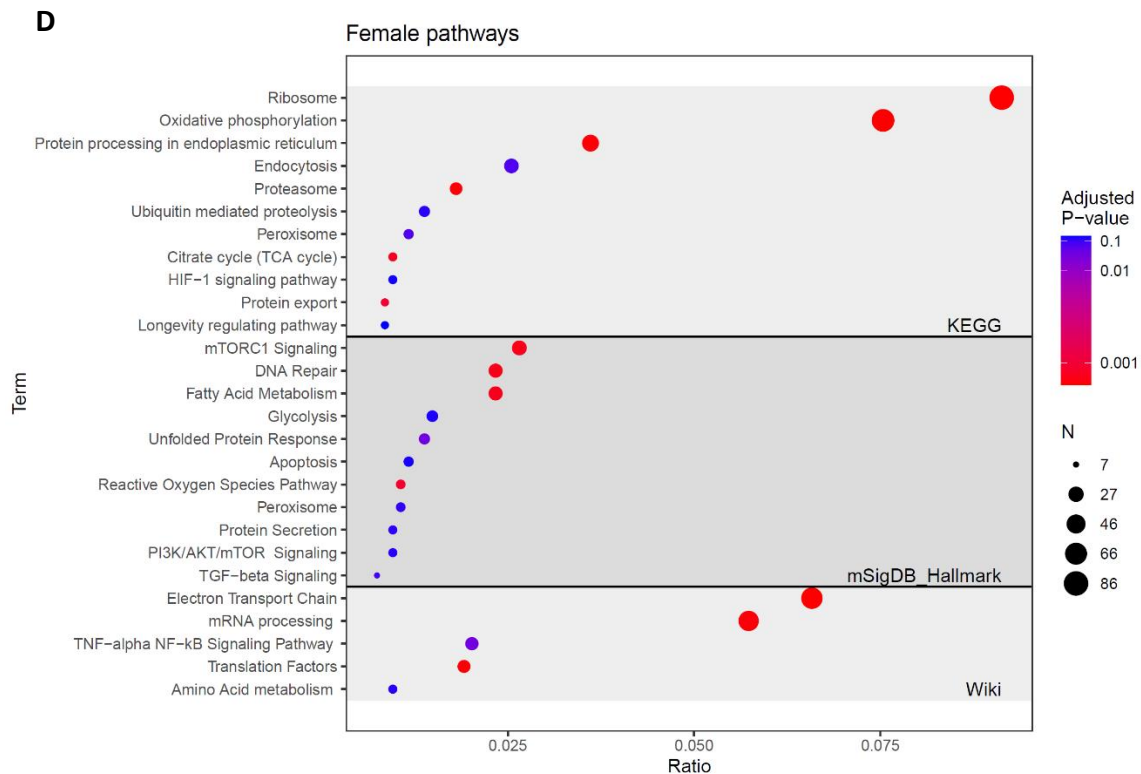


Figure 23. Gene ontology enrichment analyses of sexually dimorphic genes which were intrinsically overexpressed either in males or in females. Male and female podocytes showed 826 and 942 overexpressed genes, respectively. (A and B) Significantly enriched GO terms and pathways for significantly DE genes of podocytes from male and (C and D) female vehicle treated mice; all GO terms were statistically enriched, p value < 0.05 and FDR < 0.1. GO terms in (A and C) were extracted from panther GO-slim. B and C for pathways analysis and hallmark were extracted from Enrichr.

3.4.2.2 Gene set enrichment analyses of treatment-related differentially expressed genes

Next, treatment-related significantly DE genes were subjected to GO enrichment analyses. In male podocytes, rapamycin significantly altered the expression of 132 genes compared to vehicle (63 genes upregulated and 69 genes were downregulated) with p < 0.05 (54 genes with p < 0.01) (Figure 19B, xlx list in Appendix, Table 4). Functional annotation by panther GO and Enrichr online database of these genes resulted in only few significantly regulated GOs (p -value and FDR value < 0.05) with gene number > 4). Only “regulation of transcription, DNA-templated” was significantly upregulated after rapamycin. In contrast, “MAPK signaling pathway” was downregulated (Figure 24). None of the regulated genes were related to mTOR pathways neither podocyte-specific genes except for seven cytoskeletal proteins related/binding/activity genes

(*Gas7*, *Pdlim2*, *Mrtfb*, *Abll*, *Maco1*, *Daam2* and *Hip1r*, all of them significantly upregulated in response to treatment in male podocytes). As already described, female podocytes only significantly regulated three genes in response to rapamycin: *Ptgds*, *Dip2b* and *Ankrd33b* with p adj. value < 0.05.

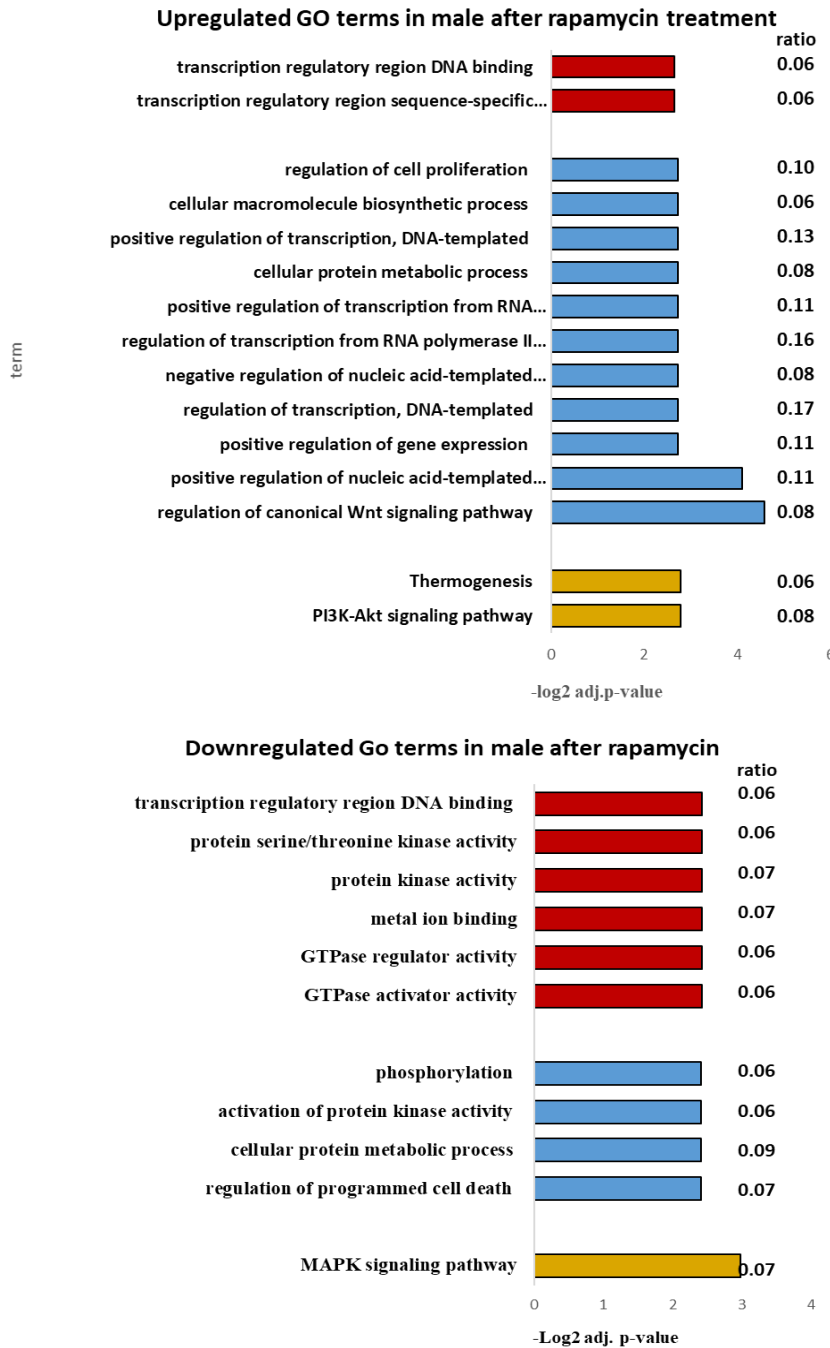
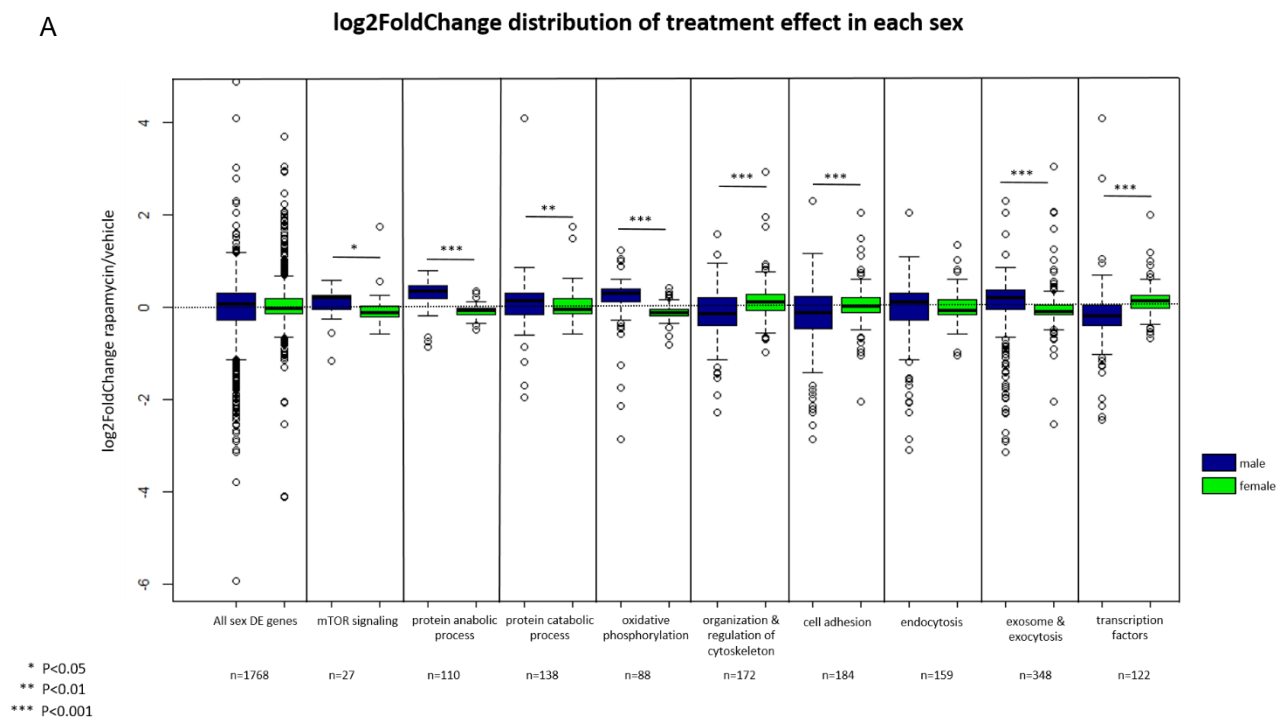


Figure 24. Functional annotation graphs for the significantly differentially regulated genes by treatment in male podocytes. Analysis for major hits for the significantly upregulated (n=66) and downregulated (n=69) genes in KEGG pathways (yellow bars), GO-BP (blue bars), and MF (red bars). Data was generated using Enrichr and results are represented as -log2 FDR (adj. p-value), all GOs with p-value < 0.05 and number of genes > 4.

3.4.2.3 Sexually dimorphic responses to rapamycin in functionally relevant gene subgroups

To investigate the rapamycin-induced expression changes of sexually dimorphic genes in both sexes in more detail, Log2FC in each sex were compared for specific subgroups of intrinsically sexually dimorphic genes which are known to be of high importance for podocyte homeostasis. Wilcoxon ranked sum test was performed to identify significantly sex-different response patterns. Results for specific terms are summarized in Figure 25A. Interestingly, females significantly upregulated sexually dimorphic genes of the terms “organization & regulation of cytoskeleton”, and “transcription factors” and deregulated genes of “mTOR signaling”, “protein anabolic and catabolic process”, “oxidative phosphorylation”, “endocytosis”, “exosome & exocytosis”. In contrast, male upregulated genes related to “mTOR signaling”, “protein anabolic and catabolic process”, “oxidative phosphorylation”, “endocytosis”, “exosome & exocytosis” and deregulated “organization & regulation of cytoskeleton” and “transcription factors” as stress response induced by rapamycin treatment. Cluster analysis and presentation as heatmap of the z-scores of the average transcript number for these GOs of interest confirmed strong intrinsic sexual dimorphism and distinct responses to rapamycin, yet showed less strong clustering for treatment responses (Figure 25B).



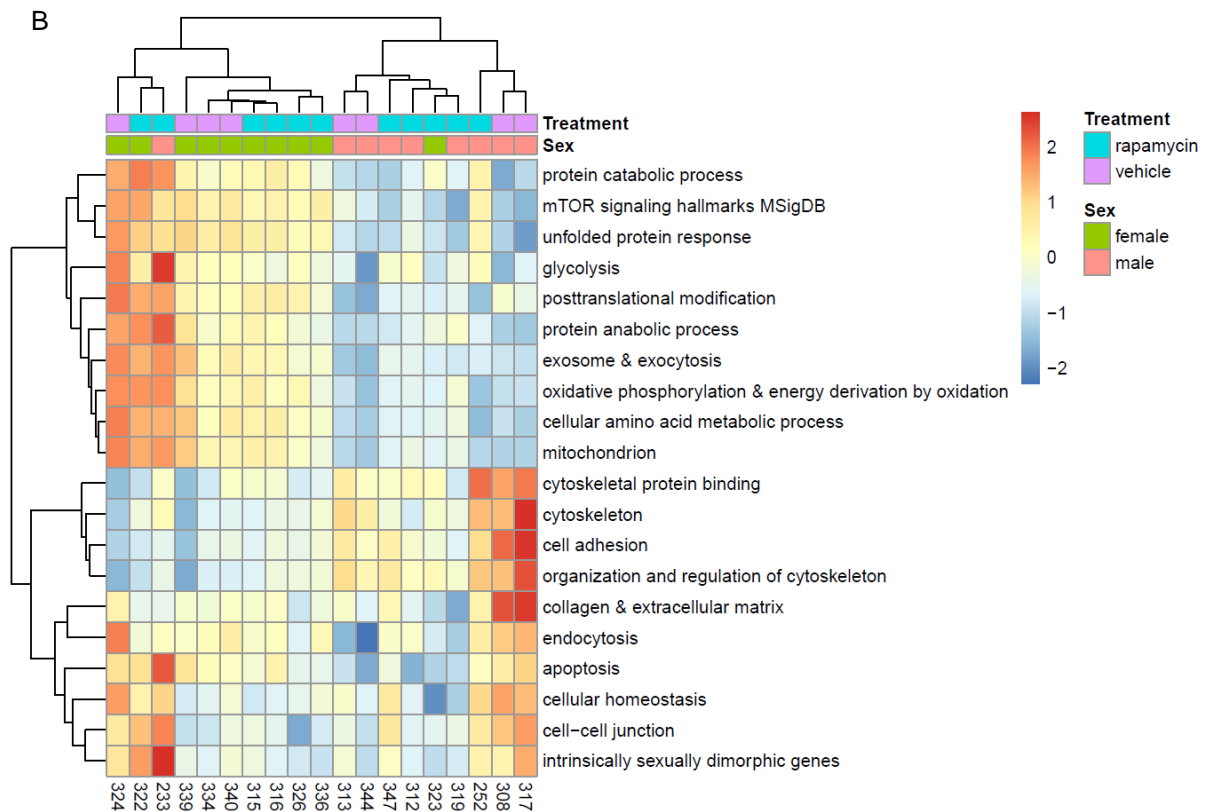


Figure 25. Sexual dimorphism in responses to rapamycin in functionally relevant subgroups of sexually dimorphic genes. Rapamycin led to a number of significantly opposed gene expression alterations comparing male and female podocytes by (A) individual Log2FC for specific gene GO subgroups displayed in whisker plots (n = number of genes within specific term, significance levels * $p < 0.05$, ** $p < 0.01$, *** $p < 0.001$ as determined by Wilcoxon ranked sum test), and as displayed in (B) heatmap of z-score of the average transcript number of all genes related to the GO term of interest.

3.4.3 Gene set enrichment analysis (GSEA) of whole transcriptome

Taking into account the whole male and female transcriptome of vehicle and rapamycin groups, gene set enrichment analysis (GSEA) resulted in comparable major GOs which had already been identified investigating only the intrinsic sexually dimorphic podocyte transcriptome (Table 12 summarizing the major hits from KEGG pathway analysis of sexually dimorphic genes using enrichr). GSEA analysis was performed with GSEA software using molecular signature database (mSigDB 7.2 released Sep.2020) (45, 101). The complete list of significantly enriched GOs for the different comparisons between male and female vehicle and rapamycin groups can be found in Appendix, Table 5, more detailed descriptions follow in the next chapter.

Table 12: Major hits of KEGG pathway analysis of significant sexually dimorphic genes.

KEGG pathway term	count	p-value	FDR	Enrichment factor
Ribosome	84	2.61E-43	7.52E-41	10.52
Oxidative phosphorylation	69	2.86E-37	4.12E-35	11.34
Protein processing in endoplasmic reticulum	41	5.47E-10	1.97E-08	3.52
FoxO signaling pathway	33	3.02E-08	9.68E-07	3.48
Proteasome	17	1.67E-07	4.36E-06	6.09
HIF-1 signaling pathway	25	2.99E-06	6.63E-05	3.29
ErbB signaling pathway	21	9.45E-06	1.94E-04	3.46
Circadian rhythm	11	2.81E-05	5.40E-04	6.00
Aldosterone-regulated sodium reabsorption	12	6.75E-05	0.00114	4.78
mTOR signaling pathway	29	7.62E-05	0.00121	2.41
Endocytosis	43	1.03E-04	0.00156	1.98
Citrate cycle (TCA cycle)	9	0.00139	0.01481	4.05
Ubiquitin mediated proteolysis	23	0.00225	0.02077	2.08
Protein export	8	0.00228	0.02077	4.14
PI3K-AKT signaling pathway	48	0.00230	0.02077	1.62
AGE-RAGE signaling pathway in diabetic complications	18	0.00309	0.02623	2.25
Wnt signaling pathway	25	0.00365	0.02963	1.92
N-Glycan biosynthesis	11	0.00370	0.02963	2.92
Adherens junction	14	0.00382	0.02980	2.50
Focal adhesion	29	0.00518	0.03930	1.77
TNF signaling pathway	18	0.00776	0.05457	2.03
Regulation of actin cytoskeleton	30	0.00952	0.06097	1.66
Apoptosis	21	0.01243	0.07022	1.81
AMPK signaling pathway	19	0.01489	0.07800	1.84
Autophagy	19	0.02022	0.09705	1.77
Ras signaling pathway	30	0.02386	0.10907	1.53

3.4.4 Transcriptional differences in selected GO terms which appeared significantly enriched in GSEA of the whole transcriptome

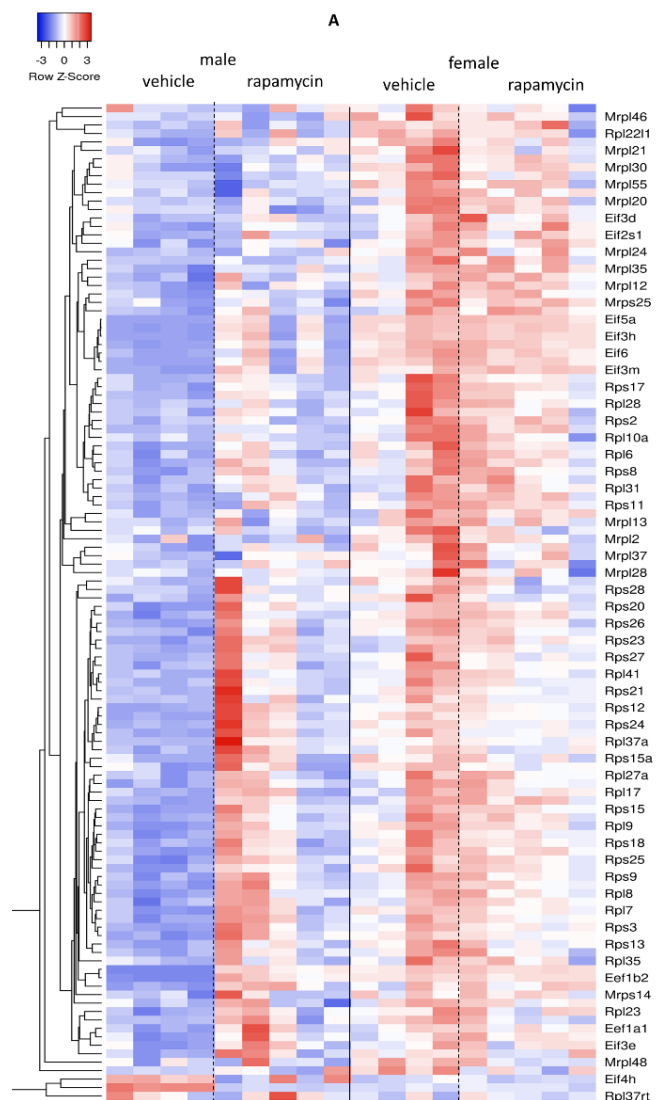
3.4.4.1 GOs including genes relevant for podocyte proteostasis

“Ribosome”, “Protein processing in ER”, “Proteasome”, and “Ubiquitin-mediated proteolysis” appeared under the strongest significantly enriched GO’s (Table 12, Appendix, Table5).

A heatmap was prepared showing the significantly differently expressed **ribosomal genes and genes involved in translation and ribosome biogenesis** (Figure 26A). Interestingly, 73

ribosomal genes coding for 2/3 of all known ribosomal proteins, 26 mitochondrial ribosomal proteins, 4 aminoacyl-tRNA synthase (*Fars*, *Nars*, *Sars* and *Mars*), 19 initiation and 6 elongation factors were intrinsically significantly higher expressed in female podocytes. Only 4 initiation factors (*Ago1*, *Ago2*, *Ago3*, *Guf1*) had a higher intrinsic transcript level in male podocytes.

After rapamycin treatment, this striking sexual dimorphism was abrogated by an increased interindividual variability in ribosomal gene expression in both sexes. Except for *Rrp36* and *Rrp7a*, male ribosomal proteins generally showed a higher expression in rapamycin treated males compared to vehicle males whereas females only responded with neglectable changes, except for moderate downregulations of *Rpl221l*, *Mrpl21* and *Rpl36al*.



Elongation and initiation factors showed comparable opposite responses to rapamycin in each sex, with males upregulating genes, e.g. *Eef1b2* and *Eif3m*, and females mostly keeping their expression levels or mildly downregulating, e.g. *Eef1*, *akmt2*, *Eif2s2*, *Eif2b3* and *Eif3l*. (Figure 26)

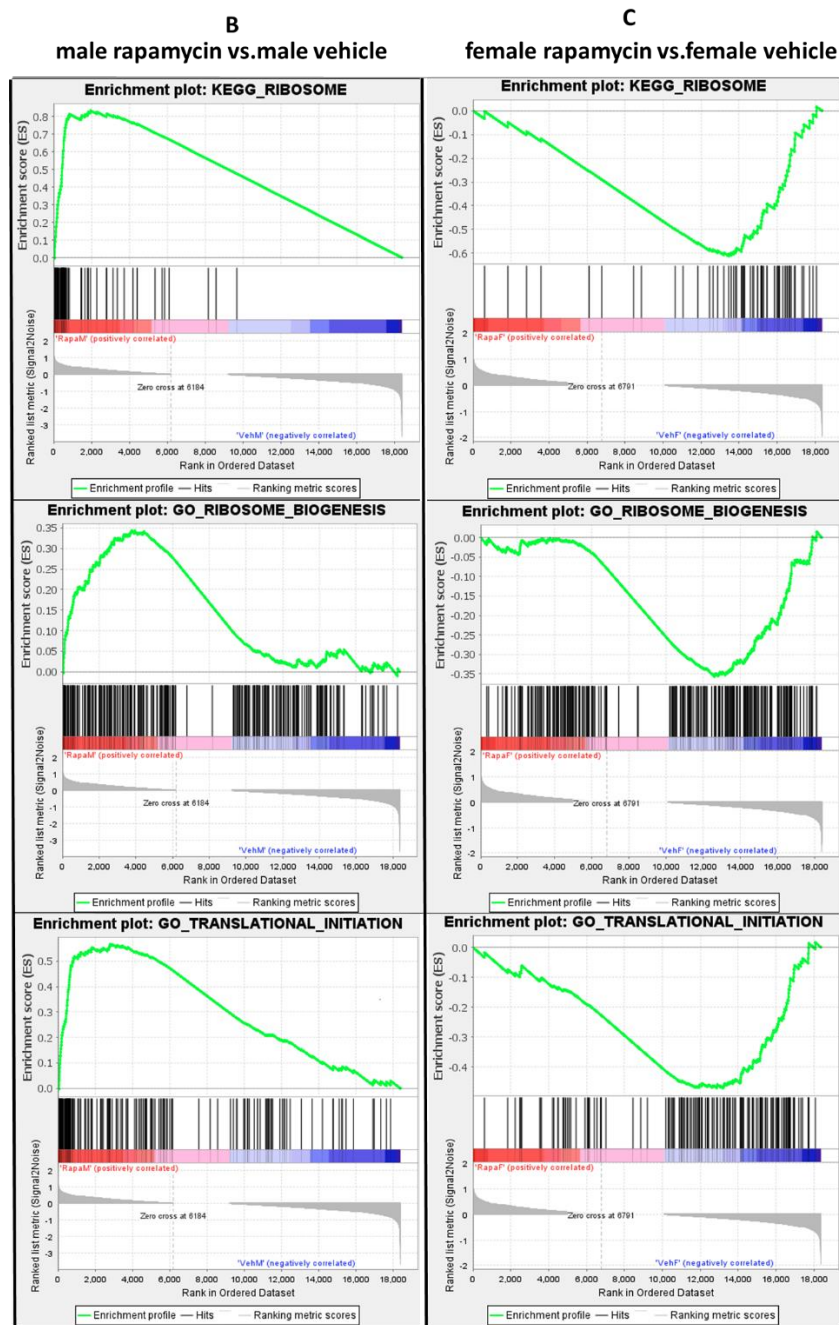
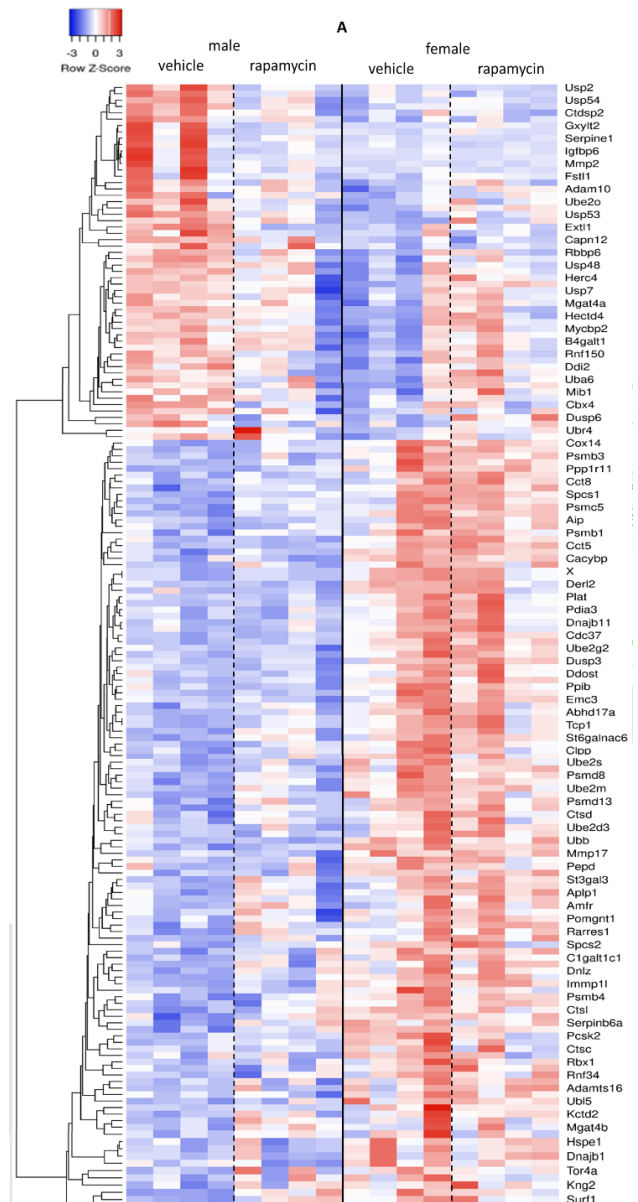


Figure 26: Heatmap of significant sexually dimorphic ribosomal genes, translational factors and genes involved in ribosome biogenesis of podocytes from all experimental groups. (A) Heatmap represents gene expression data of genes coding for ribosomal proteins and translation factors which were significantly higher expressed in female vehicle podocytes compared to male with p value <0.05. Heatmap were developed using Heatmapper (B/C) GSEA enrichment plots for treatment effects (rapamycin vs. vehicle) in each sex.

Post-translational modifications (PTMs) including **phosphorylation, glycosylation, ubiquitination and proteolysis**, change the functional diversity of the proteome by addition of functional groups or proteins, proteolytic cleavage of regulatory subunits, or degradation of entire proteins, regulating cellular activity, localization of proteins and modulating protein-protein interactions and stability. Interestingly, 11.2% of all intrinsically sexually dimorphic genes were related to PTMs (18 protein folding, 13 glycosylation, 30 ubiquitin-ligase and 24 proteasome-mediated ubiquitination related genes). Only 13 genes were differently regulated after rapamycin treatment only in males (Figure 27A, Figure 23).

It is well-known that intracellular protease activity is crucial for podocyte homeostasis (121, 122) Panther analysis identified 59 intrinsically significantly differently expressed genes with **protease activities** (PC00190) (metalloproteases, serine, cysteine and aspartic proteases) and 13 genes with **proteases inhibitor activity** (PC00191), e.g. *Serpinh1*, *Serpinh9*, *Serpinh6a* and *Rarres1*. Out of these protease genes, 35 were overexpressed in female podocytes (under them Cathepsin L (*Ctsl*), cathepsin C (*Ctsc*), *plat*, and *MMP23*) compared to 22 genes in males. In addition, 16 **proteasome subunits related genes** were sex-differently expressed with significant enrichment in females (enrichment factor 7.2, p value 0.0003 with Log2FC0.25-0.8). A strong sexual dimorphism was further observed in



response to rapamycin for genes related to **protein folding and proteasome** but not for glycosylation and ubiquitination. Yet, male downregulated *Usp2*, *Mmp2*, *Serpine1* and many glycosylation-related genes to more than half. On the other hand, female transcriptome remained rather unchanged in response to rapamycin treatment (more than 70% of all DE genes). Those few, including *Ctsl*, *Capn12*, *Usp54*, *Clpp*, *Serpinh6a* and *Rnf144b/150* (which affect BAX

proteolysis and protect from cell death), were upregulated only in females in response to rapamycin. (Figure 27)

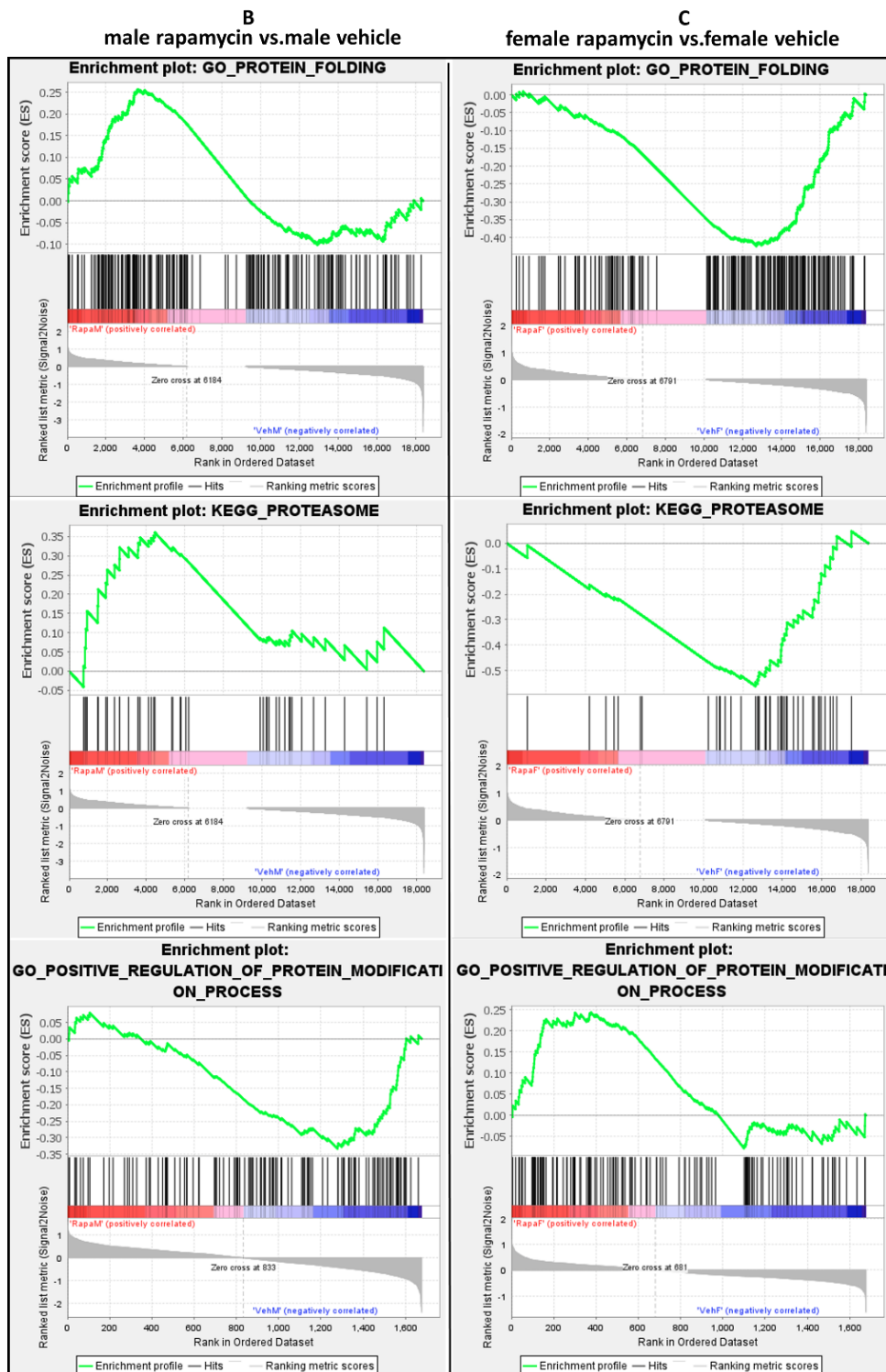


Figure 27: Sexual dimorphism of PTM-related genes. (A) enrichment analysis of protein folding- and proteasome-related genes show-significantly different regulation between sexes by rapamycin treatment. (B) Heatmap of all significantly DE genes between vehicles related to GO protease, folding proteins, ubiquitination, proteasome and glycosylation (adj. p-value<0.05).

3.4.4.2. GO's including genes relevant for podocyte energy homeostasis and metabolism

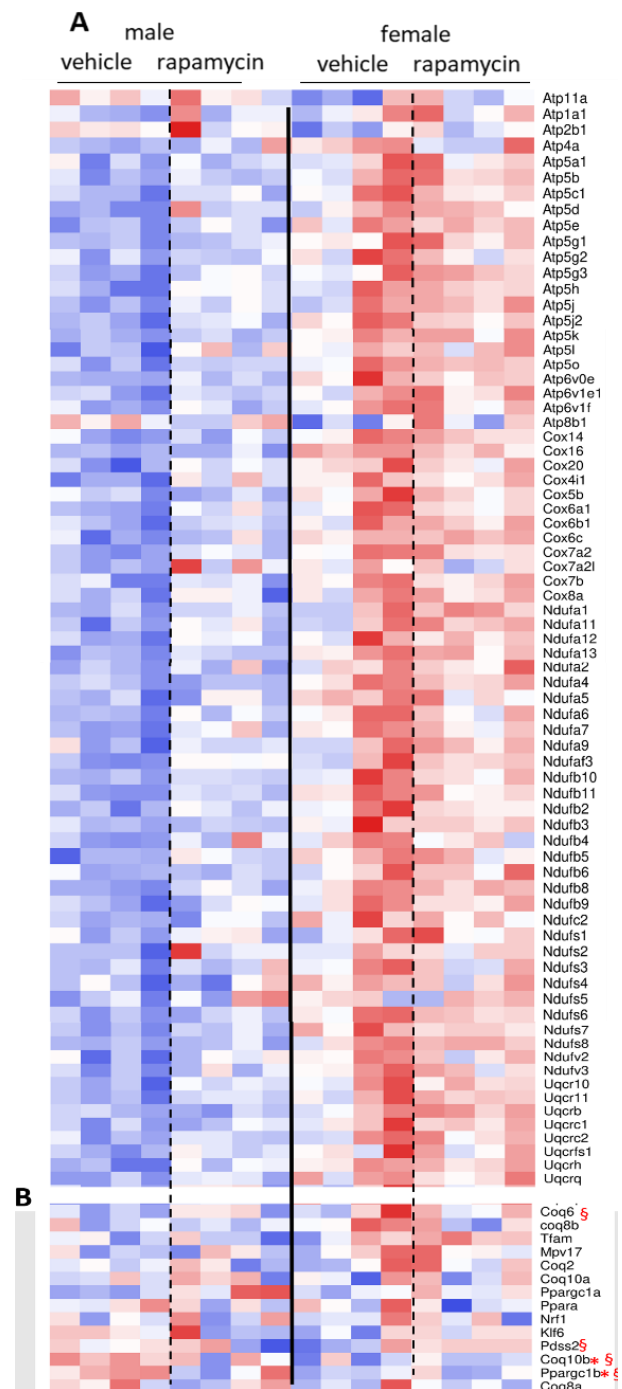
Another major significantly regulated GO term in all different experimental groups was “oxidative phosphorylation” (Table 12, Appendix Table 5).

Mitochondria are essential organelles which play a major role in energy homeostasis through oxidative phosphorylation. **76 transcripts encoding for mitochondrial proteins of the oxidative phosphorylation system** were identified to be significantly (adj. p-value < 0.05)

DE between male and female podocytes under basal condition (vehicle control), under them 54 highly significantly different with adj. p-value < 0.01. Except for three genes (*Atp8b1*, *Atp11a* and *Atp2b1*), all of the highly significant sexual dimorphic mitochondrial genes were higher expressed in female podocytes compared to males and annotated for genes of all five mitochondrial membrane complexes (enrichment factor 7.19, adj. p-value < 0.000001). Rapamycin treatment elicited again opposite changes in male and female mitochondrial gene expression levels while male responded mainly with upregulation of these genes to 1.2- up to 2-fold and females only showed slight expressional changes (Figure 25 and 28A, B).

As many **well-known mitochondrial genetic diseases are associated with nephrotic syndrome and podocytopathies** (46), mitochondrial related genes with known mutations causing nephrotic diseases were analyzed. Only *Coq10* and *Ppargc1b* showed significant sex differences at baseline and sexual dimorphic responses to rapamycin were observed

for *Coq6*, *Coq10b*, *Ppargc1b* and *Pdss2* (Figure 28C).



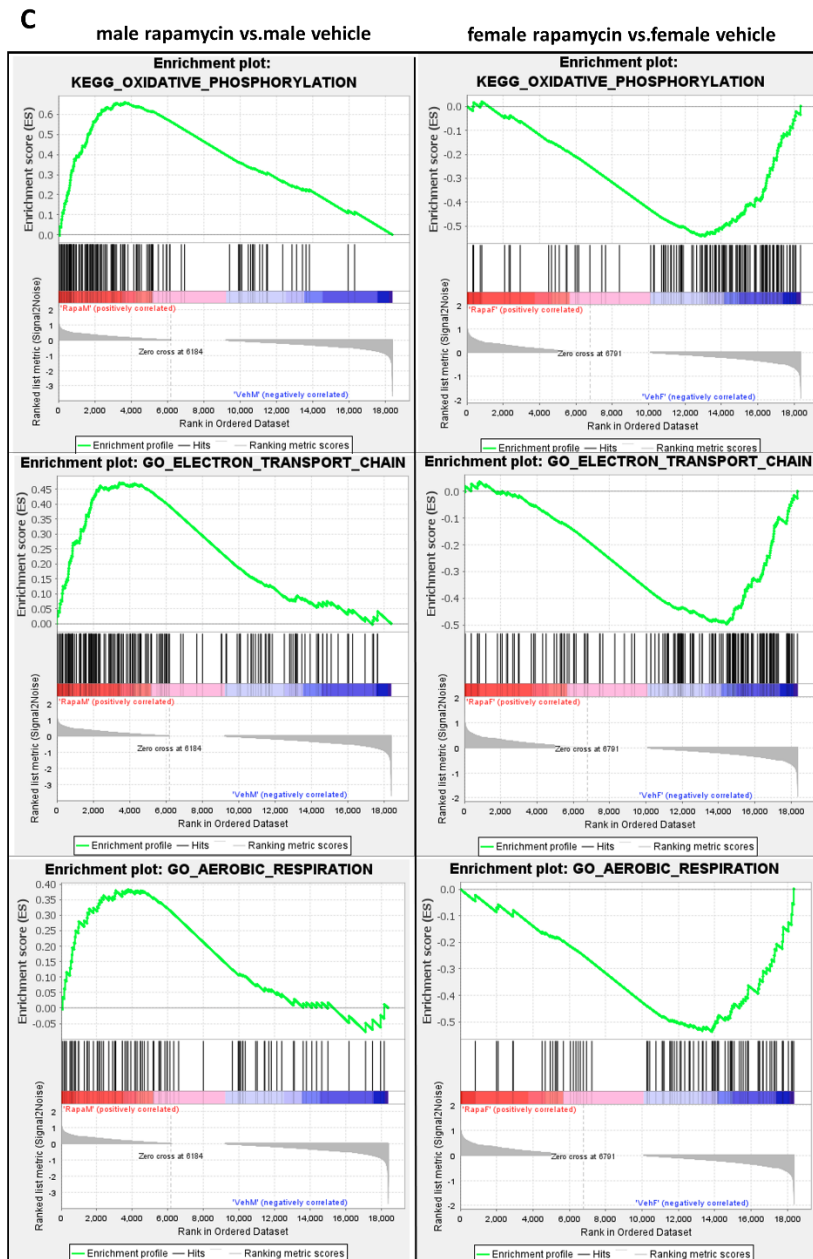
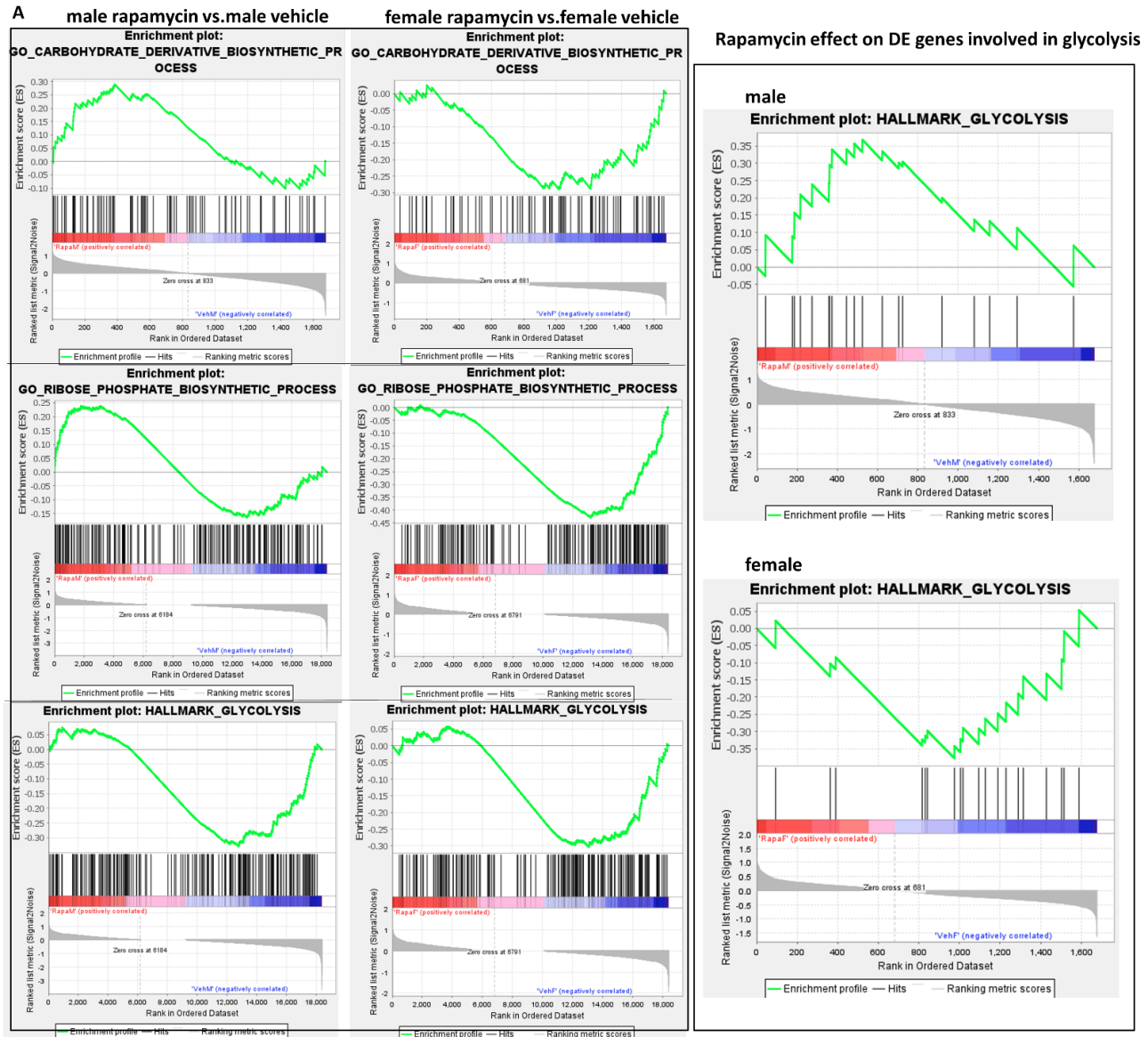


Figure 28. Sexually dimorphic response of mitochondrial genes coding for proteins of the oxidative phosphorylation system (A) Gene expression data of the normalized transcript numbers of the 79 mitochondrial specific transcripts which are significantly higher expressed in female vehicle podocytes compared to male podocytes (B) Heatmap of expression levels of nephrotic-disease-related mitochondrial genes in all experimental groups. (C) Enrichment plots of oxidative phosphorylation genes of male and female podocytes showing opposite treatment responses in both sexes.

Previous publications have demonstrated that mTOR inhibition is associated with hyperglycemia in 10-50% of patients (123). In this study, gene enrichment analyses on sexually dimorphic genes pointed to a significant overexpression of **glycolysis/TCA genes** in females (enrichment factor of

2, adj.p-value 0.009) (Figure 23). Overall, RNA-seq (GSEA analysis; KEGG pathway) showed that rapamycin significantly downregulated glycolytic genes in females (p<0.02) and non-significantly in males, yet, many genes involved in glycolysis which are significantly differently expressed between vehicles and more specifically those of rate limiting steps were upregulated in males but not in females podocyte. (Figure 29)



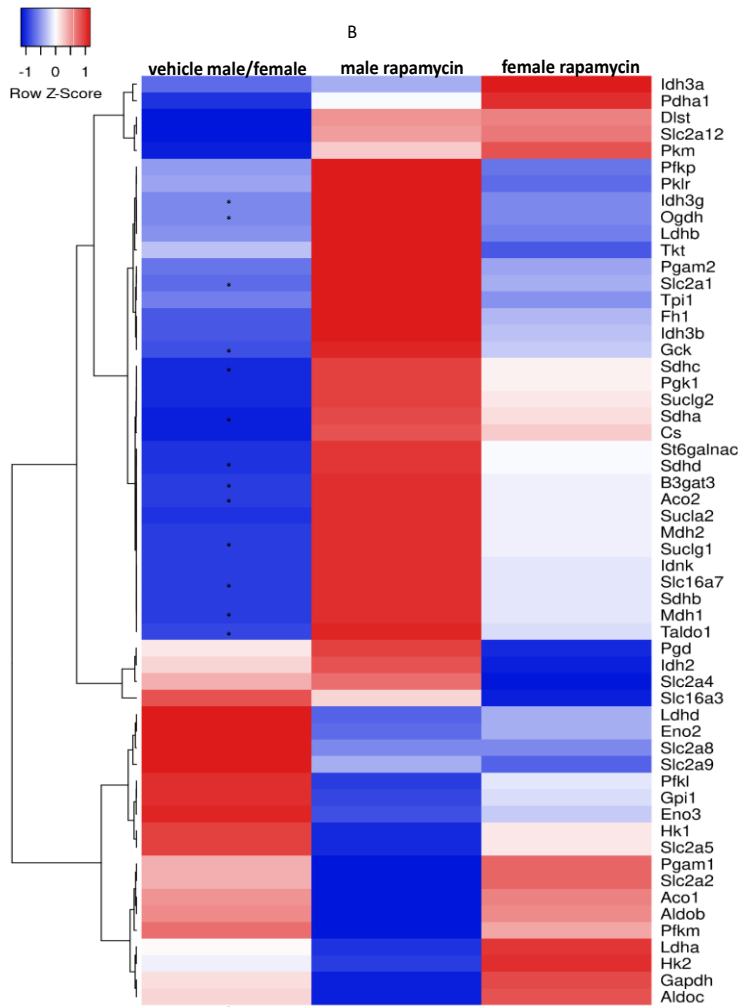


Figure 29. Gene expression changes of glycolysis and TCA cycle genes in male and female podocytes in response to rapamycin. (A) Enrichment plots point to decreased glucose synthesis and metabolism in female after rapamycin, while glucometabolic processes were increased in male. (B) Heatmap displaying the Log2FC of glycolytic, TCA and PPP genes between all experimental groups. Males had intrinsically decreased expression levels of most enzymes involved in glycolysis and TCA cycle compared to female podocytes. Response to rapamycin were sexually dimorphic, such as females maintained or reduced many gene expressions while males upregulated their expression (second and third lane). * Indicates significantly DE genes (p<0.05).

GLUT3/5/8/9, part of the known 14 GLUTs, which are relevant for the glucose uptake in cells, showed a remarkable decrease after rapamycin in both male and female podocytes, whereas GLUT 1 and GLUT12 remained largely unaffected by treatment. In contrast, GLUT2 showed a sexual dimorphic response to rapamycin, such as male dramatically downregulated GLUT2 (80% reduction compared to vehicle) and female upregulated to 1.5 times their gene expression in response to rapamycin.

Genes coding for **enzymes involved in the pentose phosphate pathway PPP** (*Taldo 1*, *pgd*, and *Tkt*) were higher expressed in female podocytes compared to males at baseline and decreased in

response to rapamycin in females, whereas males maintained/slightly increased their expression levels.

Finally, three genes related to **carbohydrate metabolism** (*St6galnac6*, *Idnk* and *B3gat3*) were found to be significantly differently regulated between male and female podocytes with sexually dimorphic response to rapamycin. The entire carbohydrate biosynthetic process appearing in the enrichment plots in Figure 29A showed an increased expression in only males upon rapamycin treatment.

In contrast to these energy-producing and anabolic processes, catabolism by **autophagy** also plays a major role in podocyte homeostasis (124). It appeared as a relevant GO when categorizing intrinsically sexually dimorphic genes. *Ambra1* and *Rb1cc1*, components that bind to ULK complex through the initiation of autophagy, showed intrinsically significantly higher expression in male podocytes. Sexual dimorphism in response to rapamycin was also observed, such as only females upregulated most autophagy-related gene expressions. Atgs involved in phagophore and sequestration steps, were slightly higher expressed in females, yet responses to rapamycin varied between different Atgs. *Map1lc3a/b*, *Sqdtm1* receptor, and *VAMP8*, involved in autophagosome formation and lysosome fusion, displayed sex-different reaction to rapamycin with downregulation in females and upregulation in males.

Interestingly, many kinases and TFs, such as *Tfeb*, *Atf4* and *Atf6*, which regulate autophagy were also significantly sexually dimorphically expressed. *Xpb1* is also among the differentially regulated genes at baseline and was upregulated in males and downregulated in females after rapamycin. *Xpb1* functions as a stress-inducible potent transcriptional activator during endoplasmic reticulum (ER) stress by inducing UPR target genes via binding to the UPR element (UPRE). Also, it improves glucose homeostasis in ER stress through both, binding and proteasome-induced degradation of the transcription factor FOXO1, resulting in suppression of gluconeogenic genes expression and in a reduction of blood glucose levels (125).

3.4.4.3 Other GO's including genes relevant for adaptation processes in response to stress

Antioxidative capacity is another important prerequisite for the cell's homeostasis under stress conditions. Female podocytes displayed enrichment for the "Reactive Oxygen Species Pathway pathway" at baseline compared to male (Figure 23). Twenty genes related to **antioxidants, redox**

genes, glutathione proteins, peroxiredoxin (Prdx), thioredoxin and genes coding for peroxisome related proteins showed mainly intrinsically significant higher expression in female podocytes. Most peroxisome genes decreased in females in response to rapamycin whereas males upregulated some, such as *Pex2*, *Pex3* and others down, such as *Pex11* and *Pex26*. (Figure 30)

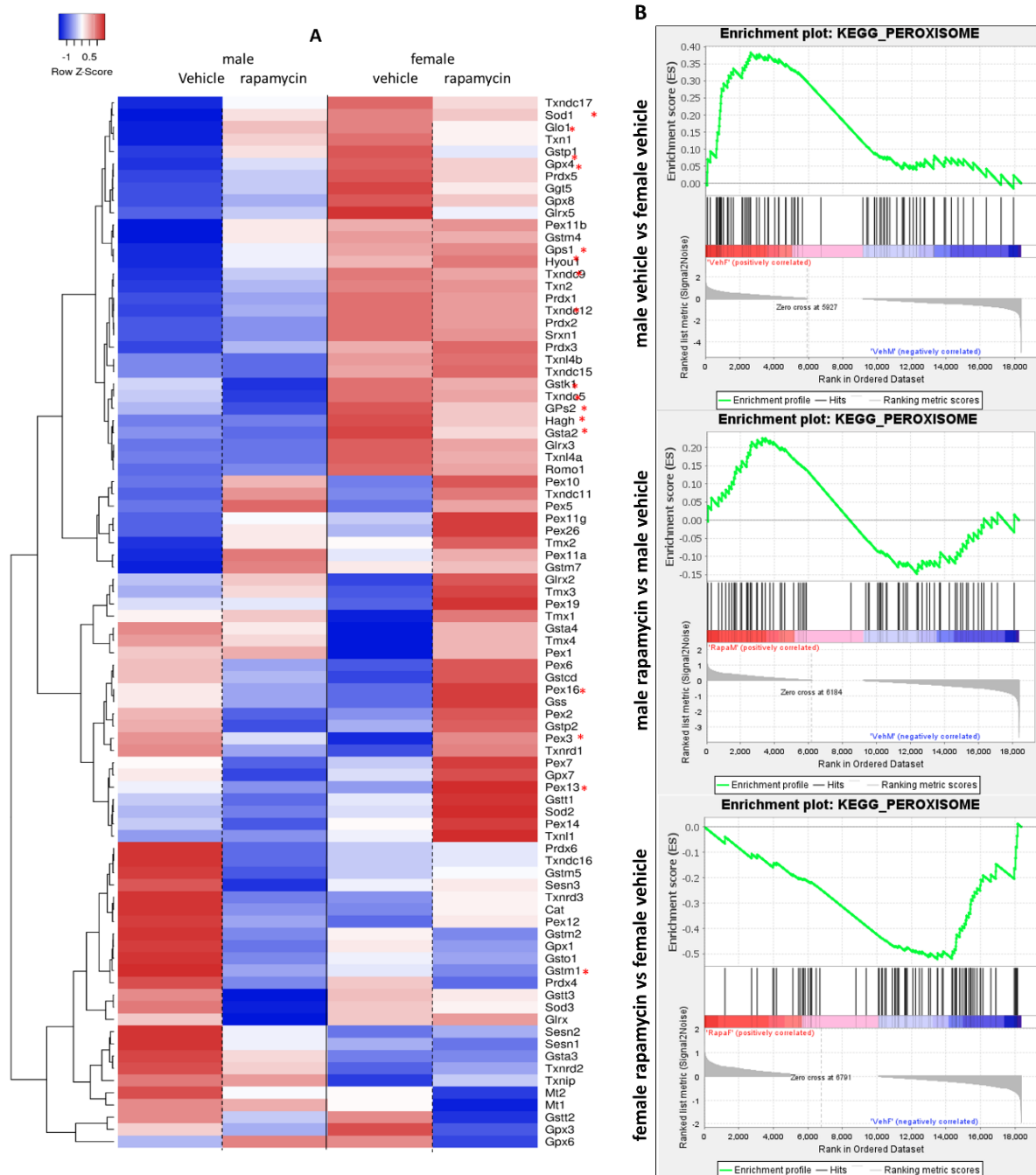


Figure 30. Redox genes show sexual dimorphic expression levels at baseline and with rapamycin. (A) Heatmap illustrating average transcript numbers of redox genes. (B) Enrichment plots for genes related to KEGG peroxisome. * indicates significantly DE genes (p-value < 0.05).

Pro- and anti-apoptotic mechanisms further regulate cell fates under stress conditions. Remarkably, **female podocytes had higher levels of most pro-apoptotic genes and positive regulators for apoptosis** such as *Bak1*, *Bcl10*, *Bax*, *Cyts* and *P62* compared to males. Respectively, the opposite could be observed for the **anti-apoptotic genes, where male podocytes showed significantly higher expression** (e.g. *Bcl211*, *Bcl6*, *Bcl9*, *Bcl3* and isoforms, $p < 0.01$).

GSEA showed that rapamycin caused an overall upregulation of apoptotic pathway in females and downregulation in males (figure 31). All identified caspases showed no sex-differences at baseline. Most of them were downregulated in males (Log2FC of -0.5 to -0.3) in response to rapamycin treatment, but not in females. *Diablo* gene increased in response to rapamycin in males which could explain the upregulation of *cytochrome c/Apaf-1* but not *Casp9* genes.

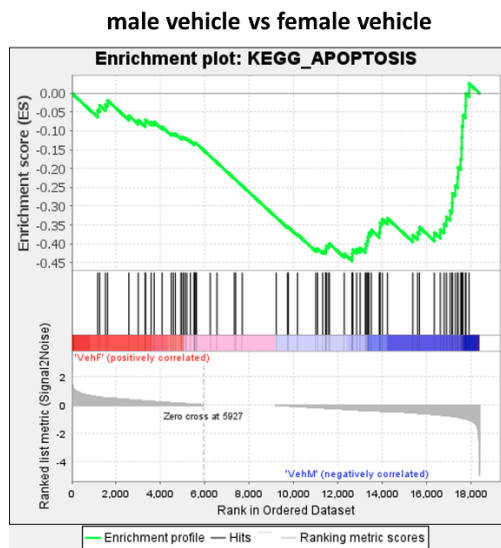
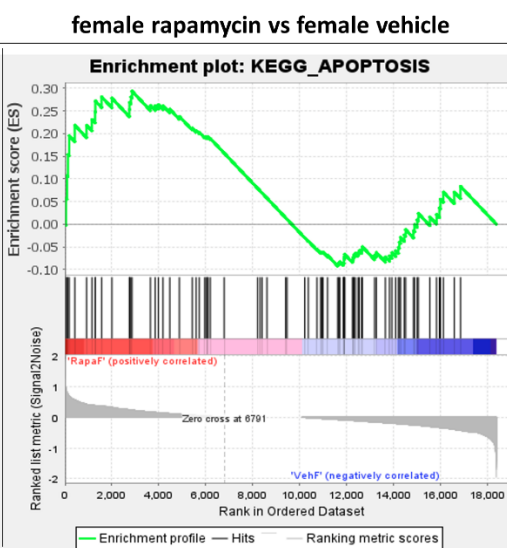
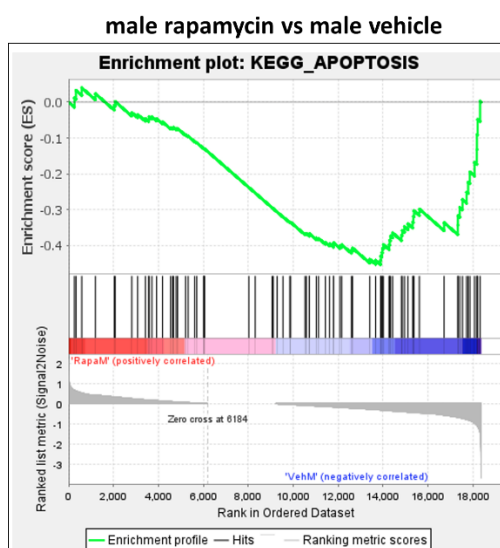


Figure 31. Apoptotic genes respond differently to rapamycin in male and female podocytes. Enrichment plots on 81 apoptotic genes analyzed by GSEA software, show a downregulation of apoptotic genes in male podocytes and upregulation in females in response to rapamycin.

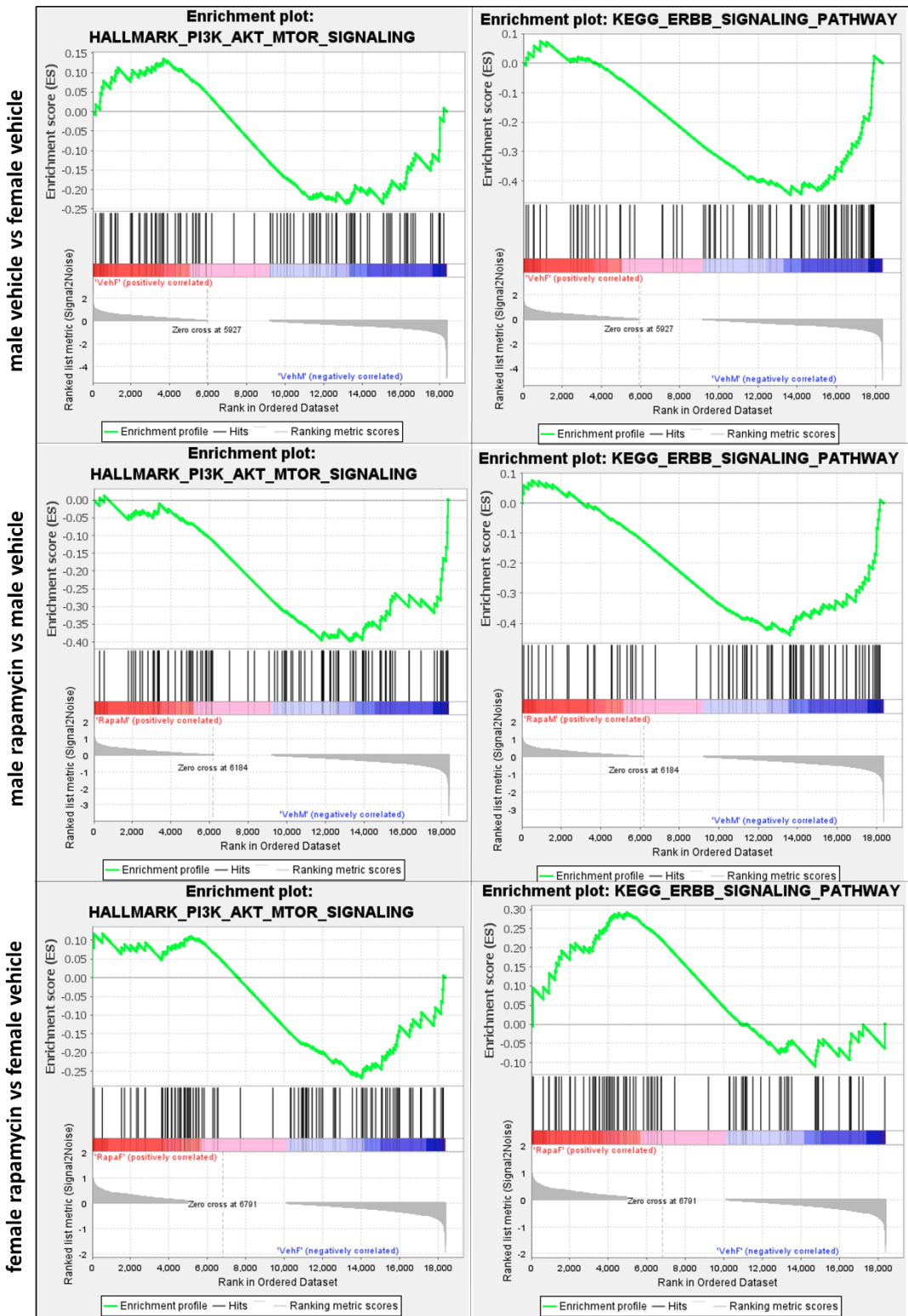


Intrinsic sexual dimorphism and sexual dimorphic stress responses to rapamycin treatment were also observed in **cell survival signaling pathways, such as the PI3K/AKT pathway, tyrosine kinases and sphingolipid signaling**. In total, 48 PI3K/AKT pathway related genes were intrinsically sex-differently expressed, such as GSK3 β , most of them less in females. Females responded to rapamycin rather with enrichment of signalling genes, whereas males mainly showed de-enrichments (Figure 32A, GSEA analysis, Appendix, Table 5).

Additionally, tyrosine kinases and phosphatases are highly enriched in podocyte (106). Four tyrosine kinases receptors genes (part of the ErBB signaling pathway), *Tyro3*, *Axl*, *Ror1* and *Abl1* and ten phosphatase kinases (*Ppp1ca*, *Ppp2ca*, *Ptpa*, *Ssu72*, *llkap*, *Ptp4a2*, *Ptpn23*, *Ptpn3* and *Ptprd*) were found to be intrinsically significantly overexpressed in male podocytes (p-value<0.05, log2FC 0.4 to 0.7 male/female). Tyrosine kinase receptors interact with AKT and MAPK pathways, regulate proliferation, cell migration and adhesion, apoptosis, etc. In response to rapamycin, male podocytes downregulated many of these genes and females mainly upregulated these kinase genes. For example, *Phlpp2* is a protein phosphatase responsible for the regulation of AKT/Pkc signaling pathway and dephosphorylates AKT specifically at Ser473 (126). Rapamycin caused downregulation of *Phlpp2* expression in males and was maintained in females after rapamycin. that could strongly explain the increased phosphorylation of AKT at 473 observed in males but not females. Other well recognized kinases which play a role in podocyte homeostasis and show sexual dimorphic response to rapamycin are *Aak1*, *Sphk2* and *Cerk*. *Aak1* regulates clathrin-mediated endocytosis which was downregulated by 40% only in males (Figure 32B).

Sphingolipids are important as structural components of cells as well as signaling molecules. Beyond regulating different cellular processes such as apoptosis, cell proliferation, cell migration and inflammation, they play a role in the synthesis of ceramides which are important for podocyte homeostasis (127). *Sphk2* (Sphingosine kinase 2) and *Cerk* (Ceramide kinase) were found to be sexually significantly differently regulated at baseline and after rapamycin. Both were overexpressed in female podocytes with almost twice higher expression compared to males (log2FC of 1.01 female/male vehicle). In response to rapamycin, males upregulated both genes, significantly for *Sphk2*, while females slightly downregulated both genes (Figure 32B).

A



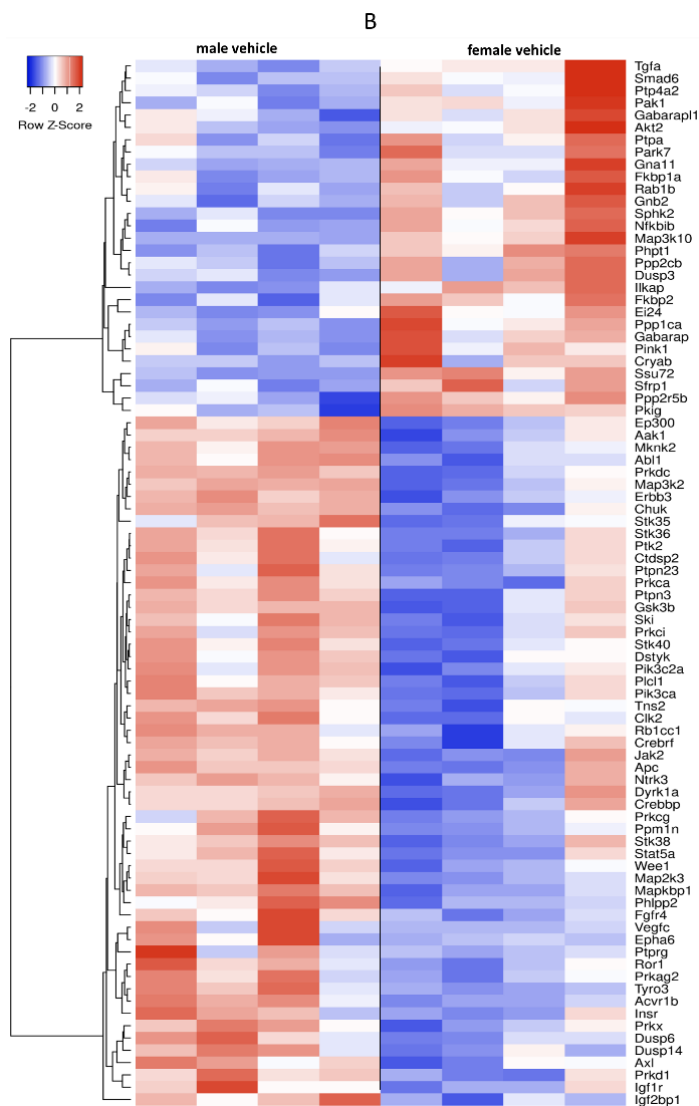


Figure 32. Gene expression changes of signaling pathway in male and female podocytes in response to rapamycin.

(A) Enrichment plots point to different response in signaling pathways expression in male and female after rapamycin.

(B) Heatmap displaying all the significantly differently expressed kinases related genes between vehicle groups. Males had intrinsically higher expression levels of most kinases compared to female podocytes. Response to rapamycin were sexually dimorphic, such as females maintained or increased many gene expressions while males downregulated their expression.

Finally, many **transcription factors (TF)** showed significant intrinsic sexual dimorphism, as identified by the GO’s “DNA-templated transcription” and “transcriptional factors” (Figure 23). 104 genes related to “DNA-binding transcription factor” (PC00218) and 13 genes of “transcription cofactor” (PC00217) showed intrinsic and treatment-related sexual dimorphism (p-value <0.05). Only 11 genes were belonged to general transcription factors which are necessary to initiate transcription (*Eloc*, *Elob*, *Med12*, *Med28*, *Med29*, *Med31*, *Supt49*, *Tceal9*, *Tcerg1*, *Taf46*, *Taf4*, *Taf10* and *Dido1*). Furthermore, more than 80% of these genes had higher expression in male podocytes, such as *Arntl*, *Osr2*, *Nfil3*, *Foxs1*, *Naca*, *Emx1*, *Smad6*, *Jund*, *Thra*, *Atf5* and *Tle5*. The heatmap in Figure 34 illustrates all intrinsically significantly DE TFs genes and the expressional changes by treatment. 26 zinc finger protein transcriptional factors were higher expressed in males, as well as eight circadian genes, under them *Per1*, *Per2*, *Per3*. Statistical analysis of treatment effects to transcription factor expression levels in each sex resulted

in significant downregulation of intrinsically sexually dimorphic transcription factors in male compared to females, with only 8 significantly downregulated genes. (Figure 25A). *Mlxip*, a TF that regulate glycolytic genes target, was intrinsically highly expressed in female podocytes, further increased in response to rapamycin, whereas it was then downregulated in males. *Tcf4*, which regulate β -catenin and the actin cytoskeleton reacted comparably. (Figure 33)

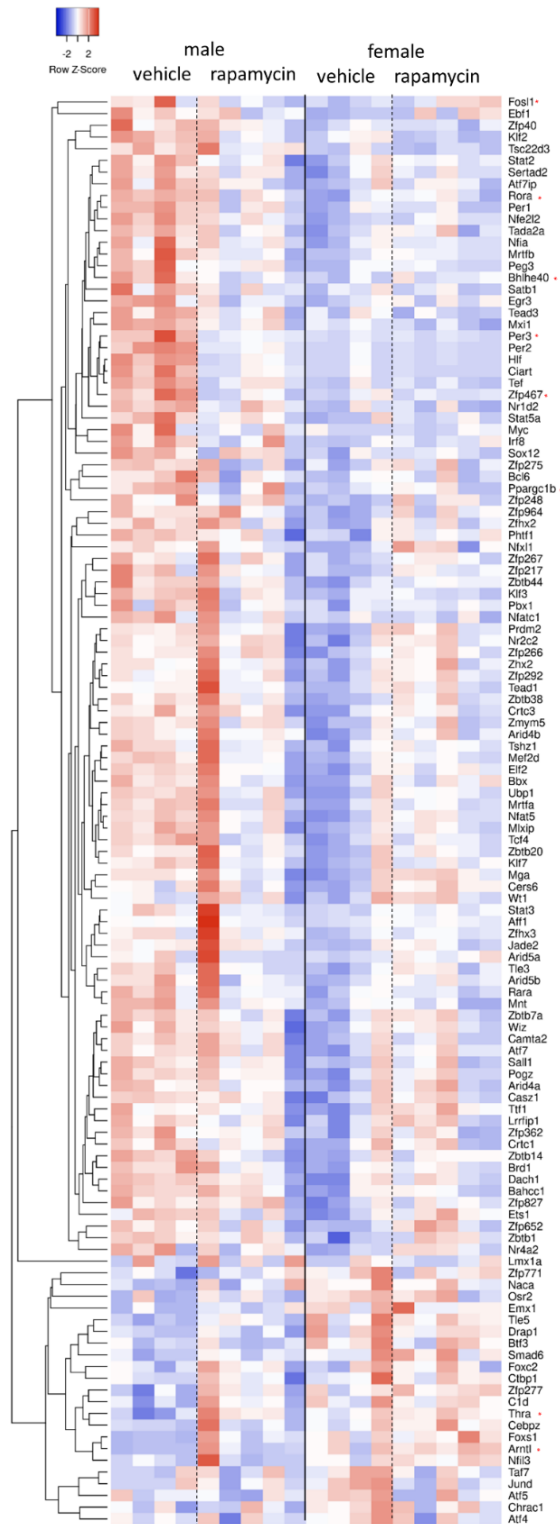
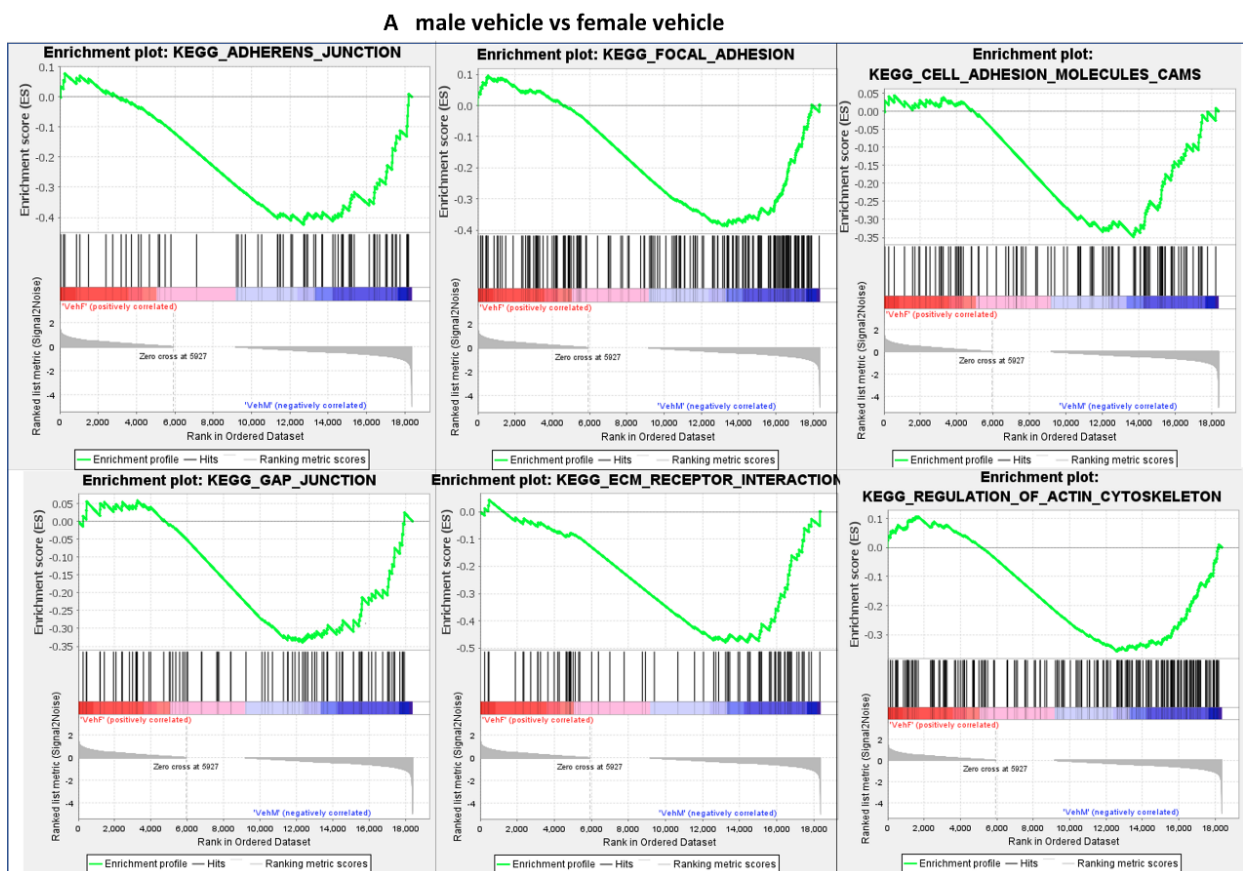


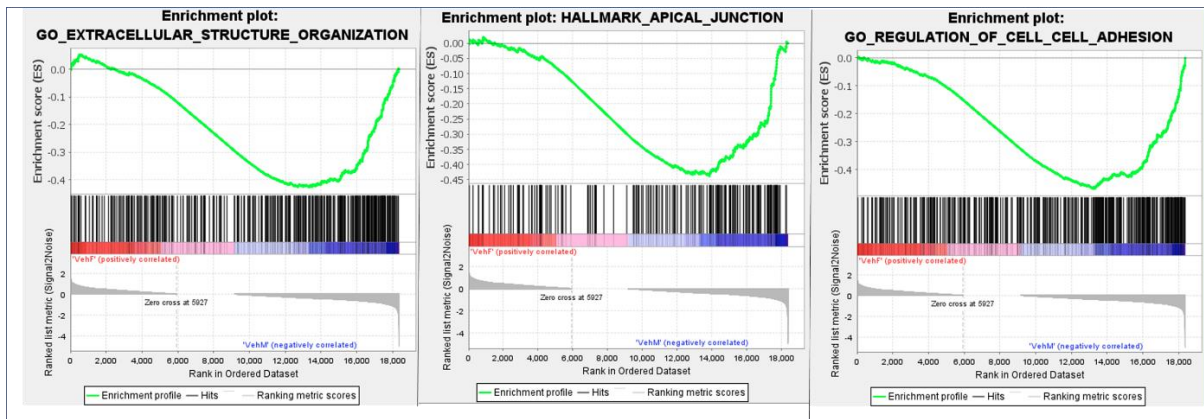
Figure 33: Sexual dimorphism in TFs genes. Heatmaps illustrate the 104 intrinsically sex-DE TF genes and expressional level changes in response to rapamycin in both sexes. * Indicates significantly DE genes in male after rapamycin (p-value < 0.05).

3.4.4.4 GO's including genes relevant for podocyte structure and cell-cell interactions

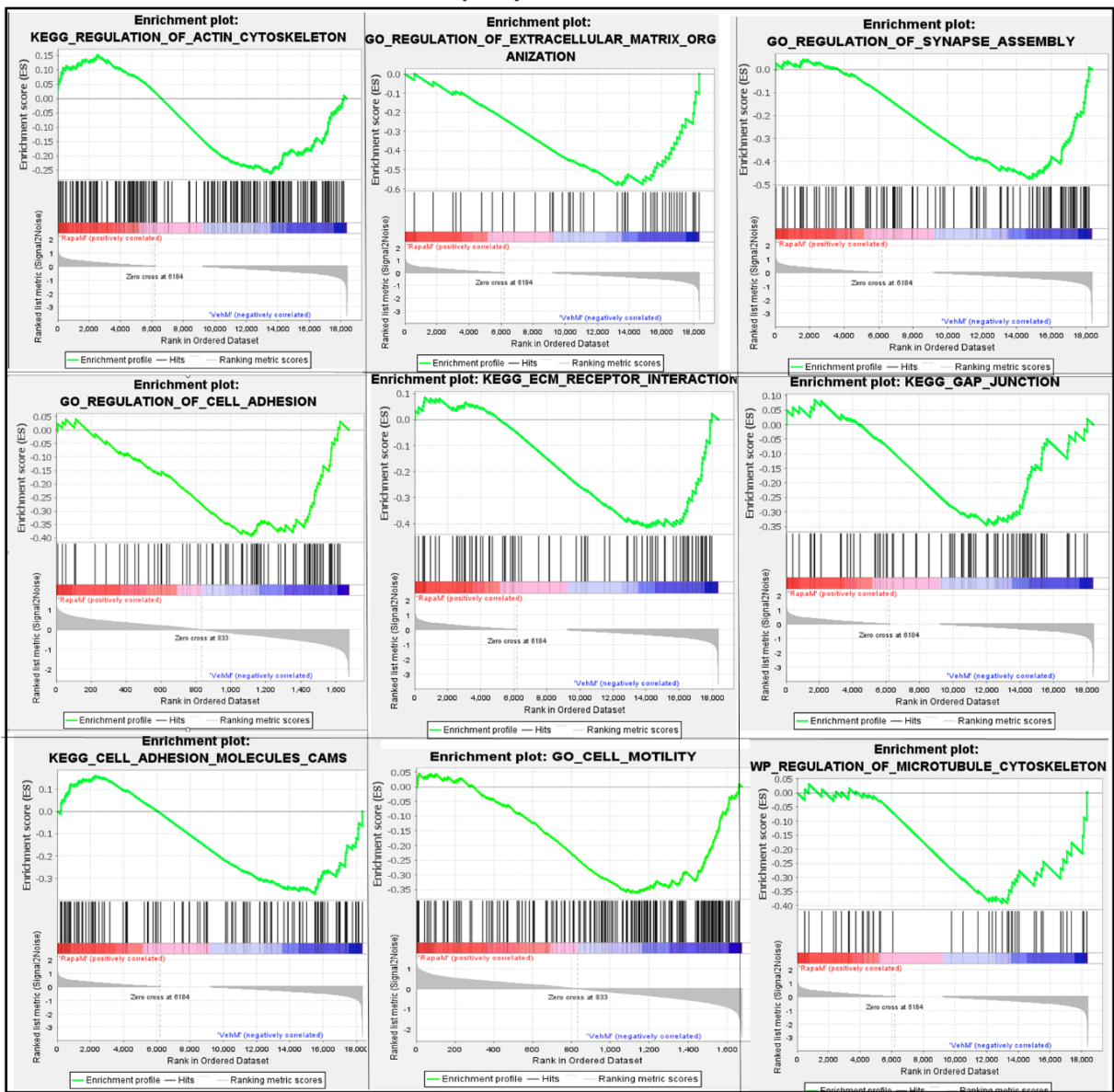
The foot process is the most characteristic structure of podocytes. A specialized junction between FPs the SD and between podocytes and the GBM through focal adhesion (FA) are crucial for maintaining integrity of the glomerular filtration barrier (128). Main components of FA and GBM are *Itgb1/a3*, *Ilk*, *Vinculin*, *Talin*, *Collagen IV (Col4a3-5)*, *laminin β 2*, *Syndecan2/4* and *Agrin* (129). Important sexual dimorphic responses to rapamycin treatment were observed in genes related to “cell adhesion molecules”, “regulation of cytoskeleton”, “focal adhesion” and “ECM-receptor interaction” (Table 4, Figure 25, Figure 34A).

Totally, 29 and 14 FA genes were found to be significantly differentially expressed between male and female podocytes with many of them higher expressed in males, such as *Col4a6*, *vinculin*, *talin1* and *paxillin (Itg β 5, Col4a5, Itga3/ β 1, syndecan4, agrin, nidogen1 and *Pavra* being intrinsically higher expressed in females) (Figure 35). Rapamycin treatment changes of the significantly DE cytoskeleton-related genes were significantly opposite in male and female podocytes whereas male mainly reduced expressions and females upregulated them (Figure 34B/C).*





B male rapamycin vs male vehicle



C female rapamycin vs female vehicle

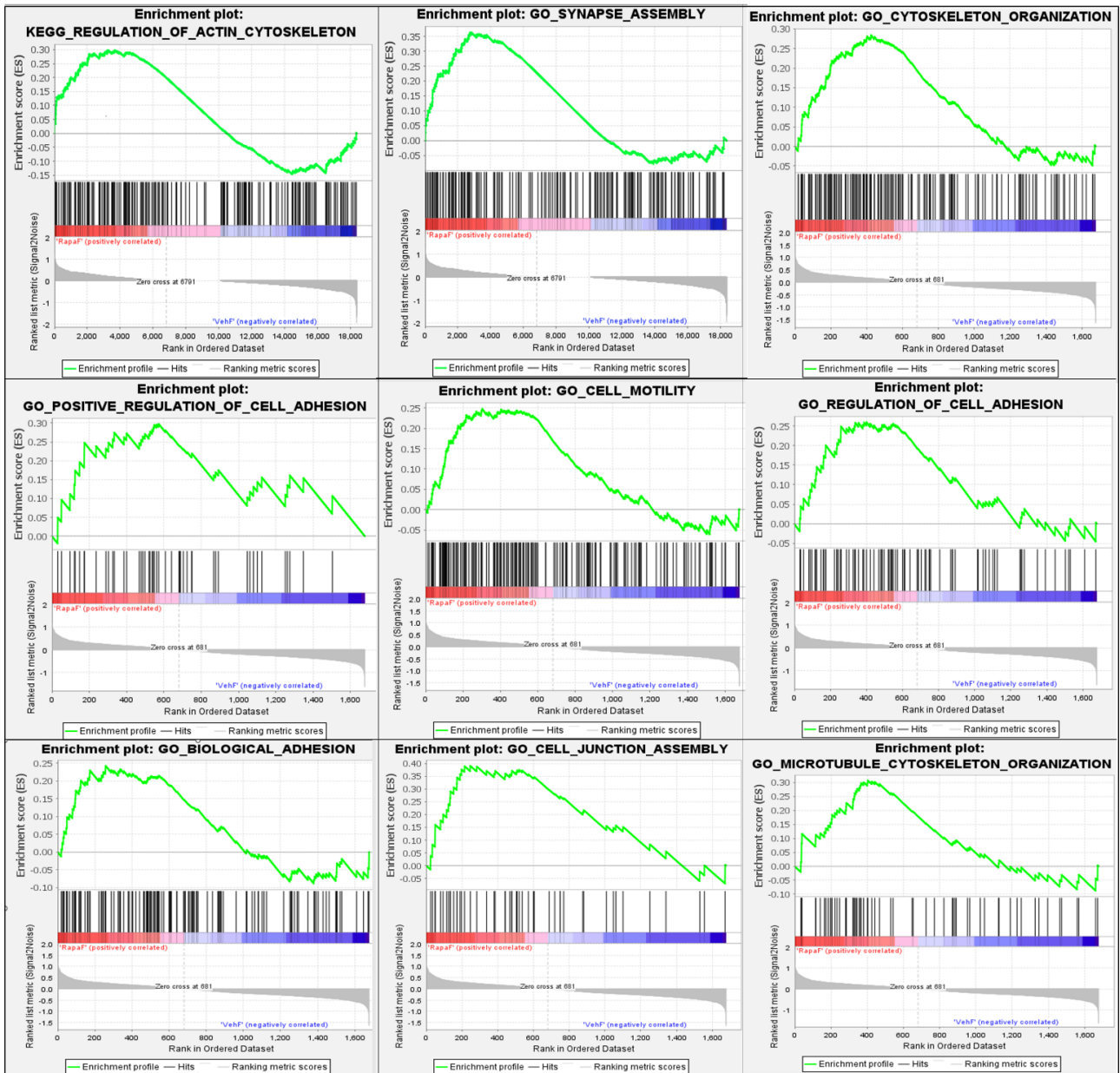


Figure 34: GSEA analysis of GOs related to focal adhesion, regulation of cytoskeleton different expression at baseline and after rapamycin. (A) At baseline, male podocytes overexpressed all GOs related to cell junction and regulation of cytoskeleton. Responses to rapamycin treatment in either (B) male or (C) female podocytes.

The SD plays a major role in podocyte function and morphology. Nephrin (*Nphs1*), podocin (*Nphs2*), *Tjp1*, *Nck1*, and *Neph1* are among the main proteins regulating the SD function, many of their genes were identified as intrinsically sexually dimorphic such as *Tjp1*(*ZO1*) and *Nphs2*

and displaying sex-different treatment responses to rapamycin. however, others genes, such as *Fat1*, *Neph1/2* were upregulated in both sexes. (Figure 35).

Other **podocyte structural proteins including focal adhesion proteins**-related genes and proteins related genes important for podocyte homeostasis such as *Cd151*, *Nphs2*, *Clic3*, *Cdkn1c*, Inverted formin-2 (*Inf2*), *Itgb5*, Cadherins and Claudins were among the significantly intrinsically sexually dimorphic genes and shows different response to rapamycin (to different levels). Many focal adhesion molecules-genes showed non-significantly higher basal levels in males, while females have higher level of ECM levels such as *Col4a3*, *Lamb2*. After rapamycin, male podocytes regulated the expression of many genes such as *CD151* and *Neph2*, whereas females mostly maintained their expression. (Figure 35)

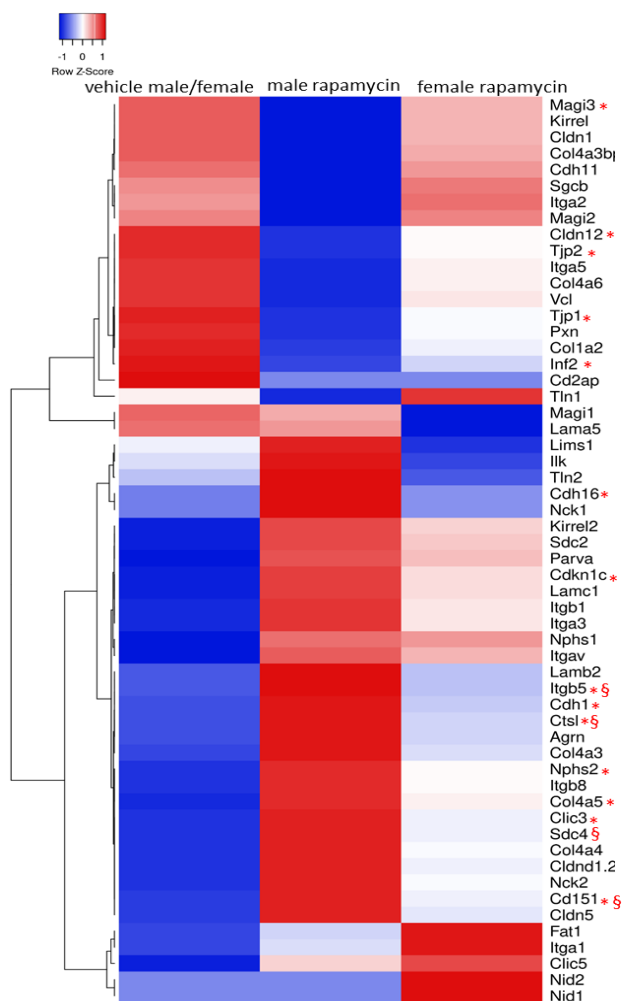


Figure 35. Heatmap of the log₂FC expression for highly expressed SD, ECM and FA molecules. between all experimental groups. * indicates intrinsically significantly regulated expression between male and female podocytes and § indicates differentially regulated genes after rapamycin in male (adj. p-value<0.05).

Cytoskeletal and actin binding proteins further contribute significantly to maintenance of podocyte structure and proper function. Male podocytes had higher levels of ACTN1, Afap1, Arhgap32/21, Tpm, Plectin, many Wipf subunits, Pdlim subunits, many Septin subunits which are involved in actin organization and actin filament binding. In contrast, females intrinsically had

higher levels of ACTN4, Gesolin, Arp2/3 complexes (Arpc, Actr), different Dynactin subunits and many more proteins involved in **cytoskeletal proteins ubiquitination and endocytosis**, such as Hipr1 and Daam2 (Appendix, Table 1).

In addition, Rho GTPases are well known regulators for cytoskeletal proteins, and genetic mutation in some Rho GTPases cause podocytopathies and nephrotic syndrome. **Regulation of cytoskeleton** GO term was significantly regulated at baseline. Panther analysis identified 9 genes directly regulating the cytoskeleton which were expressed differently between sexes such as Arpc4, Cdc42, Rhod, Tubb2b and Arhgef1. Few genes showed strong sexual dimorphic responses to rapamycin such as for Profilin2, Svll, an important FA binding modulator, and Capg, an actin filament binding proteins. Females upregulated most of these genes, and male downregulated them (Figure 28, Figure 36) as observed for Tropomodulin, Septins, Phactr4, Actn1 and Homer1, which had significantly higher level in males at baseline (xlsx gene list in Appendix, Table 1).

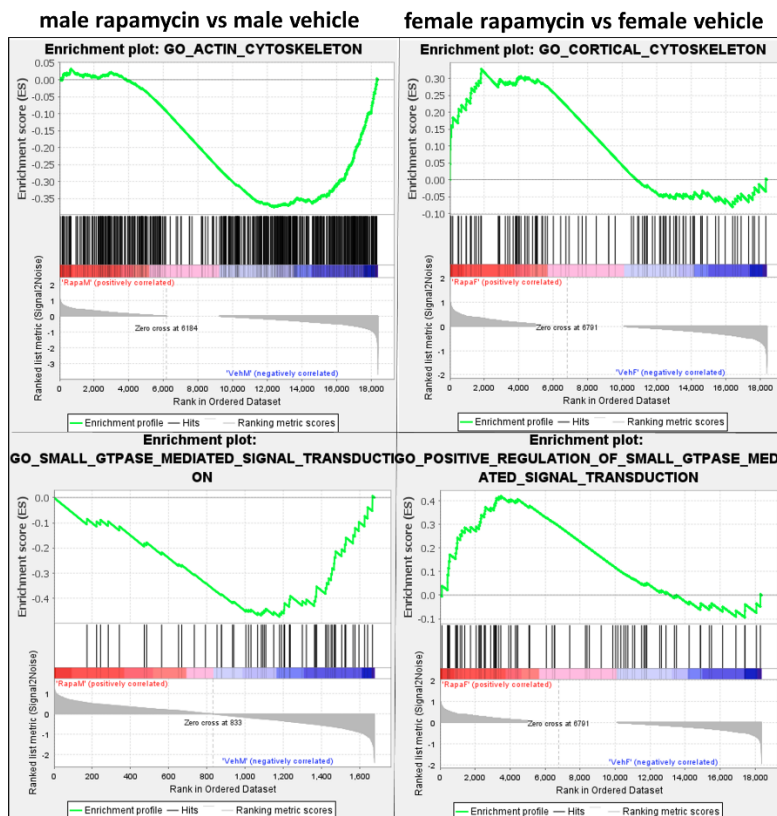


Figure 36. GSEA analysis of GOs related to podocyte-cytoskeleton specific genes. Sexual dimorphic responses to rapamycin were observed in GOs related to the actin-cytoskeleton and regulation by small GTPases.

The **endocytic process** is fundamental for the development and maintenance of the GFB. It serves as a gateway for the internalization and recovery of plasma membrane components and transmembrane receptors (130). The importance of endocytosis has been emerged by the observation of abundant endocytic vesicles in glomerular cross sections by EM and the fact that endocytosis regulates many podocyte protein functions, such as nephrin and cytoskeletal proteins.

Endocytosis is often categorized into clathrin-dependent (CME) and clathrin-independent pathway, still functional biological relevance has not been well defined so far (130, 131).

CME occurs in phosphatidylinositol-4,5-bisphosphate [PI(4,5)P₂]-enriched regions of the plasma membrane, where clathrin adaptor proteins, such as dynamin, synaptojanin 1, endophilin, auxillin/GAK and hsc70 in addition to proteins of the non-clathrin pathway, such as caveolin 1 (Cav1), Arf6, flotillin-1, and clathrin-independent carrier (Clic) are recruited. GO enrichment analysis of DE genes between vehicle pointed out that genes related to the term “endocytosis” (59 genes) were significantly enriched and sex-DE (enrichment factor 1.5, p-value 0.005) and 13 genes responded to rapamycin in males only (p-value 0.01). (Figure 37)

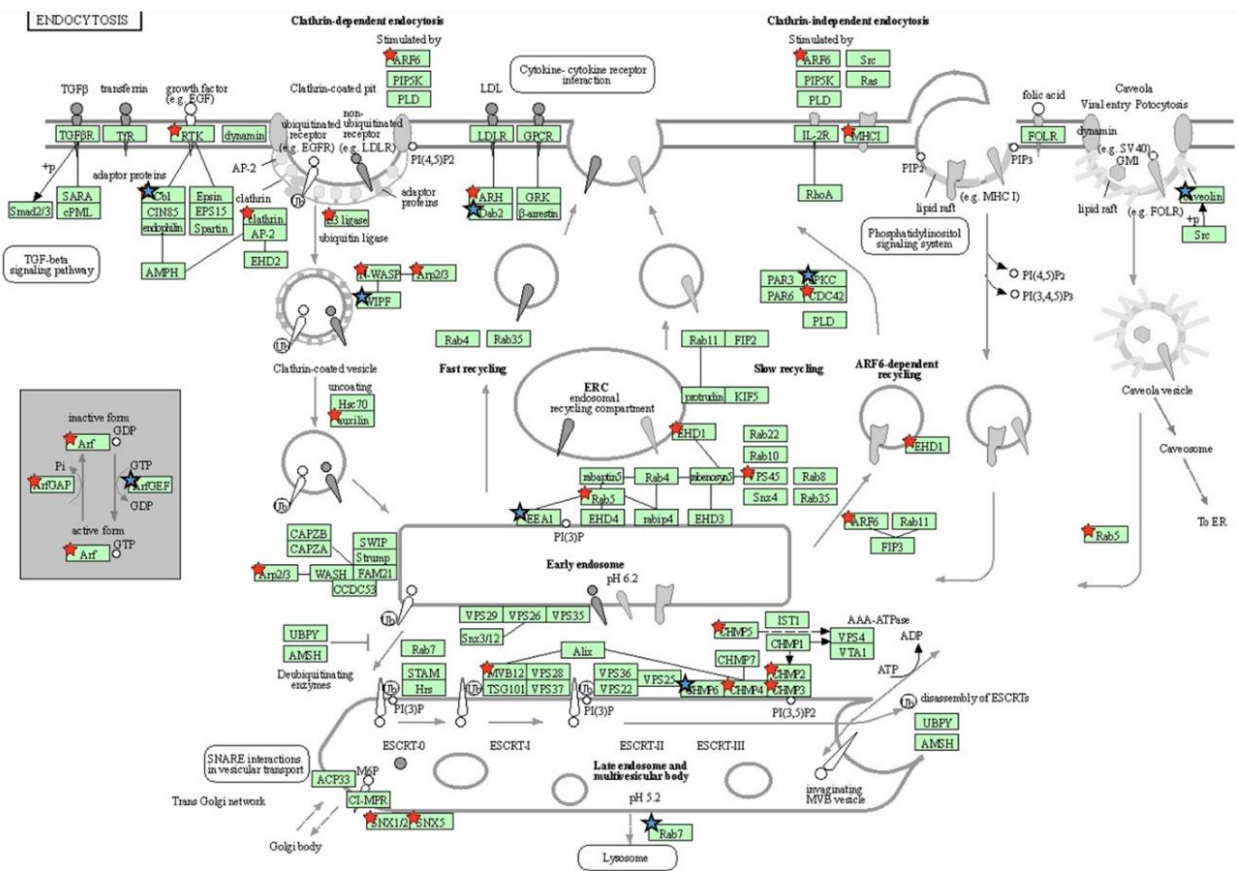


Figure 37. KEGG graph for endocytosis. Intrinsically significantly DE genes higher expressed in females are labelled with red stars and blue stars for higher expression in males.

Most DE genes were related to “membrane traffic protein” (PC00150) were already significantly differently expressed under baseline between male and female podocytes, under them 28 genes with higher expression in females, such as Chmp3/4/6 – important for endosomal sorting and multivesicular bodies (MVBs) formation. Stonin - *Ston1/2*- are important endocytosis genes

regulating FA assembly showed both intrinsic and treatment-related sexual dimorphism after rapamycin (more than 30% higher expressed intrinsically in males, downregulated in males and upregulated in females after rapamycin). Additionally, Clathrin Clta/b was higher expressed in females at baseline, and rapamycin caused upregulation in males and without changes in females. Furthermore, different Rab genes, e.g. *Rab1b/3b*, *Rab8*, *Rab11*, were intrinsically higher expressed in female podocytes. Different isoforms of Rab - Ras superfamily of GTPases control endocytic vesicle trafficking from the endoplasmic reticulum to the Golgi apparatus. (Figure 38).

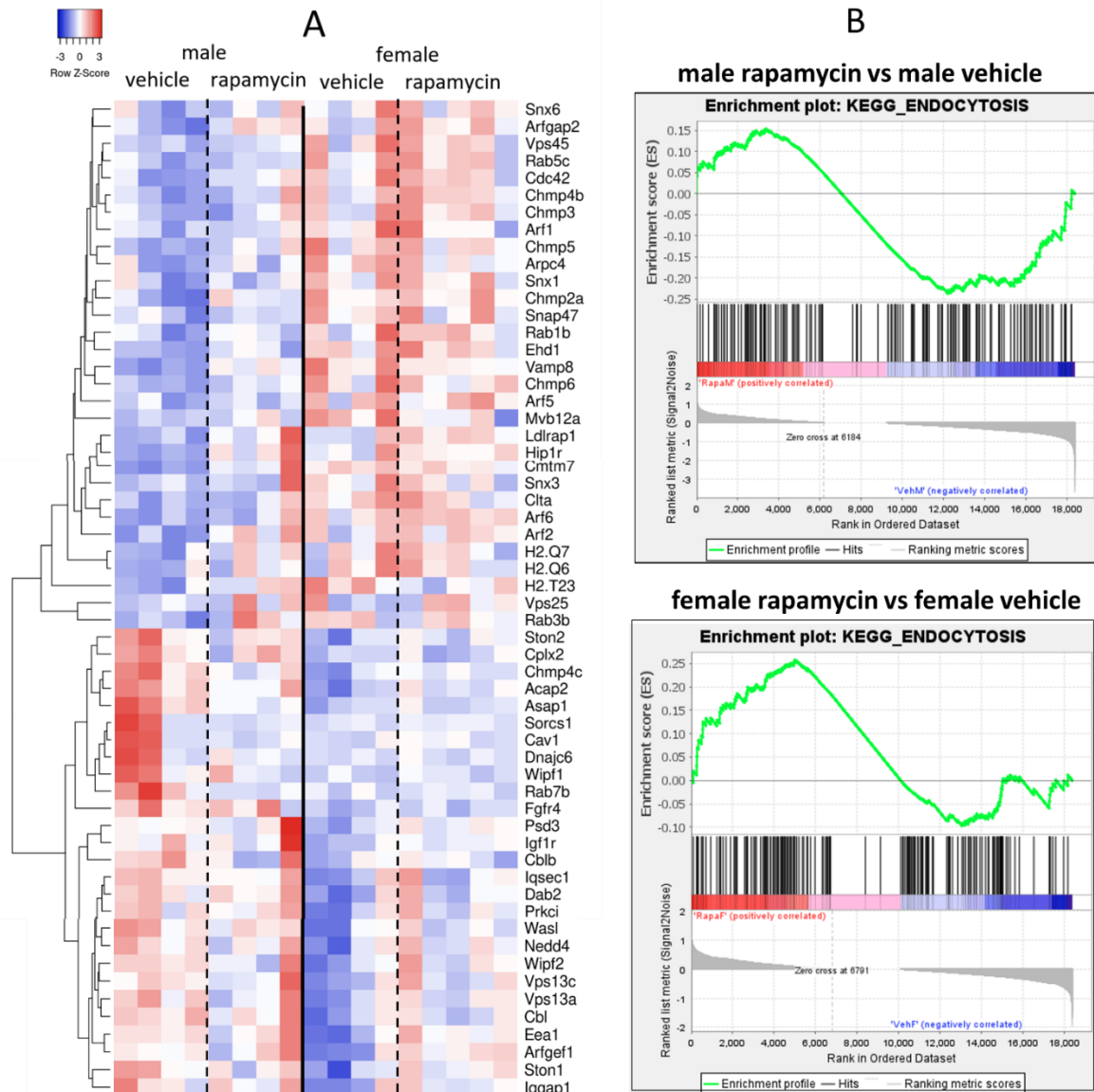


Figure 38. Sexual dimorphism in podocyte endocytic genes (A) Heatmap of the DE genes related to endocytosis show higher intrinsic expression in females. Rapamycin did not significantly alter the expression of many genes (B) GSEA of 166 endocytic genes enrichment plot shows sex-different response to rapamycin.

3.4.4.5 Sex- and treatment-specific transcriptional differences in genes coding for mTOR-signaling related proteins

As mTOR inhibition was used as a stress model, it was of specific interest whether components of the mTOR-signalling pathway were sexually dimorphically expressed or differently affected by treatment in each sex. 13 genes encoding for mTOR components and related proteins, such as *riCTOR*, and the negative regulators of mTOR, *Tsc1*, were significantly lower expressed in female vehicle podocytes *AKT1s1(PRAS40)* was also significantly differently expressed between both vehicle with higher expression in females. After rapamycin treatment, gene expressions increased in females for *Tsc1* and decreased in males compared to vehicle, indicating sexual dimorphism in response to rapamycin. Even though *riCTOR* showed 40% higher expression in males compared to females at baseline, no differences and alteration in expression was observed in *riCTOR* in both male and female podocytes after rapamycin, and males maintained their higher expression compared to females.

Furthermore, *Tsc2* showed non-significantly higher expression in males at baseline compared to female, and also showed sexual differences in response to rapamycin as was seen for *Tsc1* but to less extent. Additionally, while other genes encoding mTOR components (*mTOR*, *Dptor*, *Rheb*, *Raptor* and *Mlst8*) showed comparable expression at baseline, they showed non-significantly sexual dimorphism in response to rapamycin.

Regulator complex protein *LAMTOR1/2/3/4/5* and the Ras-related GTP-binding protein *a/b/c/d* which are involved in the cellular response to amino acid sensing and regulation of the mTORC1 signaling were analyzed. *LAMTOR1/2/4/5* were significantly DE between vehicles with higher expression in females (Log2FC 0.33-0.6). Moreover, sexual dimorphism in response to rapamycin was observed, female podocytes maintained or decreased slightly the expression of the previously mentioned genes, while male podocytes upregulated these genes.

Interestingly, several FK506- and rapamycin-binding proteins (FKBPs) were significantly higher expressed in female vehicle treated group compared to male, even though *Fkbps* are inhibited by rapamycin, response to rapamycin showed sexual dimorphic response for most quantified *Fkbps* with female downregulating the expression of most *Fkbps* genes but not males. Intrinsically DE mTOR-related genes were analyzed for rapamycin effect in each sex and showed significant DE with opposite changes (males upregulated most of the genes, whereas females downregulated expression levels in response to rapamycin) (Figure 25). GSEA showed that mTORC1 pathway

was de-enriched in both, male and female podocytes, yet to a higher degree in females (Figure 39).

Sesn3, a leucine sensor, which negatively regulates the mTORC1 signaling pathway was significantly sex-DE intrinsically and showed sexual dimorphic responses to rapamycin (male significantly downregulated the expression of *Sesn3* to half. *Sesn1* and *Sesn2* also showed higher expression in males and both were also downregulated primarily in male podocytes after rapamycin treatment.

AKT kinases, regulate many processes including metabolism, proliferation, cell survival, glucose uptake and angiogenesis and are also involved in activating mTORC1 signaling. Other than AKT1, AKT2 isoform, known to be highly expressed in podocytes (75) was significantly upregulated in female podocytes.

Rapamycin non-significantly altered gene expression in both isoforms, with a slight increase in males and slight reduction in females. *Akt3*, another isoform of AKT was only moderately expressed in podocytes with significantly higher expression level in males (p-value <0.004). The sex-difference was abrogated after rapamycin treatment due to reduction of levels in males. The role of AKT3 is yet not clear in podocytes and it appears to be predominantly expressed in brain.

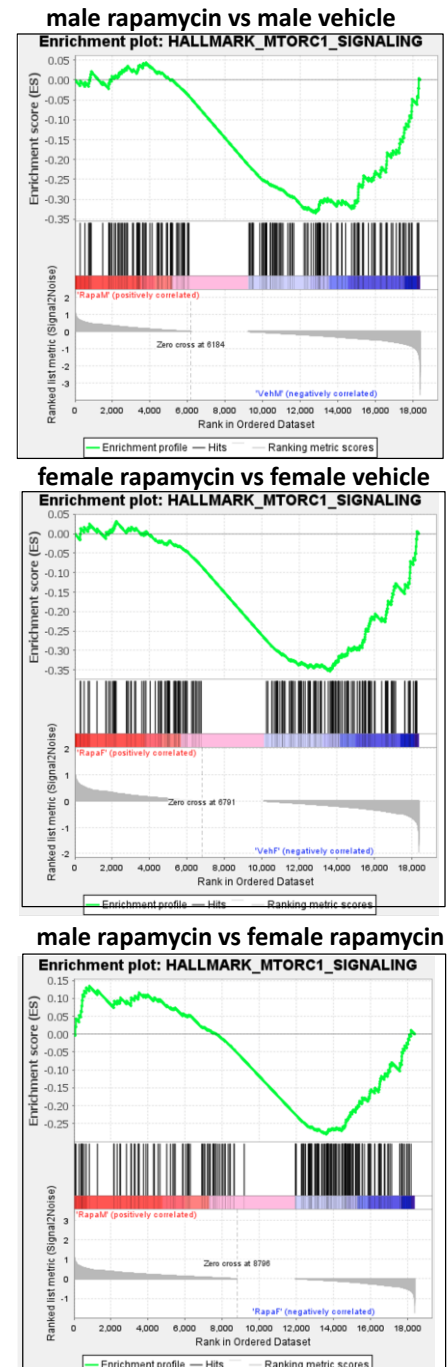


Figure 39. Effect of rapamycin on mTOR pathway. Rapamycin downregulated mTORC1 pathway and to higher level in females.

3.4.5 Validation of gene expression levels for selected genes

qRT-PCR was performed with podocyte samples from mice used for RNA-seq together with podocyte samples isolated from additional mice of the same experimental groups for sequencing data validation. Podocyte genes were selected which were intrinsically sexually dimorphically expressed, such as podocin (Nphs2), Slc6a6, Arhgap32 and Tjp1 as well as genes representing main sexual dimorphic GOs such as Bhlhe40, Rpl13 and Cox7a2 for transcription factors, ribosomal and mitochondrial genes, respectively. These genes were chosen as some of them were additionally significantly differently regulated in male after rapamycin treatment such as Daam2, Cd151, Ctstl and Arhgap32. Other criteria for gene selection were transcript level expressions higher than 1000, log₂FC differences between at least 2 experimental groups of 0.5-2.0, and biological relevance of the genes for kidney physiology or disease. All genes measured showed significant differences between male and female vehicles with p value <0.05 consistent with RNA-seq results. (Figure 40 A/B).

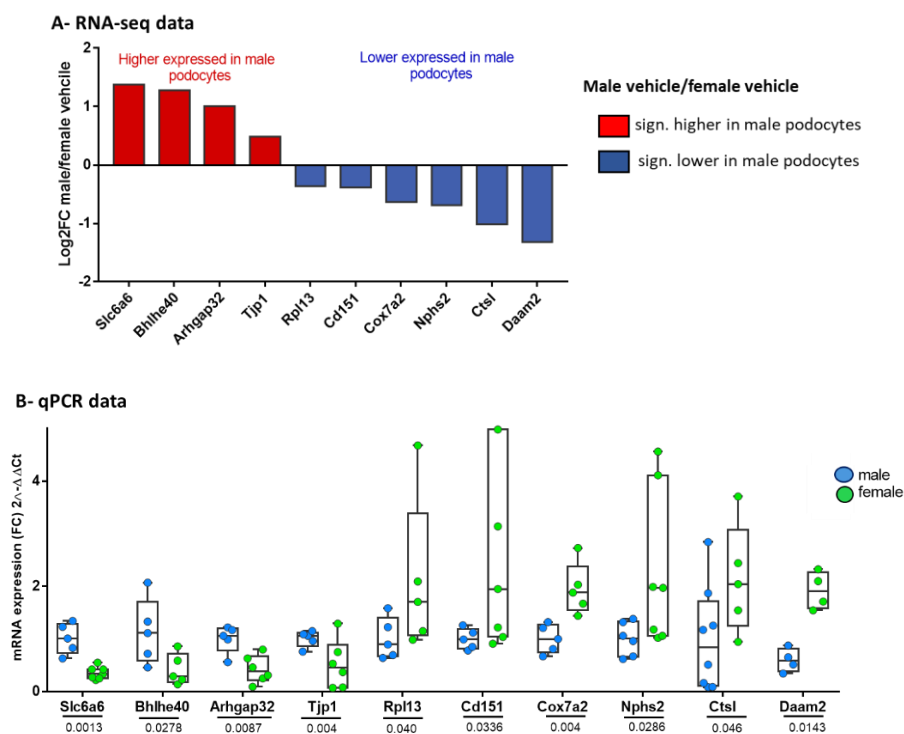


Figure 40. Validation of differentially expressed genes (DEGs) between male and female vehicle podocytes. (A) Graphical presentation of RNA-seq-derived Log₂FC of for validation selected intrinsically significantly sexually dimorphic podocyte genes. (B) qPCR results for the same genes in male and female vehicle podocytes (n=4-8 in each group). Reference genes used for normalization were Hdgf and Ywhaz genes. All genes were normalized to male vehicle, and results are expressed as mean +/- SEM, Mann-Whitney test was used for statistical comparisons, p value < 0.05.

qPCR confirmation for the significantly regulated genes in response to rapamycin treatment was only performed in males (rapamycin vs vehicle) as females mainly maintained their transcriptome with no significantly regulated genes after rapamycin except for 3 genes that were not related to podocyte homeostasis or structure. *Bhlhe40* and *Arhgap32* showed significant downregulation in male after rapamycin and *Daam2* and *Ctsl* were significantly upregulated consistent with RNA-seq data. (Figure 41 A/B). *Cd151* showed upregulation after rapamycin in qPCR, yet did not reach significance as in RNA-seq data. The two in qPCR validation included genes without significances in RNA-seq, *Nphs2* and *Rpl13*, also showed non-significant differential expressions in qPCR results. Despite female rapamycin did not show significant changes in transcriptome, additional qPCRs were performed for the following genes *Nphs2*, *Cd151*, *Ctsl* and *Bhlhe40* in podocytes isolated from rapamycin-treated females. Comparably to RNA-seq, qPCR of these genes did not show any significant differences between the podocytes from vehicle and rapamycin-treated female mice (data not shown).

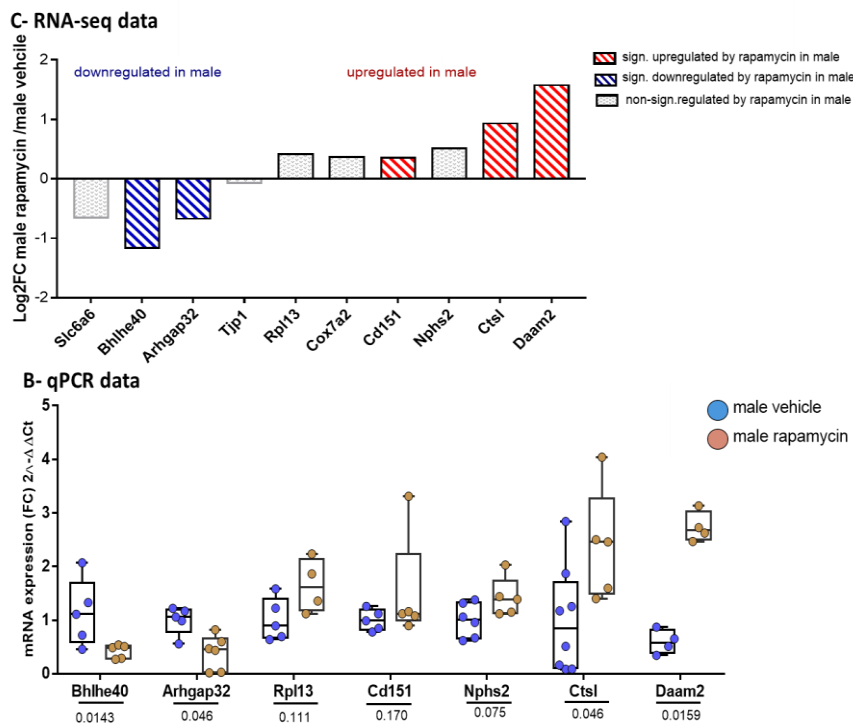


Figure 41. Validation of differentially regulated genes in response to rapamycin in male podocytes. (A) Graphical presentation of RNA-seq-derived Log₂FC of for change of gene expressions in response to rapamycin in male. (B) qPCR results for the same genes in male vehicle and male rapamycin podocytes (n=4-8 in each group). qPCR data

confirming the significant up and downregulation of genes by rapamycin. Mann-Whitney test was used, and results are expressed as mean +/- SEM. All genes showed significant differences with p value < 0.05 except for *Cd151*. Reference genes used for normalization were *Hdgf* and *Ywhaz*. All genes were normalized to male vehicle, and results are expressed as mean +/- SEM, Mann-Whitney test was used for statistical comparisons, p value < 0.05.

3.5 Podocyte-specific proteomics and effect of mTOR inhibition on protein levels of selected podocyte relevant structural and functional protein groups

To determine if the sexual dimorphism on the molecular identity of podocytes identified by RNA-seq could also be detected on protein level, isolated podocytes from each three male and female vehicle and rapamycin treated mice were subjected to mass spectrometry analysis in collaboration with Markus Rinschen, University of Cologne. However, due to the limited number of isolated podocytes per mouse and further technical problems, only proteomic results from vehicle groups were available for pilot analyses. Label-free quantification (LFQ) and global statistical analysis was performed by the collaboration partner, detailed analyses for subgroups and western blots were subject of this thesis work.

3.5.1 Podocyte-specific proteomics revealed sexual dimorphism in vehicle control mice

In total, 3881 proteins could be identified in the podocytes isolated from vehicle mice. However, only 2740 proteins were quantifiable in at least 3 samples. Podocytes did not cluster completely by gender. From the 2740 quantified proteins, female podocytes had 1114 proteins (40.6% of total proteins quantified) with more than 1.5 FC higher expression (Log₂FC of 0.54) compared to male podocytes (under them 587 proteins with > 2 FC higher expression). In contrast, male podocytes showed only 405 proteins (14.8% from total proteins) with more than 1.5 FC higher (169 protein higher than 2 FC higher expression) compared to female podocytes Table 6 appendix. Statistical analysis identified 40 proteins significantly differently expressed between male and female podocytes with p-value of < 0.05 (Figure 42).

Of these 40 proteins, 33 proteins were higher expressed in female compared to male podocytes and were related to metabolism. Table 13 displays these significant sexually dimorphic podocyte proteins and their functions. None of the significantly differently expressed protein was a podocyte-specific protein, yet, many influence podocyte homeostasis.

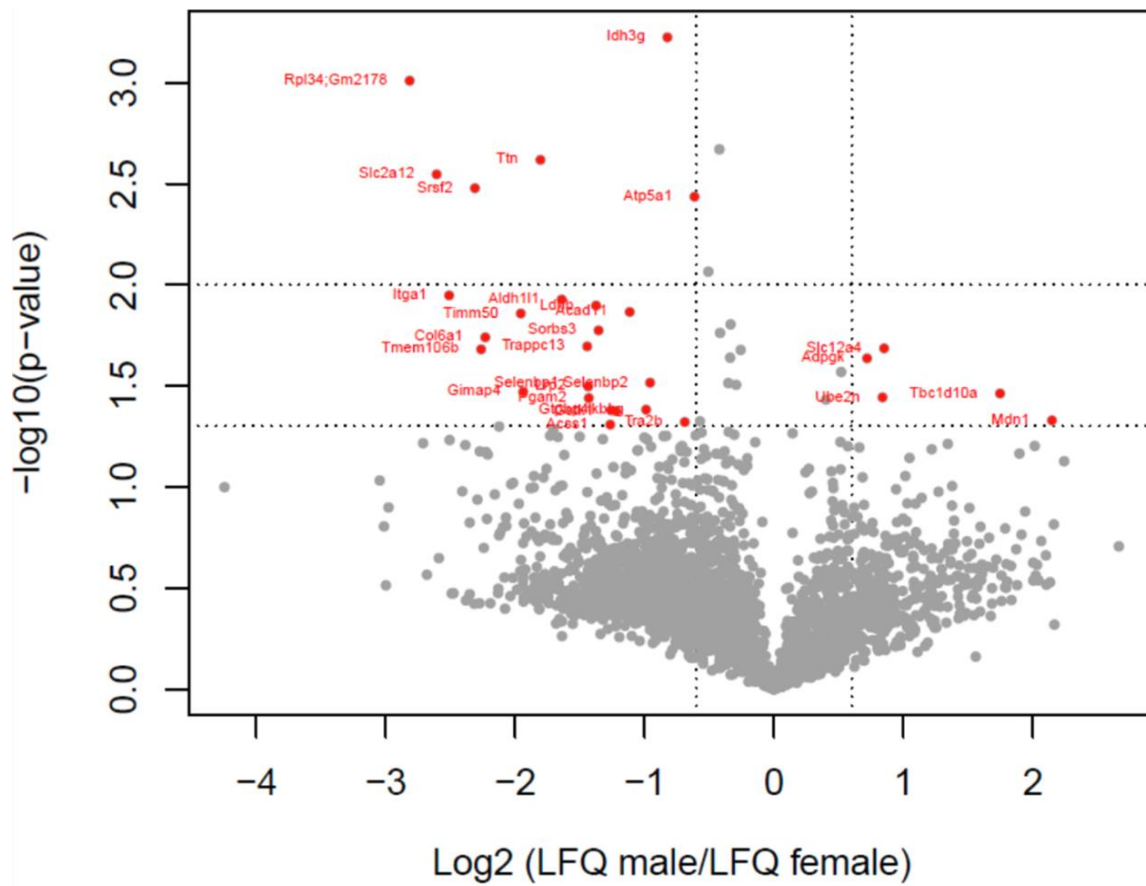


Figure 42: Volcano plot of significantly sex-DE expressed proteins. 40 proteins were significantly DE between male and female podocytes (labelled red). Shown are fold change (\log_2) values of LFQ male/LFQ female according to adjusted p-values (FDR) ($-\log_{10}$ scale) on Y-axis. FDR cut off value was set to 0.05. Black dotted lines represent cut offs.

Table 13. Overview of significantly DE sexually dimorphic proteins

Gene	Log2FC male to female	Molecular function
Mitochondrial proteins and Metabolic process		
Slc12a4	0.8510	Contribute to cell volume homeostasis in single cells and involves in chloride and potassium homeostasis
Adpgk	0.7194	Involved in the pathway glycolysis and catalyzes the phosphorylation of D-glucose to D-glucose 6-phosphate
G6pdx	0.5193	This protein is involved in the first and the rate-limiting step 1 of the pathway pentose phosphate pathway (part of C
Ispd	-0.2932	Catalyzes the formation of CDP-ribitol nucleotide sugar important for alpha-dystroglycan (DAG1)
Fh	-0.3388	Catalyzes the hydration of fumarate to L-malate in the tricarboxylic acid (TCA) cycle
Txnrd1	-0.3534	Involved in the redox homeostasis
Dad1	0.4015	This protein is involved in the pathway protein glycosylation, which is part of Protein modification.
Smek1	-0.4167	Regulatory subunit of serine/threonine-protein phosphatase 4. May regulate the activity of PPP4C at centrosomal microtub
Hadhb	-0.4219	This protein is involved in the pathway fatty acid beta-oxidation
Atp5a1	-0.6144	Part of the electron transport complexes of the respiratory chain
Idh3g	-0.8240	Regulatory subunit involved in catalyzing the decarboxylation of isocitrate (ICT) into alpha-ketoglutarate in TCA cycle
Selenbp1/2	-0.9575	Oxidative reductase protein involved in the catalyzes of methanethiol
Ikbkg	-0.9883	positive regulator for NF-kappaB-inducing kinase activity
Acad11	-1.1148	Involved in the pathway fatty acid beta-oxidation, which is part of Lipid metabolism
Gstk1	-1.2205	Involved in glutathione metabolic process and cell differentiaaion
Ldhb	-1.3750	This protein is involved in step 1 of the subpathway that synthesizes (S)-lactate from pyruvate/lactate metabolomic proces
Pgam2	-1.4312	Interconversion of 3- and 2-phosphoglycerate with 2,3-bisphosphoglycerate in Glycolysis pathway
Acss1	-1.2654	Catalyzes the synthesis of acetyl-CoA from short-chain fatty acids and provides acetyl-CoA that
Aldh1l1	-1.6407	involved in folate metabolism and has aldehyde dehydrogenase (NAD+) activity
Gimap4	-1.9378	Immunity-Associated Nucleotide 1 Protein
Timm50	-1.9570	Essential component of the TIM23 complex, mediating the translocation of transit peptide-containing proteins across the m
Slc2a12	-2.6074	Insulin-independent facilitative glucose transporter
Actin cytoskeletal related proteins		
Acap2	-0.3353	GTPase-activating protein for ADP ribosylation factor 6 (ARF6) which is important for actin filament based process and e
Ctnna1	-0.5722	involve in actin filament network, and primary importance for cadherins cell-adhesion properties.
Sorbs3	-1.3559	Promotes up-regulation of actin stress fiber formation.
Ttn	-1.8049	important for the actin filament organization
Col6a1	-2.2311	Part of the ECM
Itga1	-2.5105	Binding ECM to actin cytoskeleton
Trnaslational proteins		
Mdn1	2.1485	Nuclear chaperone required for maturation and nuclear export of pre-60S ribosome subunits
Ube2n	0.8383	Ubiquitin-dependent protein catabolic process.
Rpl22	-0.2577	Ribosomal protein
Cul4a	-0.5078	Core component of multiple cullin-RING-based E3 ubiquitin-protein ligase complexes
Tra2b	-0.6897	Involved in the control of pre-mRNA splicing.
Gtpbp4	-1.2591	Involved in the biogenesis of the 60S ribosomal subunit.
Srsf2	-2.3112	Necessary for the splicing of pre-mRNA.
Rpl34	-2.8159	Ribosomal protein
Endocytosis/protein trafficking		
Lrp2	-1.4361	Endocytic receptor involved in endocytosis , and in phagocytosis of apoptotic cells
Trappc13	-1.4436	May play a role in vesicular transport from endoplasmic reticulum to Golgi.
Tbc1d10a	1.7471	GTPase-activating protein for RAB27A, small GTPase which regulate homeostasis of late endocytic pathway and exocyto
Tmem106b	-2.2634	Involved in dendrite morphogenesis and maintenance by regulating lysosomal trafficking via its interaction with MAP6

3.5.2 GO enrichment analysis of proteomics of vehicle control podocytes revealed that females have an increased abundance of mitochondrial oxidative phosphorylation proteins and basal cell proteins

Different databases considered for GO enrichment analysis showed that female podocytes had an increased abundance of mitochondrial, specifically oxidative phosphorylation proteins which were significantly higher expressed in female podocytes, as well as basal cell proteins. These expression differences were concordant to the RNA-seq results. However, in contrast to higher transcripts for genes related to translation in female podocytes, proteins involved in translation

appeared to be higher in male podocytes, and cytoskeletal structure in females rather than males (Figure 43).

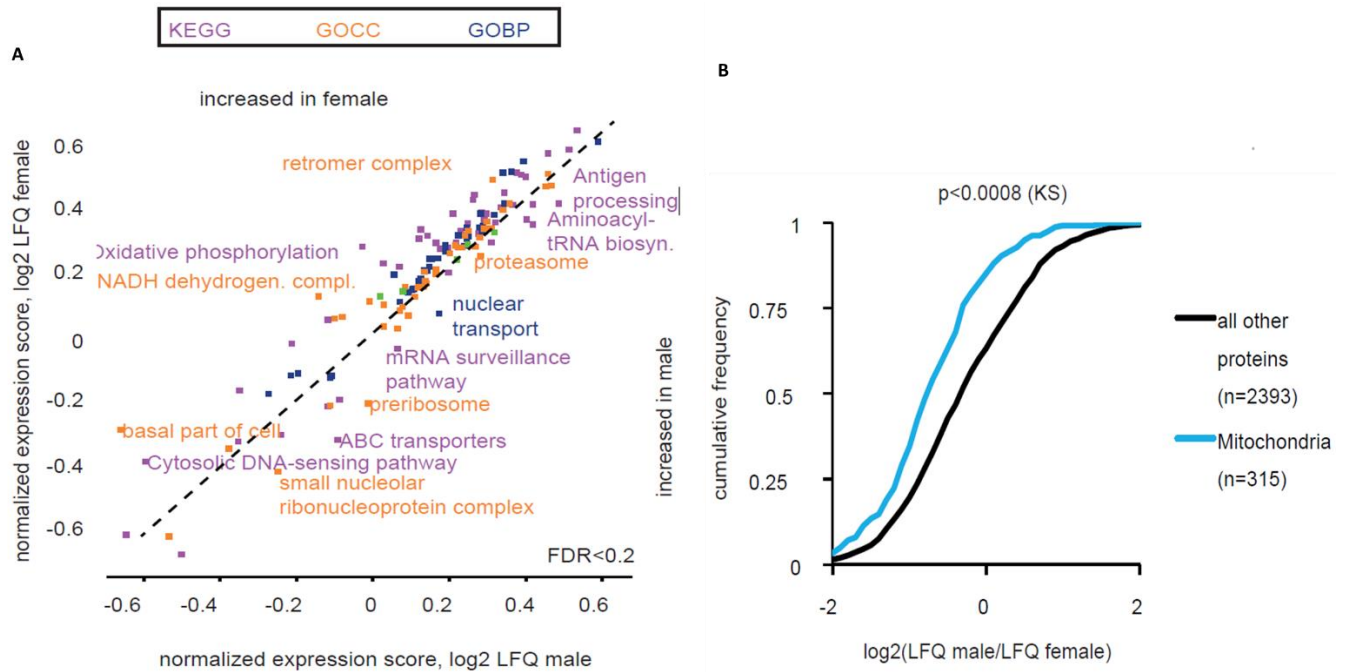


Figure 43. GO enrichment analysis revealed enrichment of cell part and mitochondrial proteins in female podocytes (A) Female podocytes had an increased abundance for basal cell proteins as well as oxidative phosphorylation proteins whereas male podocytes had an increased abundance of ribosomal proteins using different databases (B) Female podocytes showed significantly higher expression of total mitochondrial proteins compared to male podocytes.

Further GO terms-enrichment was performed using Enrichr functional annotation tool for proteins with > 2FC DE between male and female podocytes (Figure 44). “Metabolic pathway”, “endocytosis”, “oxidation phosphorylation”, “carbon metabolism”, “regulation of actin cytoskeleton”, “focal adhesion” were from the top KEGG pathways found to be significantly enriched in female podocytes compared to males.

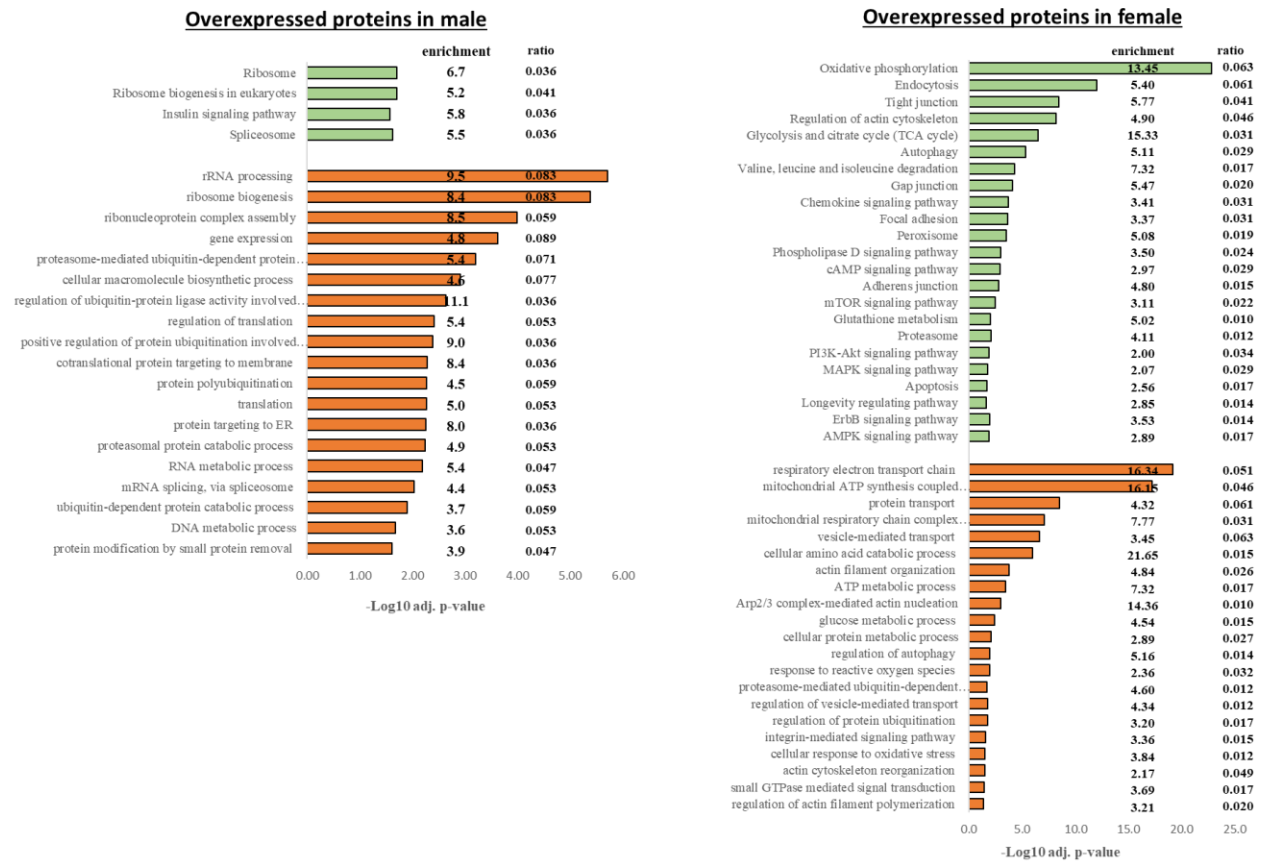


Figure 44. GO-term overexpressed in male and female podocyte protein vehicle groups with FC>2. Enrichr analysis of proteins with sex-differential expression (FC>2). GO terms include biological process (orange bars) and KEGG pathway (green bars) in 587 proteins in female podocyte and 169 proteins in male.

5.3.3 Focus on sexual dimorphism in mitochondrial respiratory chain proteins and metabolic proteins related to glycolysis, TCA cycle and pentose phosphate pathway

Further detailed analysis for this thesis work using Panther gene ontology revealed that 72 proteins with “oxidative-reductase activity” (GO:0016491) were more than 2-fold higher expressed in female podocytes compared to only 18 proteins in male podocytes from the same category.

Figure 44 gives an overview of the sex differentially expressed proteins related to oxidative phosphorylation in the mitochondria. 51 enzymes involved in oxidative phosphorylation and electron transport chain were found to be upregulated in female podocytes (Log2FC male/female range -3.0 – -0.2) compared to only 4 of 58 identified proteins in male podocytes (Figure 45).

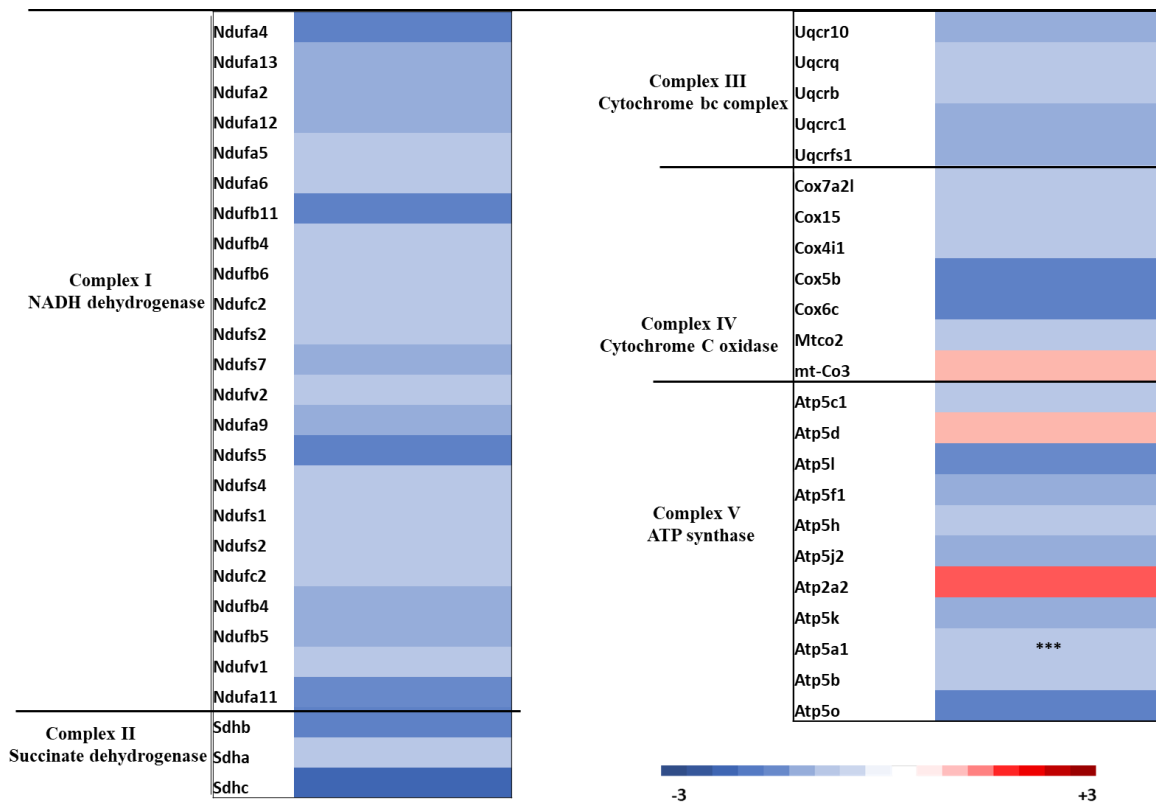


Figure 45. Log2FC of LFQ values of male versus female podocyte proteins of the oxidative chain. Heatmap of mean Log2FCs shows higher expression of most respiratory chain proteins in female podocytes indicate by green colour. (*, significantly DE with $p < 0.05$, **, with $p < 0.01$).

Interestingly, panther gene ontology database identified differences and increased expression in females at baseline of major enzymes involved in “glycolysis”, “TCA cycle” and “pentose phosphate pathway” similar to what had been observed in the RNA-seq results (enrichment factor 2, p -value < 0.05). Four enzymes and one carrier were significantly overexpressed in female podocytes (Fh, ldh3g, ldhb, pgam2 and the glucose transporter Slc2a12) and showed a Log2FC male/female of -0.3 to -2.0, of these both ldh3g and Slc2a12 were also significantly overexpressed as well on the transcriptional level in female podocyte, represented in figure 46.

Other enzymes showed higher expression in female podocytes are the rate-limiting enzymes of the glycolysis pathway, such as mdh1/2, Suclg1, ogdh, Aco2, Sdhc and two enzymes in PPP Taldo1, Gpi which showed 1.2 to 6 times higher expression in female podocytes compared to male podocytes.

of all quantified heat shock proteins compared to male podocytes, as well as other chaperone which were significantly regulated on the transcriptional level

Recently, sirtuins have been associated with oxidative stress signaling and antioxidant defense in the cell through different effectors to enhance cellular defense mechanisms (133). Proteomics revealed Sirt2 protein to be intrinsically higher expressed in female compared to male podocytes (Log2FC male to female of -0.83 / 80% more expression in female).

3.5.5 Focus on sexual dimorphism in proteins related to the post-translational modification in podocytes

Protease activity is essential for physiological podocyte maintenance (122). Several studies support the diverse capacity of ubiquitin proteases to affect the cytoskeletal and proteomic composition of podocytes(121). The strong sexual differences identified in RNA-seq earlier in ubiquitination and proteases activity genes between male and female podocytes were not completely reflected by the protein level. Proteomics identified around 120 proteins related to **proteolysis and ubiquitination**, but only Ube2n was significantly differently expressed between sexes with p value <0.05. Nevertheless, Panther analysis identified a large number of differently expressed proteins with proteases activity (PC00190), ubiquitinated genes (and 4 genes with proteases inhibitor activity), with > 2 FC.

Calpain, a calcium-dependent cysteine **protease**, is a protease that cleaves talin, a cytoskeletal protein important in regulation of cell-cell contacts. Three Calpain proteins were identified in this analysis; calpain-1 and calpain-2 which were only slightly higher expressed in female podocytes compared to male podocytes (1.3 FC).

Cathepsins, a further protease group, contribute to both, podocyte maintenance and response to acute injury. Cathepsin D, an aspartic protease, which has been shown to be relevant for integrity of slit diaphragm and prevention of proteinuria (134) was expressed equally between male and female podocytes. Cathepsin L is a serine protease, which activity is increased in some kidney diseases and is considered to have a destructive effect, could not be quantified in this proteomics. Among the quantified proteins involved in ubiquitination were glutamyl aminopeptidase (Enpep), carboxypeptidase Q (Cpq), neprilysin (Mme), pyroglutamyl peptidase 1 (Pgpep1), rhomboid-related protein-3 (Rhbdl3), dipeptidyl peptidase 4 (Dpp4), serine protease HTRA1 (Htra1), metalloproteinase domain-containing protein-10 (Adam10), carboxypeptidase D (Cpd), and nardilysin (Nrd1). Most of them showed a higher expression in female podocytes compared to male podocytes. The function of these proteins is generally well known, however a special role in

podocytes has not been described yet (122). In summary, female podocytes displayed a higher capacity of ubiquitination and proteases compared to males, still their role in modulating the ECM composition requires further studies.

3.5.6 Focus on sexual dimorphism in podocyte-specific structural proteins and proteins related to podocyte homeostasis and function.

Interestingly six of the significantly differently expressed proteins in this proteomics study were related to the actin cytoskeletal or regulators of the actin filaments, including titin, vinexin, catenin alpha 1, integrin alpha1 and collagen VI which are important for podocyte function.

First, podocyte-specific structural proteins were investigated in more detail. Interestingly, the majority of **podocyte-specific proteins**, such as synaptopodin, podocalyxin and nephrin were higher expressed in females, in addition to **cell junction and focal adhesion molecules**, such as ZO-1, Magi-2, ACTN4, vimentin, Itg β 5, Itg β 1, focal adhesion kinases, such as Ilk with 2.5 times (log₂FC 1.3) higher expression in female podocytes. Female podocytes showed abundant expression of integrin-related proteins with 48 proteins involved in integrin signaling and only 4 being overexpressed in male podocytes, such as Talin-1/2. Proteomics further revealed higher expression of ECM components in female podocytes, such as Col3 α 4, Col6, Laminin β 2, syndecan-4, dystroglycan (Figure 47A/B), as well as for proteins involved in exocytic/endocytic pathway, such as clathrin light chain (data not shown).

In contrast to RNA-seq results, cytoskeletal proteins, binding and regulators were enriched in female podocyte. 34 **cytoskeletal proteins** (PC:00085) and 9 adaptor proteins were highly expressed in female podocytes with > 2 FC compared to only 5 in males, such as ACTN4 and Vimentin. Furthermore, 11 proteins with Rho-GTPase activities regulating cytoskeletal function, such as Cofilin1/2, Myo10, Rock1 and Rheb proteins were higher expressed in female podocytes, also 6 upregulated Arp2/3 protein complexes. The Arp2/3 machinery is required for proper podocyte process formation, adaptation and adhesion for regulation of the GFB (Figure 47C/D).

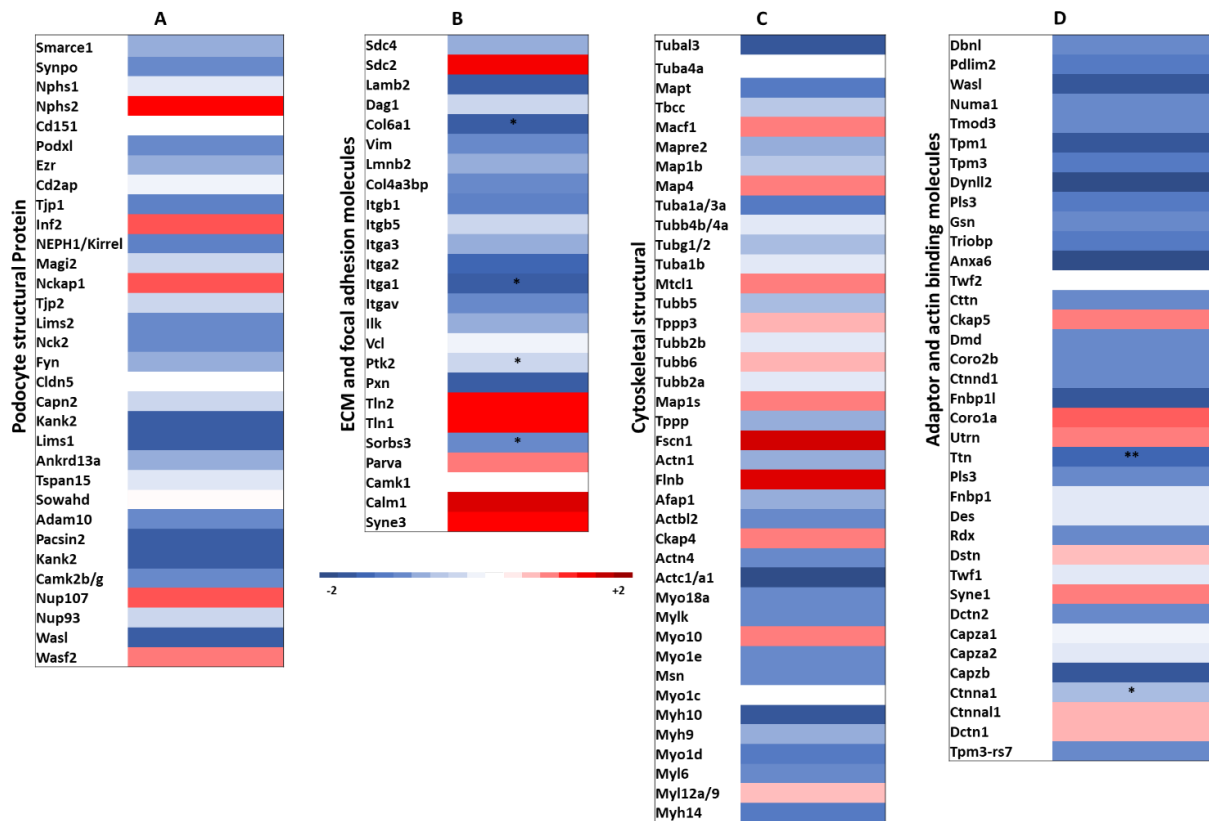


Figure 47. Log2FC of LFQ values of male versus female podocyte proteins for podocyte-specific and structural proteins. (A/B) Major structural podocyte proteins, focal adhesion molecules and ECM proteins were higher expressed in female compared to male podocytes. (C/D) cytoskeletal and binding proteins indicate by blue colour, red colour indicates higher expression in male. (*, significantly DE with $*p < 0.05$, **, with $p < 0.01$, *** $p < 0.0001$).

3.5.7 Sexual dimorphism in proteins involved in major cellular response and cell fate pathways

In contrast to transcriptomics, proteomic analysis using Panther database showed that several signalling pathway proteins were overexpressed in female podocytes compared to males of vehicle groups with $\log_2FC > 0.57$ / $FC > 1.5$ times. For example, different AMPK subunits and ERK1/2 were more than twice higher expressed in female podocytes, as well as AKT1 and AKT2. Moreover, 22 additional protein kinases, tyrosine and phosphatase enriched kinases were sex-DE with 1.2 -1.5 FC (data not shown).

3.6 Integration of transcriptomics and proteomics data

As both transcriptomic and proteomic analyses relied on podocytes of mice treated under same experimental settings, it was of special interest whether the transcriptomic sex differences were translated into the proteome. Corresponding genes/proteins from transcriptomic and proteomic datasets were overlaid and analyzed. Only 6 significantly sex-regulated transcripts were significantly sex-DE on protein level. Nevertheless, the biological consequences of the protein differentially expression with $FC > 1.5$ were analyzed using Enrichr and major hits were similar such as for the terms oxidation phosphorylation, glycolysis, proteasome, metabolic process were among the common pathways concordantly enriched in both, proteomics and transcriptomics of male and female podocytes. Others were enriched in an opposite manner, such as e.g. males enriched proteins related to translational factors and ribosomal proteins, whereas females showed a higher expression of cytoskeleton, focal adhesion and regulation of cytoskeleton-related proteins. (Figure 48).

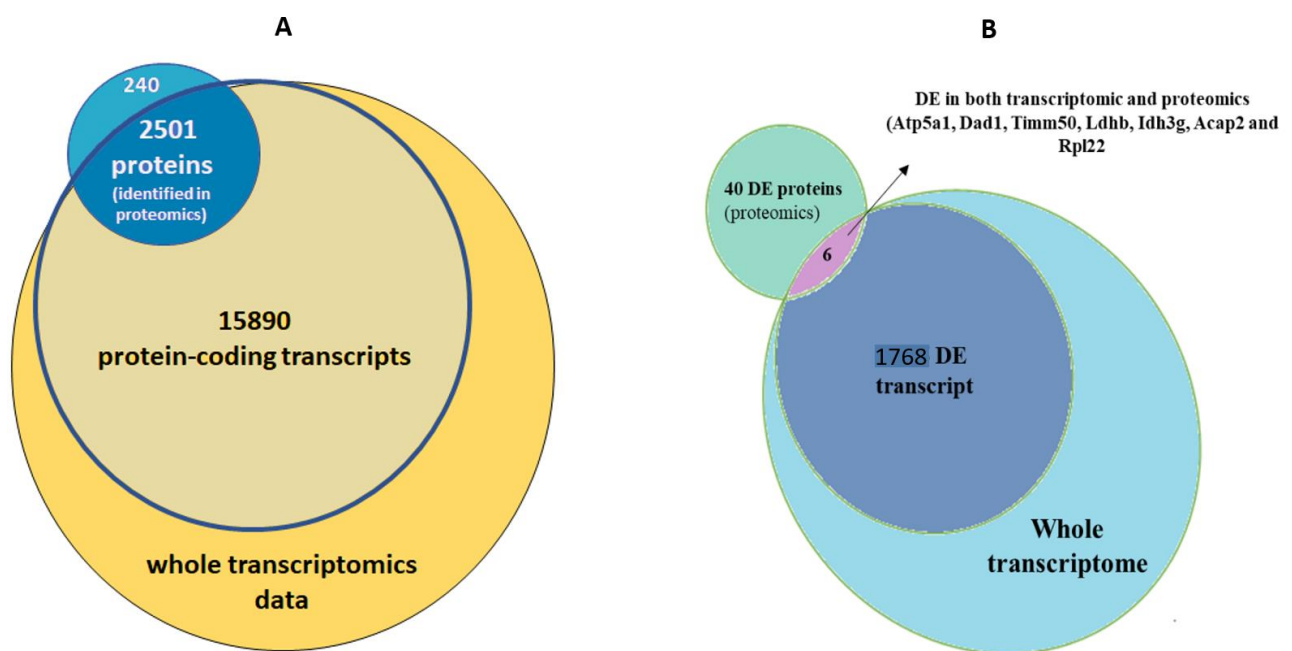


Figure 48. Integration of transcriptomics and proteomics data. (A) Overlaying protein-encoding transcripts with identified proteins from current proteomics (B) only 6 genes and their corresponding proteins showed significant sex-DE in both RNA sequencing and proteomics.

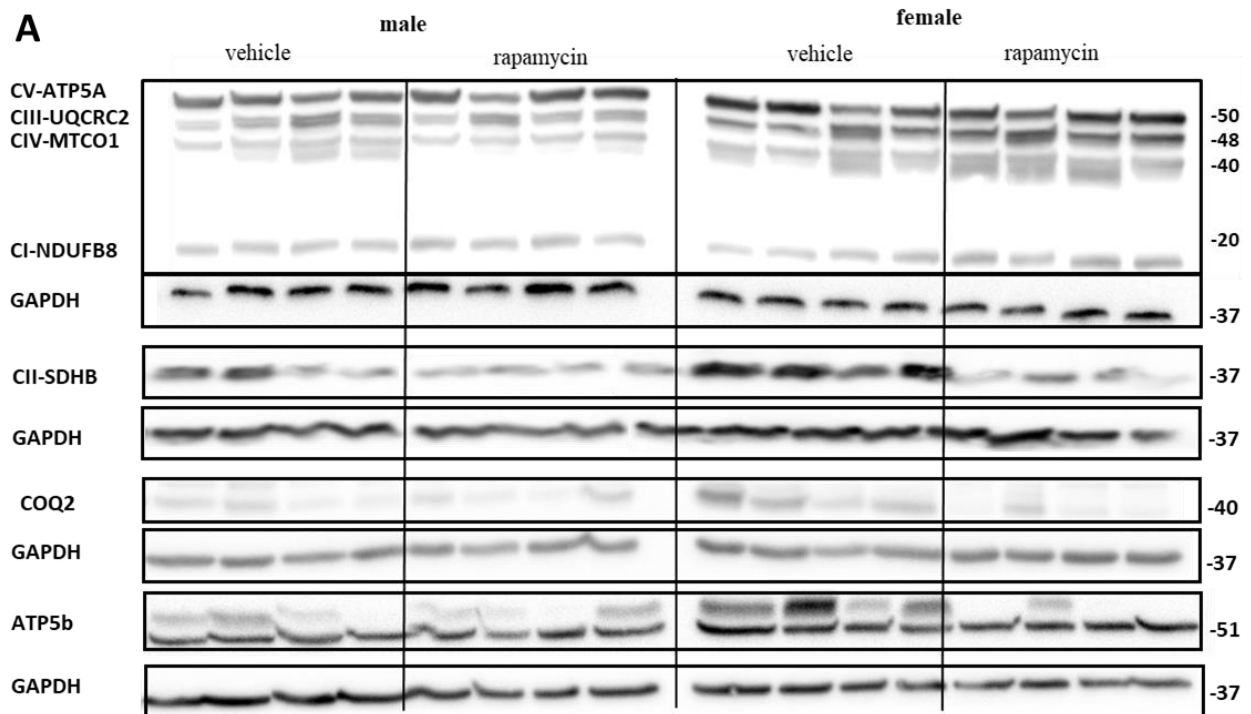
3.7 Analyses of selected protein expression levels in renal cortex tissues of all experimental groups to investigate sexually dimorphic responses to rapamycin treatment on protein level

Due to limited protein material to be obtained from isolated podocytes, kidney cortex sections of female and male vehicle and rapamycin treated mice (each at least 4 mice/group) were immunostained and subjected to tissue lysis and subsequent protein detection using immunoblots with specific antibodies to validate proteomics data and to further study the effects of rapamycin treatment on protein levels.

3.7.1 Sexual dimorphic responses to mTOR inhibition on expression of mitochondrial oxidative proteins

Both, RNA-seq and proteomics had shown intrinsic sex-differences for podocyte-specific expression at the mitochondrial and oxidative phosphorylation (respiratory chain) levels.

To confirm proteomics results concerning changes of OXPHOS complexes in mouse mitochondria between vehicle groups and to investigate the responses to rapamycin, Western blots were performed from cortex-renal tissue and the total OXPHOS rodent WB Antibody Cocktail was used (Figure 49).



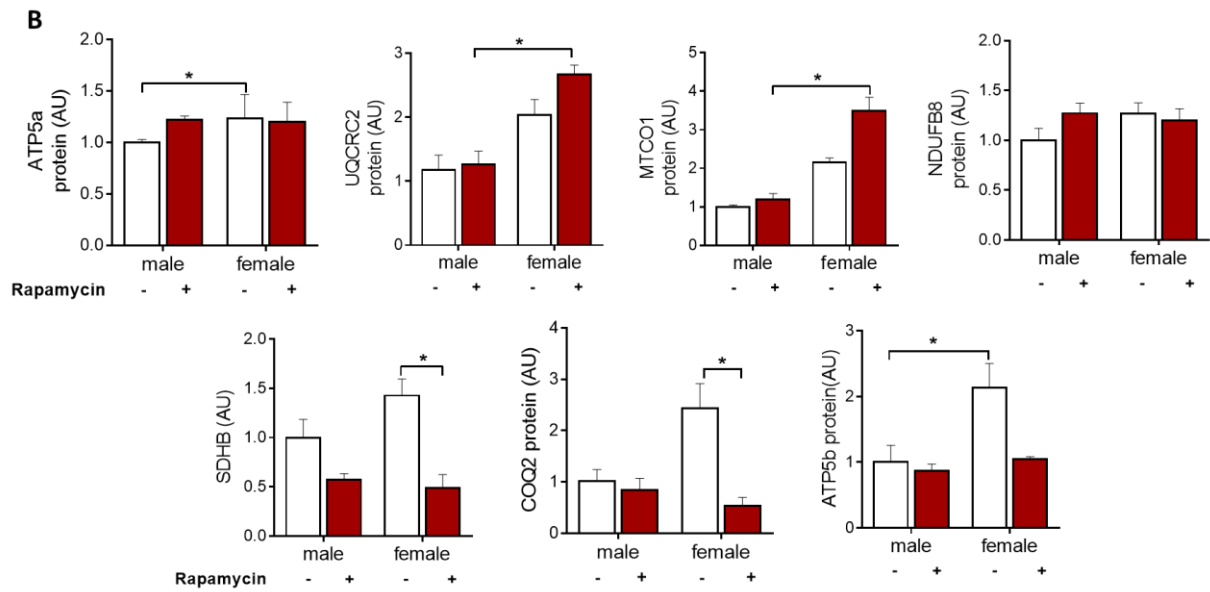


Figure 49: Sexual dimorphic expression of mitochondrial proteins. Higher expression of OXPHOS complex proteins was observed intrinsically in females and responses to rapamycin were sexually dimorphic (A) Representative western blots are shown for OXPHOS complex and COQ2 (n=4 for each experimental group) (B) Densitometric quantification showed a higher level of mitochondrial proteins in females compared to males. GAPDH was used as loading control. Kruskal–Wallis test was used and results are expressed as mean +/- SEM, *p<0.05, **p<0.01.

Increased expression of ATP5a and ATP5b (complex V) was confirmed by WB in female vehicle with comparable FC of 1.3 in proteomics. MTCO1 and UQCRC2 (complex IV) were not quantified in proteomics, however, WB showed increase in females compared to male vehicles. Proteomics detected several Cytochrome b-c1 complex (UQCRC component) and all were upregulated in female vehicle podocytes as well as for MTCO2 with log2FC more than 0.5.

Complex II core protein SDHB was not successfully quantifiable with cocktail OXPHOS antibody, however use of another monoclonal AB showed concordantly to RNA and proteomics results significantly higher expression in females. After rapamycin, levels remained the same or decreased such as in SDHB that was decreased significantly in females, whereas MTCO1 and UQCRC2 only increased in females. In male cortex tissues no major changes were detectable between vehicle and rapamycin groups for these proteins.

The mitochondrial COQ2 enzyme functions in the biosynthesis of CoQ (ubiquinone), a redox carrier in the mitochondrial respiratory chain and a lipid-soluble antioxidant, and is part of the

coenzyme Q10 pathway which plays an essential role in oxidative phosphorylation working as antioxidant. Mutations in this gene cause coenzyme Q10 deficiency and cause nephrotic syndrome symptoms (135). WB analysis showed higher baseline of COQ2 in female mice, both males and female enzyme levels were reduced after rapamycin treatment, to higher extent in females.

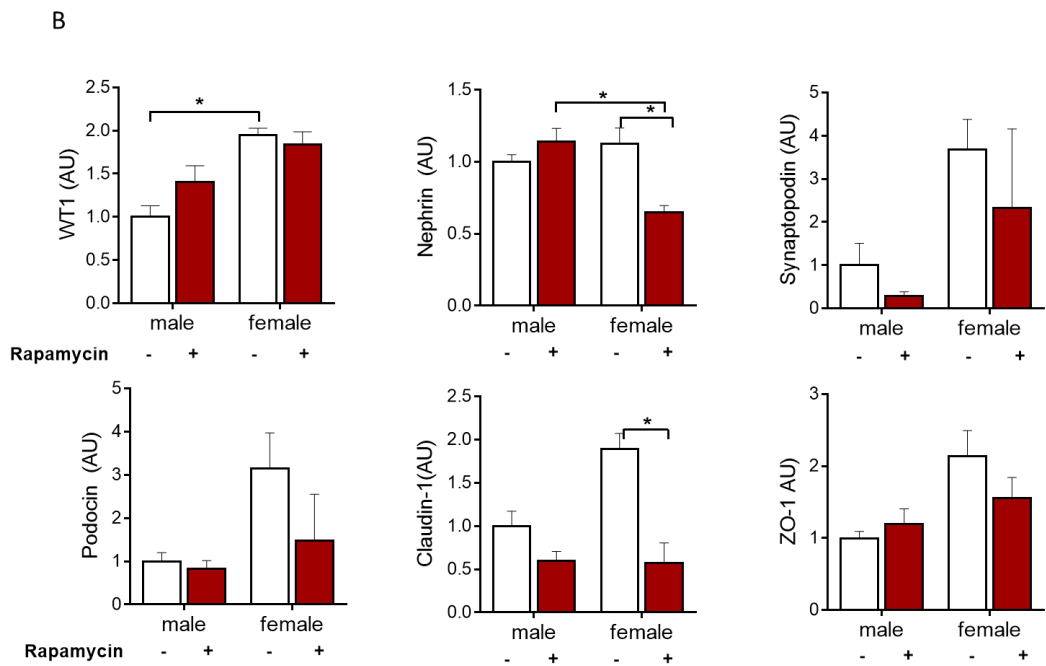
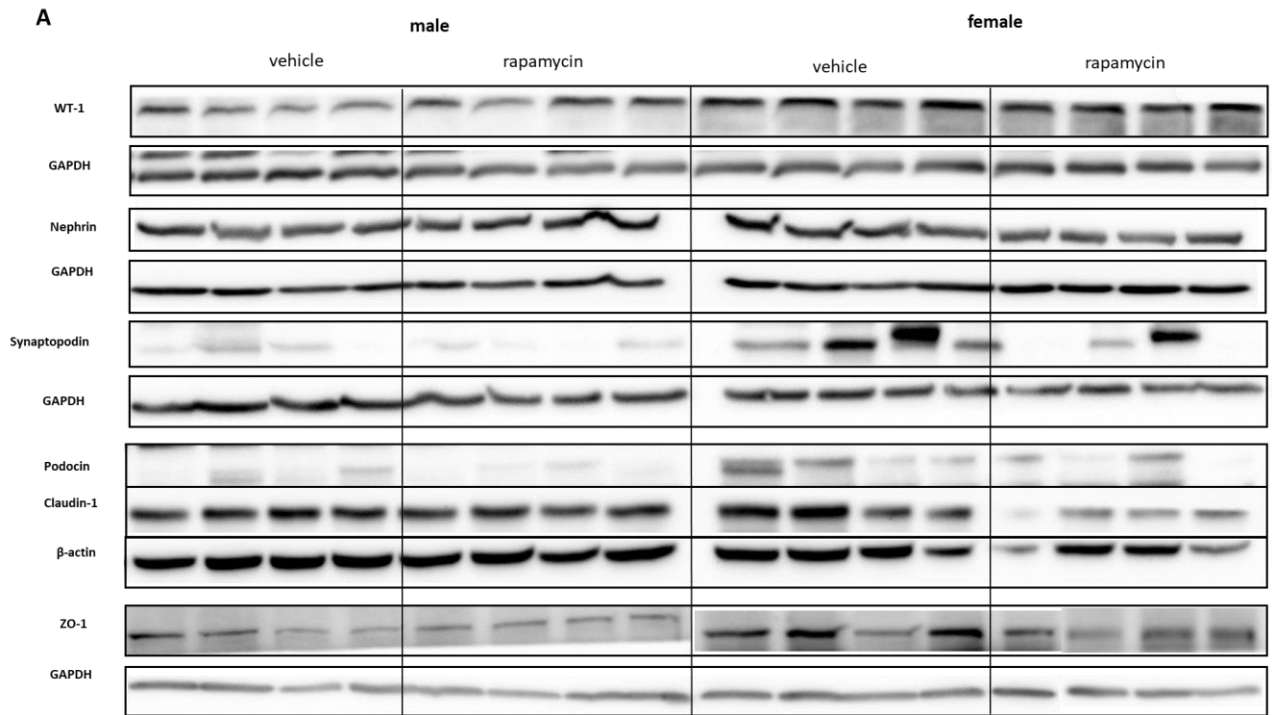
3.7.2 Sexual dimorphic responses to mTOR inhibition on podocyte-specific proteins

Nephrin and ZO-1 control the slit diaphragm integrity and function and work also as signaling molecules (27). Podocin and synaptopodin importantly regulate actin cytoskeleton and function. In proteomics, the majority of these podocyte-specific proteins were intrinsically higher expressed in female podocytes. Selected proteins were now investigated for their expressional changes in response to mTOR inhibition in renal cortex tissues.

Podocin appeared almost 3 times higher expressed in female compared to male renal cortex tissues, which was contrary to expression levels in podocytes in proteomics. Yet LFQs in proteomics showed high interindividual variability for podocin which might have led to the discrepant results.

Yet, ZO-1 levels were highly expressed in female vehicle group compared to male as detected by proteomics. After rapamycin, levels of podocin, nephrin, synaptopodin, claudin-1 and ZO-1 decreased in females whereas remained almost constant in males except for synaptopodin and claudin-1 which also decreased in males. Another podocyte marker, WT1 could not be determined in proteomics most probably due to low abundancy in the analyzed podocyte samples. WB revealed that females had a two times higher intrinsic protein expression of WT1 compared to males. In response to mTOR inhibition, levels slightly decreased in females and on the contrary increased in males. (Figure 50A/B). It is well documented that defects of WT1 cause several types of renal disease and nephrotic syndrome as Fraiser and Denys-Drash syndrome, and the reduction in the number of podocytes correlates with the progression of renal diseases. Podocyte number is usually measured by counting of positive signals for nuclear WT1 staining. For further confirmation of surprising WB results, immunohistochemistry of WT1 was performed, and results were quantified by counting all positive signals in all glomeruli of 6 mice per group. Female mice had a higher podocyte number indicated by WT1 positive signal. After rapamycin, the number increased in male and decreased in female. Also, it was visually noticed that the signal intensity

of WT1 was much stronger in female compared to male in both, vehicle and rapamycin groups. (Figure 50C/D).



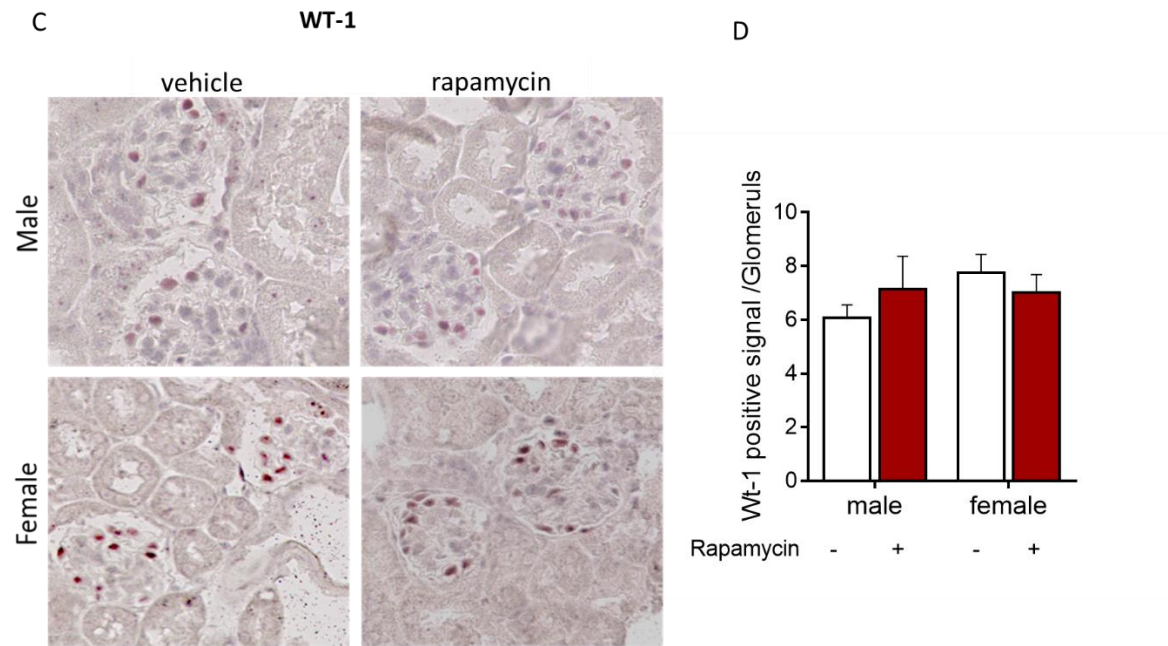


Figure 50: Sexual dimorphism in selected podocyte-specific proteins. (A) Western blots showing a higher expression of WT1, Synaptopodin, nephrin, podocin, ZO-1 and Claudin-1 in female vehicle (n= 4 for each experimental group). ZO-1 band was detected at 130 kDa, not as expected 200 kDa, this could be due to post modification or isoform from ZO-1 (as manufacturer info). (B) Relative protein levels as determined by densitometry of WBs, * $p < 0.05$, ** $P < 0.01$. (C) Immunohistochemistry of WT1 in vehicle and rapamycin treated groups showed significantly more nuclei stained positive for WT1 in females. Rapamycin increased WT1 staining in podocytes in males, but not females, (D) Quantification of staining for WT1, renal cortex slide staining from 6 mice per group were analyzed.

3.7.3 Effect of rapamycin on cytoskeletal and focal adhesion proteins

The cytoskeleton is composed of three types of filaments, F-actin fibers, intermediate filaments and microtubule filaments. One representative protein from each filament type was analyzed by WB in podocyte-enriched cortex samples. ACTN4, Vimentin, and α -tubulin proteins were highly enriched in podocytes, all three proteins were higher expressed in female vehicle group compared to male consistent to podocyte-specific proteomics results, vimentin and α -tubulin protein levels were reduced after rapamycin treatment mainly in females. (Figure 51)

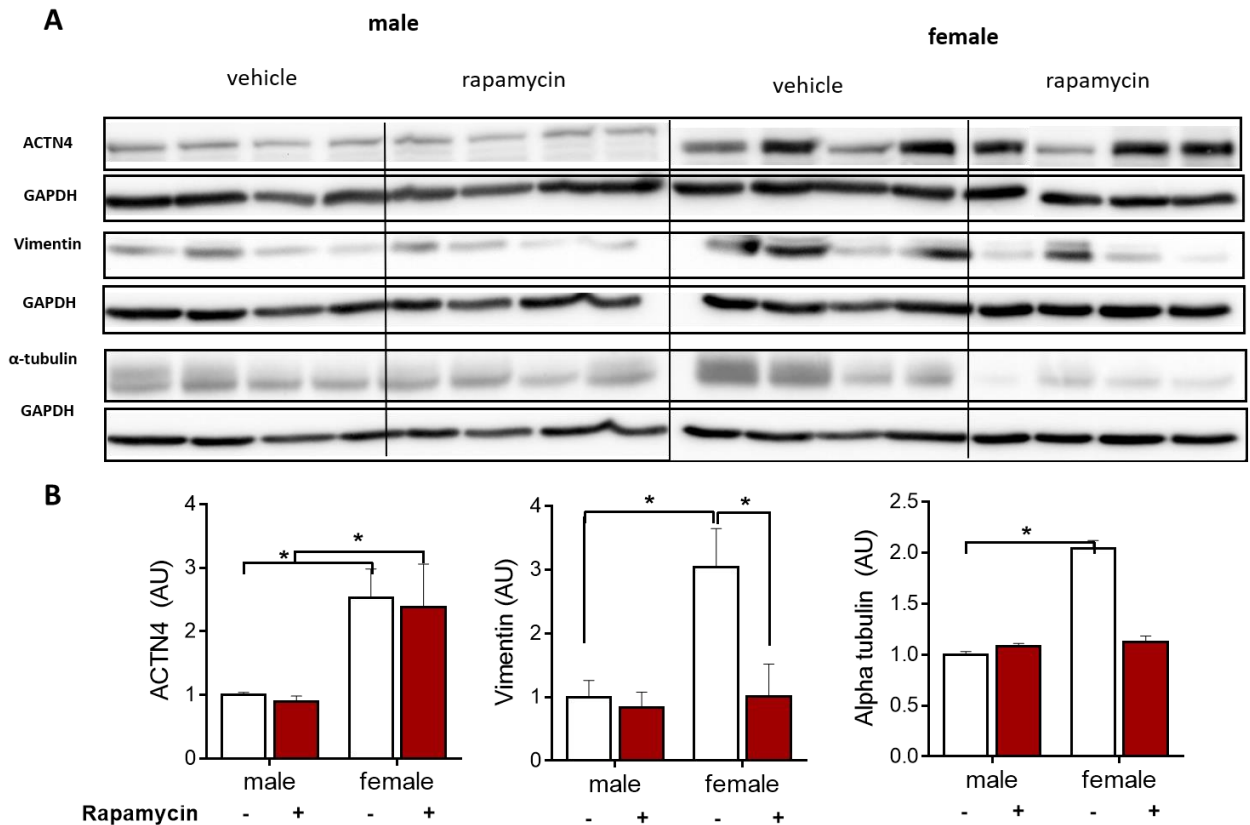


Figure 51. Sexual dimorphism in cytoskeletal filament proteins. (A) ACTN4 representing actin filaments, α -tubulin representing microtubules and vimentin as candidate protein for intermediate filaments were determined in renal cortex tissue sections of mice from all four experimental groups. (n=4 per group) (B) Densitometric quantification showed a higher level of cytoskeleton proteins in females compared to males. GAPDH was used as loading control. Kruskal–Wallis test was used and results are expressed as mean \pm SEM, * p <0.05, ** p <0.01.

Additionally, as Phalloidin staining is frequently used to analyze the actin cytoskeleton, this staining was used to validate the proteomics results of female podocytes which showed higher abundance of actin cytoskeletal proteins compared to male podocytes. Figure 52 displays representative staining and quantification of the average intensity per glomerulus (70-80 glomeruli per group were quantified). Rapamycin treatment led to reduced expression of actin fibers in both sexes.

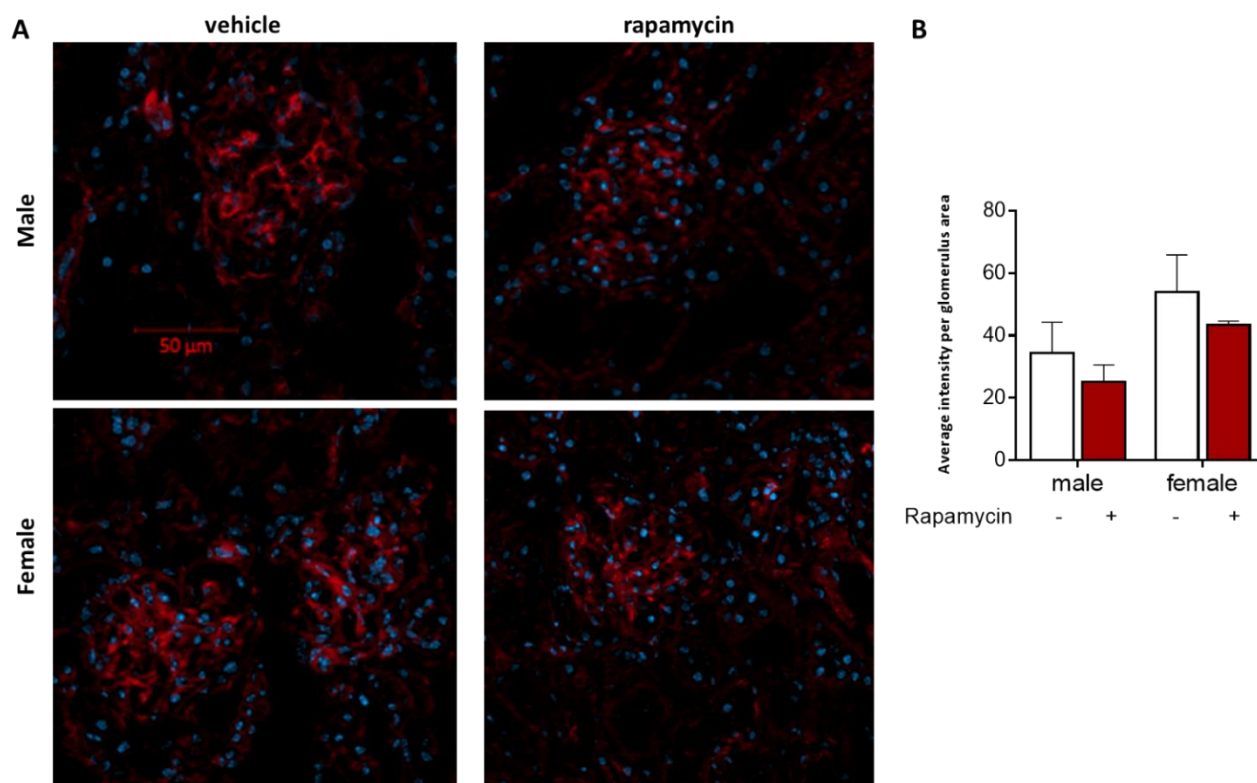


Figure 52. Cytoskeletal staining of renal cortex tissue sections from vehicle and rapamycin treated male and female mice and quantification. (A) Representative fluorescent microscopy images of phalloidin-649 staining of renal cortex tissue sections from vehicle and rapamycin treated male and female mice. (B) Average fluorescent intensities were determined per glomerulus and are shown in arbitrary units. Staining of four mice were analyzed per group, 70-80 glomeruli were quantified per group.

Rho-GTPases influence podocyte cytoskeleton and function. Therefore, WB were performed for RhoA, Rac1 and Cdc42 to investigate the cytoskeletal regulation after rapamycin treatment. Females had higher intrinsic levels of RhoA and Rac1 proteins, and lower level of Cdc42 compared to males which was concordant to proteomics with similar fold change differences. In response to rapamycin treatment, females had significantly reduced Rac1 levels with almost no changes in RhoA and Cdc42 expressions. However, males increased Cdc42 after rapamycin treatment with slight, non-significant reductions in Rac1 and RhoA. (Figure 53)

It has been reported that Rho GTPases Rac1 and Cdc42 have divergent functions in podocyte injury (136). Reduced levels of Cdc42 in podocytes result in congenital nephropathy and renal failure. Furthermore, Cdc42 regulates podocyte apoptosis and protects against proteinuria (137) .

The observed increase in Cdc42 in male rapamycin treated group might indicate a compensatory response to rapamycin counteracting the stress induced by the drug.

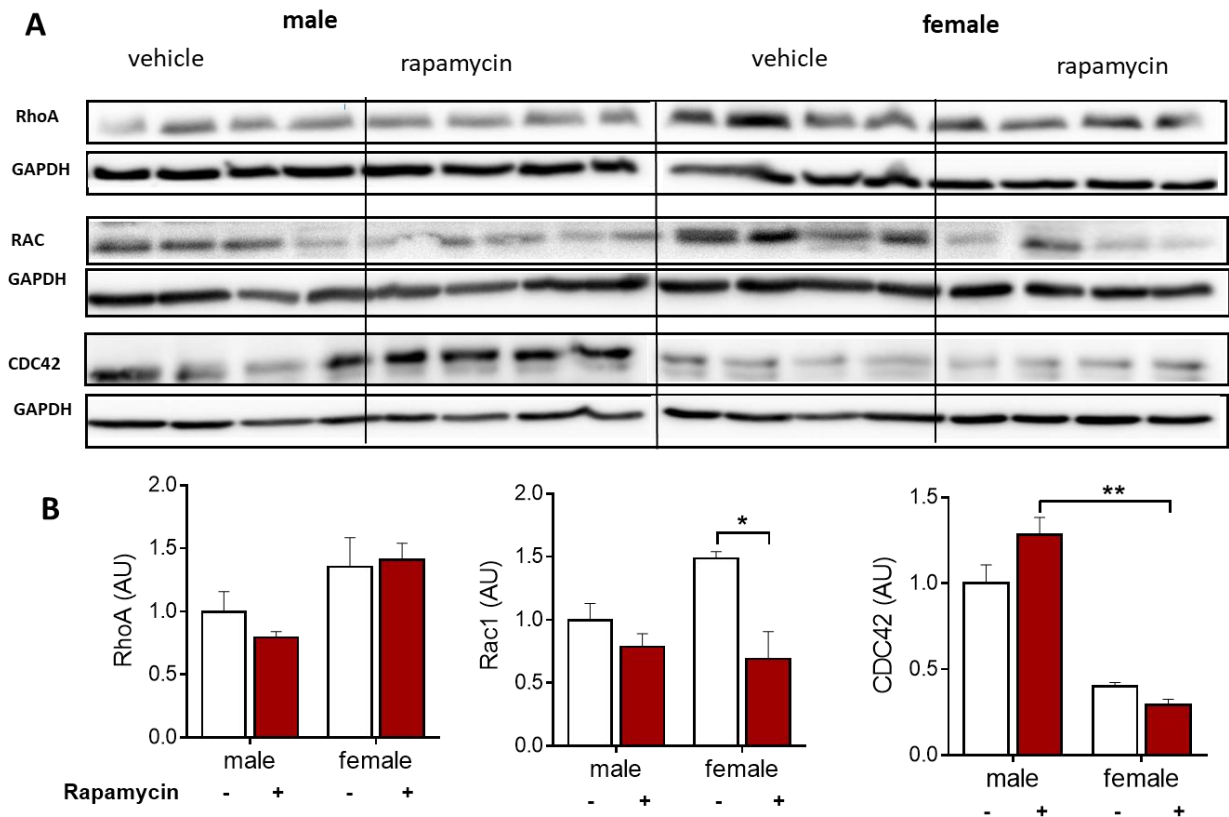
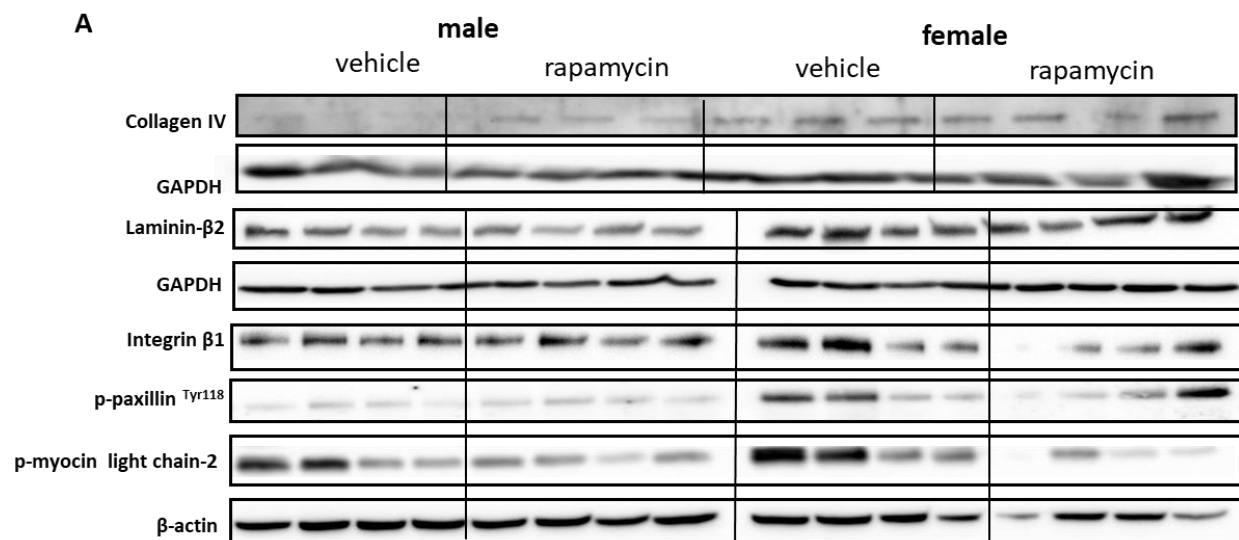


Figure 53. Expression of Rho-GTPases and sexual dimorphic responses to rapamycin treatment in renal cortex tissue. (A) WB and densitometric analysis show higher intrinsic expressions of RhoA, Cdc42 and Rac1 in females. Rapamycin significantly reduced Rac1 in females and increased Cdc42 in males (n=4 per group) (B) Densitometric quantification showed a higher level of GTPase proteins in females compared to males. GAPDH was used as loading control. Kruskal–Wallis test was used and results are expressed as mean +/- SEM, *p<0.05, **p<0.01

FA and integrins connect the actin cytoskeleton to the GBM, laminin β 2 and Collagen IV α 3 α 4 α 5 (128). They are considered to be the major proteins in the GBM and serve as a scaffolding layer for the podocytes. Laminin β 2 and Col IV (α 3 α 4 α 5) were intrinsically significantly higher expressed in female compared to male. Levels reduced non-significantly in females after rapamycin treatment. Mainly integrin α 3 β 1 mediates cell adhesion to the extracellular matrix in podocytes (129).

Unfortunately, integrin $\alpha 3$ detection by WB was not successful, yet, Wb analysis of integrin $\beta 1$ showed that females had 1.3 fold higher expression compared to males in vehicle group. In proteomics 5 types of integrins α and β could be quantified and were more than 1.2 fold higher expressed in female compared to male podocytes. Integrins are linked to the actin cytoskeleton via many molecules, such as talin, vinculin, paxillin and integrin-linked kinase (ILK). Paxillin is an adaptor protein and considered as a key component of integrin signaling. Proteomics had shown more than three times higher intrinsic expression of paxillin in female podocytes. The tyrosine phosphorylation is required for integrin-mediated cytoskeletal reorganization. WB in Figure 54 shows a higher intrinsic level of phosphorylated paxillin in females which was reduced to almost half after rapamycin treatment, suggesting that male podocyte increase phosphorylation in face of stress caused by rapamycin to increase integrity and adhesion between podocyte cytoskeleton with ECM and integrin signaling.

Further key component of focal adhesion formation is myosin II. Activation of myosin II through light chain phosphorylation allows myosin to bind to actin filaments (138). Proteomics detected twelve myosin proteins, most of them were highly expressed in female vehicle compared to males, such as Myo1c, Myo9 and Myo1e. WB could be performed for phosphorylated myosin light chain-2 and revealed higher activation levels in females and decrease after rapamycin treatment in both sexes. (Figure 54)



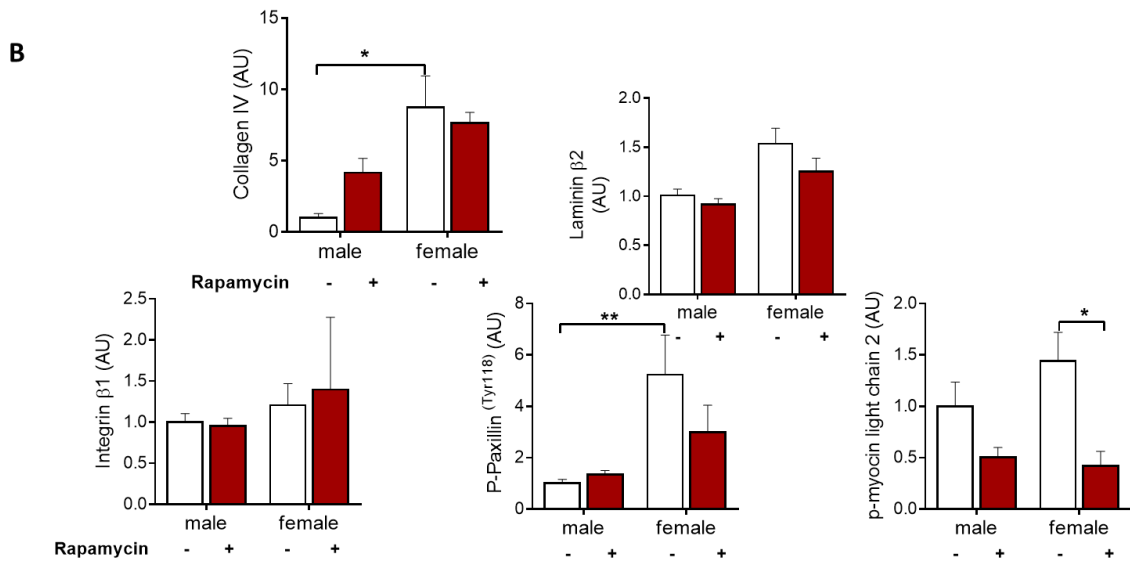


Figure 54. Expression and regulation of selected ECM and focal adhesion proteins in renal cortex tissue of male and female vehicle and rapamycin treated mice. (A) WB and densitometric analysis show higher intrinsic expressions of collagen IV, Lamininβ2, Integrinβ1, phosphorylated Paxillin and Myosin light chain in females (n=3 per group for Collagen IV, n=4 per group for Laminin β2, Integrinβ1, Paxillin and myosin light chain). Laminin β-2 was detected at around 130-150 kDa molecular weight, possibly post-modification changes as manufacturer info. (B) Densitometric quantification of WB, GAPDH was used as loading control. Kruskal–Wallis test was used and results are expressed as mean +/- SEM, * $p < 0.05$, ** $p < 0.01$.

3.7.4 Sexual dimorphism in autophagy and apoptosis marker protein expressions

RNA-seq had shown a higher transcriptional level of autophagic and apoptotic genes in podocytes. Therefore, several marker proteins involved in autophagy and apoptosis were investigated for possible sexual dimorphism on the translational level.

Autophagy is controlled by mTOR signalling and inhibition of mTORC1 leads to induction of autophagy. Measurements of p62 (Sqstm1) degradation and increase of LC3Iib, which is involved in autophagosome formation, are established marker proteins to investigate autophagy. Females had intrinsically higher levels of LC3Iib which only in females further increased in response to rapamycin together with slight reduction of p62 indicating induction of autophagy in response to mTOR inhibition. Male did not change LC3Iib levels after rapamycin treatment yet displayed a non-significant increase in p62 protein. (Figure 55)

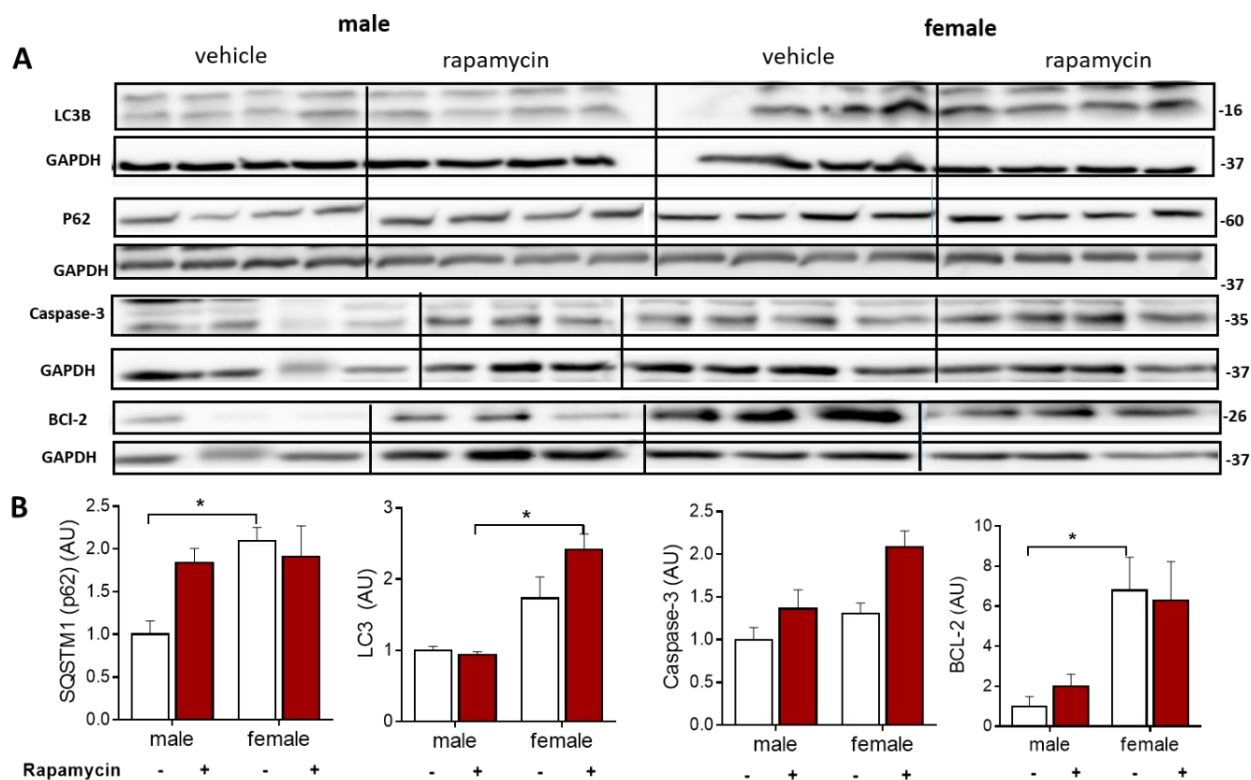


Figure 55. Marker protein expressions for autophagy and apoptosis in renal cortex tissue of male and female vehicle and rapamycin treated mice. (A) Autophagy marker LC3IIB was significantly higher in female vehicle mice and further increased after rapamycin treatment in female only. No cleaved caspase 3 could be detected indicating absence of apoptosis in all experimental groups. Furthermore, p62 and BCL2 were significantly higher in female compared to male vehicle group (n=4 per group for LC3B, P62 and Caspase-3, n=3 per group for BCL2) (B) Quantification of WB using image J., Kruskal Wallis test was used* p < 0.05, ** p < 0.01, *** p < 0.001).

Concerning apoptosis, proteomics analysis had detected 12 apoptosis related proteins to be upregulated in female, under them caspase-3, CytoC and Bag1, and only 3 proteins in male, under them Cad, a caspase activated Dnase. In Wb of renal cortex tissues, caspase 3 increased in response to rapamycin in females whereas levels remained largely unchanged in males. However, increased caspase-3 was not indicative for increased apoptosis in females treated with rapamycin, as the caspase-3 band was only detected at 35 kDa and not at lower bands which would have indicated cleaved protein levels indicative for apoptosis, suggesting “healthy” glomerular compartment in mice even after 3 weeks rapamycin treatment. In addition, the antiapoptotic protein Bcl2 was quantified and showed significantly higher levels in female vehicle, with non-significant changes after rapamycin in both sexes.

3.8 Effect of mTOR inhibition on renal cortex metabolism

RNA sequencing revealed an important sexual dimorphism in genes related to metabolism. To determine whether this relevant finding translated into sex differences in renal metabolites, and to get further insight into the effect of rapamycin on glycol-metabolic activity, seven kidney cortex tissue specimen from male and female vehicle and rapamycin groups were prepared for GS/MS which was performed in collaboration with BIH Metabolomics Facility lead by Jennifer Kirwan. GS/MS measurements and statistical analyses were done by Dr. Raphaela Fritsche. Four samples could not be analyzed due to injection failure, yet a minimum of at least 5 biological replicates per group remained for further analyses.

In total, 104 metabolites were identified (Appendix, Table7). Metabolites were valid when they appeared in a minimum of 3 biological replicates. 41 metabolites involved in central carbon metabolism could be analyzed in detail. Biological variabilities were generally low in the four experimental groups; however a slightly higher variance was detected in the sum of normalized peak area in female mice treated with rapamycin (data not shown).

The main findings of the metabolite analyses were that independently of sex, most of the amino acids (except for tryptophan, tyrosine and lysine) were significantly higher in rapamycin-treated mice. This accumulation was more pronounced and significant in a higher number of single amino acids in males compared to females suggesting that rapamycin might affect protein synthesis to a higher extent in males compared to females (Figure 56). Among the amino acids, serine, threonine and isoleucine showed the largest relative increased in intracellular pools that reached more than 70% increase. In this study, tryptophan, lysine and tyrosine were not accumulated, and the levels were decreased largely in females. These amino acids are known to be metabolized and used for Acetyl CoA synthesis - the first intermediate in TCA cycle- and might serve in females as a compensation for the reduced TCA cycle.

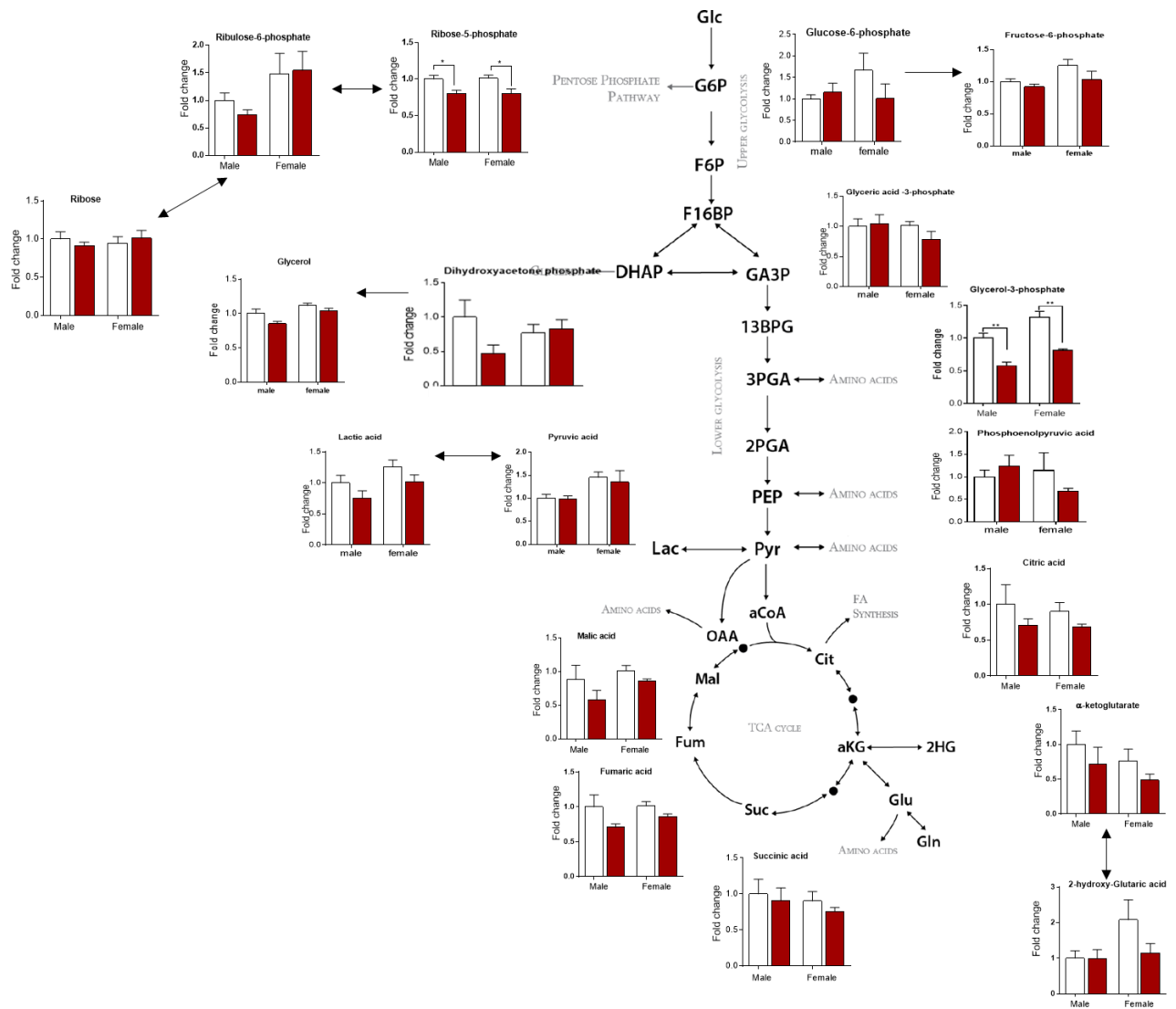


Figure 57. Rapamycin effect on main metabolites of the central carbon metabolism. (A) Scheme of rapamycin effect in each sex for glycolysis, TCA cycle and PPP pathway. (B) Heatmap of log₂FC of the mean of the normalized peak areas of glycolysis metabolites, TCA cycle and pentose phosphate pathways in male and female renal cortex tissue in response to rapamycin in each sex separately and male and female combined (rapamycin/vehicle) showing decreased glycolytic metabolism in both male and female in response to rapamycin. Blue indicates decreased level - white (no regulation) – red (increased), * p < 0.05, ** p < 0.01, ***p < 0.001. Dashed line represents significance for the group of glycolysis and TCA after univariate scaling, n=7 biological replicates in each group.

Only three metabolites showed sexual dimorphic response to rapamycin: Glucose-6-phosphate (G6P), phosphoenolpyruvate (PEP) and α -ketoglutarate. The relatively higher metabolite levels in males compared to females could be explained by enhanced glycolytic metabolism in males to compensate for ATP reduction caused by rapamycin. Interestingly, males had upregulated genes for oxidation phosphorylation and glycolysis, whereas many enzyme expressions were maintained or decreased in females, suggesting higher stress resistance in females. Since many amino acids are metabolized and converted to metabolites entering glycolytic pathways in many steps, the increase in amino acid pool in males could partially explain why males had relatively higher metabolite levels compared to females. Concordant to RNA-seq and proteomics, metabolomics showed that female mice had higher intrinsic levels of glycolytic metabolites and PPP (except for succinate and citrate).

Nucleobases analyzed in this metabolomics study were adenosine, uracil, and cytosine. All of them were reduced after rapamycin treatment in both, males and females without significant differences. Nucleobase levels were reduced although amino acids, responsible for nucleobases synthesis were accumulated after rapamycin. mTORC1 is involved in de novo synthesis of nucleotides (139), and inhibition by rapamycin might have additionally prevented amino acid conversion to pyrimidine/purine nucleobases. Nevertheless, adenosine showed a sexual dimorphic response to rapamycin. Males reduced adenosine levels by 50% and females increased their level by twice. (figure 58)

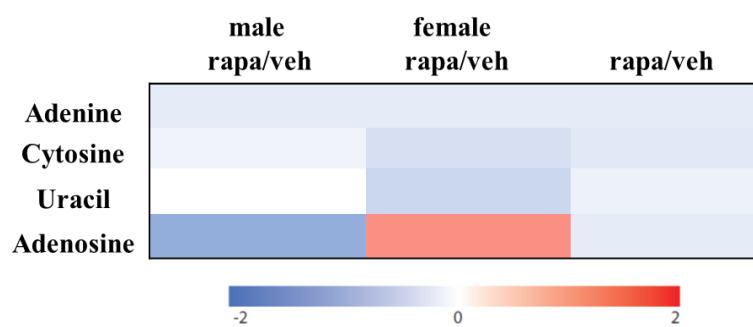


Figure 58. Rapamycin effect on nucleobases metabolites. Heatmap of log₂FC of the mean of the normalized peak areas of the four nucleobases showing a decrease in nucleobase metabolism in both, male and female, after rapamycin treatment, except for adenosine. Blue indicates decreased level - white (no regulation) – red (increased), * p<0.05, Wilcoxon test on the normalized peak areas.

4. DISCUSSION

In 2001, the Institute of Medicine (IOM) published a report, indicating that “Sex matters” is an important basic human variable that should be considered when designing and analyzing studies in all health-related research. Still, many studies are only conducted with males or failed to report the sex of animals (140). This thesis work about the sexual dimorphism of the molecular signature of podocytes under physiological and stress conditions might contribute essentially to fill that lack of scientific knowledge.

Sex differences in kidney function and renal diseases are well documented in animals and humans with the incidence of ESRD being higher in males compared to females. Further, the mean age at the start of dialysis is also higher in women compared to men (13). To this date, the exact molecular mechanisms underlying these sex biases are largely unknown. Sex hormones and the fact that 10-20 % of X chromosome genes escape silencing on the inactive X and cause an increases of gene expression in females with different expressions in different organs could explain this partially (141). A better understanding of the molecular cell compositions and response patterns in male and female might help to develop sex-specific therapeutics in today’s precision medicine to support intrinsic defense mechanisms and to limit or even reverse pathologies.

One of the most important cell types of the kidney which determine progressive kidney diseases are podocytes. Podocytes are terminally differentiated cells of the glomerulus and represent the essential cell-type to maintain the integrity of the GFB. Recently, several papers have focused on the molecular identity of podocytes. However, despite of the known sexual dimorphism of renal diseases and clinical courses there is only one report including male and female podocytes for transcriptomic analysis, yet focusing on podocyte aging processes rather than on sex-differences (115).

This is the first study which investigated in detail the sex-specific molecular signature of podocytes by deep transcriptomics and proteomics, accomplished with signaling studies and metabolomics of renal cortex tissues from male and female mice under vehicle control conditions and in a stress model using mTOR inhibition. In order to obtain highly pure podocyte fractions for molecular analyses, a transgenic mouse line (NPHS2Cre*mT/mG mice) was used which allowed highly efficient isolation of GFP-labelled podocytes by FACS sorting (95). Even though no microalbuminuria, renal functional changes or histological pathologies could be detected in all vehicle and rapamycin treated animals after 3 weeks of treatment, significant transcriptional

changes of podocytes genes, proteins and metabolites were observed. Sex differences were most prominent between vehicle groups, yet rapamycin treatment mostly abolished differences with a shift of the male transcriptome towards female vehicle phenotype. Moreover, on proteome levels, a high number of proteins involved in mitochondrial oxidative phosphorylation, metabolism and glycolysis were significantly higher expressed in female podocytes with many of them showing concordant expression with the transcriptome. Whereas females downregulated many podocyte structural and functional related genes and proteins in response to rapamycin treatment, they seemed less affected by consequences of mTOR inhibition on protein synthesis and other metabolic changes as determined by metabolomics of podocyte-enriched renal cortex tissue.

4.1 Mouse model and experimental design

4.1.1 Mouse model

Mice expressing GFP-positive podocytes and tomato-positive non-podocyte kidney cells (NPHS2Cre*mT/mG) were used as they enabled highly specific isolation of podocytes by FACS sorting. The podocyte isolation technique was adapted from Borries et al. 2013 which was superior to previous reported isolation techniques yielding to an average of 500,000 podocyte per mouse (95). In the current study, using the same mouse line, the average podocyte yield per mouse was 330,000, which was comparable to the previous cited study and corresponded to about one third of all glomerular cells. It should be added that the age of the mice used in this study (12-18 weeks old) was chosen to be comparable to 20 - 30 year-old human, representing healthy mature adults prior to relevant changes caused by aging or disease development.

Different mouse strains are found to have different susceptibilities to various diseases. Mice used in this study were on a C57BL/6 background. Unfortunately, C57BL/6 mice show sometimes resistance to proteinuria in contrast to 129/Sv mice and considered sensitive to only certain renal models (142). This might be a reason that in spite of strong molecular changes, rapamycin did not lead to functional renal impairment during the 3 weeks of treatment even with rapamycin concentrations reaching clinically significant trough levels which have been reported to cause renal functional impairment in human. However, C57BL/6 strain is a good breeder and therefore most commonly used to generate transgenic mice and its entire genome is published and can be related. Further to that, several studies used C57BL/6 strain before to investigate podocytes, proteinuria and various kidney diseases (95, 143).

4.1.2 Choice for the use of mTOR inhibition to investigate sexual dimorphic stress responses in podocytes

The mTOR signaling network represents a key pathway controlling renal epithelial cells and regulating a variety of renal epithelial processes ranging from podocyte size control (51, 144). More extensive evidence points to the importance of the mTOR signaling pathway in both, control of physiological podocyte function and in podocyte injury and changes could be modulated by mTORC1 inhibition (67, 68). Because of the strong relevance of mTOR activation in the development of glomerular diseases, the aim of this study was to test the hypothesis if the response to inhibition of mTOR signaling by rapamycin occurs differently in male and female. In addition, recent work from Dragun's lab has shown sex-specific regulation of distinct mTOR complexes – mTORC1 and mTORC2 in terminally differentiated cells, the cardiomyocytes (145, 146). mTORC2 was essential for female endogenous cardioprotection which was lost upon mTOR inhibition with rapamycin whereas male mice displayed improved cardiac function in response to rapamycin treatment. Like cardiomyocytes, podocytes are postmitotic cells with limited regenerative capacity. Another reason not to work with a specific disease model, such as FSGS to test for sexual dimorphic stress responses, was to exclude secondary effects.

The dose and frequency of rapamycin given in this study was based on previous work from Dragun's lab that ensured a therapeutic level of rapamycin trough concentration in the blood comparable to humans.

4.1.3 Sample size

In designing animal and clinical experiments, selecting and calculating the appropriate number of animals or patients is a decision to be taken with care, taking into consideration cost, precision required, getting ethical approval from specialized authorities and the nature of the experiment, in addition to the breeding efficacy to be able to detect small differences of treatment. It is known, that increased number of mice or patients recruited increases sensitivity of results and detecting even small real differences which means robust results.

In this work, more than 80 mice were used to reach the requirements for reliable results for the different read-outs for all four experimental groups. Recently, the number of biological replicates needed to ensure biological interpretation for RNA-seq result was studied by 11 statistical known tools in RNA-seq. It was found that 12 biological replicates for each condition allowed the identification of > 90% of the true significantly differentially expressed (SDE) genes for all fold changes. Yet, it was recommended that a minimum of three to six replicates per condition should be used and analyzed using edgeR (excat) or DESseq2 tools to detect SDE (147). In this thesis

work 12 mice of each experimental group were used for podocytes isolation. Five to six podocytes-biological replicates each were initially sent for RNA-seq. However, due to some technical problem, only 4 mice vehicle treated could be further analyzed and 5 male rapamycin treated mice, whereas a total of 6 female mice of both treatment groups could be included and further analyzed by DESeq2.

Other RNA-seq studies, which have been published in high ranked journals, have been used the same or less number of biological replicates (95, 115, 148) Yet, some podocyte RNA-seq studies have done pooling of 4-5 biological replicates and further performed technical replicates (95, 106, 114, 115). Such pooling makes it impossible to assess the underlying variability of individuals in an experiment and cannot produce a valid inference but could be acceptable if variation between samples were tested in advance and found to be low. Considering the difficulty, precision in isolation technique, time needed for isolation and with the before-known limited number of podocytes isolated per mouse, the plan to use 6 mice each group was considered appropriate. For proteomics however, due to low protein yield from single preparations, 6 biological replicates per experimental group were not possible and finally only three samples per vehicle group could be analyzed by mass spectrometry to yield a proteome unfortunately only without high deepness.

For metabolomics, use of at least 5 biological replicates is common and recommended for each condition and preferably as many biological replicates as possible per treatment and control to take into account usually high subject to subject variation. In the current study, 7 samples were used per each experimental group leading to quantifiable results which all succeeded the required quality checks.

4.1.4 Validation of RNA-seq and proteomics data

Validation for RNA-seq and proteomics was done by qPCR and western blot, four to eight biological replicates were each used. For qPCR, firstly qPCR was performed for selected mRNAs using cDNA prepared for RNA sequencing (library cDNA-podocyte RNA). However, quality of cDNA for that much later than RNA-seq performed qPCRs was not good enough anymore that this approach could not be followed further. Therefore, RNA was freshly extracted from podocyte isolated cells which had been snap frozen directly after the end of the treatment period and used further for RNA sequencing validation. In addition, validation of proteomics could also not be done on podocyte isolated cell lysates due to the limited number of podocytes, but from glomeruli enriched kidney tissue which were isolated from individual mice. To further evaluate proteomics findings, immunohistochemical stainings were performed proving expression levels of several important proteins to be concordant to proteomics results.

4.2 Lack of physiological and morphological alterations in response to mTOR inhibition with rapamycin in both sexes

mTOR inhibition may have diverse effects on GFR and urinary albumin excretion dependent on kidney disease prevalence or other yet unknown factors. Rapamycin is more and more frequently used as immunosuppressant in renal transplantation to avoid the nephrotoxic effects of calcineurin inhibitors; some patients develop relevant proteinuria, others not (70, 149). In addition, whereas rapamycin has been proven to be nephroprotective in some glomerular diseases in animals, some patients contrarily respond with strong increase in proteinuria which even persists after withdrawal of the drug (150, 151). Therefore, it was completely unknown how the mice would react to the rapamycin treatment. Rapamycin was effective in reducing mTORC1 activities in renal cortex tissues in both, male and female mice. However, concerning the functional and morphological effects in the kidneys no significant changes could be detected. Vehicle and rapamycin treated mice maintained normal levels of serum creatinine and other physiological parameters during the 3 weeks of treatment. However, males showed a reduction in body weight of 1.5% compared to male vehicle. This might have been related to a decrease in protein synthesis, as suggested by the fact of downregulation of mTORC1 activity as measured by decreased p-p70S6 and the observed increase in amino acid pool detected in metabolomics in males after rapamycin treatment.

Previous publications have demonstrated that mTOR inhibition is associated with hyper-glycemia in 10-50% of patients and that rapamycin can induce glucose intolerance by reducing secreted insulin (123, 152). Furthermore it is known that mTOR regulates glucose uptake and GLUT1 /4 expression, which allows insulin independent transmembrane transport of glucose (153, 154). The findings of increased glucose levels in two males and females of the rapamycin group and the accumulation of glycolytic metabolites together with decreased GLUT mRNA expression levels after rapamycin in both sexes could be related to decreased uptake of glucose and the findings of GSEA were rapamycin in both male and female podocyte downregulated carbohydrate transport and glycolysis explain therefore higher excretion in the urine, though did not reach statistically significant value, which maybe would have been occurred with longer rapamycin treatment. Moreover, a correlation between decreased glucose renal tubular reabsorption with decreased AKT2 expression - which is required for the regulation of the Na⁺-linked glucose transporter SGLT1-has been reported (155). On the transcriptomic and translational level, AKT2 expression was decreased in females, in addition to reduced expression of p-AKT2 Ser473 and Thr308 after rapamycin, treatment which might have influenced both GLUT expression and renal reabsorption to a higher degree in females than in males.

Renal structural changes were investigated by PAS staining, which showed a normal morphology in controls and after rapamycin treatment. To obtain more information on changes at the ultrastructural level of podocytes, two mice of each sex and treatment groups were perfused with glutaraldehyde for samples preparation for electron microscopy in collaboration with Prof. Bachmann's group at Charité. Electron microscopic analyses showed normal podocyte structure and foot processes, regular slit diaphragm and normal fenestrated endothelium in all groups. However, female mice appeared to have more structural and microtubule components in renal cortices compared to males under physiological condition (data not shown).

Rapamycin as an immunosuppressant agent modulates the immune system and decreases IL-2 and other cytokine receptor-dependent signal transduction mechanisms, through protein FK-binding protein 12 binding. Importantly, GSEA analysis showed downregulation of many interleukins, immune response signaling molecules and cytokines. Some displayed sexual dimorphism in response to rapamycin, e.g. the GO "cytokine-cytokine interaction" (table 5 appendix). However, no increased mRNA transcripts or protein levels were detectable for pro-inflammatory molecules such as IL-6, TNF α , TGF β or MCP-1 before or after treatment. Furthermore histological analyses did not show any lymphocyte recruitment or other signs of inflammation.

4.3 Sexual dimorphic expressions of mTOR complex components, related signaling molecules and responses to rapamycin treatment

A recent study of Prof. Dragan's lab has reported sexual dimorphism in mTOR complex components in cardiac tissue and dimorphic responses to rapamycin treatment on mTORCs activation levels (145, 146). mTORC2 function as measured by p-AKT Ser473 increased in males after rapamycin treatment, whereas it significantly decreased in females, which was concordant to the results obtained in podocytes in this study. Moreover, the downstream targets of mTORC1 p-p70s6 and p-AKT Ser473 showed higher levels in female compared to male hearts at baseline, which was also consistent with the findings in podocytes.

Comparable results were reported in a study with brain lysates of old mice, where females displayed a higher baseline expression of mTOR, p-mTOR, AKT and p-AKT (156) and a study in brain hippocampus, where females showed 11-20% higher baseline levels of mTOR, p-mTOR, Raptor, AKT, p-AKT, p-p70s6 and p-4EBP1 and other kinases including AMPK and GSK3 β (157). In addition to these intrinsic sex differences, further sex differences in response to mTOR

inhibition were reported in different tissues such as glioblastoma (158) microglial (159) cardiomyocytes (145) and liver (160, 161).

In the current study, mTOR, p-mTOR and p-4EBP1 protein expressions were reduced in renal cortex tissues with no sexual dimorphism after rapamycin treatment, still expressions remained higher in females. Only AKT and phosphorylated Akt at Ser473 and Thr308 showed a sexual dimorphism in response to rapamycin treatment, such as that males had increased levels of AKT and p-AKT Ser473 and p-AKT Thr308. This could be a tissue specific effect. The fact of tissue specific sexually dimorphic responses is supported by a study with caloric restriction which mimics rapamycin inhibition and reduces PI3K/mTOR activity where opposite to S6 phosphorylation, pAktSer473 increased in fasted males but not in females in liver, adipose tissue, and heart (160).

To rule out different serum concentration levels in male and female mice responsible for the observed signaling differences, steady-state rapamycin levels were measured biochemically by LC/MS. LC/MS values of blood samples pointed to a trough concentration of 19-25 ng/ml and were comparable in both sexes. Yet, these findings alone could not rule out a possible different metabolism of the drug or permeability to reach the kidney tissue between males and females as cause for the observed differences. Yet, functional monitoring of the phosphorylation status of the main downstream target p70S6 in renal cortex tissues proved sufficient mTORC1 inhibition in both sexes.

4.4 Intrinsic and treatment-related sexual dimorphism of podocyte genes and proteins

4.4.1 Sexual dimorphic GO enrichments in podocyte genes and proteins

This is the first study which evaluated sex differences on gene and protein levels in isolated podocytes. Years ago, whole kidney tissue has been investigated for possible sexual dimorphism on the gene expression pattern in mouse and human. Only three papers could be found investigating primarily the differences on the transcriptomic level between healthy male and female (18-20). On the glomerular level, significantly regulated gene expression was detected, but not to such an extent as within the current study. Si et. al reported only less than 30 genes related to metabolism, translation and angiogenesis which were differently expressed between male and female glomeruli. Transporters were also among the differently regulated genes as well as genes related to steroid metabolism. Another study used rats of different ages and performed gene

analysis by microarray. More than 400 genes related to metabolism, signaling, protein synthesis, oxidative stress and cell death were sex-differently regulated in the young rats (age comparable to this thesis study between 8-12 weeks). Interestingly, GO-functional analysis of differently regulated genes showed different functional categories based on age (18). Another recent single-cell study of renal cells showed strong clustering by sex for the proximal tubular region mainly for transporters and metabolism (118). Concordant, to these studies, the current work showed an enrichment and differently regulated genes on metabolism, translation, protein synthesis and oxidative stress, though a larger number of genes were differently regulated on the podocyte level compared to whole kidney tissue. Moreover, human kidney cortex tissue investigated in the frame of the Genotype-Tissue Expression project, revealed sex-biased expression especially in transcription factors. However, as samples were mixed healthy and diseased, it was not possible to relate these data to this thesis study (120).

Transcriptomic changes during aging have additionally been investigated in male and female cells of renin lineage and mouse podocytes (115, 148). In aged podocytes, yet sex-dependent differences were rather attributed to small biological variations within the groups and no specific pathway enrichments were reported (115). However, in cells of renin-lineage from 2 month-old young mice, 79 out of 113 genes were significantly upregulated in females compared to males, mostly related to metabolic process (148).

In this thesis study, 1768 significantly differentially expressed genes accounted for about 6.5% of the total transcriptome. GO enrichment analyses showed that females were enriched in GO term mitochondria and related process, translation, cell part including adaptor proteins in addition to plasma and intracellular proteins (as endocytosis), proteolysis and glycolysis, all processes which are fundamental for podocyte homeostasis. Enrichments in these GO terms were also observed in the female podocyte proteome.

In contrast, male podocytes displayed increased levels of cytoskeletal, focal adhesions, cytokine chemokine inflammatory response and immune system activation which are known to relate to the pathophysiology and progression of CKD (162), in addition to GO terms related to kinase activity, transcription, and apoptotic process. Furthermore, exosome and extra-cellular exocytosis were among the differently expressed gene ontologies under baseline, and were significantly differently regulated after rapamycin with significant upregulation in male podocytes. Exosomes are known to mediate intercellular communication, regulate immune system and antigen presentation (163). Upregulation of these gene sets mainly in male indicate that males might have been functionally stronger affected by rapamycin treatment compared to females. However, in

addition to ribosomal proteins, cytoskeletal proteins showed opposite enrichments for males and females in the proteome, therefore these differences remained untranslated from the genome to the proteome.

Interesting was the following observation, that the number of significantly sex-differently expressed genes which were observed intrinsically, decreased dramatically between podocytes of male and female rapamycin treated mice. Females showed much less changes in response to rapamycin treatment compared to males which might indicate a higher stress resistance compared to males and what became even more obvious when taking into account the results of metabolomics which will be discussed later.

In the proteome study almost 3200 proteins could be identified, but only 2700 proteins were quantifiable compared to around 7000 quantifiable proteins in a recent paper of Rinschen M (106). The reason for that lower number of quantifiable proteins might be due to the low amount of material and the limited number of mice analyzed, not allowing to perform deep analysis and quantification as had been performed on the genomic level. Yet, Borries 2013, described only 1451 proteins in SILAC based proteomes and quantified only 991 based on LFQ values. Due to high inter-individual variation of LFQ values of podocyte proteins of male vehicle group, the mean and/or log₂FC differences between male and female podocytes were considered for functional analyses. Only 40 proteins showed significantly different expression between male and female and in total, expression levels of around 70 % of the podocyte proteins were found to be higher expressed in females with more than 1.5 fold change. Still, many of the GOs which showed enrichment in the transcriptome, only displayed enrichment in the proteome, such as oxidative phosphorylation, redox homeostasis, ubiquitination and apoptosis. Yet, overall correlation between DE single genes and proteins was poor. Both RNA-seq and proteomics had been performed with by the same method isolated podocytes, but from different mice. Therefore, inter-individual variation, together with low number of replicates especially for the proteomics and the differences in sequencing and proteomics depth might have increased this lacking correlation. However, earlier studies have also shown only poor correlation between transcriptomics and proteomics (95, 164).

The analysis of GO terms enrichment and functional annotation was performed using three databases, mainly Panther database for the GO-Slim, Enrichr for extracting KEGG, Wiki pathways in addition to Hallmark gene ontology and GSEA software was used for gene enrichment from the whole transcriptome. All these databases are well established, regularly updated and provide a comprehensive set of functional annotation tools.

4.4.2 Sexual dimorphism in major podocyte-specific genes and proteins relevant for podocyte structure

Nephrin, Podocin and Neph1 (Kirrel) are the major components in the slit diaphragm, which ensure that essential proteins and macro-molecules are retained in the blood and not lost into the urine. Its integrity depends on the cytoplasmic interaction with podocin. Loss of function of these three proteins disrupts the slit diaphragm formation and causes proteinuria (27). Podocin is important for nephrin recruitment and stabilization at the podocyte foot processes, enhances its signaling, acts as mechano-sensor and links tight junction proteins to the actin cytoskeleton (165). Nephrin works as a signaling molecule and is involved in podocyte polarity, cell survival, membrane trafficking and actin organization (31). All these mentioned proteins are known for their critical role in podocyte homeostasis, many mutations or loss of expression are known to cause nephrotic syndrome and proteinuria (22, 25, 27, 28, 34, 38, 40, 41).

In this study, both RNA-seq and WB showed intrinsically higher levels of podocin in females compared to males. Rapamycin treatment led to increased expressions in males suggesting higher sensitivity of males to rapamycin concerning podocin gene expression. Transcripts for *Tjp1*, *Itgb5* as well as *CD151* were also significantly different between female podocytes compared to males at baseline. Only on protein levels, sexual dimorphism was observed for nephrin in response to rapamycin, where male podocytes showed upregulation of nephrin tyrosine phosphorylation compared to vehicle and downregulation in females. As rapamycin was given systematically via intraperitoneal injection, glucose intolerance induced by nephrin downregulation on pancreatic islet cells could be a possible explanation for the differences in higher accumulation of glycolytic metabolites and glucosuria in females after rapamycin treatment, as reported before (166). Rapamycin-induced downregulation of nephrin with decreased GLUT4 expression and trafficking and glucokinase enzymes in females might have resulted in decreased glucose uptake in females, while male upregulated both GLUT4 and glucokinase expression and enhanced glycolysis as observed in the metabolomics study.

Another major podocyte-specific protein which showed sexual dimorphism at protein level was WT1. WT1 is a transcriptional factor developmentally regulated, but present throughout life. And play a role in homeostasis of the mature glomeruli. It is well documented that defects of WT1 cause several types of renal diseases and nephrotic syndrome as Fraiser and Denys-Drash syndrome. The WT1-dependent transcriptional network directs podocyte development and maintenance by regulation of more than 200 podocytes-associated genes (114). WT1 is shown to initiate nephrin transcription as a nuclear transcriptional factor through binding to the promoter region of nephrin (167). It is also responsible for the induction of endogenous podocalyxin, one

of the major structural membrane proteins of glomerular podocytes (168). Moreover, WT1 has been related to influence the transcription of other proteins such as ACTN4, CD2ap, Col4a3, inf2, podocin, Itga3, laminin β 2, Myo9 and plce1 (114).

The present work here showed significant sexually dimorphic regulations of WT1 in response to rapamycin. Rapamycin increased WT1 protein expression in male cortex tissues by 1.5 times whereas it decreased in females. This increase in WT1 in males might have triggered the increased transcription of genes regulated by WT1, such as nephrin (slightly), ACTN4, CD2ap, podocin, col4a3 and laminin β 2. Yet, on protein levels, only nephrin and Col4a3 increased concordantly to the increased gene expressions in males in response to rapamycin. This might be also caused by the fact that more than one transcriptional factors influences the podocyte protein, such as podocin which is transcribed by WT1 and Lmxib. In contrast to this work, a recent study conducted in male Sprague Dawley rats, showed that levels of nephrin and podocin which decreased after one week of rapamycin treatment, were restored after 4 weeks of rapamycin administration on both mRNA and protein levels (169). Whether same adaptation mechanisms would occur in mouse podocytes remains to be tested.

Several other studies report on effects of rapamycin and everolimus on podocyte-specific proteins, however without investigation of sex differences. WT1, SD proteins and other cytoskeletal related proteins were mainly reduced by treatment (89, 90, 92) whereas apoptosis increased (88). Everolimus furthermore regulated microtubular genes in podocyte, such as TUBB2B and DCDC2, which are both involved in MT assembly and podocyte morphology (170).

In addition, endocytic genes and proteins were intrinsically differentially expressed in male and female podocytes, including several vesicular transporters and non-clathrin endocytic pathway proteins. It has been reported that the loss of key CME proteins, dynamin, synaptojanin 1 or endophilin and class II PI 3-kinase C2 α (*Pi3kc2a*), result in proteinuria and foot process effacement (130). This can be explained by the fact that many podocyte proteins are regulated by endocytic proteins of clathrin dependent and independent pathway, mainly dynamin and synaptojanin 1, slit-diaphragm proteins, Nephrin, ZO-1, actin regulatory proteins such as Arp2/3, Myo1e, CD2AP, and Nck, cortactin, β 1-integrins, focal adhesion kinase as well as free fatty acid and albumin (130, 131). Still, little is known about sex differences in this aspect of podocyte function. There is one report on microglia (phagocytosis machine and one form of endocytosis) which showed sexual dimorphism such as that males had more microglia in brain, whereas females showed higher engulfment efficiency with additional sex differences upon inflammation, stroke and aging (171). Sexual dimorphism observed in endocytic machinery, in addition to sexual

dimorphism seen in PMTs and catabolism with or without rapamycin induced stress, might partially explain the sexual dimorphism observed in podocyte structural protein differences.

The regular function of podocytes depends on their structural integrity and motility which is mainly regulated by the cytoskeleton, focal adhesions, small GTPases and ECM interaction. As for podocytes, cytoskeletal structure and viable function are important in brain. In a recent study, sexual dimorphism has been reported in cytoskeletal genes and proteins in microglia mainly in myosin related proteins with high expression in male (164). In this thesis study, male podocytes showed intrinsically increased expressions of many cytoskeletal, focal adhesion, ECM proteins on the transcriptional levels, yet, on protein level, females showed enrichment in the GOs cytoskeleton, Rho GTPases, ECM and focal adhesion proteins, such as Actn4, vimentin, integrins and Col3a4, which has been discussed before.

Rapamycin has been reported to inhibit F-actin reorganization by inhibition of the phosphorylation of focal adhesion proteins, such as FAK and paxillin by raptor complex disruption and by reduction of protein synthesis of RhoA, Rac1 and Cdc42 (172). These findings were only partly concordant to this study where gene expressions of RhoA and Cdc42 decreased in both sexes in response to rapamycin treatment, whereas protein levels did not change significantly in both sexes except for Rac1 in females. Additionally, GSEA analysis showed a pattern of downregulation in cytoskeletal gene expression in both male and female. Interestingly, rapamycin effects were not consistent between sexes for all genes and proteins of these groups. Some, such as Actn4, F-actin decreased in both, male and female podocytes, as also confirmed by phalloidin staining. In contrast, some showed a sexual dimorphic response to rapamycin, such as vimentin and tubulin proteins, two main cytoskeletal proteins in podocytes, which decreased significantly by rapamycin treatment in females, but levels remained almost constant in males.

Moreover, p-paxillin showed sex-specific differences after rapamycin treatment. Phosphorylation was increased in males and reduced in female. As mentioned before, paxillin phosphorylation is important for adhesion between ECM/integrins and cytoskeletal structure in podocyte FB and cell body, which in addition to the GSEA findings (down regulation of cytoskeletal proteins, focal adhesion, cytoskeletal organization) suggest that males had to upregulate genes involved in cytoskeletal integrity and stability as a stress response to ensure podocyte homeostasis whereas females were less susceptible to stress induced by rapamycin treatment concerning the cytoskeletal structure and adhesion/cell-cell junction molecules.

Rho family of small GTPases is a family of small (~21 kDa) signaling G proteins, which are key players in the regulation of actin dynamics, focal adhesion assembly and cell polarity. Rac and cdc42 are crucially involved in cytoskeletal reorganization and cell motility by regulating

filopodia, lamellipodia and stress fibers. In contrast, RhoA promotes the formation of contractile actin–myosin containing stress fibers in the cell body and at the rear of the migrating cell in a highly coordinated manner (173). Furthermore, the podocyte adapter protein synaptopodin has been shown to induce stress fibers by stabilizing RhoA and suppressing filopodia (34). Rac1 is also known as critical regulator of the expression of mTOR and of cellular size control. Several studies have suggested an involvement of the small GTPases RhoA, Rac1 and cdc42 in podocytes during glomerular disease, reviewed in (40). In neurons, other postmitotic cells like podocytes, Rho family of GTPases are involved in several crucial processes including actin dynamics, axon growth, stabilization and guidance and neuronal survival and death.

Here, in both, transcriptome and proteome a significant sexual dimorphism was identified not only in the cytoskeletal structures, but also in their regulators including RhoGTPases, Actin2/3 proteins, actin binding proteins and RhoGTPase downstream targets such as cofilin and rophilin with higher expression in female podocytes compared to males. Results from western blots of renal cortex tissues showed that in males, cdc42 significantly increased in response to rapamycin whereas it remained unchanged in females. In contrast, Rac1 did not change in males whereas protein levels significantly decreased in females in response to rapamycin. The different effect of changes caused by rapamycin needs to be further studied functionally in addition to the effects of downstream regulators.

4.4.3 Intrinsic and treatment-related sexual dimorphism in podocyte cellular energy homeostasis

Podocytes express a high number of mitochondrial proteins and many mutations in mitochondrial genes cause kidney diseases, such as different types of FSGD and nephrotic syndrome, e.g. by mutation in *COQ2* (135). Mitochondrial biogenesis and OXPHOS are regulated by energy demand, mTOR and AMPK pathway in addition to PGC-1 α . Overexpression of PGC-1 α has been reported to protect podocytes against damage caused for example by aldosterone-mitochondrial depletion (174). In both, RNA-seq and proteomic significant enrichment of genes and proteins related to oxidation process were found with higher expressions in female podocytes, including PGC-1 α and nuclear factors NRF-1 and TFAM. These differences were abolished after rapamycin treatment indicating loss of sexual dimorphism under stress condition with mTOR inhibition.

Furthermore, a recent study showed that anaerobic glycolysis is the main pathway to generate ATP in podocytes (175). By analyzing main enzymes involved in this pathway, females also

showed higher enzyme expressions compared to males which was additionally reflected at the metabolite levels in the metabolomics of the renal cortex tissues, which will be discussed in more detail below.

It was not surprising to observe a sexual dimorphism in the mitochondrial proteins/OXPHOS, as it is well known that estrogen controls mitochondrial function and increases the expression of nuclear factors which drive mitochondrial biogenesis (176). This was also observed in other cells, namely cardiomyocytes (177). However, the response after rapamycin was interesting, females showed reduced mitochondrial gene levels whereas male levels increased abrogating the before existing sexual dimorphism. This might indicate a compensatory mechanism of male podocytes to counteract the stress induced by mTOR inhibition whereas females might compensate by different ways as discussed later in the metabolomics part.

Finally, AMPK, a central regulator of both lipid and glucose metabolism, is activated in response to stress and ATP depletion, such as low glucose and hypoxia. Many AMPK subunits were found sex-differently expressed in vehicle control groups. Additionally, AMPK phosphorylation at Thr172 was upregulated in males in response to rapamycin but not in females to enhance and restore reduced mitochondrial function, which is not the case in females, where they showed better adaptation toward stress. Increased AMPK phosphorylation was accompanied with less accumulation of glycolytic metabolites in males. This indicated a sex-specific response to rapamycin in energy metabolism in the kidney. AMPK sexual dimorphic phosphorylation after rapamycin might also explain the sexual dimorphism observed in autophagic response to rapamycin, even though autophagy is a downstream target for mTOR, and rapamycin was therefore expected to activate autophagy in both sexes. However, the observation of sex differences in AMPK phosphorylation - a master regulator for autophagy when AMP/ATP ratio is elevated- could explain the sexual dimorphic response for many autophagic genes.

4.4.4 Sexual dimorphism in redox proteins

Oxidative stress influences cell antioxidant defense enzyme homeostasis and is considered to be an important mechanism for the development of many cardiovascular as hypertension, renal failure and ischemia/reperfusion injury such as Sod, catalyze and glutathione system (178). Under normal condition, cells are protected from ROS by. In general females due to estrogen are more resistant to cellular oxidative stress and have higher antioxidant capacity than males (179).

Interestingly, sexually dimorphic responses have been reported for mediators involved in the transition of AKI to CKD, such as HIF-1 α and catalyses (94). Sexual dimorphism in redox enzymes has been reported in cardiomyocytes with female cells showing lower levels of oxidative stress and ROS production. However, male cardiomyocytes exhibited higher levels of glutathione peroxidase and other related enzymes and lower SOD1 than females (179). Moreover, glutathione related genes/proteins showed tissue specific sex differences (180). In the current study, significantly sex-different gene expressions were found in SOD enzymes, glutathione, and thioredoxin, furthermore translated into significantly differentially expressed thioredoxin related proteins and many enzymes with $\log_2FC > 1.5$. Rapamycin upregulated expression of many glutathione and SOD genes in males but not in females. In proximal tubules, it was shown that females due to hormonal effect maintain the GSH content in extreme conditions such as ischemic reperfusion injury and protect kidney from injury (94) this can explain that changes caused by rapamycin in male podocytes were not seen in females, and females kidney cells are resistant to redox protein changes caused by different stimuli/stress, here by rapamycin.

Hmgb1 functions as endogenous redox-sensitive promoter of the immune response, involved in podocyte injury and induces EMT and apoptosis and its inhibition has been found to be protective against podocyte injury (181). In this study, males showed higher expression at baseline compared to female on gene level with \log_2FC of 0.8. Rapamycin reduced 10% of Hmgb1 expression in males, while females increased the expression. The same effect was observed for MT-1 and sirtuin, which both have antiapoptotic and antioxidative function.

4.4.5 Sexual dimorphism in proteostasis-regulating genes and proteins

To maintain proteostasis, unfolded protein response and molecular chaperones are key players to maintain healthy podocyte against proteinuric kidney disease (182). There are several reports on intrinsic sexual dimorphism of proteolytic activity-chaperone expressions in various tissues, such as brain, liver and fat tissue. Furthermore, it has been shown that rapamycin influences proteolytic activity in brain and fat tissue in a tissue and sex-specific manner (156). In this study, rapamycin increased chaperone and folding protein related gene expressions in males whereas chaperone transcript levels slightly decreased or were maintained in female podocytes. This suggests a higher need to promote the turnover and removal of damaged and misfolded proteins in male podocytes as a stress response to rapamycin treatment. This was supported by GSEA analysis which showed that male podocytes upregulated genes/GOs related to ubiquitination/ proteolysis compared to only minor changes in females.

Another important pathway in regulation of proteostasis is autophagy which is a regulated mechanism of the cell to remove unnecessary or dysfunctional organelles and proteins and recycle essential molecular components. Previously, it has been shown that females treated with rapamycin showed significant changes in the expression of longevity-related genes including, circadian rhythm genes, ubiquitin-proteasome and autophagy pathways (LC3) and selected genes involved in response to ER stress pathways, such as the unfolded protein response (UPR), which showed a sex-specific response to rapamycin with higher expressions of such proteins in females but no changes in males (161). In the current study, genes of the UPR were upregulated in male podocytes, whereas downregulated slightly in females in response to rapamycin treatment. In contrast, female podocytes upregulated macroautophagy related genes (GSEA table). LC3IIb, as an autophagy marker, increased in both, male and female cortex tissues in response to rapamycin, which corresponds to reported effects of mTORC1 inhibition on autophagy, but not for the other autophagic genes as discussed earlier. Additionally, upon accumulation of misfolded proteins, IRE1 α – part of the unfolded protein response - is activated and induces genes that encode chaperones, autophagy mediators, and metabolic adaptations resulting in protection from injury in an experimental focal segmental glomerulosclerosis model (183). In this thesis work, IRE1 α was upregulated only in females and downregulated to the same extent in male podocytes, strengthening protective adaptation processes in females.

4.4.6 Sexual dimorphism in kinases relevant for podocyte homeostasis

Various protein kinases are enriched in podocytes and are shown to be dysregulated upon stress and podocyte injury (106). For example, the importance of AKT kinase has been studied in podocytes. Akt is highly expressed in podocytes (75, 106) and loss of AKT2 expression or reduced activation resulted in podocyte apoptosis and FP effacement and subsequently proteinuria, in addition to changes in cytoskeletal structures through Rac1. Moreover, in the same study, rapamycin treatment in human kidney transplant patients decreased AKT2 expression possibly via mTORC2 inhibition and eventually lead to proteinuria. Additionally, in response to stress activated AKT2 mimicked nephrin loss during CKD induced by subtotal nephrectomy (75). In this thesis work, AKT2 was intrinsically higher expressed in female podocytes at both, RNA and protein levels, as well as for AKT1. Both levels were reduced after rapamycin treatment only in females.

Further protein kinases were found to be differently upregulated in female podocytes after rapamycin such as *prkcy*, *prkci* and *prkca* in addition to phospholipase *Plc1* and *prkd1/3*, *pik3c2a*.

All of these sexually dimorphic kinases play a major role in podocyte homeostasis, proliferation, apoptosis, and many other cellular signaling processes and are involved in further pathways, such as β -receptor activation, dopamine, 5-HT pathway and FGF pathways. For example, β -adrenergic receptor activation accelerates podocyte recovery through the induction of mitochondrial biogenesis (184). Higher intrinsic expression of kinases and different regulation after rapamycin in females or male suggest different endogenous capacities to counteract harmful stress conditions.

4.4.7 Sexual dimorphism in transcription factors

Among the significantly differently expressed and regulated genes detected between male and female podocytes were almost 100 TFs, under them Dicer1, Stat3, Nfat5 and Foxs1 ($p < 0.01$) with higher expression in male podocytes. The sexual dimorphism in TF expressions was also seen in response to rapamycin and could strongly mediate the sexually dimorphic gene expression observed. However, this approach was not followed and analyzed by specific software and databases at this point, as this could be a full thesis by its own. Nevertheless, few TFs will be discussed shortly.

First, and most importantly, there was a significant differential expression in the core circadian rhythm genes between vehicles (Figure 23). Expression decreased significantly only in males after rapamycin. It is widely known that many circadian genes influence various different physiological systems, sleep to metabolism, immune system and aging (185). In a recent study, circadian transcriptome profiling was performed on isolated glomeruli from control and cKO mice and revealed their influence on multiple genes encoding protein expressions essential for normal podocyte function. Rho GTPase Activating Protein, cytoskeleton, Cathepsin L among others were altered and influenced the kidney function (186). The effect on circadian genes expression after rapamycin on the significantly expressed genes between vehicle and differently regulated after rapamycin in males was not further investigated at this point, however, the cross talk between many circadian genes and podocyte homeostasis should be further investigated deeply.

Dicer is the enzyme responsible for miRNA generation and thereby regulation of protein synthesis. In a Dicer mutation specific to podocyte mouse model 120 significantly upregulated genes were found in mutant mice, among them vimentin, Hsp20, Tagln which are important for cytoskeleton structure and other genes important for apoptosis and for integrin signaling (50). High expression of Dicer in males might contribute to the higher expression of focal adhesion and most cytoskeletal genes in male podocytes. Rapamycin upregulated slightly Dicer1 expression in

females (and also to little extent in males) which might provide beneficial effects of rapamycin on the cytoskeletal structure, were female upregulated many cytoskeletal proteins-related actin binding proteins. Yet, this conclusion could not be based only on Dicer1 expression levels, since many kinases, endocytic genes and transcription factors influence focal adhesion molecules, cytoskeletal proteins and their regulators.

4.5 Sexual dimorphic metabolic responses to rapamycin

Sexual dimorphism in metabolism has been well documented in different tissues, with higher glucose metabolism in females compared to males (187, 188). Female hormones have been attributed a major role in these differences. Estradiol has been reported to enhance glycolytic metabolism and to increase glucose uptake (189) in a PI3K/AKT-dependent manner through the pentose phosphate pathway (190).

Investigating renal cortex tissues from male and female vehicle treated mice, females showed higher intrinsic levels of glycolytic metabolites and PPP (except for succinate and citrate). However male mice showed higher levels of amino acid pools compared to females (except for isoleucine and serine) indicating possibly enhanced protein turnover compared to females. Yet, differences between sexes under control conditions were overall small for AA pools and glycolytic metabolites reaching only significant levels in 4 out of 12 of the measured AA and glycolytic metabolites.

Effects of rapamycin and other mTOR inhibitors on glucose homeostasis have been investigated before in skeletal muscle cells and adipocytes (191). Rapamycin induced metabolomic changes have been shown to extend lifespan in multiple animal models (192). Prolonged exposure to rapamycin led to decreased glycolysis in rat pancreatic islets (166), which has also been observed in this thesis study. Moreover, metabolomic changes in response to rapamycin have been shown to be tissue-specific. In brain, rapamycin did not change the metabolomics profile but did in liver (192). In muscle cells, everolimus has been reported to reduce glucose uptake as well as intracellular glucose levels during 48 h treatment, which was accompanied by reduced levels of main glucose transporters and main enzymes such as Cs and Ogdh on mRNA and protein levels (123).

In females, rapamycin effects has been also studied in mice hearts after at least one week of rapamycin treatment. Glycolysis was reduced and the main two metabolites in TCA cycle, oxaloacetate and ketoglutarate, were increased as well as amino acid such as glutamine, aspartic acid and levels of valine and isoleucine. Interestingly, these increased levels went back to normal

with prolonged treatment (193), whereas in another study the metabolites changes caused by rapamycin lasted even after cessation of rapamycin treatment (194). Podocytes as cardiomyocytes, both postmitotic cells, depend mainly on energy consumption for their function, and therefore these similar changes in female mice in response to rapamycin are not surprising.

Sexual dimorphism in metabolomics has been investigated in response to mTOR inhibition before (123, 188, 195). A recent study on HUVEC cells showed sexual dimorphism on glycolysis, TCA and amino acid metabolism after starvation, where females showed higher levels of glycolytic metabolites compared to males as well as an increase in amino acid pool.

As transcriptomics and proteomics revealed major differences between male and female animals in amino acid, nitrogen, glycolysis and mitochondrial phosphorylation chain reaction, focus was directed towards the three major glucose metabolic pathways: glycolysis, the tricarboxylic acid (TCA) cycle, and the pentose phosphate pathway (PPP). Independent of whether a combined or individual single analysis of male and female samples were used, amino acids showed increased pools while glycolysis, PPP and TCA cycle pathways were decreased in mice treated with rapamycin. Yet, AA accumulation was higher in male compared to female and the decrease in glycolysis metabolism was higher in female compared to male (detected as higher level of metabolites in rapamycin-treated male mice) in response to rapamycin which was in contrast to the results reported in HUVEC in response to starvation. Here, metabolic results were concordant to RNA-seq and suggested that females were less susceptible to changes in metabolic activity in response to rapamycin compared to males and the downregulation in mitochondrial function including glycolysis was reflected by less glycolytic metabolites. Whereas males showed strong increases in glycolytic enzyme gene expressions to adapt/compensate, such as GLUT expression and with reduction in protein synthesis causing an accumulation of amino acids, resulting most probably in more amino acids available to convert to Acetyl CoA and entering TCA cycle, females showed less changes in response to rapamycin, at least concerning the accumulation of AA. Amino acids can yield TCA cycle intermediates following the catabolism of their carbon skeletons (e.g. tryptophan, isoleucine, tyrosine, and valine yielding Acetyl CoA; tyrosine yielding fumarate) and replenish depleted levels of TCA cycle intermediates at any time point. In this study, tryptophan, lysine and tyrosine were not accumulated, and the levels were decreased largely in females. To note, these amino acids are known to be metabolized and used for Acetyl CoA synthesis - the first intermediate in TCA cycle- and, in addition to the minimal changes in glycolytic enzyme expression after rapamycin in females, this could explain the higher accumulation of TCA metabolites in females compared to males. Moreover, metabolomics results

follow GSEA analysis, where females downregulated the glycolysis/TCA cycle processes causing less metabolites whereas male upregulated the same pathways.

In this study, *Pgd* and *Taldo1* involved in PPP showed stable levels in response to rapamycin. Therefore, the decrease in PPP metabolites observed in renal cortex tissues in response to rapamycin might be rather explained by the reduction of precursors in the glycolytic pathway.

Transcriptomics and proteomics had been indicated that oxidative phosphorylation was not largely and significantly affected by rapamycin in females, yet carbohydrate metabolism related genes were strongly reduced by rapamycin and showed sexual dimorphic responses. Analysis of enzymes involved in glycolysis and in the TCA cycle revealed that several enzymes regulating glucose metabolism were changed specifically for the two of the three limiting rate steps responsible enzymes in glycolysis, were sex-differently regulated in response to rapamycin. *Gck*, a glucose sensor, was upregulated in males maybe as a compensation for higher Glut reduction in males. Also pyruvate kinase (*pkm*, *pklr*), a key rate-limiting step of glycolysis, showed a different pattern of *pklr* expression in male and female podocytes in response to mTOR inhibition. Rapamycin-treated male podocytes showed a dramatic increased level after rapamycin treatment with log₂FC of 2.2, while female rapamycin treated group showed suppressed expression compared to baseline. The increase in the expression of *pklr* enzymes in males compared to females could be due to the excessive accumulation of glycolytic intermediate products in males. As response, they might have increased enzyme expression to promote the metabolism of the accumulated intermediates in the previous steps.

The rate limiting step in the TCA cycle is the conversion of isocitrate to α -ketoglutarate via isocitrate dehydrogenase *ldh*. Four isoforms were detected in sequencing (*Idh2*, *Idh3a*, *Idh3b* and *Idh3g*), and three genes were non-significantly reduced after rapamycin in females but remained unchanged in males (*Idh2*, *Idh3b* and *Idh3g*). For other enzymes involved in TCA cycle (*Aco2*, *Cs*, *mdh1/2*, *sdha/b/c/d*) RNA expression slightly decreased in females (less than 10% and 20% decrease for *Idh2*). However, males responded differently to rapamycin. RNA levels for the enzymes involved increases from 7% up to 30% in response to rapamycin, which might have favored a higher metabolism of fumarate and malate by increased expression of the enzymes involved in TCA cycle (*mdh1* and *fh1* mainly) as well as increased RNA expression of *sdhb*. A possible explanation for higher g6p in male compared to female, could be the finding that *Gck* enzyme, responsible for the irreversible conversion of glucose to glucose 6 phosphate, was increased only in male and GLUT expression in response to rapamycin decreased less in males compared to females.

The finding that α -ketoglutarate showed a sexual dimorphic response to rapamycin is interesting, since recently, it has been shown that α -ketoglutarate is responsible for delayed age-related phenotype and prolonged life span (196). Furthermore, it is known that p-AMPK increases α -ketoglutarate, and as increased phosphorylation of AMPK was observed only in male, it was not surprising to observe a sexual dimorphism in α -ketoglutarate levels. Moreover, one of the major source for α -ketoglutarate is amino acid turnover. Actually, amino acids accumulated more in males which might contribute to the higher levels of α -ketoglutarate in males compared to females.

The AA response to rapamycin treatment was also metabolically profiled and demonstrated significant accumulation of AA except for few. The observed increase in intracellular levels of certain AA occurred largely in males. Interesting was in this aspect the GSEA findings on expression changes in genes related to uptake via transporters, synthesis or metabolism. In both, male and female rapamycin treated podocytes, rapamycin downregulated the gene expression of many transporters including AA transporters, AA synthesis and metabolic process and that significantly stronger in males. Yet, some of these transporter genes were sex-differently expressed after rapamycin which might have essentially contributed together with sex-differences in AA metabolism/degradation to the higher accumulation of AA in males. Males might normally have a higher protein synthesis which was dampened by mTORC1 inhibition in the rapamycin group, contributing to reduced body weight in rapamycin-treated male mice.

In this study, tryptophan, lysine and tyrosine were not accumulated, and the levels were decreased largely in females. These amino acids are known to be metabolized and used for Acetyl CoA synthesis - the first intermediate in TCA cycle- and in addition to the minimal changes in glycolytic enzyme expression after rapamycin in females, this might have triggered a compensatory mechanism in females of converting mainly these three amino acids to metabolites entering the TCA cycle to overcome the reduced TCA cycle.

Finally, GSEA analysis showed a downregulation of purine synthesis and catabolic process after rapamycin in both sexes, as was translated into reduced levels of nucleobases in the metabolomics even with the accumulation of AA, which was related to mTOR inhibition and reduced protein synthesis. However, this could not explain the sexual dimorphism observed for adenosine. Sex-different levels of adenosine might have been influenced by sexual dimorphism observed in AMPK phosphorylation. Adenosine is a precursor for AMP/ADP/ATP. Increased level of AMP:ADP ratio activates AMPK to enhance and restore reduced mitochondrial function by increased ATP synthesis (113).

4.6 Study limitations

Unfortunately, podocyte-specific proteomics could not be performed in such a depth as the podocyte-specific sequencing. Due to the limited number of podocytes and the low number of biological replicates, analyzing 3 vehicle-treated females and 3 males (2 biological replicates, one pooled sample) prevented strong quantitative analysis. In addition, samples from rapamycin-treated mice yielded not enough protein extracts to enable proper analysis and could therefore not be reported within this study. Western blots, even if glomerular enriched from lysates of renal cortices, could provide some further data on protein expressions and signal transduction, yet could never completely substitute results from isolated podocytes. Immunofluorescent stainings were another approach to overcome the limitations of proteomics, yet quantification has always to be interpreted cautiously due to technical limitations for highly comparable staining methods.

Another limitation of proteomics in general is bias towards high abundant proteins. In this proteomic study, important podocyte proteins were missing, not identified or not quantifiable, such as WT1. In addition, the analysis of posttranslational protein modifications was not performed.

Further limitations of the present study concerned metabolomics. Metabolomic data only address static changes of pathways between vehicle controls and after three-weeks exposure to rapamycin. Intracellular glucose uptake or ATP consumption were not measured. Measuring intracellular or extracellular glucose levels would have been helpful in interpretation of the metabolomics findings.

All previously mentioned differences after rapamycin were only determined after one dosage and one time point of 1.5mg/kg and three weeks of rapamycin treatment. Alterations in gene expression and protein levels could have been restored with longer/chronic treatment duration as many patients do as part of adaptation. Hence, longer treatment durations should be planned in the future together with investigations in specific disease models. Finally, these significant findings and observations were detected in healthy young mice. However, in pathological conditions the responses might be completely different and further studies need to be conducted using different rapamycin doses and duration and young and aged mice.

4.7 Conclusions and outlook

This thesis is first to report on podocyte-specific sexual dimorphic gene regulation and protein expression patterns which may potentially account for significant sex differences in susceptibilities and progression of glomerular pathologies. Additionally, sex-different molecular changes and response patterns to mTOR inhibition attribute to this sexual dimorphism and might influence the high interindividual variation observed clinically after rapamycin treatment. According to metabolomic results, females appeared less susceptible towards stress caused by mTOR inhibition and might possess a higher compensatory molecular buffer capacity compared to males which reacted with a high diversity of significant gene expression changes. Further investigation of podocyte adaptation upon acute or chronic pathological conditions with simultaneous mTORi with different dosages is warranted. Furthermore, proteomics analysis from isolated podocytes of both, control and rapamycin treated male and female mice is encouraged to cell-specifically investigate the protein expression changes in podocytes under stress conditions. Moreover, more advanced techniques which are currently under development to target cell-specific metabolomics could lead to further knowledge about this critical, organ function determining cell-type of the glomerular filtration barrier. Importantly, these thesis results and further detailed knowledge of sex-specific response patterns of podocytes will substantially contribute to the development of target-specific advanced molecular therapies optimized for male and female patients.

REFERENCES

1. Pollitzer E. Biology: Cell sex matters. *Nature*. 2013;500(7460):23-4.
2. Neugarten J, Golestaneh L. Gender and the prevalence and progression of renal disease. *Adv Chronic Kidney Dis*. 2013;20(5):390-5.
3. Pinares-Garcia P, Stratikopoulos M, Zagato A, Loke H, Lee J. Sex: A Significant Risk Factor for Neurodevelopmental and Neurodegenerative Disorders. *Brain Sci*. 2018;8(8).
4. Regitz-Zagrosek V, Kararigas G. Mechanistic Pathways of Sex Differences in Cardiovascular Disease. *Physiol Rev*. 2017;97(1):1-37.
5. Zheng D, Trynda J, Williams C, Vold JA, Nguyen JH, Harnois DM, Bagaria SP, McLaughlin SA, Li Z. Sexual dimorphism in the incidence of human cancers. *BMC Cancer*. 2019;19(1):684.
6. Wang S, Cowley LA, Liu XS. Sex Differences in Cancer Immunotherapy Efficacy, Biomarkers, and Therapeutic Strategy. *Molecules*. 2019;24(18).
7. Momper JD, Misel ML, McKay DB. Sex differences in transplantation. *Transplant Rev (Orlando)*. 2017;31(3):145-50.
8. Carrero JJ, Hecking M, Chesnaye NC, Jager KJ. Sex and gender disparities in the epidemiology and outcomes of chronic kidney disease. *Nat Rev Nephrol*. 2018;14(3):151-64.
9. Silbiger S, Neugarten J. Gender and human chronic renal disease. *Gend Med*. 2008;5 Suppl A:S3-S10.
10. Aufhauser DD, Jr., Wang Z, Murken DR, Bhatti TR, Wang Y, Ge G, Redfield RR, 3rd, Abt PL, Wang L, Svoronos N, Thomasson A, Reese PP, Hancock WW, Levine MH. Improved renal ischemia tolerance in females influences kidney transplantation outcomes. *J Clin Invest*. 2016;126(5):1968-77.
11. Pinches M, Betts C, Bickerton S, Burdett L, Thomas H, Derbyshire N, Jones HB, Moores M. Evaluation of novel renal biomarkers with a cisplatin model of kidney injury: gender and dosage differences. *Toxicol Pathol*. 2012;40(3):522-33.
12. Neugarten J, Golestaneh L. Influence of Sex on the Progression of Chronic Kidney Disease. *Mayo Clin Proc*. 2019;94(7):1339-56.
13. Iseki K. Gender differences in chronic kidney disease. *Kidney Int*. 2008;74(4):415-7.
14. Yabuki A, Suzuki S, Matsumoto M, Nishinakagawa H. Sexual dimorphism of proximal straight tubular cells in mouse kidney. *Anat Rec*. 1999;255(3):316-23.
15. Seppi T, Prajczek S, Dorler MM, Eiter O, Hekl D, Nevinny-Stickel M, Skvortsova I, Gstraunthaler G, Lukas P, Lechner J. Sex Differences in Renal Proximal Tubular Cell Homeostasis. *J Am Soc Nephrol*. 2016;27(10):3051-62.
16. Li Q, McDonough AA, Layton HE, Layton AT. Functional implications of sexual dimorphism of transporter patterns along the rat proximal tubule: modeling and analysis. *Am J Physiol Renal Physiol*. 2018;315(3):F692-F700.
17. Veiras LC, Girardi ACC, Curry J, Pei L, Ralph DL, Tran A, Castelo-Branco RC, Pastor-Soler N, Arranz CT, Yu ASL, McDonough AA. Sexual Dimorphic Pattern of Renal Transporters and Electrolyte Homeostasis. *J Am Soc Nephrol*. 2017;28(12):3504-17.
18. Kwekel JC, Desai VG, Moland CL, Vijay V, Fuscoe JC. Sex differences in kidney gene expression during the life cycle of F344 rats. *Biol Sex Differ*. 2013;4(1):14.
19. Rinn JL, Rozowsky JS, Laurenzi IJ, Petersen PH, Zou K, Zhong W, Gerstein M, Snyder M. Major molecular differences between mammalian sexes are involved in drug metabolism and renal function. *Dev Cell*. 2004;6(6):791-800.
20. Si H, Banga RS, Kapitsinou P, Ramaiah M, Lawrence J, Kambhampati G, Gruenwald A, Bottinger E, Glicklich D, Tellis V, Greenstein S, Thomas DB, Pullman J, Fazzari M, Susztak K. Human and murine kidneys show gender- and species-specific gene expression differences in response to injury. *PLoS One*. 2009;4(3):e4802.

21. Reiser J, Altintas MM. Podocytes. *F1000Res*. 2016;5.
22. Toblli JE, Bevione P, Di Gennaro F, Madalena L, Cao G, Angerosa M. Understanding the mechanisms of proteinuria: therapeutic implications. *Int J Nephrol*. 2012;2012:546039.
23. Schlondorff D, Wyatt CM, Campbell KN. Revisiting the determinants of the glomerular filtration barrier: what goes round must come round. *Kidney Int*. 2017;92(3):533-6.
24. Pavenstadt H, Kriz W, Kretzler M. Cell biology of the glomerular podocyte. *Physiol Rev*. 2003;83(1):253-307.
25. Brinkkoetter PT, Ising C, Benzing T. The role of the podocyte in albumin filtration. *Nat Rev Nephrol*. 2013;9(6):328-36.
26. Arif E, Nihalani D. Glomerular Filtration Barrier Assembly: An insight. *Postdoc J*. 2013;1(4):33-45.
27. Grahammer F, Schell C, Huber TB. The podocyte slit diaphragm--from a thin grey line to a complex signalling hub. *Nat Rev Nephrol*. 2013;9(10):587-98.
28. Wiggins RC. The spectrum of podocytopathies: a unifying view of glomerular diseases. *Kidney Int*. 2007;71(12):1205-14.
29. Michaud JL, Kennedy CR. The podocyte in health and disease: insights from the mouse. *Clin Sci (Lond)*. 2007;112(6):325-35.
30. Perico L, Conti S, Benigni A, Remuzzi G. Podocyte-actin dynamics in health and disease. *Nat Rev Nephrol*. 2016;12(11):692-710.
31. Martin CE, Jones N. Nephrin Signaling in the Podocyte: An Updated View of Signal Regulation at the Slit Diaphragm and Beyond. *Front Endocrinol (Lausanne)*. 2018;9:302.
32. Welsh GI, Saleem MA. The podocyte cytoskeleton--key to a functioning glomerulus in health and disease. *Nat Rev Nephrol*. 2011;8(1):14-21.
33. Lal MA, Andersson AC, Katayama K, Xiao Z, Nukui M, Hultenby K, Wernerson A, Tryggvason K. Rhophilin-1 is a key regulator of the podocyte cytoskeleton and is essential for glomerular filtration. *J Am Soc Nephrol*. 2015;26(3):647-62.
34. He FF, Chen S, Su H, Meng XF, Zhang C. Actin-associated Proteins in the Pathogenesis of Podocyte Injury. *Curr Genomics*. 2013;14(7):477-84.
35. Perisic L, Rodriguez PQ, Hultenby K, Sun Y, Lal M, Betsholtz C, Uhlen M, Wernerson A, Hedin U, Pikkarainen T, Tryggvason K, Patrakka J. Schip1 is a novel podocyte foot process protein that mediates actin cytoskeleton rearrangements and forms a complex with Nherf2 and ezrin. *PLoS One*. 2015;10(3):e0122067.
36. Sistani L, Duner F, Udumala S, Hultenby K, Uhlen M, Betsholtz C, Tryggvason K, Wernerson A, Patrakka J. Pdlim2 is a novel actin-regulating protein of podocyte foot processes. *Kidney Int*. 2011;80(10):1045-54.
37. Levi M, Myakala K, Wang X. SRGAP2a: A New Player That Modulates Podocyte Cytoskeleton and Injury in Diabetes. *Diabetes*. 2018;67(4):550-1.
38. Nagata M. Podocyte injury and its consequences. *Kidney Int*. 2016;89(6):1221-30.
39. Gorriz JL, Martinez-Castelao A. Proteinuria: detection and role in native renal disease progression. *Transplant Rev (Orlando)*. 2012;26(1):3-13.
40. Mundel P, Reiser J. Proteinuria: an enzymatic disease of the podocyte? *Kidney Int*. 2010;77(7):571-80.
41. Mundel P, Shankland SJ. Podocyte biology and response to injury. *J Am Soc Nephrol*. 2002;13(12):3005-15.
42. Cheng YC, Chen CA, Chen HC. Endoplasmic reticulum stress-induced cell death in podocytes. *Nephrology (Carlton)*. 2017;22 Suppl 4:43-9.
43. Manda G, Checherita AI, Comanescu MV, Hinescu ME. Redox Signaling in Diabetic Nephropathy: Hypertrophy versus Death Choices in Mesangial Cells and Podocytes. *Mediators Inflamm*. 2015;2015:604208.

44. Lohmann F, Sachs M, Meyer TN, Sievert H, Lindenmeyer MT, Wiech T, Cohen CD, Balabanov S, Stahl RA, Meyer-Schwesinger C. UCH-L1 induces podocyte hypertrophy in membranous nephropathy by protein accumulation. *Biochim Biophys Acta*. 2014;1842(7):945-58.
45. Mootha VK, Lindgren CM, Eriksson KF, Subramanian A, Sihag S, Lehar J, Puigserver P, Carlsson E, Ridderstrale M, Laurila E, Houstis N, Daly MJ, Patterson N, Mesirov JP, Golub TR, Tamayo P, Spiegelman B, Lander ES, Hirschhorn JN, Altshuler D, Groop LC. PGC-1alpha-responsive genes involved in oxidative phosphorylation are coordinately downregulated in human diabetes. *Nat Genet*. 2003;34(3):267-73.
46. Muller-Deile J, Schiffer M. The podocyte power-plant disaster and its contribution to glomerulopathy. *Front Endocrinol (Lausanne)*. 2014;5:209.
47. Smoyer WE, Ransom RF. Hsp27 regulates podocyte cytoskeletal changes in an in vitro model of podocyte process retraction. *FASEB J*. 2002;16(3):315-26.
48. Sanchez-Nino MD, Sanz AB, Sanchez-Lopez E, Ruiz-Ortega M, Benito-Martin A, Saleem MA, Mathieson PW, Mezzano S, Egido J, Ortiz A. HSP27/HSPB1 as an adaptive podocyte antiapoptotic protein activated by high glucose and angiotensin II. *Lab Invest*. 2012;92(1):32-45.
49. Beeken M, Lindenmeyer MT, Blattner SM, Radon V, Oh J, Meyer TN, Hildebrand D, Schluter H, Reinicke AT, Knop JH, Vivekanandan-Giri A, Munster S, Sachs M, Wiech T, Pennathur S, Cohen CD, Kretzler M, Stahl RA, Meyer-Schwesinger C. Alterations in the ubiquitin proteasome system in persistent but not reversible proteinuric diseases. *J Am Soc Nephrol*. 2014;25(11):2511-25.
50. Shi S, Yu L, Chiu C, Sun Y, Chen J, Khitrov G, Merckenschlager M, Holzman LB, Zhang W, Mundel P, Bottinger EP. Podocyte-selective deletion of *dicer* induces proteinuria and glomerulosclerosis. *J Am Soc Nephrol*. 2008;19(11):2159-69.
51. Yao Y, Inoki K. The role of mechanistic target of rapamycin in maintenance of glomerular epithelial cells. *Curr Opin Nephrol Hypertens*. 2016;25(1):28-34.
52. Grahammer F, Haenisch N, Steinhardt F, Sandner L, Roerden M, Arnold F, Cordts T, Wanner N, Reichardt W, Kerjaschki D, Ruegg MA, Hall MN, Moulin P, Busch H, Boerries M, Walz G, Artunc F, Huber TB. mTORC1 maintains renal tubular homeostasis and is essential in response to ischemic stress. *Proc Natl Acad Sci U S A*. 2014;111(27):E2817-26.
53. Grahammer F, Ramakrishnan SK, Rinschen MM, Larionov AA, Syed M, Khatib H, Roerden M, Sass JO, Helmstaedter M, Osenberg D, Kuhne L, Kretz O, Wanner N, Jouret F, Benzing T, Artunc F, Huber TB, Theilig F. mTOR Regulates Endocytosis and Nutrient Transport in Proximal Tubular Cells. *J Am Soc Nephrol*. 2017;28(1):230-41.
54. Fantus D, Rogers NM, Grahammer F, Huber TB, Thomson AW. Roles of mTOR complexes in the kidney: implications for renal disease and transplantation. *Nat Rev Nephrol*. 2016;12(10):587-609.
55. Huber TB, Walz G, Kuehn EW. mTOR and rapamycin in the kidney: signaling and therapeutic implications beyond immunosuppression. *Kidney Int*. 2011;79(5):502-11.
56. Liko D, Hall MN. mTOR in health and in sickness. *J Mol Med (Berl)*. 2015;93(10):1061-73.
57. Martelli AM, Buontempo F, McCubrey JA. Drug discovery targeting the mTOR pathway. *Clin Sci (Lond)*. 2018;132(5):543-68.
58. Saxton RA, Sabatini DM. mTOR Signaling in Growth, Metabolism, and Disease. *Cell*. 2017;168(6):960-76.
59. Wataya-Kaneda M. Mammalian target of rapamycin and tuberous sclerosis complex. *J Dermatol Sci*. 2015;79(2):93-100.
60. Haissaguerre M, Saucisse N, Cota D. Influence of mTOR in energy and metabolic homeostasis. *Mol Cell Endocrinol*. 2014;397(1-2):67-77.

61. Lamming DW, Ye L, Katajisto P, Goncalves MD, Saitoh M, Stevens DM, Davis JG, Salmon AB, Richardson A, Ahima RS, Guertin DA, Sabatini DM, Baur JA. Rapamycin-induced insulin resistance is mediated by mTORC2 loss and uncoupled from longevity. *Science*. 2012;335(6076):1638-43.
62. Fantus D, Thomson AW. Evolving perspectives of mTOR complexes in immunity and transplantation. *Am J Transplant*. 2015;15(4):891-902.
63. Sciarretta S, Forte M, Frati G, Sadoshima J. New Insights Into the Role of mTOR Signaling in the Cardiovascular System. *Circ Res*. 2018;122(3):489-505.
64. Johnson SC, Rabinovitch PS, Kaerberlein M. mTOR is a key modulator of ageing and age-related disease. *Nature*. 2013;493(7432):338-45.
65. Godel M, Hartleben B, Herbach N, Liu S, Zschiedrich S, Lu S, Debreczeni-Mor A, Lindenmeyer MT, Rastaldi MP, Hartleben G, Wiech T, Fornoni A, Nelson RG, Kretzler M, Wanke R, Pavenstadt H, Kerjaschki D, Cohen CD, Hall MN, Ruegg MA, Inoki K, Walz G, Huber TB. Role of mTOR in podocyte function and diabetic nephropathy in humans and mice. *J Clin Invest*. 2011;121(6):2197-209.
66. Inoki K, Mori H, Wang J, Suzuki T, Hong S, Yoshida S, Blattner SM, Ikenoue T, Ruegg MA, Hall MN, Kwiatkowski DJ, Rastaldi MP, Huber TB, Kretzler M, Holzman LB, Wiggins RC, Guan KL. mTORC1 activation in podocytes is a critical step in the development of diabetic nephropathy in mice. *J Clin Invest*. 2011;121(6):2181-96.
67. Inoki K, Huber TB. Mammalian target of rapamycin signaling in the podocyte. *Curr Opin Nephrol Hypertens*. 2012;21(3):251-7.
68. Zschiedrich S, Bork T, Liang W, Wanner N, Eulenbruch K, Munder S, Hartleben B, Kretz O, Gerber S, Simons M, Viau A, Burtin M, Wei C, Reiser J, Herbach N, Rastaldi MP, Cohen CD, Tharaux PL, Terzi F, Walz G, Godel M, Huber TB. Targeting mTOR Signaling Can Prevent the Progression of FSGS. *J Am Soc Nephrol*. 2017;28(7):2144-57.
69. Rachubik P, Szejder M, Rogacka D, Audzeyenka I, Rychlowski M, Angielski S, Piwkowska A. The TRPC6-AMPK Pathway is Involved in Insulin-Dependent Cytoskeleton Reorganization and Glucose Uptake in Cultured Rat Podocytes. *Cell Physiol Biochem*. 2018;51(1):393-410.
70. Viana SD, Reis F, Alves R. Therapeutic Use of mTOR Inhibitors in Renal Diseases: Advances, Drawbacks, and Challenges. *Oxid Med Cell Longev*. 2018;2018:3693625.
71. Um SH, D'Alessio D, Thomas G. Nutrient overload, insulin resistance, and ribosomal protein S6 kinase 1, S6K1. *Cell Metab*. 2006;3(6):393-402.
72. Lieberthal W, Levine JS. The role of the mammalian target of rapamycin (mTOR) in renal disease. *J Am Soc Nephrol*. 2009;20(12):2493-502.
73. Jiang L, Xu L, Mao J, Li J, Fang L, Zhou Y, Liu W, He W, Zhao AZ, Yang J, Dai C. Rheb/mTORC1 signaling promotes kidney fibroblast activation and fibrosis. *J Am Soc Nephrol*. 2013;24(7):1114-26.
74. Lu M, Wang J, Ives HE, Pearce D. mSIN1 protein mediates SGK1 protein interaction with mTORC2 protein complex and is required for selective activation of the epithelial sodium channel. *J Biol Chem*. 2011;286(35):30647-54.
75. Canaud G, Bienaime F, Viau A, Treins C, Baron W, Nguyen C, Burtin M, Berissi S, Giannakakis K, Muda AO, Zschiedrich S, Huber TB, Friedlander G, Legendre C, Pontoglio M, Pende M, Terzi F. AKT2 is essential to maintain podocyte viability and function during chronic kidney disease. *Nat Med*. 2013;19(10):1288-96.
76. Das F, Ghosh-Choudhury N, Lee DY, Gorin Y, Kasinath BS, Choudhury GG. Akt2 causes TGFbeta-induced dephosphorylation facilitating mTOR to drive podocyte hypertrophy and matrix protein expression. *PLoS One*. 2018;13(11):e0207285.
77. Muller-Krebs S, Weber L, Tsoaneli J, Kihm LP, Reiser J, Zeier M, Schwenger V. Cellular effects of everolimus and sirolimus on podocytes. *PLoS One*. 2013;8(11):e80340.

78. Laplante M, Sabatini DM. mTOR signaling at a glance. *J Cell Sci.* 2009;122(Pt 20):3589-94.
79. Lieberthal W, Levine JS. Mammalian target of rapamycin and the kidney. I. The signaling pathway. *Am J Physiol Renal Physiol.* 2012;303(1):F1-10.
80. MacKeigan JP, Krueger DA. Differentiating the mTOR inhibitors everolimus and sirolimus in the treatment of tuberous sclerosis complex. *Neuro Oncol.* 2015;17(12):1550-9.
81. Robert T, Abraham JJG, Edmund I, Graziani. *Chemistry and Pharmacology of Rapamycin and Its Derivatives*, . The Enzymes. 27: Elsevier; 2010. p. 329-66.
82. Sarbassov DD, Ali SM, Sengupta S, Sheen JH, Hsu PP, Bagley AF, Markhard AL, Sabatini DM. Prolonged rapamycin treatment inhibits mTORC2 assembly and Akt/PKB. *Mol Cell.* 2006;22(2):159-68.
83. Morelon E KH. Sirolimus therapy without calcineurin inhibitors: Necker Hospital 8-year experience. . *Transpl Proc.* 2003;35:52S-7S.
84. Fernandes-Silva G, Ivani de Paula M, Rangel EB. mTOR inhibitors in pancreas transplant: adverse effects and drug-drug interactions. *Expert Opin Drug Metab Toxicol.* 2017;13(4):367-85.
85. Murakami N, Riella LV, Funakoshi T. Risk of metabolic complications in kidney transplantation after conversion to mTOR inhibitor: a systematic review and meta-analysis. *Am J Transplant.* 2014;14(10):2317-27.
86. Rossi AP, Vella JP. Acute Kidney Disease After Liver and Heart Transplantation. *Transplantation.* 2016;100(3):506-14.
87. Ventura-Aguiar P, Campistol JM, Diekmann F. Safety of mTOR inhibitors in adult solid organ transplantation. *Expert Opin Drug Saf.* 2016;15(3):303-19.
88. Vollenbroeker B, George B, Wolfgart M, Saleem MA, Pavenstadt H, Weide T. mTOR regulates expression of slit diaphragm proteins and cytoskeleton structure in podocytes. *Am J Physiol Renal Physiol.* 2009;296(2):F418-26.
89. Letavernier E, Bruneval P, Vandermeersch S, Perez J, Mandet C, Belair MF, Haymann JP, Legendre C, Baud L. Sirolimus interacts with pathways essential for podocyte integrity. *Nephrol Dial Transplant.* 2009;24(2):630-8.
90. Stallone G, Infante B, Pontrelli P, Gigante M, Montemurno E, Loverre A, Rossini M, Schena FP, Grandaliano G, Gesualdo L. Sirolimus and proteinuria in renal transplant patients: evidence for a dose-dependent effect on slit diaphragm-associated proteins. *Transplantation.* 2011;91(9):997-1004.
91. Biancone L, Bussolati B, Mazzucco G, Barreca A, Gallo E, Rossetti M, Messina M, Nuschak B, Fop F, Medica D, Cantaluppi V, Camussi G, Segoloni GP. Loss of nephrin expression in glomeruli of kidney-transplanted patients under m-TOR inhibitor therapy. *Am J Transplant.* 2010;10(10):2270-8.
92. Kim BS, Lee JG, Cho Y, Song SH, Huh KH, Kim MS, Kim YS. Reduction of Slit Diaphragm-associated Molecules by Sirolimus: Is it Enough to Induce Proteinuria? *Transplant Proc.* 2017;49(5):1165-9.
93. Deng W, Tan X, Zhou Q, Ai Z, Liu W, Chen W, Yu X, Yang Q. Gender-related differences in clinicopathological characteristics and renal outcomes of Chinese patients with IgA nephropathy. *BMC Nephrol.* 2018;19(1):31.
94. Lima-Posada I, Portas-Cortes C, Perez-Villalva R, Fontana F, Rodriguez-Romo R, Prieto R, Sanchez-Navarro A, Rodriguez-Gonzalez GL, Gamba G, Zambrano E, Bobadilla NA. Gender Differences in the Acute Kidney Injury to Chronic Kidney Disease Transition. *Sci Rep.* 2017;7(1):12270.
95. Boerries M, Grahammer F, Eiselein S, Buck M, Meyer C, Goedel M, Bechtel W, Zschiedrich S, Pfeifer D, Laloe D, Arrondel C, Goncalves S, Kruger M, Harvey SJ, Busch H,

- Dengjel J, Huber TB. Molecular fingerprinting of the podocyte reveals novel gene and protein regulatory networks. *Kidney Int.* 2013;83(6):1052-64.
96. Lawrence M, Huber W, Pages H, Aboyoun P, Carlson M, Gentleman R, Morgan MT, Carey VJ. Software for computing and annotating genomic ranges. *PLoS Comput Biol.* 2013;9(8):e1003118.
97. Liao Y, Smyth GK, Shi W. The Subread aligner: fast, accurate and scalable read mapping by seed-and-vote. *Nucleic Acids Res.* 2013;41(10):e108.
98. Love MI, Huber W, Anders S. Moderated estimation of fold change and dispersion for RNA-seq data with DESeq2. *Genome Biol.* 2014;15(12):550.
99. Mi H, Ebert D, Muruganujan A, Mills C, Albou LP, Mushayamaha T, Thomas PD. PANTHER version 16: a revised family classification, tree-based classification tool, enhancer regions and extensive API. *Nucleic Acids Res.* 2021;49(D1):D394-D403.
100. Mi H, Muruganujan A, Huang X, Ebert D, Mills C, Guo X, Thomas PD. Protocol Update for large-scale genome and gene function analysis with the PANTHER classification system (v.14.0). *Nat Protoc.* 2019;14(3):703-21.
101. Subramanian A, Tamayo P, Mootha VK, Mukherjee S, Ebert BL, Gillette MA, Paulovich A, Pomeroy SL, Golub TR, Lander ES, Mesirov JP. Gene set enrichment analysis: a knowledge-based approach for interpreting genome-wide expression profiles. *Proc Natl Acad Sci U S A.* 2005;102(43):15545-50.
102. Chen EY, Tan CM, Kou Y, Duan Q, Wang Z, Meirelles GV, Clark NR, Ma'ayan A. Enrichr: interactive and collaborative HTML5 gene list enrichment analysis tool. *BMC Bioinformatics.* 2013;14:128.
103. Kuleshov MV, Jones MR, Rouillard AD, Fernandez NF, Duan Q, Wang Z, Koplev S, Jenkins SL, Jagodnik KM, Lachmann A, McDermott MG, Monteiro CD, Gunderson GW, Ma'ayan A. Enrichr: a comprehensive gene set enrichment analysis web server 2016 update. *Nucleic Acids Res.* 2016;44(W1):W90-7.
104. Xie Z, Bailey A, Kuleshov MV, Clarke DJB, Evangelista JE, Jenkins SL, Lachmann A, Wojciechowicz ML, Kropiwnicki E, Jagodnik KM, Jeon M, Ma'ayan A. Gene Set Knowledge Discovery with Enrichr. *Curr Protoc.* 2021;1(3):e90.
105. Babicki S, Arndt D, Marcu A, Liang Y, Grant JR, Maciejewski A, Wishart DS. Heatmapper: web-enabled heat mapping for all. *Nucleic Acids Res.* 2016;44(W1):W147-53.
106. Rinschen MM, Godel M, Grahammer F, Zschiedrich S, Helmstadter M, Kretz O, Zarei M, Braun DA, Dittrich S, Pahmeyer C, Schroder P, Teetzen C, Gee H, Daouk G, Pohl M, Kuhn E, Schermer B, Kuttner V, Boerries M, Busch H, Schiffer M, Bergmann C, Kruger M, Hildebrandt F, Dengjel J, Benzing T, Huber TB. A Multi-layered Quantitative In Vivo Expression Atlas of the Podocyte Unravels Kidney Disease Candidate Genes. *Cell Rep.* 2018;23(8):2495-508.
107. Reiling JH, Sabatini DM. Stress and mTOR signaling. *Oncogene.* 2006;25(48):6373-83.
108. Chen G, Chen H, Wang C, Peng Y, Sun L, Liu H, Liu F. Rapamycin ameliorates kidney fibrosis by inhibiting the activation of mTOR signaling in interstitial macrophages and myofibroblasts. *PLoS One.* 2012;7(3):e33626.
109. Wiza C, Nascimento EB, Ouwers DM. Role of PRAS40 in Akt and mTOR signaling in health and disease. *Am J Physiol Endocrinol Metab.* 2012;302(12):E1453-60.
110. Hay N, Sonenberg N. Upstream and downstream of mTOR. *Genes Dev.* 2004;18(16):1926-45.
111. Choo AY, Yoon SO, Kim SG, Roux PP, Blenis J. Rapamycin differentially inhibits S6Ks and 4E-BP1 to mediate cell-type-specific repression of mRNA translation. *Proc Natl Acad Sci U S A.* 2008;105(45):17414-9.

112. Copp J, Manning G, Hunter T. TORC-specific phosphorylation of mammalian target of rapamycin (mTOR): phospho-Ser2481 is a marker for intact mTOR signaling complex 2. *Cancer Res.* 2009;69(5):1821-7.
113. Garcia D, Shaw RJ. AMPK: Mechanisms of Cellular Energy Sensing and Restoration of Metabolic Balance. *Mol Cell.* 2017;66(6):789-800.
114. Kann M, Ettou S, Jung YL, Lenz MO, Taglienti ME, Park PJ, Schermer B, Benzing T, Kreidberg JA. Genome-Wide Analysis of Wilms' Tumor 1-Controlled Gene Expression in Podocytes Reveals Key Regulatory Mechanisms. *J Am Soc Nephrol.* 2015;26(9):2097-104.
115. Wang Y, Eng DG, Kaverina NV, Loretz CJ, Koirala A, Akilesh S, Pippin JW, Shankland SJ. Global transcriptomic changes occur in aged mouse podocytes. *Kidney Int.* 2020;98(5):1160-73.
116. Lu Y, Ye Y, Bao W, Yang Q, Wang J, Liu Z, Shi S. Genome-wide identification of genes essential for podocyte cytoskeletons based on single-cell RNA sequencing. *Kidney Int.* 2017;92(5):1119-29.
117. Park J, Shrestha R, Qiu C, Kondo A, Huang S, Werth M, Li M, Barasch J, Susztak K. Single-cell transcriptomics of the mouse kidney reveals potential cellular targets of kidney disease. *Science.* 2018;360(6390):758-63.
118. Ransick A, Lindstrom NO, Liu J, Zhu Q, Guo JJ, Alvarado GF, Kim AD, Black HG, Kim J, McMahon AP. Single-Cell Profiling Reveals Sex, Lineage, and Regional Diversity in the Mouse Kidney. *Dev Cell.* 2019;51(3):399-413 e7.
119. Lopes-Ramos CM, Chen CY, Kuijjer ML, Paulson JN, Sonawane AR, Fagny M, Platig J, Glass K, Quackenbush J, DeMeo DL. Sex Differences in Gene Expression and Regulatory Networks across 29 Human Tissues. *Cell Rep.* 2020;31(12):107795.
120. Oliva M, Munoz-Aguirre M, Kim-Hellmuth S, Wucher V, Gewirtz ADH, Cotter DJ, Parsana P, Kasela S, Balliu B, Vinuela A, Castel SE, Mohammadi P, Aguet F, Zou Y, Khramtsova EA, Skol AD, Garrido-Martin D, Reverter F, Brown A, Evans P, Gamazon ER, Payne A, Bonazzola R, Barbeira AN, Hamel AR, Martinez-Perez A, Soria JM, Consortium GT, Pierce BL, Stephens M, Eskin E, Dermitzakis ET, Segre AV, Im HK, Engelhardt BE, Ardlie KG, Montgomery SB, Battle AJ, Lappalainen T, Guigo R, Stranger BE. The impact of sex on gene expression across human tissues. *Science.* 2020;369(6509).
121. Rinschen MM, Hoppe AK, Grahmmer F, Kann M, Volker LA, Schurek EM, Binz J, Hohne M, Demir F, Malisic M, Huber TB, Kurschat C, Kizhakkedathu JN, Schermer B, Huesgen PF, Benzing T. N-Degradomic Analysis Reveals a Proteolytic Network Processing the Podocyte Cytoskeleton. *J Am Soc Nephrol.* 2017;28(10):2867-78.
122. Rinschen MM, Huesgen PF, Koch RE. The podocyte protease web: uncovering the gatekeepers of glomerular disease. *Am J Physiol Renal Physiol.* 2018;315(6):F1812-F6.
123. Yoshida K, Imamura CK, Hara K, Mochizuki M, Tanigawara Y. Effect of everolimus on the glucose metabolic pathway in mouse skeletal muscle cells (C2C12). *Metabolomics.* 2017;13(8):98.
124. Yasuda-Yamahara M, Kume S, Tagawa A, Maegawa H, Uzu T. Emerging role of podocyte autophagy in the progression of diabetic nephropathy. *Autophagy.* 2015;11(12):2385-6.
125. Zhou Y, Lee J, Reno CM, Sun C, Park SW, Chung J, Lee J, Fisher SJ, White MF, Biddinger SB, Ozcan U. Regulation of glucose homeostasis through a XBP-1-FoxO1 interaction. *Nat Med.* 2011;17(3):356-65.
126. Gao T, Furnari F, Newton AC. PHLPP: a phosphatase that directly dephosphorylates Akt, promotes apoptosis, and suppresses tumor growth. *Mol Cell.* 2005;18(1):13-24.
127. Woo CY, Baek JY, Kim AR, Hong CH, Yoon JE, Kim HS, Yoo HJ, Park TS, Kc R, Lee KU, Koh EH. Inhibition of Ceramide Accumulation in Podocytes by Myriocin Prevents Diabetic Nephropathy. *Diabetes Metab J.* 2020;44(4):581-91.

128. Lennon R, Randles MJ, Humphries MJ. The importance of podocyte adhesion for a healthy glomerulus. *Front Endocrinol (Lausanne)*. 2014;5:160.
129. Sterk LM, de Melker AA, Kramer D, Kuikman I, Chand A, Claessen N, Weening JJ, Sonnenberg A. Glomerular extracellular matrix components and integrins. *Cell Adhes Commun*. 1998;5(3):177-92.
130. Inoue K, Ishibe S. Podocyte endocytosis in the regulation of the glomerular filtration barrier. *Am J Physiol Renal Physiol*. 2015;309(5):F398-405.
131. Soda K, Ishibe S. The function of endocytosis in podocytes. *Curr Opin Nephrol Hypertens*. 2013;22(4):432-8.
132. Nistala R, Whaley-Connell A, Sowers JR. Redox control of renal function and hypertension. *Antioxid Redox Signal*. 2008;10(12):2047-89.
133. Singh CK, Chhabra G, Ndiaye MA, Garcia-Peterson LM, Mack NJ, Ahmad N. The Role of Sirtuins in Antioxidant and Redox Signaling. *Antioxid Redox Signal*. 2018;28(8):643-61.
134. Yamamoto-Nonaka K, Koike M, Asanuma K, Takagi M, Oliva Trejo JA, Seki T, Hidaka T, Ichimura K, Sakai T, Tada N, Ueno T, Uchiyama Y, Tomino Y. Cathepsin D in Podocytes Is Important in the Pathogenesis of Proteinuria and CKD. *J Am Soc Nephrol*. 2016;27(9):2685-700.
135. Starr MC, Chang IJ, Finn LS, Sun A, Larson AA, Goebel J, Hanevold C, Thies J, Van Hove JLK, Hingorani SR, Lam C. COQ2 nephropathy: a treatable cause of nephrotic syndrome in children. *Pediatr Nephrol*. 2018;33(7):1257-61.
136. Blattner SM, Hodgins JB, Nishio M, Wylie SA, Saha J, Soofi AA, Vining C, Randolph A, Herbach N, Wanke R, Atkins KB, Gyung Kang H, Henger A, Brakebusch C, Holzman LB, Kretzler M. Divergent functions of the Rho GTPases Rac1 and Cdc42 in podocyte injury. *Kidney Int*. 2013;84(5):920-30.
137. Scott RP, Hawley SP, Ruston J, Du J, Brakebusch C, Jones N, Pawson T. Podocyte-specific loss of Cdc42 leads to congenital nephropathy. *J Am Soc Nephrol*. 2012;23(7):1149-54.
138. Hatch V, Zhi G, Smith L, Stull JT, Craig R, Lehman W. Myosin light chain kinase binding to a unique site on F-actin revealed by three-dimensional image reconstruction. *J Cell Biol*. 2001;154(3):611-7.
139. Ben-Sahra I, Howell JJ, Asara JM, Manning BD. Stimulation of de novo pyrimidine synthesis by growth signaling through mTOR and S6K1. *Science*. 2013;339(6125):1323-8.
140. Lee SK. Sex as an important biological variable in biomedical research. *BMB Rep*. 2018;51(4):167-73.
141. Berletch JB, Yang F, Xu J, Carrel L, Distèche CM. Genes that escape from X inactivation. *Hum Genet*. 2011;130(2):237-45.
142. Ishola DA, Jr., van der Giezen DM, Hahnel B, Goldschmeding R, Kriz W, Koomans HA, Joles JA. In mice, proteinuria and renal inflammatory responses to albumin overload are strain-dependent. *Nephrol Dial Transplant*. 2006;21(3):591-7.
143. Lv Z, Hu M, Fan M, Li X, Lin J, Zhen J, Wang Z, Jin H, Wang R. Podocyte-specific Rac1 deficiency ameliorates podocyte damage and proteinuria in STZ-induced diabetic nephropathy in mice. *Cell Death Dis*. 2018;9(3):342.
144. Grahammer F, Wanner N, Huber TB. mTOR controls kidney epithelia in health and disease. *Nephrol Dial Transplant*. 2014;29 Suppl 1:i9-i18.
145. Gurgun D, Kusch A, Klewitz R, Hoff U, Catar R, Hegner B, Kintscher U, Luft FC, Dragun D. Sex-specific mTOR signaling determines sexual dimorphism in myocardial adaptation in normotensive DOCA-salt model. *Hypertension*. 2013;61(3):730-6.
146. Kusch A, Schmidt M, Gurgun D, Postpieszala D, Catar R, Hegner B, Davidson MM, Mahmoodzadeh S, Dragun D. 17 β -Estradiol regulates mTORC2 sensitivity to rapamycin in adaptive cardiac remodeling. *PLoS One*. 2015;10(4):e0123385.
147. Schurch NJ, Schofield P, Gierlinski M, Cole C, Sherstnev A, Singh V, Wrobel N, Gharbi K, Simpson GG, Owen-Hughes T, Blaxter M, Barton GJ. How many biological replicates are

- needed in an RNA-seq experiment and which differential expression tool should you use? *RNA*. 2016;22(6):839-51.
148. Wang Y, Eng DG, Pippin JW, Gharib SA, McClelland A, Gross KW, Shankland SJ. Sex differences in transcriptomic profiles in aged kidney cells of renin lineage. *Aging (Albany NY)*. 2018;10(4):606-21.
149. Rangan GK. Sirolimus-associated proteinuria and renal dysfunction. *Drug Saf*. 2006;29(12):1153-61.
150. Amer H, Cosio FG. Significance and management of proteinuria in kidney transplant recipients. *J Am Soc Nephrol*. 2009;20(12):2490-2.
151. Diekmann F, Rovira J, Carreras J, Arellano EM, Banon-Maneus E, Ramirez-Bajo MJ, Gutierrez-Dalmau A, Brunet M, Campistol JM. Mammalian target of rapamycin inhibition halts the progression of proteinuria in a rat model of reduced renal mass. *J Am Soc Nephrol*. 2007;18(10):2653-60.
152. Yang SB, Lee HY, Young DM, Tien AC, Rowson-Baldwin A, Shu YY, Jan YN, Jan LY. Rapamycin induces glucose intolerance in mice by reducing islet mass, insulin content, and insulin sensitivity. *J Mol Med (Berl)*. 2012;90(5):575-85.
153. Buller CL, Loberg RD, Fan MH, Zhu Q, Park JL, Vesely E, Inoki K, Guan KL, Brosius FC, 3rd. A GSK-3/TSC2/mTOR pathway regulates glucose uptake and GLUT1 glucose transporter expression. *Am J Physiol Cell Physiol*. 2008;295(3):C836-43.
154. Kohn AD, Summers SA, Birnbaum MJ, Roth RA. Expression of a constitutively active Akt Ser/Thr kinase in 3T3-L1 adipocytes stimulates glucose uptake and glucose transporter 4 translocation. *J Biol Chem*. 1996;271(49):31372-8.
155. Kempe DS, Siraskar G, Frohlich H, Umbach AT, Stubs M, Weiss F, Ackermann TF, Volkl H, Birnbaum MJ, Pearce D, Foller M, Lang F. Regulation of renal tubular glucose reabsorption by Akt2/PKCb β . *Am J Physiol Renal Physiol*. 2010;298(5):F1113-7.
156. Rodriguez KA, Dodds SG, Strong R, Galvan V, Sharp ZD, Buffenstein R. Divergent tissue and sex effects of rapamycin on the proteasome-chaperone network of old mice. *Front Mol Neurosci*. 2014;7:83.
157. Block A, Ahmed MM, Dhanasekaran AR, Tong S, Gardiner KJ. Sex differences in protein expression in the mouse brain and their perturbations in a model of Down syndrome. *Biol Sex Differ*. 2015;6:24.
158. Ostrom QT, Rubin JB, Lathia JD, Berens ME, Barnholtz-Sloan JS. Females have the survival advantage in glioblastoma. *Neuro Oncol*. 2018;20(4):576-7.
159. Inyang KE, Szabo-Pardi T, Wentworth E, McDougal TA, Dussor G, Burton MD, Price TJ. The antidiabetic drug metformin prevents and reverses neuropathic pain and spinal cord microglial activation in male but not female mice. *Pharmacol Res*. 2019;139:1-16.
160. Baar EL, Carbajal KA, Ong IM, Lamming DW. Sex- and tissue-specific changes in mTOR signaling with age in C57BL/6J mice. *Aging Cell*. 2016;15(1):155-66.
161. Yu Z, Sunchu B, Fok WC, Alshaikh N, Perez VI. Gene expression in the liver of female, but not male mice treated with rapamycin resembles changes observed under dietary restriction. *Springerplus*. 2015;4:174.
162. Mihai S, Codrici E, Popescu ID, Enciu AM, Albuлесcu L, Necula LG, Mambet C, Anton G, Tanase C. Inflammation-Related Mechanisms in Chronic Kidney Disease Prediction, Progression, and Outcome. *J Immunol Res*. 2018;2018:2180373.
163. Zhang Y, Liu Y, Liu H, Tang WH. Exosomes: biogenesis, biologic function and clinical potential. *Cell Biosci*. 2019;9:19.
164. Guneykaya D, Ivanov A, Hernandez DP, Haage V, Wojtas B, Meyer N, Maricos M, Jordan P, Buonfiglioli A, Gielniewski B, Ochocka N, Comert C, Friedrich C, Artiles LS, Kaminska B, Mertins P, Beule D, Kettenmann H, Wolf SA. Transcriptional and Translational Differences of Microglia from Male and Female Brains. *Cell Rep*. 2018;24(10):2773-83 e6.

165. Huber TB, Kottgen M, Schilling B, Walz G, Benzing T. Interaction with podocin facilitates nephrin signaling. *J Biol Chem*. 2001;276(45):41543-6.
166. Shimodahira M, Fujimoto S, Mukai E, Nakamura Y, Nishi Y, Sasaki M, Sato Y, Sato H, Hosokawa M, Nagashima K, Seino Y, Inagaki N. Rapamycin impairs metabolism-secretion coupling in rat pancreatic islets by suppressing carbohydrate metabolism. *J Endocrinol*. 2010;204(1):37-46.
167. Zhou L, Liu Y. Wnt/beta-catenin signalling and podocyte dysfunction in proteinuric kidney disease. *Nat Rev Nephrol*. 2015;11(9):535-45.
168. Palmer RE, Kotsianti A, Cadman B, Boyd T, Gerald W, Haber DA. WT1 regulates the expression of the major glomerular podocyte membrane protein Podocalyxin. *Curr Biol*. 2001;11(22):1805-9.
169. Stylianou K, Petrakis I, Mavroeidi V, Stratakis S, Kokologiannakis G, Lioudaki E, Liotsi C, Kroustalakis N, Vardaki E, Stratigis S, Perakis K, Kyriazis J, Nakopoulou L, Daphnis E. Rapamycin induced ultrastructural and molecular alterations in glomerular podocytes in healthy mice. *Nephrol Dial Transplant*. 2012;27(8):3141-8.
170. Jeruschke S, Jeruschke K, DiStasio A, Karaterzi S, Buscher AK, Nalbant P, Klein-Hitpass L, Hoyer PF, Weiss J, Stottmann RW, Weber S. Everolimus Stabilizes Podocyte Microtubules via Enhancing TUBB2B and DCDC2 Expression. *PLoS One*. 2015;10(9):e0137043.
171. Kerr N, Dietrich DW, Bramlett HM, Raval AP. Sexually dimorphic microglia and ischemic stroke. *CNS Neurosci Ther*. 2019;25(12):1308-17.
172. Liu L, Luo Y, Chen L, Shen T, Xu B, Chen W, Zhou H, Han X, Huang S. Rapamycin inhibits cytoskeleton reorganization and cell motility by suppressing RhoA expression and activity. *J Biol Chem*. 2010;285(49):38362-73.
173. Mouawad F, Tsui H, Takano T. Role of Rho-GTPases and their regulatory proteins in glomerular podocyte function. *Can J Physiol Pharmacol*. 2013;91(10):773-82.
174. Zhao M, Yuan Y, Bai M, Ding G, Jia Z, Huang S, Zhang A. PGC-1alpha overexpression protects against aldosterone-induced podocyte depletion: role of mitochondria. *Oncotarget*. 2016;7(11):12150-62.
175. Brinkkoetter PT, Bork T, Salou S, Liang W, Mizi A, Ozel C, Koehler S, Hagmann HH, Ising C, Kuczkowski A, Schnyder S, Abed A, Schermer B, Benzing T, Kretz O, Puelles VG, Lagies S, Schlimpert M, Kammerer B, Handschin C, Schell C, Huber TB. Anaerobic Glycolysis Maintains the Glomerular Filtration Barrier Independent of Mitochondrial Metabolism and Dynamics. *Cell Rep*. 2019;27(5):1551-66 e5.
176. Klinge CM. Estrogenic control of mitochondrial function. *Redox Biol*. 2020;31:101435.
177. Ventura-Clapier R, Moulin M, Piquereau J, Lemaire C, Mericskay M, Veksler V, Garnier A. Mitochondria: a central target for sex differences in pathologies. *Clin Sci (Lond)*. 2017;131(9):803-22.
178. Mitchell T, De Miguel C, Gohar EY. Sex differences in redox homeostasis in renal disease. *Redox Biol*. 2020;31:101489.
179. Cruz-Topete D, Dominic P, Stokes KY. Uncovering sex-specific mechanisms of action of testosterone and redox balance. *Redox Biol*. 2020;31:101490.
180. Wang L, Ahn YJ, Asmis R. Sexual dimorphism in glutathione metabolism and glutathione-dependent responses. *Redox Biol*. 2020;31:101410.
181. Jin J, Gong J, Zhao L, Zhang H, He Q, Jiang X. Inhibition of high mobility group box 1 (HMGB1) attenuates podocyte apoptosis and epithelial-mesenchymal transition by regulating autophagy flux. *J Diabetes*. 2019;11(10):826-36.
182. Cybulsky AV. The intersecting roles of endoplasmic reticulum stress, ubiquitin-proteasome system, and autophagy in the pathogenesis of proteinuric kidney disease. *Kidney Int*. 2013;84(1):25-33.

183. Navarro-Betancourt JR, Papillon J, Guillemette J, Iwawaki T, Chung CF, Cybulsky AV. Role of IRE1 α in podocyte proteostasis and mitochondrial health. *Cell Death Discov.* 2020;6(1):128.
184. Arif E, Solanki AK, Srivastava P, Rahman B, Fitzgibbon WR, Deng P, Budisavljevic MN, Baicu CF, Zile MR, Megyesi J, Janech MG, Kwon SH, Collier J, Schnellmann RG, Nihalani D. Mitochondrial biogenesis induced by the beta2-adrenergic receptor agonist formoterol accelerates podocyte recovery from glomerular injury. *Kidney Int.* 2019;96(3):656-73.
185. Rijo-Ferreira F, Takahashi JS. Genomics of circadian rhythms in health and disease. *Genome Med.* 2019;11(1):82.
186. Ansermet C, Centeno G, Nikolaeva S, Maillard MP, Pradervand S, Firsov D. The intrinsic circadian clock in podocytes controls glomerular filtration rate. *Sci Rep.* 2019;9(1):16089.
187. Goita Y, Chao de la Barca JM, Keita A, Diarra MB, Dembele KC, Chabrun F, Drame BSI, Kassogue Y, Diakite M, Mirebeau-Prunier D, Cisse BM, Simard G, Reynier P. Sexual Dimorphism of Metabolomic Profile in Arterial Hypertension. *Sci Rep.* 2020;10(1):7517.
188. Lorenz M, Blaschke B, Benn A, Hammer E, Witt E, Kirwan J, Fritsche-Guenther R, Gloaguen Y, Bartsch C, Vietzke A, Kramer F, Kappert K, Brunner P, Nguyen HG, Dreger H, Stangl K, Knaus P, Stangl V. Sex-specific metabolic and functional differences in human umbilical vein endothelial cells from twin pairs. *Atherosclerosis.* 2019;291:99-106.
189. Chen JQ, Brown TR, Russo J. Regulation of energy metabolism pathways by estrogens and estrogenic chemicals and potential implications in obesity associated with increased exposure to endocrine disruptors. *Biochim Biophys Acta.* 2009;1793(7):1128-43.
190. Sun Y, Gu X, Zhang E, Park MA, Pereira AM, Wang S, Morrison T, Li C, Blenis J, Gerbaudo VH, Henske EP, Yu JJ. Estradiol promotes pentose phosphate pathway addiction and cell survival via reactivation of Akt in mTORC1 hyperactive cells. *Cell Death Dis.* 2014;5:e1231.
191. Sipula IJ, Brown NF, Perdomo G. Rapamycin-mediated inhibition of mammalian target of rapamycin in skeletal muscle cells reduces glucose utilization and increases fatty acid oxidation. *Metabolism.* 2006;55(12):1637-44.
192. Siegmund SE, Yang H, Sharma R, Javors M, Skinner O, Mootha V, Hirano M, Schon EA. Low-dose rapamycin extends lifespan in a mouse model of mtDNA depletion syndrome. *Hum Mol Genet.* 2017;26(23):4588-605.
193. Chiao YA, Kolwicz SC, Basisty N, Gagnidze A, Zhang J, Gu H, Djukovic D, Beyer RP, Raftery D, MacCoss M, Tian R, Rabinovitch PS. Rapamycin transiently induces mitochondrial remodeling to reprogram energy metabolism in old hearts. *Aging (Albany NY).* 2016;8(2):314-27.
194. Quarles E, Basisty N, Chiao YA, Merrihew G, Gu H, Sweetwyne MT, Fredrickson J, Nguyen NH, Razumova M, Kooiker K, Moussavi-Harami F, Regnier M, Quarles C, MacCoss M, Rabinovitch PS. Rapamycin persistently improves cardiac function in aged, male and female mice, even following cessation of treatment. *Aging Cell.* 2020;19(2):e13086.
195. Mercken EM, Crosby SD, Lamming DW, JeBailey L, Krzysik-Walker S, Villareal DT, Capri M, Franceschi C, Zhang Y, Becker K, Sabatini DM, de Cabo R, Fontana L. Calorie restriction in humans inhibits the PI3K/AKT pathway and induces a younger transcription profile. *Aging Cell.* 2013;12(4):645-51.
196. Asadi Shahmirzadi A, Edgar D, Liao CY, Hsu YM, Lucanic M, Asadi Shahmirzadi A, Wiley CD, Gan G, Kim DE, Kasler HG, Kuehnemann C, Kaplowitz B, Bhaumik D, Riley RR, Kennedy BK, Lithgow GJ. Alpha-Ketoglutarate, an Endogenous Metabolite, Extends Lifespan and Compresses Morbidity in Aging Mice. *Cell Metab.* 2020;32(3):447-56 e6.

Appendix Table 1. List of intrinsically significantly differently expressed genes (male 826, female 942)

male vehicle significantly overexpressed genes						adj.p-value < 0.01											adj.p-value 0.01 > 0.05																																																																																																																																																																																																																																																																																																																																																																																																																																																																												
Ddx3y	Cep250	Fndc3a	Mgam	Polr2a	Stgp3	0610010F05F	Bicra	Dclre1c	Hdac4	Lmln	Plk1	Secisbp2l	Tns1	1700012D01F	Bod1l	Ddi2	Hdac5	Loxl1	Plk5	Sept6	Tpm1	2510009E07F	Bok	Dennd4a	Herc2	Lrch3	Plod2	Sept8	Traf3	4833420G17F	Brd1	Desi2	Herc4	Lrrc56	Plxna1	Serac1	Trafd1	4933427D14F	Brd4	Dgkq	Hipk1	Lrrfip1	Pnpla7	Serpine1	Trak1	5930430L01F	C1rl	Dhx33	Hipk4	Lrrk1	Pogz	Sertad2	Trerf1	A530013C23F	C2cd3	Dicer1	Hk1	Mamld1	Ppox	Sf3b1	Trim8	Actn1	C3	Dll1	Hnrnpu	Map7d1	Ppp4r1l-p	Sh3rf1	Trpm7	Acvr1l	Cabin1	Dnajc6	Homer1	Mbtd1	Prdm2	Shank3	Trpv4	Adamts5	Cables2	Dnmt3a	Hoxa3	Mdc1	Prickle3	Shroom4	Tshz1	Adarb1	Camta2	Dock6	Htt	Med13	Prkag2	Slc17a9	Tspan18	Adh1	Caprin2	Dstyk	Huwe1	Med13l	Prkca	Slc25a37	Ttcl3	Afaf1	Cav1	Dtna	Icam1	Mfhas1	Prkcg	Slc26a2	Ttc28	Aff1	Cbl	Dyrk1a	Icosl	Mga	Prkci	Slc30a1	Ttc39b	Ahctf1	Cbx4	E430016F16F	Ifitm1	Mgat4a	Prkdc	Slc43a3	Tubb6	Akap7	Ccbe1	Efnb2	Igf1	Mia3	Prkx	Slc9a1	Tubg2	Aldh1a1	Ccdc186	Elmsan1	Igf1r	Mib1	Prr12	Slmap	Uaca	Ambra1	Ccdc6	Enah	Igf2bp1	Mpdz	Prr14l	Slpi	Uba6	Amt	Ccdc9b	Endou	Igfbp6	Mrtfa	Prrc1	Smarca1	Ubr4	Angel2	Ccn2	Eogt	Inmt	Msh6	Prrc2b	Smyd1	Ucp2	Ank	Ccnt1	Ep400	Ino80	Mxi1	Prrc2c	Snpc4	Uhrf1bpl1	Ankrd13d	Ccnt2	Epb41	Ino80dc	Myc	Prrg4	Snx24	Ulk3	Ankrd29	Cd109	Erbp3	Inpp1	Myliip	Psd3	Sorbs3	Usp48	Ankrd6	Cd47	Erc6	Inpp5f	Myo9b	Ptbp3	Sox5	Usp49	Aox1	Cd55os	Ern1	Insr	Nbeal1	Ptk2	Spag1	Usp7	Ap3m2	Cd68	Fam135a	Ints6	Nbeal2	Ptpn3	Spen	Uvssa	Apba1	Cd74	Fam13a	Iqcn	Ncoa3	Ptprg	Spns2	Vangl2	Appbp2	Cdc42bpt	Fam171a2	Iqgap1	Ncoa6	Pus7	Srrm2	Vit	Ar	Cdk19	Fam199x	Iqsec1	Nedd4	Pwwp2b	St5	Vps13c	Arc	Cdkl5	Fam214a	Irf8	Nfatc1	Rab12	Stac3	Wasl	Arfgef1	Cemip2	Fam53b	Itprid2	Nfia	Rara	Star	Wbp1l	Arhgap17	Cep192	Fam76a	Itpripl2	Nfxl1	Rasa1	Stat2	Wdr19	Arhgef10	Champ1	Fancm	Jade2	Npat	Rasal2	Stat3	Wdr6	Arhgef40	Chd3	Fbxl18	Jag1	Npc1	Rassf5	Stk36	Wipf1	Arhgef7	Chd4	Fbxo21	Jak2	Nphp3	Rb1cc1	Ston1	Wipf2	Arid1a	Chd7	Fbxo32	Jmjd1c	Nr1d2	Rbbp6	Sulf2	Wiz	Arid2	Chd8	Fgd1	Jmy	Nr2c2	Rbm33	Swap70	Wwc2	Arid4a	Chd9	Fhl1	Jup	Nr3c2	Rbm38	Syngap1	Xndc1	Arid4b	Chuk	Fhod1	Kat6a	Osmr	Rc3h2	Tacc2	Xrn1	Arid5a	Clasp2	Fmnl3	Kdm7a	Pan2	Rcc2	Tada2a	Xylt1	Ash1l	Cldn12	Fosl1	Khdc4	Pan3	Rel1	Taf4	Zbtb1	Atad2	Clk2	Foxj2	Kif1b	Parp8	Rhbd13	Taok3	Zbtb20	Atf7	Clstn2	Foxk1	Klf2	Paxbp1	Rhof	Tbc1d2b	Zbtb7a	Atf7ip	Cnot6	Foxn2	Klf7	Pbx1	Ric1	Tbc1d8	Zdhhc21	Atp11a	Cog3	Foxo3	Klhl21	Pdlim1	Rictor	Tcaf2	Zer1	Atp8b1	Col16a1	Foxp4	Kmt2b	Pdlim7	Rnase4	Tchp	Zfhx2	Atr	Cp	Fstl1	Kmt2c	Per1	Rnaseh2l	Tead1	Zfhx3	Atxn1	Cplx2	Gabbr1	Krit1	Phactr1	Robo1	Tead3	Zfp267	Atxn2l	Crebbp	Gbp9	Lag3	Phc1	Rprd2	Tet2	Zfp273	Axl	Crebrf	Gclm	Lama3	Phka1	Rreb1	Tfeb	Zfp362	B430010I23R	Creg2	Gcnt2	Larp4	Phlda3	Safb2	Tjp2	Zfp592	Bach1	Cry2	Gm35339	Larp4b	Phldb1	Sall1	Tm6sf1	Zfp652	Bahcc1	Csnk1g1	Gpsm2	Larp6	Phlpp2	Samd8	Tmcc1	Zfp827	Baiap2	Ctdsp2	Gramd1b	Lbp	Phtf1	Satb1	Tmem13l	Zfp862-ps	Baz2b	Cx3c1	Grb10	Lcat	Pias1	Sbf1	Tmem176	Zmiz1	Bbx	Dab2	Gsk3b	Lhfp	Pik3c2a	Scara5	Tmem184	Zmyz5	BC024386	Dab2ip	Guf1	Limk1	Pik3r1	Sdk1	Tmem94	Zmynd8	Bcl3	Dach1	Hacd4	Lgl1	Pik3r2	Sec16b	Tnks2	Zpbp	Bcor1l	Dcbl2	Hbegf	Lmbr1l	Pkd1l3	Sec24a	Tnpo1	Zswim8

female vehicle significantly overexpressed genes

adj. p-value<0.01							adj. p- value 0.01> <0.05							
1110002L01Rik	Ctla	Gas7	Mrpl35	Pea15a	Rpl37a	Spp1	1110008P14Rik	Cct5	Dynlrb1	Guk1	Morn2	Pex7	Rplp2	Tex264
2310022B05Rik	Cmtm7	Gatm	Mrpl52	Pex14	Rpl41	Spr	1110065P20Rik	Cct6a	Ebna1bp2	H1f2	Mplkip	Pgrmc1	Rpp30	Thra
2310039H08Rik	Cnbp	Gck	Mrpl57	Pfdn5	Rpl5	Sqstm1	2210016L21Rik	Cct8	Echs1	H2-Q6	Mrfap1	Phpt1	Rps16	Timm8b
2410022M11Rik	Coa3	Gdi2	Mrpl58	Pgls	Rpl6	Srpr	5031425E22Rik	Cd320	Eef1b2	H2-Q7	Mrpl13	Pin1	Rps18	Tm2d1
2810001G20Rik	Commdd6	Gfod1	Mrps12	Phb	Rpl7	Ssu72	5530601H04Rik	Cdc37	Eef1e1	H3f3a	Mrpl2	Pink1	Rps19	Tm2d3
3830406C13Rik	Cope	Ggt5	Mrps18a	Phyh	Rpl7a	St3gal3	5830408C22Rik	Cdc42se2	Eef1g	H4c8	Mrpl20	Plekha2	Rps23	Tmbim4
6330418K02Rik	Cops9	Gja3	Mrps24	Pkig	Rpl8	St6galnac6	Abhd6	Cdh1	Efh1	Habp4	Mrpl24	Ppp3	Rps25	Tmco1
Aagab	Cotl1	Gm15501	Mrps28	Pla2g7	Rpl9	Stx8	Acaa1a	Cdipt	Ei24	Haus2	Mrpl27	Pmpcb	Rps28	Tmed2
Abhd17a	Cox14	Gm5617	Mtfr1	Plat	Rplp1	Suclg2	Acadm	Cdk2ap2	Eif2b2	Hax1	Mrpl28	Pno1	Rps6	Tmed3
Acot2	Cox16	Gm5	Mtln	Polb	Rpn1	Supt4a	Acads	Cebpz	Eif2b3	Hba-a1	Mrpl37	Polr1d	Rrp36	Tmem115
Acot9	Cox20	Gna11	Mvb12a	Pold4	Rpph1	Taf10	Aco2	Cenpx	Eif2b5	Hcfc1r1	Mrpl46	Polr2c	Rrp7a	Tmem183a
Adamts16	Cox41	Gnb2	Myl12a	Polr2g	Rps10	Tbc1d22a	Actr1b	Cept1	Eif2s1	Higd2a	Mrpl48	Polr2f	Rsl24d1	Tmem199
Adprh	Cox5b	Gnptg	Myl7	Pomp	Rps11	Tbcb	Adh5	Cetn2	Eif3d	Hnrnpc	Mrpl54	Pomgnt1	Rtcb	Tmem234
Adsl	Cox6a1	Gpx4	Mylk3	Ppib	Rps12	Tbgr1	Adipor1	Cetn3	Eif3e	Hotairm1	Mrpl55	Ppa1	Sar1a	Tmem238
Agpat4	Cox6c	Gpx8	Naa10	Ppp1ca	Rps13	Tgfa	Aip	Cfdp1	Eif3g	Hprt	Mrps14	Ppil2	Sar1b	Tmem242
Aif1l	Cox7a2	Gramd4	Naa20	Ppp1r11	Rps14	Timm13	Akt1s1	Chchd10	Eif3h	Idh3b	Mrps25	Ppp2cb	Scoc	Tmem256
Akr1a1	Cox7b	H13	Naca	Ppp1r1a	Rps15	Timm50	Akt2	Chmp2a	Eif3i	Idh3g	Mrps34	Prdx1	Sdf4	Tmem54
Alkbh6	Creb3l1	H2-Ke6	Nans	Ppp2r5b	Rps15a	Tle5	Amfr	Chmp3	Eif3l	Idnk	Mtch1	Prrm1	Sdhaf3	Tmem59
Alkbh7	Csdc2	H2-T23	Naxe	Prdx5	Rps17	Tmem134	Anapc13	Chmp4b	Eif4a3	Ift22	Mthfsl	Prrm7	Sdhf	Tmem60
Antxr2	Ctsc	Hagh	Ncaph2	Prr13	Rps2	Tmem140	Ankrd40	Chmp5	Eif5a	Igfbp7	Mydgf	Prx	Sdk2	Tmem70
Arf6	Ctsl	Hint1	Ndfip1	Psenen	Rps20	Tmem160	Appl1	Chrac1	Eif6	Il11ra1	MYL6	Prxl2a	Sec61a1	Tmprss2
Arl10	Cwc15	Hip1r	Ndufa12	Psmab	Rps21	Tmem219	Arf1	Churc1	Elob	Ilkap	Naa38	Psm1a	Sec61g	Tmsb4x
Arntl	Cyb5a	Hmgcl	Ndufa13	Psmb3	Rps24	Tmem52b	Arf2	Ciao2b	Eloc	Imp3	Nars	Psm2	Selenof	Tomm40l
Arvcf	Cyba	Hs3st6	Ndufa2	Psmb4	Rps26	Tmsb10	Arf5	Cisd1	Emb	Itm2c	Naxd	Psmb1	Selenos	Tomm5
Asb13	Cyc1	Hsbp1	Ndufa4	Psmb5	Rps27	Triap1	Arfgap2	Cnp	Emc3	Josd2	Nbl1	Psmc3	Serf2	Tomm7
Atp4a	Cyp4a14	Hsp90aa1	Ndufa5	Psmb6	Rps27a	Trim3	Arfrp1	Cnpy3	Emc4	Jund	Ndufa1	Psmd6	Serpinb9	Tonsl
Atp5b	Daam2	Hspb8	Ndufa6	Psmb7	Rps29	Trp53i11	Arhgap44	Col4a5	Eml2	Kank1	Ndufa11	Psm2e	Serpinh1	Tor1a
Atp5c1	Dad1	Hspe1	Ndufa7	Psmc4	Rps3	Tspan15	Arl2	Comp	Emx1	Kcng2	Ndufa9	Ptp4a2	Sf3b5	Tor4a
Atp5d	Dcdc2a	Ifi27	Ndufaf3	Psmc5	Rps4x	Tspan3	Arl6ip1	Comtd1	Ergic1	Kcnj1	Ndufb1-ps	Ptpa	Sh2d4a	Tpt1
Atp5e	Dctn5	Ifngr1	Ndufb10	Psmd13	Rps5	Tuba1b	Arpc4	Cops4	Erp29	Kctd2	Ndufb3	Pthr2	Slc16a7	Trappc4
Atp5g1	Dda1	Immp1l	Ndufb11	Psmd8	Rps7	Tubb2b	As3mt	Cops5	Exosc5	Kdm6a	Ndufc2	Pttg1ip	Slc25a17	Trmt112
Atp5g3	Ddx3x	Ints3	Ndufb2	Ptgds	Rps9	Txn2	Asl	Cox6b1	Fahd1	Kng2	Ndufs1	Pxm2	Slc25a39	Tspan31
Atp5j2	Defb1	Itgb5	Ndufb4	Pthr1d	Rpsa	Txndc17	Asna1	Cox7a2l	Fam136a	Kremen1	Ndufs2	Pycr2	Slc25a5	Tspo
Atp5k	Degs1	Itm2b	Ndufb5	Pvalb	Rtraf	Uap11	Atf4	Cox8a	Fam204a	Krtcap2	Ndufs3	R3hdm4	Slc35b1	Tsta3
Atp5md	Dnajb11	Jtb	Ndufb6	Pyclr	S100a1	Ubb	Atf5	Cpt2	Fars2	Kti12	Ndufs4	Rab1b	Slc39a3	Ttc1
Atp5o	Dnajc15	Klc2	Ndufb8	Qdpr	S100a10	Ube2g2	Atf6b	Cr1l	Fkbp1a	Lamtor1	Ndufs5	Rab3b	Slc41a2	Ttc27
Atp5pb	Dnlz	Lamtor4	Ndufb9	Rab13	Saraf	Ube2m	Atp1a1	Crb2	Fkbp2	Lamtor2	Nedd8	Rab5c	Snap47	Tusc3
Atp60e	Dpm3	Lamtor5	Ndufs6	Rab17	Sars	Ube2s	Atp5a1	Creg1	Fkbp7	Laptm4a	Nelfe	Rab5if	Snrnp27	Txn1
Avp1	Ech1	Ldrap1	Ndufs7	Rabac1	Scand1	Ubl5	Atp5g2	Crelld1	Fkbp1	Lasp1	Neu1	Rbis	Snrpb	Txndc9
B3gat3	Edf1	Lemd2	Ndufs8	Rack1	Sdf2	Ubxn6	Atp5h	Crls1	Fmc1	Lcmt2	Nlk	Rbx1	Snrpb	Txn14a
Babam1	Eef1a1	Leo1	Ndufv2	Raly	Sdhb	Ufc1	Atp5j	Cryab	Fnta	Ldhb	Nme2	Rer1	Snrpd1	Ube2d3
Bag1	Eef1akmt2	Lingo1	Ndufv3	Rarres1	Sec61b	Ugt1a2	Atp5l	Cst3	Fopnl	Litaf	Nol12	Rexo2	Snx1	Ube2e1
BC031181	Eef1d	Map3k10	Nectin2	Rdm1	Selenok	Uqcr10	Atp5mpl	Ctsd	Gabarap	Lman2	Nop16	Rhbdd2	Snx6	Ube2ql1
Bckdk	Egf	Mars	Nenf	Rex1bd	Selenop	Uqcr11	Atp6v1e1	Cwh43	Gabarap1	Lrp5	Npc2	Rnaseh2c	Spag7	Uck1
Bloc1s2	Ehd1	Mcrip1	Nfkbib	Rgs3	Selenow	Uqcrb	Atp6v1f	Cyb561d2	Gadd45gjlrrc	Lrrc59	Ociad1	Rnf141	Spsc2	Ufm1
Bri3	Eid1	Mdh1	Ngb	Rhod	Serpinb6a	Uqcrcl	Aurkaip1	Cystm1	Gatd3a	Lsm4	Ogfod3	Rnf34	Spp2	Unc5c
Bsg	Eif2s2	Med28	Nme1	Rin3	Setd3	Uqcrcl	B230118H07Rik	D8Ertld738	Gcat	Ltbr	Osr2	Rnf7	Spsb3	Urm1
Btf3	Eif2s3x	Med31	Nop10	Rn7sk	Sfrp1	Uqcrfs1	B230319C09Rik	Dctd	Get4	Mal	Ost4	Romo1	Sptssa	Use1
C1galt1c1	Eif3k	Mesd	Npas2	Rnf187	Sgk3	Uqcrh	Banf1	Dctn2	Gfod2	Mal2	Oxtcl	Rpl10a	Sqor	Vapa
Calr	Eif3m	Mettl23	Nphs2	Rpl10	Slc27a3	Uqcrq	BC004004	Dctn6	Ghdc	Manf	Pa2g4	Rpl11	Srp14	Vdac3
Ccdc91	Eif4h	Mgat5b	Npl	Rpl14	Slc38a10	Vamp8	BC005624	Ddost	Ghitm	Mcf2	Paip2	Rpl12	Srxn1	Vps45
Cct7	Elmo2	Nicu1	Npr1	Rpl15	Slirp	Vkorc1	Bod1	Derl2	Gipc1	Mdh2	Pak1	Rpl13	Ssr2	Vstm4
Cd151	Elof1	Mien1	Nudt16l1	Rpl18	Smad6	Xist	Brk1	Dgcr6	Glrx3	Mea1	Pam16	Rpl17	Stk16	Vti1b
Cdc42	Fau	Mlf2	Nxph3	Rpl19	Smdt1	Yif1a	Bsnd	Dhcr7	Gm1821	Mecr	Park7	Rpl18a	Stub1	Wdr18
Cdh16	Fis1	Mmp17	Oaz1	Rpl21	Smim4	Yif1b	Bub3	Diablo	Gmppb	Med29	Pbdc1	Rpl23a	Sugt1	Wdr83os
Cdkn1c	Fkbp3	Mmp23	Ormdl3	Rpl22l1	Smim7	Ywhae	C1qtnf1	Dnajb1	Gpr39	Metrl	Pcbp1	Rpl27	Surf1	Wnt8b
Cerk	Fkbp8	Mocs1	P4hb	Rpl23	Snrpd2	Ywhaq	Cacybp	Dohh	Gps1	Mettl1	Pcmt1	Rpl27a	Swi5	Xbp1
Chchd2	Foxs1	Mpc2	Pcsk2	Rpl26	Snu13	Zfand6	Capns1	Dpcd	Grccl0	Mettl26	Pcna	Rpl28	Tac4	Yars
Chmp6	Fth1	Mrm3	Pdia4	Rpl31	Snx21	Zmat5	Car14	Drap1	Grpel1	Mgat4b	Pdap1	Rpl35	Tbca	Zc3hc1
Ckb	Ftl1	Mrpl12	Pdia6	Rpl32	Sod1		Ccdc107	Drg1	Gsn	Micos13	Pdhh	Rpl36a	Tbxas1	Zcrb1
Clnkb	Fxyd2	Mrpl17	Pdlim2	Rpl35a	Spcs1		Ccdc124	Drg2	Gsta2	Mif4gd	Pdia3	Rpl37	Tceal9	Zfp207
Clic3	Gadd45a	Mrpl21	Pdrg1	Rpl36	Sphk2		Ccdc92	Dusp3	Gstp1	Mlec	Pebp1	Rpl38	Tcp1	Zfp277
Clpp	Galnt10	Mrpl30	Pdzd11	Rpl36al	Spint2		Cct2	Dynll2	Gtf2f1	Mob2	Pepd	Rpl4	Tesc	Znhit1

Appendix Table 2. List of significantly differently regulated genes after between male and female podocytes of rapamycin-treated groups with p-value<0.05 (53 genes)

male rapamycin vs. female rapamycin			
male upregulated		female upregulated	
Adj.p-value<0.01	Adj.p-value0.01> <0.05	Adj.p-value<0.01	Adj.p-value0.01> <0.05
Ddx3y	Tmem176b	Xist	Prlr
Eif2s3y	Steap3	Ugt1a2	Rps4l
Uty	Slc6a6	Slc22a29	Apoo
Kdm5d	Ccnl2	Kitl	5530601H04Rik
Kap	Cyp27a1	Tgm2	Socs3
Cyp2j13	Acy3	Kdm6a	Sod3
Mfap2	Hdac7	Eif2s3x	
Dlk2	March7	Pbdc1	
Slc7a13	Camta1	Ddx3x	
Cyp4b1	Zbtb16	Armc5	
Apaf1	Pi16		
Tacr1	Hsf2bp		
Prrt1	Chst11		
Ces1f	Lrtm2		
Chil1	Tmem176a		
Cyp2d9	Hnrnp1		
Grik5			
Pros1			
Cyp2e1			
Cd36			
A930016O22Rik			
Rtn2			

Appendix Table 3. List of significantly differentially expressed genes in treatment and sex interaction analysis (32 genes)

Upregulated in male	Upregulated in female
Arntl	Bhlhe40
Stat6	Asap1
Rarres1	Pitpnm2
Mgat4b	Sspn
Cnbp	Maco1
Sgk3	Dip2b
Pdlim2	Mrtfb
Agpat4	Arhgap32
Mocs1	Sesn3
H1f2	Rnf150
Sphk2	Map2k3
Hip1r	Abl1
Cmtm7	Chmp4c
Ggt5	
Ctsl	
Daam2	
Ifngr1	
Csdc2	
Creb3l1	

Appendix Table 4. List of significantly differently regulated genes after rapamycin in male podocytes with p-value<0.05 (132 genes)

upregulated genes after rapamycin			downregulated genes after rapamycin		
Adj. p-value<0.01	Adj. p-value 0.01> <0.05		Adj. p-value<0.01	Adj. p-value 0.01> <0.05	
Daam2	Eif3m	Rps6	Mael	Tcaf2	Zchc2
Egf	Tgfa	Eef1a1	Maco1	Plk5	Megf10
Cmtm7	Pdrg1	Pros1	Sesn3	Parm1	S1pr2
Mocs1	Eif4a2	Nectin2	Map2k3	Arhgap32	Adtrp
Creb3l1	Sybu	Ppargc1a	Sspn	Finc	Igsf9
Agpat4	Ldlrap1	Abtb2	Extl1	Adamts15	Arfgap3
Ifngr1	Pea15a	Myl12a	Ccbe1	Mustn1	Ifit3b
Arntl	2310022B05Rik		Rorc	Sorcs1	Igfals
Rarres1	Luzp2		Pitpnm2	Pgm2l1	Smyd1
Npas2	Lasp1		Man1a2	Tspan18	Fhod1
Thra	Cd151		Abl1	Taok3	Creg2
Gramd4	Itm2b		Sod3	Col1a1	Usp2
Csdc2	Arf2		Pik3ip1	Glul	Nckap5
Sgk3	Dusp15		Ywhah	Stk38	Phactr1
Hip1r	St6galnac6		Cys1	Cpeb1	Fbn1
Kremen1	Ctdp1		Mrtfb	Chmp4c	Aldh1a1
Foxs1	Selenow		Per3	Gm34655	Igfbp6
Pdlim2	Npr1		Bhlhe40	Ccdc9b	
5830408C22Rik	Rpl4		Ago1	Trim58	
Tmem248	Lrp5		Zfp467	Ppp1r15b	
Ctsl	Tmem140		Asap1	Plekho2	
Sphk2	Pkig		B3gnt9	Ndrgr1	
Amfr	St3gal3		Hfe	Mknk2	
Acot9	Cnbp		Stc2	Fmo5	
Mgat4b	Anxa3		Il1r1	Gfra1	
Cerk	Setd3		Bok	Plekha6	
Slc41a2	Gas7				
Tspan15	Pfdn5				

Appendix Table 5. Selected up and down-regulated GO terms after rapamycin in male and female podocyte (Biological process mSigDB and KEGG pathway) by GSEA software

upregulated male vehicle vs female vehicle				
KEGG pathway	size	Normalized	Nom p va	FDR
Ecm_Receptor_Interaction	83	0	0.138	0.65
Mapk_Signaling_Pathway	259	0	0.165	0.795
Jak_Stat_Signaling_Pathway	141	0.001	0.173	0.587
Wnt_Signaling_Pathway	145	0.002	0.166	0.911
Notch_Signaling_Pathway	45	0.01	0.159	0.635
ErbB_Signaling_Pathway	83	0.012	0.178	0.97
Apoptosis	81	0.012	0.178	0.973
Focal_Adhesion	194	0.012	0.183	1
P53_Signaling_Pathway	62	0.02	0.171	0.934
Cytokine_Cytokine_Receptor_Interaction	233	0.02	0.233	1
Chemokine_Signaling_Pathway	165	0.035	0.229	1
Adherens_Junction	72	0.036	0.188	1
Regulation_Of_Actin_Cytoskeleton	208	0.039	0.266	1
GO-BP				
Regulation_Of_Protein_Depolymerization	82	0	0.151	0.695
Negative_Regulation_Of_Cell_Adhesion	277	0	0.178	0.962
Regulation_Of_Phosphatidylinositol_3_Kinase_Signaling	127	0	0.17	0.964
Regulation_Of_Cell_Cell_Adhesion	402	0	0.145	0.966
Inositol_Lipid_Mediated_Signaling	193	0	0.139	0.966
Phosphatidylinositol_3_Kinase_Signaling	153	0	0.128	0.973
Endothelial_Cell_Apoptotic_Process	62	0	0.128	0.975
Regulation_Of_Microtubule_Depolymerization	30	0	0.135	0.997
Rhythmic_Process	297	0	0.139	0.997
Actin_Filament_Depolymerization	54	0	0.14	0.998
Circadian_Rhythm	212	0	0.139	1
Rhythmic_Behavior	50	0	0.152	1
Positive_Regulation_Of_Cell_Projection_Organization	389	0	0.215	1
Regulation_Of_Inflammatory_Response	377	0	0.221	1
Synapse_Organization	423	0	0.227	1
Cell_Junction_Assembly	421	0	0.23	1
Regulation_Of_Stress_Activated_Protein_Kinase_Signaling_Cascade	225	0.001	0.21	1
Stress_Activated_Protein_Kinase_Signaling_Cascade	281	0.001	0.216	1
upregulated Female vehicle vs male vehicle				
KEGG pathway	size	Normalized	Nom p va	FDR
Oxidative_Phosphorylation	124	3.38	0	0
Ribosome	59	3.28	0	0
Proteasome	43	2.5	0	0
Protein_Export	23	2.44	0	0
Citrate_Cycle_Tca_Cycle	30	1.82	0	0.009
Propanoate_Metabolism	31	1.81	0	0.009
Antigen_Processing_And_Presentation	52	1.6	0	0.045
Valine_Leucine_And_Isoleucine_Degradation	44	1.75	0.005	0.014
Peroxisome	77	1.58	0.008	0.046
N_Glycan_Biosynthesis	44	1.46	0.011	0.088
Phenylalanine_Metabolism	18	1.64	0.012	0.034
Spliceosome	115	1.48	0.012	0.085
Pyruvate_Metabolism	39	1.52	0.014	0.068
Snare_Interactions_In_Vesicular_Transport	33	1.44	0.051	0.1
Glycolysis_Gluconeogenesis	57	1.29	0.063	0.208
Lysosome	116	1.19	0.075	0.284
Arachidonic_Acid_Metabolism	53	1.27	0.09	0.217
Go-Bp				
Oxidative_Phosphorylation	137	3.3	0	0
Atp_Synthesis_Coupled_Electron_Transport	90	3.27	0	0
Mitochondrial_Respiratory_Chain_Complex_Assembly	99	3.22	0	0
Mitochondrial_Translation	133	3.06	0	0
Protein_Localization_To_Endoplasmic_Reticulum	114	3.04	0	0
Translational_Termination	103	2.99	0	0
Translational_Elongation	129	2.76	0	0
Cellular_Respiration	179	2.75	0	0
Cristae_Formation	33	2.73	0	0
Protein_Targeting_To_Membrane	168	2.6	0	0
Atp_Synthesis_Coupled_Proton_Transport	22	2.47	0	0
Protein_Targeting	388	2.44	0	0
Atp_Metabolic_Process	289	2.15	0	0.001
Ribosome_Biogenesis	281	2.07	0	0.003
Energy_Derivation_By_Oxidation_Of_Organic_Compounds	267	2.06	0	0.003
Protein_Folding	203	2	0	0.005
Amine_Metabolic_Process	136	1.65	0	0.067
Peroxisome_Organization	78	1.59	0	0.089
Peroxisomal_Transport	68	1.58	0	0.093

Up-regulated terms in male rapamycin vs.vehicle				
GS	size	Normalize	p-value	FDR
KEGG pathway				
Ribosome	59	3.21	0	0
Oxidative Phosphorylation	124	2.82	0	0
Protein Export	23	1.7	0	0.023
Allograft Rejection	24	1.38	0.067	0.166
Proteasome	43	1.3	0.07	0.252
GO-BP				
Atp Synthesis Coupled Electron Transport	90	2.81	0	0
Oxidative Phosphorylation	137	2.69	0	0
Translational Initiation	158	2.6	0	0
Mitochondrial Electron Transport Nadh To Ubiquinone	52	2.59	0	0
Respiratory Electron Transport Chain	108	2.54	0	0
Protein Targeting To Membrane	168	2.29	0	0
Cristae Formation	33	2.23	0	0.001
Atp Synthesis Coupled Proton Transport	22	2.21	0	0.001
Ribosomal Large Subunit Biogenesis	62	2.17	0	0.002
Ribosome Assembly	54	2.13	0	0.003
Electron Transport Chain	171	2.08	0	0.005
Cytoplasmic Translation	85	2.06	0	0.006
Cellular Respiration	179	2.03	0	0.007
Atp Biosynthetic Process	47	1.98	0	0.011
Translational Elongation	129	1.87	0	0.027
Protein Targeting	388	1.77	0	0.05
Mitochondrial Translational Termination	89	1.76	0	0.052
Ribosome Biogenesis	281	1.62	0	0.14
Atp Metabolic Process	289	1.61	0	0.148
Mitochondrial Translation	133	1.6	0	0.15
Aerobic Respiration	83	1.59	0	0.159
Rrna Metabolic Process	220	1.58	0	0.159
Translational Termination	103	1.58	0	0.16
Mitochondrial Gene Expression	160	1.47	0	0.269
Energy Derivation By Oxidation Of Organic Compounds	267	1.4	0	0.329
Rna Catabolic Process	374	1.37	0	0.35
Regulation Of Natural Killer Cell Mediated Immunity	33	1.39	0.036	0.33
Protein Folding	203	1.2	0	0.57
Down-regulated terms in male rapamycin vs.vehicle				
KEGG pathway				
Pentose Phosphate Pathway	24	-1.57	0.015	0.428
Apoptosis	81	-1.41	0.015	0.385
Notch Signaling Pathway	45	-1.48	0.017	0.458
ErbB Signaling Pathway	83	-1.38	0.033	0.463
Cytokine Cytokine Receptor Interaction	233	-1.26	0.042	0.494
Mapk Signaling Pathway	259	-1.24	0.047	0.513
Ecm Receptor Interaction	83	-1.3	0.055	0.471
GO-BP				
L Amino Acid Transport	69	-1.71	0	0.504
Response To Type I Interferon	80	-1.65	0	0.471
Regulation Of Organic Acid Transport	66	-1.57	0	0.441
Cytokine Production Involved In Immune Response	94	-1.55	0	0.416
Extracellular Structure Organization	382	-1.51	0	0.402
Rhythmic Process	297	-1.49	0	0.402
Regulation Of Inflammatory Response	377	-1.4	0	0.487
Regulation Of Ion Transmembrane Transport	464	-1.31	0	0.531
Regulation Of Extracellular Matrix Organization	44	-1.69	0.001	0.481
Amino Acid Transmembrane Transport	87	-1.55	0.001	0.412
Negative Regulation Of Cell Cell Adhesion	174	-1.5	0.001	0.391
Circadian Rhythm	212	-1.42	0.001	0.49
Response To Interferon Gamma	163	-1.49	0.002	0.393
Toll Like Receptor Signaling Pathway	138	-1.46	0.002	0.43
Collagen Metabolic Process	106	-1.52	0.003	0.405
Arginine Metabolic Process	19	-1.64	0.004	0.455
Carbohydrate Transport	142	-1.4	0.005	0.485
Positive Regulation Of Cytokine Production	416	-1.29	0.005	0.55
L Alpha Amino Acid Transmembrane Transport	58	-1.53	0.006	0.4
Wound Healing	491	-1.23	0.008	0.599
Regulation Of Amino Acid Transport	36	-1.56	0.009	0.439
Extracellular Matrix Assembly	43	-1.53	0.01	0.394
Microtubule Depolymerization	45	-1.57	0.012	0.434
Aminoglycan Metabolic Process	167	-1.36	0.012	0.491
Carbohydrate Catabolic Process	187	-1.31	0.017	0.536
Actin Filament Organization	411	-1.23	0.02	0.598
Calcineurin Mediated Signaling	47	-1.45	0.022	0.46
Positive Regulation Of Autophagy	126	-1.36	0.022	0.496
Cellular Modified Amino Acid Metabolic Process	169	-1.3	0.022	0.536
Neutral Amino Acid Transport	42	-1.45	0.027	0.459
Positive Regulation Of Endocytosis	97	-1.34	0.03	0.514
Synapse Assembly	179	-1.29	0.031	0.548
Phospholipid Metabolic Process	439	-1.2	0.033	0.631
Regulation Of Response To Reactive Oxygen Species	39	-1.44	0.034	0.472
Alpha Amino Acid Metabolic Process	189	-1.27	0.034	0.567
Regulation Of Microtubule Cytoskeleton Organization	184	-1.27	0.038	0.567

Up-regulated terms in female rapamycin vs.female vehicle				
Term	size	Enriched score ES	p-value	FDR
KEGG pathway				
O_Glycan_Biosynthesis	29	1.42	0.047	1.00
Cytokine_Cytokine_Receptor_Interaction	233	1.32	0.004	1.00
Jak_Stat_Signaling_Pathway	141	1.25	0.048	1.00
Regulation_Of_Actin_Cytoskeleton	208	1.24	0.054	0.97
Mtor_Signaling_Pathway	52	1.24	0.114	0.87
Go-Bp				
Synapse_Assembly	179	1.48	0	0.63
Regulation_Of_Small_Gtpase_Mediated_Signal_Transduction	315	1.37	0	0.68
Interleukin_6_Mediated_Signaling_Pathway	32	1.71	0.003	0.43
T_Cell_Migration	60	1.64	0.003	0.47
Leukocyte_Cell_Cell_Adhesion	333	1.3	0.004	0.73
T_Cell_Activation_Involved_In_Immune_Response	98	1.42	0.007	0.67
Protein_Localization_To_Cytoskeleton	57	1.49	0.008	0.63
Positive_Regulation_Of_Phosphatidylinositol_3_Kinase_Signaling	88	1.41	0.009	0.68
Adaptive_Immune_Response	444	1.21	0.012	0.82
Regulation_Of_Phosphatidylinositol_3_Kinase_Signaling	127	1.36	0.013	0.69
Regulation_Of_Cell_Cell_Adhesion	402	1.2	0.013	0.83
Positive_Regulation_Of_Interleukin_10_Production	35	1.54	0.014	0.57
Endothelial_Cell_Apoptotic_Process	62	1.39	0.015	0.69
Regulation_Of_T_Cell_Activation	305	1.26	0.016	0.80
Gene_Silencing	406	1.19	0.02	0.82
Microtubule_Cytoskeleton_Organization_Involved_In_Mitosis	140	1.33	0.021	0.73
Protein_Localization_To_Microtubule_Organizing_Center	33	1.51	0.022	0.60
T_Cell_Activation	444	1.25	0.027	0.81
Synapse_Organization	423	1.16	0.029	0.82
Regulation_Of_Lymphocyte_Differentiation	172	1.26	0.032	0.80
Interferon_Gamma_Production	99	1.33	0.033	0.73
Regulation_Of_Gtpase_Activity	435	1.14	0.033	0.83
Negative_Regulation_Of_Inflammatory_Response	175	1.22	0.036	0.82
Positive_Regulation_Of_P38Mapk_Cascade	28	1.5	0.038	0.62
Cell_Junction_Assembly	421	1.16	0.038	0.82
Interleukin_10_Production	57	1.36	0.04	0.70
Regulation_Of_Leukocyte_Differentiation	275	1.19	0.04	0.82
Positive_Regulation_Of_Cell_Adhesion	401	1.16	0.04	0.82
Cytoplasmic_Microtubule_Organization	63	1.33	0.044	0.72
Negative_Regulation_Of_Adaptive_Immune_Response	44	1.38	0.045	0.70
Leukocyte_Migration	419	1.17	0.045	0.82
Down-regulated terms in female rapamycin vs.female vehicle				
Term	size	Enriched score ES	p-value	FDR
KEGG pathway				
Ribosome	59	-1.96	0.000	0.003
Oxidative_phosphorylation	124	-1.93	0.000	0.002
Protein_export	23	-1.75	0.003	0.026
Lysosome	116	-1.71	0.000	0.026
Proteasome	43	-1.7	0.002	0.027
Citrate_cycle_(TCA)	30	-1.53	0.024	0.136
Base_excision_repair	31	-1.53	0.026	0.127
Valine_leucine_and_isoleucine_degradation	44	-1.52	0.011	0.132
Arachidonic_acid_metabolism	53	-1.49	0.012	0.141
Tryptophan_metabolism	39	-1.44	0.040	0.215
Nglycan_biosynthesis	44	-1.41	0.035	0.239
Glycerophospholipid_metabolism	76	-1.34	0.037	0.305
mSig-Hallmark				
Xenobiotic_metabolism	191	-1.49	0.000	0.040
Fattyacidmetabolism	155	-1.52	0.001	0.038
Reactive_oxygen_species_pathway	47	-1.67	0.002	0.014
Peroxisome	102	-1.41	0.012	0.059
P53Pathway	188	-1.37	0.015	0.094
Apoptosis	155	-1.34	0.020	0.102
Mtorc1Signaling	188	-1.34	0.022	0.097
Epithelial_mesenchymal_transition	195	-1.29	0.039	0.112
Hypoxia	197	-1.27	0.039	0.113
GO-BP				
Atp_Synthesis_Coupled_Electron_Transport	90	-2.04	0.000	0.005
Mitochondrial_Translational_Termination	89	-2.02	0.000	0.005
Translational_Termination	103	-1.92	0.000	0.018
Mitochondrial_Translation	133	-1.89	0.000	0.026
Cellular_Respiration	179	-1.88	0.000	0.026
Electron_Transport_Chain	171	-1.87	0.000	0.029
Mitochondrial_Gene_Expression	160	-1.82	0.000	0.046
Cristae_Formation	33	-1.54	0.021	0.430
Translational_Elongation	129	-1.79	0.000	0.073
Translational_Initiation	158	-1.73	0.000	0.146
Atp_Metabolic_Process	289	-1.67	0.000	0.230
Fatty_Acid_Biosynthetic_Process	161	-1.63	0.000	0.311
Protein_Folding	203	-1.6	0.000	0.340
Energy_Derivation_By_Oxidation_Of_Organic_Compounds	267	-1.57	0.000	0.377
Fatty_Acid_Metabolic_Process	370	-1.5	0.000	0.464
Cellular_Amino_Acid_Metabolic_Process	307	-1.43	0.000	0.543
Ribosome_Biogenesis	281	-1.39	0.003	0.584
Regulation_Of_Integrin_Mediated_Signaling_Pathway	15	-1.68	0.007	0.221
Lipid_Oxidation	111	-1.42	0.009	0.541
Collagen_Metabolic_Process	106	-1.43	0.018	0.540
Positive_Regulation_Of_Chemokine_Production	56	-1.44	0.022	0.547
Chaperone_Mediated_Protein_Folding	54	-1.47	0.027	0.504
Intrinsic_Apoptotic_Signaling_Pathway_In_Response_To_Oxidative_Stress	41	-1.41	0.048	0.566

Appendix Table 6: List of proteins with FC > 2 in male and female podocytes (used for figure 44).

Overexpressed proteins in male podocyte with Log2FC>2			Overexpressed proteins in female podocyte with Log2FC>2									
Aacs	Ipo4	Snrpe	Mar-2	Atp1b1	Cyp4b1	Gna13	Mapt	Pecr	Rala	Snx2	Uck2	
Abcb10	Itch	Snrpf	Sep-2	Atp1b2	D10Jhu81	Gnai3	Mat2b	Pepd	Raly	Snx27	Ugp2	
Abracl	Jup	Sos2	Sep-7	Atp5f1	Dab2	Gnao1	Mcc	Pfkip	Ran;1700009	Snx4	Ugt1a7c;Ugt1a10	
Acaca	Kdsr	Stk39	Sep-11	Atp5j;Atp5	Dach1	Gnas	Mccc1	Pgam2	Ranbp1	Snx9	Uqcc1	
Acot13	Kpna2	Stt3b	0610037L13Rik	Atp5j2	Dbi	Gnb2	Mcu	Pgls	Rap1a	Sod2	Uqcr10	
Ahnak	Krt14	Syne3	5730455P16Rik	Atp5l	Dbnl	Gng12	Mcur1	Pgm2	Rap1b	Sorbs3	Uqcrb	
Ak2	Larp7	Tap2	Abat	Atp5o	Dctn4	Golim4	Mdh1	Pgrmc1	Rap2c	Sord	Uqcrcl	
Akr1b8	Lcp1	Tbc1d10a	Abhd12	Atp6v1e1	Dhrs4	Gpaa1	Mdh2	Pgrmc2	Raver2	Spcs2	Uqcrcc2	
Alad	Lgals7	Tecr	Acad10;Acad12	Atp6v1h	Dld	Gpd1l	Mfn2	Pik3c3	Rbbp9	Srgap2	Uqcrrfs1	
Alg12	Lmf2	Tgtp1	Acad11	Auh	Dlst	Gpr39	Mgat5	Pip4k2c	RbmX;RbmXl	Srp72	Uqcrq	
Alyref2;Alyref	Lsm8	Tjap1	Acad8	BC026585	Dnajb11	Gpx8	Mgll	Pitpnb	Rexo2	Srsf2	Usmg5	
Anapc1	Ltn1	Tln2	Acadl	Bdh1	Dnajc8	Grb2	Micu2	Plod2	Rhog	Ssbp1	Vamp8	
Anapc4	Mcm3	Tmem205	Acadsb	Brc3	Dnm3	Grpel1	Mme	Pls3	Rhog	Ssr3	Vapa	
Ap3m1	Mcm5	Tmem9	Acat1	Bub3	Dnpep	Gsn	Mpc2	Pnp	Rilp	Ssr4	Vapb	
Aprt	Mcm6	Tomm70a	Acdb3	Cacybp	Dpp4	Gstk1	Mpp5	Podxl	Ripk1	St13	Vim	
Arpin	Mdn1	Tor1a	Acot2	Cadm4	Dynll2	Gstm1	Mta2	Poglut1	Rmdn1	Steap3	Vps26a	
Asns	Mfsd10	Trrap	Acox1	Capzb	Eci2	Gstm2	Mtap	Polr2e	Rmdn3	Stip1	Vps26b	
Ass1;Gm5424	Mroh1	Tspan8	Acox3	Capzb	Ehd3	Gtf2i	Mtatp6	Polr2h	Rmdn1	Stk38	Vps29	
Atp13a1	Mtpn	Ube3b	Acp1	Cardk	Ehd4	Gtpbp4	Mtmr2	Pon2	Rnf121	Ston1	Vps33a	
Atp6v1f	Mvd	Ubr2	Acp6	Cbr1	Eif1;Eif1b	H1f0	Mtx1	Ppa2	Rpl28	Strap	Vps36	
Babam1	Naa35	Ugdh	Acsm2	Ccar2	Eif2b1	Hao2	Myh10	Ppap2a	Rpl34;Gm217	Sts	Vps45	
Bag6	Nasp	Urb2	Acss1	Ccz1	Elavl1	Hist1h1d	Myl6	Ppiib	Rpl35;Gm84	Stxbp1	Vps4b	
Btaf1	Nat10	Vars	Actb2	Cd59a	Elp2	Hist1h1e	Myo1d	Ppp1cb	Rpl35a	Stxbp3	Wasl	
Btf3	Nelfb	Vwa8	Actc1;Actg2;Acta2;Actn4	Cdc23	Emc2	Hmgb1	Myom2	Ppt1	Rpl38	Suclg1	Wdr37	
Bzw1	Nif31	Wdfy3	Actn4	Cdc37	Eml4	Hmgb3	Myzap;Gc	Prdx4	Rpr1b	Suclg2	Wdr48	
Cad	Nmt2	Wdr3	Actr2	Cdk5rap3	Enpep	Hnmt	Naga	Prkaca	Rps11	Sumo1	Xpnpep2	
Calm1	Nol11	Wdr77	Acy3	Cdkn1c	Epn1	Hnrnpa2b	Nampt	Prkacb	Rps19	Synpo	Ybx1	
Cd209c	Nphs2	Wip1	Adk	Cfl2	Epn2	Hook3	Nck2	Prkag1	Rps20	Tbca	Yes1	
Cirbp	Nqo1	Xrcc5	Aifm2	Cgnl1	Epn3	Hsd17b10	Ncln	Prkar2a	Rps3	Tbcb	Ykt6	
Ckb	Nrm	Xrn2	AK3	Chmp5	Erc1	Hsp90b1	Ndufa10	Prkcs	Rps9	Tceb2	Ywhae	
Cicc1	Nudcd3	Yipf3	Akap2;Pakap	Cisd1	Erlin2	Hspa4l	Ndufa11	Prkg1	Rragc;Rragb	Thop1	Ywhag	
Cog1	Nudt14		Akr1a1	Cisd2	Ero1l	Htatip2	Ndufa12	Prpf6	Rragc;Rragb	Thumpud1	Ywhah	
Cog7	Oplah		Akr1e2;Akr1e1	Clic3	Etfb	Idh1	Ndufa13	Prune	Rras	Tial1	Zak	
Coro1a	Pa2g4		Akt1;Akt3	Clic4	Etl4;Skt	Ilk	Ndufa2	Pasma1	Rras2	Timm50		
Cpsf2	Pgfdh		Akt2	Clic5	F11r	Impa1	Ndufa4	Pma6	RtcA;Rtca	Tjp1		
Ctsp1	Phkb		Aldh1l1	Clint1	Faf2	Inpp1	Ndufa6	Psmb5	Ruvbl2	Tmed3		
Cyp2s1	Pik3r4		Aldob	Clip1	Fam129b	Itga1	Ndufa8	Psmd6	Sat2	Tmed5		
Dhx30	Plekhh2		Anp32b	Cltb	Fam162a	Itga2	Ndufa9	Psmd8	Sbds	Tmem106b		
Dock8	Ppp4c		Anpep	Cmpk1	Fam20b	Itgav	Ndufb10	Psmc3	Scp2	Tmem150c		
Dpysl5	Psat1		Anxa3	Cnp	Farp1	Itgb1	Ndufb11	Ptges2	Sdhb	Tmem245		
Eef1b;Eef1b2	PsmA4		Anxa4	Col4a3bp	Fbxo6	Itsn2	Ndufb4	Ptges3	Sdhc	Tmem30a		
Eif2ak2	Psmb2		Anxa6	Col6a1	Fermt2	Ivd	Ndufb5	Ptgr2	Sec11a	Tmod3		
Eif3f	Psmb7		Anxa6	Colgalt2	Fis1	Kank2	Ndufs3	Ptpn1	Sec13	Tnfaip8		
Eif5a	Psmd7		Ap1m1	Comt	Fkbp1a	Khsrp	Ndufs5	Ptpn11	Sec22b	Top1		
Eif6	Ptbp1		Ap1s1	Cops2	Fkbp3	Kirrel	Ndufs7	Ptpn14	Sec23a	Tpd52		
Exosc7	Ptgr1		Ap2m1	Cops5	Fkbp4	Klc1	Nebi	Ptpn21	Serinc1	Tpm1		
Fasn	Rbm3		Apoo	Copz2	Fkbp9	Kras	Nhlrc2	Ptpra	Serpinb9	Tpm3		
Fbl	Rbm39		App	Coro1b	Fnk3rp	Lactb2	Nos1ap	Ptprj	Serpinh1	Tpm3-rs7		
Fbxo9	Rnpep		Arcn1	Cox4i1	Fnbp1l	Lamb2	Npl	Puf60	Set	Tppp		
Fdps	Rpl23		Arf1	Cox5b	Fnta	Lamp1	Nptn	Pura	Sfxn1	Trappc13		
Fen1	Rpl5		Arf4	Cox6c	Fubp1	Lamtor1	Nqo2	Purb	Sfxn3	Trappc3		
Flnb	Rps12		Arhgap18	Cpne3	Fxr1	Lancl1	Nras	Pxn	Sh2d4a	Trappc5		
Fscn1	Rps14		Arhgap28	Cpt1a	Galc	Lasp1	Nudt16l1	Pycrl	Sh3bgrl	Trim3		
Fuk	Rps15		Arhgdia	Crip2	Galk2	Ldhd	Nudt19	Qdpr	Sh3bgrl2	Triobp		
GlrX3	Rps2;Gm5786;Gm6576;Gm18025		Arhgef12	Crk	Galnt10	Lgalsl	Nudt5	Qki	Slc12a3	Trnt1		
Gorasp2	Rps6		Arhgef18	Cryl1	Gatm	Lims1	Numa1	Rab10	Slc25a10	Trove2		
Gspt1;Gspt2	Rrm1		Arl8a	Cryz	Gbas	Lims2	Os9	Rab14	Slc25a11	Try10		
Gsto1	Rtn2		Armc1	Cs	Gbe1	Lin7c	Ostf1	Rab18	Slc25a12	Tsg101		
H2-Q6	S100a4		Armc10	Csnk1a1	Ggt1	Lman2	Pacsin2	Rab22a	Slc25a24	Tst		
H3f3a;H3f3c	Scyl2		Arpc1a	Csrp2	Gimap4	Lman2l	Pafah1b1	Rab23	Slc25a4	Tsta3		
Hbb-b1	Sdc2		Arpc1b	Cstb	Glg1	Lmnb2	Palld	Rab2a;Rat	Slc25a5	Ttn		
Hdac6	Serpib2		Arpc2	Ctsb	Glod4	Lrp2	Park7	Rab35	Slc2a12	Tuba1a;Tuba3a		
Hid1	Sf3a3		Arpc3	Cttn	GlrX	Lrrc7	Pcbp1	Rab3a	Slc9a3r1	Tubal3		
Hist1h3a	Sfn		Arpc5	Cttnbp2	Glyat	Lta4h	Pcca	Rab5b	Slk	Uaca		
Hist1h3b	Sh3bgrl3		Arrb1	Cul3	Gm10250;Lztf1	Pdcd10	Rab6a	Smc3	Ube2m			
Hspb1	Skivl2		Asph	Cxadr	Gm10260;Manba	Pdia4	Rab7a	Smg1	Ube3a			
Hspbp1	Slc12a9		Atad1	Cyb5a	Gm20390;Maoa	Pdk2	Rab8a	Snf8	Ubtf			
Htra1	Slc30a6		Atg7	Cyb5b	Gm20441	Maob	Pdlim2	Rab8b	Snx1	Ubxn1		
Ints3	Snrpd1		Atox1	Cyc1	Gmds	Mapk3	Pdxx	Rac1;Rac3	Snx12	Uchl5		

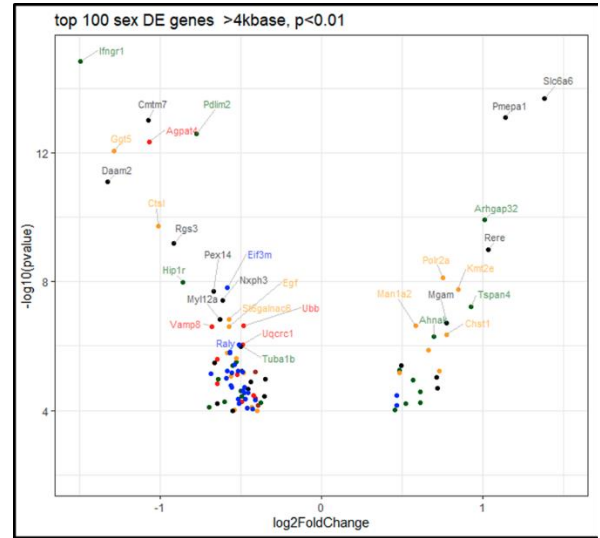
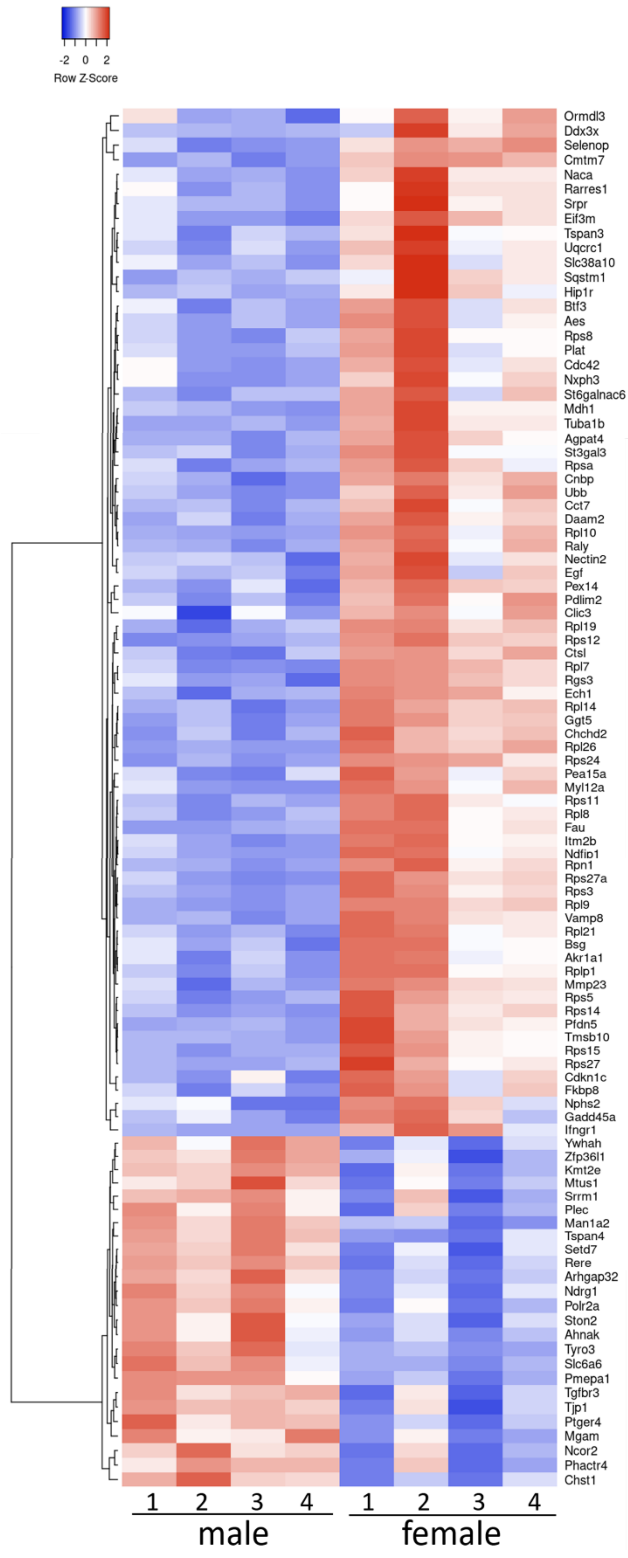
Appendix Table 7. List of metabolites identified in metabolomics

Acetoacetate	Fructose-6-phosphate	Glycerol-3-phosphate	Pyruvic acid
Aconitic acid, cis-	Fumaric acid	Glycine	Pyruvic acid, 3-hydroxy-
Adenine	Galactitol	Homocysteine	Ribitol (Adonitol)
Adenosine	Galactosamine	Hypotaurine	Ribose
Alanine	Galactosamine, N-acetyl	Hypoxanthine	Ribose, 2-deoxy-
Alanine, beta-	Galactose	Inosine	Ribose-5-phosphate
AMP	Galacturonic acid	Inositol, myo-	Ribulose-5-phosphate
Arabitol	Gluconic acid	Isobutanoic acid, 3-amino-	Serine
Arginine	Gluconic acid-6-phosphate	Isocitric acid	Sorbitol
Asparagine	Glucosamine	Isoleucine	Spermidine
Aspartic acid	Glucosamine, N-acetyl	Lactic acid	Spermine
Butanoic acid, 2-amino-	Glucose	Lactose, alpha-	Succinic acid
Butanoic acid, 3-hydroxy-	Glucose, 2-deoxy-	Leucine	Sucrose
Butanoic acid, 4-amino-	Glucose-1-phosphate	Lysine	Taurine
Citric acid	Glucose-6-phosphate	Maleic acid	Threonine
Creatinine	Glucuronic acid	Malic acid	Thymine
Cystathionine	Glutamic acid	Maltose	Trehalose, a-a-
Cysteine	Glutamic acid, N-acetyl-	Mannose	Tryptophan
Cytosine	Glutamine	Methionine	Tyrosine
Dihydroxyacetone phosphate	Glutaric acid	Ornithine	Uracil
Erythritol	Glutaric acid, 2-hydroxy-	Pantothenic acid, D-	Urea
Erythrose-4-phosphate	Glutaric acid, 2-oxo-	Phenylalanine	Uric acid
Ethanolaminephosphate	Glyceraldehyde 3-phosphate	Phosphoenolpyruvic acid	Uridine
Fructose	Glyceric acid	Proline	Uridine-5-monophosphate
Fructose 1,6-bisphosphate	Glyceric acid-3-phosphate	Putrescine	Valine
Fructose-1-phosphate	Glycerol	Pyroglutamic acid	Xylose

Appendix Table 8. Relative standard deviation of sum of normalized peak areas and median from individual metabolites. BR: biological replicates, QC: quality control pooled samples from technical variance

Type	BR	RSD [%]	Median RSD [%]
QC	4	8	16
Male control	6	11	37
Male rapamycin	6	5	32
Female control	7	10	33
Female rapamycin	5	14	25

Appendix Figure 1. Heatmap of the top 100 DE genes (Adj.p-value <0.01 and RPKB>4Kb) and treatment effect between sex



- term
- cell junction/focal adhesion
 - metabolic
 - mitochondrial
 - other
 - transcription factor
 - translation-ribosome

STATUTORY DECLARATION

“I, [**Al Diab Ola**], by personally signing this document in lieu of an oath, hereby affirm that I prepared the submitted dissertation on the topic [**Molecular profiling of sex-specific podocyte stress response in response to mTOR inhibition**], independently and without the support of third parties, and that I used no other sources and aids than those stated.

All parts which are based on the publications or presentations of other authors, either in letter or in spirit, are specified as such in accordance with the citing guidelines. The sections on methodology (in particular regarding practical work, laboratory regulations, statistical processing) and results (in particular regarding figures, charts and tables) are exclusively my responsibility.

Furthermore, I declare that I have correctly marked all of the data, the analyses, and the conclusions generated from data obtained in collaboration with other persons, and that I have correctly marked my own contribution and the contributions of other persons (cf. declaration of contribution). I have correctly marked all texts or parts of texts that were generated in collaboration with other persons.

My contributions to any publications to this dissertation correspond to those stated in the below joint declaration made together with the supervisor. All publications created within the scope of the dissertation comply with the guidelines of the ICMJE (International Committee of Medical Journal Editors; www.icmje.org) on authorship. In addition, I declare that I shall comply with the regulations of Charité – Universitätsmedizin Berlin on ensuring good scientific practice.

I declare that I have not yet submitted this dissertation in identical or similar form to another Faculty.

The significance of this statutory declaration and the consequences of a false statutory declaration under criminal law (Sections 156, 161 of the German Criminal Code) are known to me.”

Date

Signature

CURRICULUM VITAE

“My curriculum vitae does not appear in the electronic version of my paper for reasons of data protection”

ACKNOWLEDGMENT

First, most grace and praise to Allah to give me the strength to complete this work.

It's a pleasure to thank all people who made this thesis possible, many people I owe thanks. First and most importantly my advisor Dr. Angelika Kush for her patience, kindness, valuable assistance, guidance and encouragement all the time in many ways and in both personal life and work. You always see the good in students, support and criticize in balanced perfect way. You taught me that research is about mentality and good practice with good critical thinking, I cannot thank you enough, it is a pleasant to be monitored by you, I am forever grateful, you always make things easy and doable.

I would also like to thank all members in AG Dragun lab for their support and guide of my research starting from Dr.rer.nat Dennis Gürgen , Dr.rer.nat Aurelie Phillipe, Dr.rer.nat Rusan Catar on both personal and teaching levels. Dr.Raphella, Dr.Christen and Dr.Eric thank you for your collaboration and answering every questions and helping in the preliminary analysis.

Thanks to my supervisor, Prof. Duska Dragun, for accepting me in her esteemed lab. It was a pleasure to be one of her students, giving me the time and support, may her soul rest in peace.

I would like to thank my second supervisor Prof. G. Duda for his support and valuable comments during our committee meetings, thanks for the time you dedicated to me.

I owe thanks to each of the members of the Dragun lab who I work with every day, Marc thanks for helping me in experiment especially during my pregnancy, my colleagues Sumin, Lei, Peng and Chen, it was nice companion. No research is possible without infrastructure and requisite materials and resources. For this I extend thanks to Charité – Universitätsmedizin Berlin facilities.

Here, I acknowledge the people who mean the world to me, my lovely parent, this work is dedicated to you. You always supported us to follow our dream even if it is apart from you and taught us not to quit no matter how hard it comes. Your prayers, your daily phone calls, show unconditional love and support. I could not make it without hearing my voice in my heart every day. Me, my brothers and sisters are always thankful for ever, we cannot pay you back enough, may Allah bless you

Abeer, Lama, Ahmad and Mohammad, maybe it was hard in the last years not to see each other frequently, but you never showed this. Your love, concern, caring and calls, all gave me the

strength, Love you all. Abeer I cannot thank you enough for helping, care and dedicated efforts you did even a part, thanks for your spiritual support, you are my soul mate, without sister love, life is not easy.

My deepest thanks and appreciation would be to my lovely husband Ibrahim, you were always around at times I thought that it is impossible to continue, you helped me to keep things in perspective and to stay calm, it was a long journey, but you made it easy for me. Thanks for coming with me I could not imagine being alone through this tough time alone, you always encouraged, support me to be the person I want to be. Your carness, taking care of the kids, and continuous love you showed me always even in my worst moments you showed what true love is, I cannot thank you enough, I love you. Sarah and Malek, it was a hard journey with you both and on you, never imagined I would be a mom for the first time during a PhD study and away from family. Maybe you will never remember this, but you had to tolerate me during my stressful time, especially at the end. I will always share the nice pictures and moments with you and while staying with me late night, I love you both, I am the luckiest to have all the three of you in my life and may Allah bless our family.

I would like to thank all my friends, in particular Needa, Nirmeen and Basmalah, my family in Jordan and Germany.

Doing a PhD abroad was one of my dream, Germany was the first place to think about, this would not be possible without the scholarship I had from the DAAD in 2015. Thanks for Deutscher Akademischer Austauschdienst (DAAD)- German Academic Exchange Service- for granting me the scholarship and financial support for me and my family for 5 years, you made my dream comes true.

It is not the finish line that matters, it is the journey getting there

Dedicated to my beloved parent

**TO ME
Ola Al Diab**